Flame Spread Measurements Of New Zealand Timber Using An Adaptation Of The Cone Calorimeter Apparatus

VI CUONG MICHAEL HUYNH

Fire Engineering Research Report 03/5

May 2003

ISSN 1173-5996

FLAME SPREAD MEASUREMENTS OF NEW ZEALAND TIMBER USING AN ADAPTATION OF THE CONE CALORIMETER APPARATUS

BY

VI CUONG MICHAEL HUYNH

Supervised by

Michael Spearpoint

Fire Engineering Research Report 03/5

June **2003**

A thesis submitted in partial fulfilment of the requirements for the
Degree of Masters of Engineering in Fire Engineering
at the University of Canterbury

School of Engineering
University of Canterbury
Private Bag 4800
Christchurch, New Zealand
Phone +64-3 364-2250, Fax +64-3 364-2758
www.civil.canterbury.ac.nz

Abstract

This report investigates the use of an adaptation of the Cone Calorimeter to measure opposed flow flame spread. Cone Calorimeters are typically used in a horizontal orientation for ignition testing, this report looks at using the Cone Calorimeter in a vertical orientation to test flame spread, and compare results to those from Lateral Ignition Flame Transport (LIFT) experiments. This work arises from the LIFT apparatus being bulky and cumbersome which makes it an undesirable apparatus to have in the laboratory. The adaptation of the Cone Calorimeter is to provide an alternative method of obtaining the same material data in fire conditions.

This work has followed on from work which was started by Azhakesan et al (1998) at Fire SERT at the University of Ulster, by developing a small scale opposed flow flame spread apparatus. The Reduced scale Ignition and Flame spread Technique (RIFT) was the result of adapting the Cone Calorimeter. This research was conducted in the Chemical and Process Engineering department at the University of Newcastle, which had conducted some work in this field. This research used this technique to examine opposed flow flame spread over a number of species of New Zealand timber and timber products.

The research lead to an application of a view factor developed from horizontal Cone Calorimeter tests by Wilson et al (2002). This was modified and applied to the vertical orientation of the Cone Calorimeter. The use of the view factor is to estimate the profile of the heat flux along the length of the sample. The results obtained indicated a correlational nature however modifications are required to confirm findings.

The application of Quintiere's model on opposed flow flame spread used in LIFT tests is applied to the RIFT test to obtain material properties. The results from the RIFT analysis have shown that the flame spread variables are comparable with those obtained from LIFT tests. Results at this stage are preliminarily, recommendations are suggested to substantiate current results.

Acknowledgements

I would like to thank the following people for their assistance and support in helping me to complete this project:

- My supervisor, Michael Spearpoint for his support and guidance throughout this work.
- The New Zealand Fire Service Commission for their financial help and continued support of the M.E. Fire program.
- The Civil Engineering Department at the University of Canterbury for financial assistance to travel to Australia to conduct the experiments, otherwise this research may not have been possible.
- The Chemical Engineering Department at the University of Newcastle who supplied the laboratory time and access to the Cone Calorimeter which was used for the experiments and the financial assistance given for accommodation. Special thanks to Behdad Moghtaderi for his input and guidance during my time at the University of Newcastle and Jane Connelly whose help and assistance in the lab was greatly appreciated.
- The technicians at the University of Canterbury and the University of Newcastle for their help in various ways, particular thanks to Grant Dunlop whose help at Newcastle was greatly appreciated and his knowledge of the Cone Calorimeter assisted in the testing phase.
- The engineering librarians particularly Christine McKee for her assistance in obtaining the countless requests for information.
- And finally Amanda Johnston, for her patience and support during my return to University and who helped read and proof various sections of the report.

Table of Contents

List of Figures

List of Tables

Nomenclature

Flame Spread/Ignition Calculations

b	ignition correlation parameter, $s^{-½}$
C	flame spread, heat transfer factor, $m^{s/2}/kW \cdot s^{½}$
$F(t)$	specimen thermal response function
$F(x)$	surface flux configuration invariant, $(kW/m^2)/mV$
h	heat loss coefficient. $kW/m^2 \cdot K$
h_{ig}	heat loss coefficient at ignition, $kW/m^2 \cdot K$
$k\rho c$	thermal inertia – heating property, $(kW/m^2 \cdot K)^2 s$
$\dot{q}''_{0,ig}$	critical flux for ignition, kW/m^2
$\dot{q}''_{0,s}$	critical flux for spread, kW/m^2
$\dot{q}''_{e}$	measured incident flux, kW/m^2
t	time, s
t^*	thermal equilibrium time, s
t_{ig}	ignition time under incident flux, s
t_s	flame spread time, s
T_∞	ambient/initial temperature, °C
T_{ig}	ignition temperature, °C
$T_{s,\,min}$	minimum temperature for spread, °C
ΔT_f	flame heating temperature, °C
ΔT_e	external heat flux temperature, °C
V	flame velocity, m/s
$x,\ x_p$	flame front position along specimen, m
ε	surface emissivity
ϕ	flame heating parameter, kW^2/m^3
σ	Stefan-Boltzmann constant, 5.67×10^{-8}, $kW/m^2 \cdot K^4$
δ_f	flame heating distance, mm
Δ	heat transfer depth into the solid, mm

Configuration/View factor

a	distance from centerline
A_3	area of surface 3
dA_1	elemental area on the sample's surface
$F_{3\text{-}d1}$	configuration factor between surface 3 and elemental area dA_1
$F_{d1\text{-}2}$	configuration factor between elemental area dA_1 and surface 2
$F_{d1\text{-}3}$	configuration factor between elemental area dA_1 and surface 3
$F_{d1\text{-}4}$	configuration factor between elemental area dA_1 and surface 4
h	height of the frustum (65 mm for standard cone)
H_2, H_4	parameters defined as $H_2 = z/a$ and $H_4 = (h + z)/a$, respectively
$\dot{q}''$	local radiant heat flux on the specimen's surface, W/m^2
R_2, R_4	parameters defined as $R_2 = r_2/a$ and $R_4 = r_4/a$, respectively
r_2, r_4	radii of the base and top of the frustum (80 mm, and 40 mm, respectively)
T	average surface temperature of the heating element, K
z	vertical distance from the lower base of the frustum to the sample surface
Z_2, Z_4	parameters defined as $Z_2 = 1 + H_2^2 + R_2^2$ and $Z_4 = 1 + H_4^2 + R_4^2$
ε	emissivity of the heating element
σ	Stefan-Boltzmann constant, 5.67×10^{-8}, kW/m^2·K^4
ω_2, ω_4	angle of elemental point to the surface of the cone

1 Introduction

The concept of flame spread is to examine the fire spread along materials. The materials of interest are generally those with application to building designs and furnishings. Building components affect the spread of fire through various modes these include wall and ceiling linings; such as wood panelling and paint finishes to floor coverings such as; types of carpet; tiles, and wooden floors. Fire hazards in buildings are controlled by regulations and codes that define what is acceptable. To assist in this process are "reaction to fire" tests which allow observations of the material's behaviour in fire.

The fundamental aspects and measurement of flame spread have provided a foundation for application in the design of buildings and formulas have been developed for use in modelling. A testament to this work can be seen in such computer software developments such as BRANZFire, and Fire Dynamic Simulator (FDS). It is still recognised that the use of these formulas and models are limited due to a lack of material data that are available in fire conditions.

The lack of information is a particular problem with respect to indigenous New Zealand timbers and common timber products. This report focuses on experiments on indigenous New Zealand timbers and timber products that were carried out at the University of Newcastle, Newcastle, New South Wales, Australia. The Cone Calorimeter apparatus was used to measure the flame spread of the specimens of indigenous NZ timbers and timber products. The results of these tests have been compared with the results and work undertaken overseas.

1.1 Flame Spread Tests

Early flame spread tests have produced numerous outputs representing flame spread properties. The outputs from these tests however have no uniformity and little ability for useful comparison between the many types of tests therefore this inconsistency led to the adoption of standardised testing. The early fire models developed at the National Bureau of Standards were for the military, these required a large number of

material constants to be entered as data inputs, de Ris (1969). These early modellers had to thoroughly search numerous experimental papers and reports before such data could be found, de Ris and Williams (1976). During the 1980s it was realised that for any model the input data describing fire properties should be determined from standard tests. A range of fire tests were developed to met the American Society for Testing and Materials (ASTM), standards.

There are many different tests for assessing the flammability of materials such as:

- *ASTM E 84* - The test method for determining the surface burning characteristics of building materials;
- *ASTM E 162* - The test method for determining the surface flammability of materials using radiant heat energy source;
- *ASTM E 286* - The test method for determining the surface flammability of building materials using an 8 ft (2.44m) tunnel furnace;
- *ASTM E 684* - The test method for determining the critical radiant flux of floor covering systems using a radiant heat energy source;
- *ASTM E 970* - The test method for determining the critical radiant flux of exposed attic floor insulation using a radiant heat energy;
- *ASTM E 1317* - The test method for determining the flammability of marine surface finishes; and
- *ASTM E 1321 – 97a* - The test method for determining material ignition and flame spread properties.

The majority of these tests are for evaluating interior finish materials and products, (in particular wall and ceiling applications). All of these tests mentioned above express their results in terms of some observations or measurements. The results are then used to derive a relative ranking scale on which to evaluate materials. The bases of these ranking scales however are only arbitrary and therefore the results between tests highlight the problem that they may not necessarily agree with each other and are meaningful between tests.

The research undertaken in this project utilises the procedure and theory of the Lateral Ignition and Flame Transport (LIFT) test. The properties derived from the test

provide the material properties in fire conditions which can be used in ignition and opposed flow flame spread models. In particular the properties include:

- The thermal inertia property, $k\rho c$;
- The ignition temperature, T_{ig};
- The minimum temperature required for lateral flame spread, T_s;
- The corresponding heat fluxes for ignition and flame spread and, $\dot{q}''_{0,ig}$, $\dot{q}''_{0,s}$
- A numerator of the governing equation for opposed flow flame spread, ϕ

1.2 Impetus for Research

The reason for this research is explained in this section. The *ASTM E 1321*, uses the Lateral Ignition and Flame Transport (LIFT) apparatus. The LIFT apparatus is bulky and cumbersome which makes it an undesirable apparatus to have in the laboratory. The adaptation of the Cone Calorimeter, which is also an American standard ASTM E-1354-90, could provide an alternative method of obtaining the same material data in fire conditions. The Cone Calorimeter is a more practical size and is reported to be more widely used in laboratories, Babrauskas (1995).

The Cone Calorimeter has been found to fill a very useful role in fire applications because it is not a single variable test as many other fire tests are. It is already recognised the properties needed for wind aided flame spread are readily obtained from the Cone Calorimeter, Babrauskas (1999). However one type of data not found among standard Cone Calorimeter outputs is that needed to calculate the opposed flow flame spread. For that purpose the LIFT test has often been recommended.

Researchers at The University of Newcastle in Australia have continued the work, which was started by Azhakesan et al (1998) at Fire SERT at the University of Ulster, by developing a small scale opposed flow flame spread apparatus. The Reduced scale Ignition and Flame spread Technique (RIFT) was the result of adapting the Cone Calorimeter. The proposed research was conducted in the Chemical and Process Engineering department at the University of Newcastle. This research intends to use

this technique to examine opposed flow flame spread over a number of species of New Zealand timber and timber products.

By careful application of the existing LIFT theory to the RIFT experiments, it is hoped that the analysis of Cone Calorimeter data would provide sufficient information so that it could be obtained for predicting opposed flow flame spread, then reliance could be placed upon using a single test method for collecting bench scale fire property data.

Advantages includes cost savings, in terms of reduced labour and laboratory time, this would be of significant advantage as it is widely accepted that the Cone Calorimeter's specimens are much easier to prepare and to test than the equivalent LIFT specimens. It has been noted by past researchers, Babrauskas (1999), that the expected time needed for Cone Calorimeter testing is less than half of that required for by the LIFT tests. Babrauskas (1995) has reported that it is estimated that the Cone Calorimeter apparatuses are located in over 150 laboratories while the number of laboratories possessing the LIFT test apparatus are in the vicinity of 20. Consequently modelling input data could be generated at many more institutions, if Cone Calorimeter data alone was seen to be sufficient.

1.3 Objectives

The aim of the research is to be able to compare our results to the work conducted at the University of Newcastle, the results generated by Azhakesan et al and also the results obtained from the traditional flame spread test, the LIFT experiments. Experiments were carried out using the modified Cone Calorimeter and the results were analysed using the same theory as applied to the LIFT experiments. A correlation is hoped to be found between the two apparatus as the modified Cone Calorimeter could then be used for future opposed flow flame spread analysis instead of the LIFT apparatus.

The objectives of this study can be broken down into five main areas these are:

- To conduct a thorough literature review of past work in the field of opposed flow flame spread and to gauge the current developments in the field of bench scale flame tests.
- To measure the irradiance that the specimen sample is exposed too while held in the sample holder.
- To find or derive a configuration/view factor in order to be able to predict the irradiance down the length of the sample.
- To apply the opposed flow flame spread theory, derived by Quintiere (1981) which is used in LIFT experiments, to the Cone Calorimeter experiments.
- To conduct experimental tests on New Zealand timbers and timber products, and compare the results of the material properties in fire conditions (relating to flame spread), to that of the Australian and Northern Ireland studies and also from published LIFT results.

The outputs that will be compared between the studies are as follows:

- The minimum ignition surface flux, $\dot{q}''_{0,ig}$
- The minimum ignition temperature, T_{ig}
- The minimum lateral spread flux, $\dot{q}''_{0,s}$
- The minimum lateral spread temperature, $T_{s,min}$
- The thermal inertia value, $k\rho c$
- The flame heating parameter, Φ

1.4 Previous Work at the Universities of Canterbury and Newcastle

Mentioned earlier was the work conducted at the University of Newcastle, Australia. This work has been based upon a study conducted by Azhakesan, Shields and Silcock at Fire SERT at the University of Ulster who have examined flame spread using a reduced scale ignition and flame spread technique (RIFT) incorporating the use of the Cone Calorimeter. Initial work at The University of Newcastle was conducted as a final year research project by Pease (2001) where modifications to the sample holder of the Cone Calorimeter were made to allow surface flame spread experiments to take place. In this study three wood species were tested and compared to results obtained from LIFT test results published in literature. The following year at the University of

Newcastle a further study was conducted by Perrin (2002), the emphasis was on the irradiance along the length of each sample. This study is a continuation of these works.

The University of Canterbury is involved in research in the field of ignitability this has included work on timber products, Ngu (2001) and upholstered furniture such as the New Zealand Combustion Behaviour of Upholstered Furniture (NZ CBUF) studies undertaken by Enright (1999). The ignition properties of New Zealand timbers and timber products were examined using the ISO ignitability apparatus by Ngu (2001). In the study by Ngu (2001) various ignition correlations such those by Mikkola and Wichman (1989), Quintiere and Harkleroad (1985) and Spearpoint and Quintiere (2000) were applied to the test results to gauge which presented the best method. The species of timber tested in this work included: Radiata Pine; Rimu; Beech; Macrocarpa; Medium Density Fibre Board (MDF), Plywood, Particle Board and Laminated Veneer Lumber (LVL). The experimental work conducted in this research used these same New Zealand timbers and timber products as Ngu's to provide cohesion between the two studies.

1.5 Report Outline

The remainder of this report is divided into various sections. Section 2 will provide a brief overview on flame spread, outlining the two main forms of flame spread; Wind aided and Opposed flow flame spread. Section 3 will detail the LIFT apparatus and the Cone Calorimeter, providing further details of these two apparatus and a brief history. Section 4 will give a literature review outlining the development of flame spread theory particularly the pioneering work carried out in the late 1960s. A look at past experimental works in the area of ignition and flame spread tests, and also a discussion of the mathematical models that have been developed. Section 5 will provide the details of the theory by Quintiere that is applied to the LIFT tests, covering the opposed flow flame spread and ignition calculations. Section 6 will explain the experimental design, outlining the materials tested, testing conditions and the experimental layout. The results and discussion of the report will be divided to address each of the objectives. Section 7 will present the results and discussion on the

irradiance mapping along the length of the sample, while section 8 will present the results and discussion of the ignitability tests. Section 9 will present the results and discussion of the flame spread tests. The application of Quintiere's model to the data and comparison of the material properties derived. Section 10 will provide the overall conclusions of the research, summarising the results, limitations and future work. An appendix is included which includes the raw data used in the calculations.

2 Flame Spread

Flame spread is the name for the process in which a fire grows. Flame spread is a complex process, which is affected by physical, geometrical and chemical parameters. At times the term flame spread maybe misleading as flame spread is not referring to the extension of the flames but in fact the fire growth or spread. The term flame spread specifically refers to the extension of the burning region, where the region is undergoing vapourisation and therefore supplying the necessary fuel.

The affecting parameters include the:

- surface orientation;
- direction of flame spread;
- specimen (sample) size;
- initial fuel temperature;
- external radiant flux;
- roughness of the specimen's surface;
- flow velocity of the environment such as wind;
- gravitational effects;
- composition of the material and
- composition of the atmosphere such as humidity.

Many studies have been undertaken in the past such as by Atreya (1986) and Spearpoint (2000), which have specifically focused on parameters such as grain and sample orientations. To effectively deal with these factors when evaluating the performance of materials it is necessary to integrate the material data with mathematical models.

The gravitational and wind effects are the most prominent factors affecting flame spread. The flows resulting from the fire buoyancy or the natural wind of the atmosphere can either assist, which is often referred to as wind-aided flame spread or inhibit, which is known as opposed flow flame spread. Figure 1 and Figure 2 illustrate these two forms of flame spread.

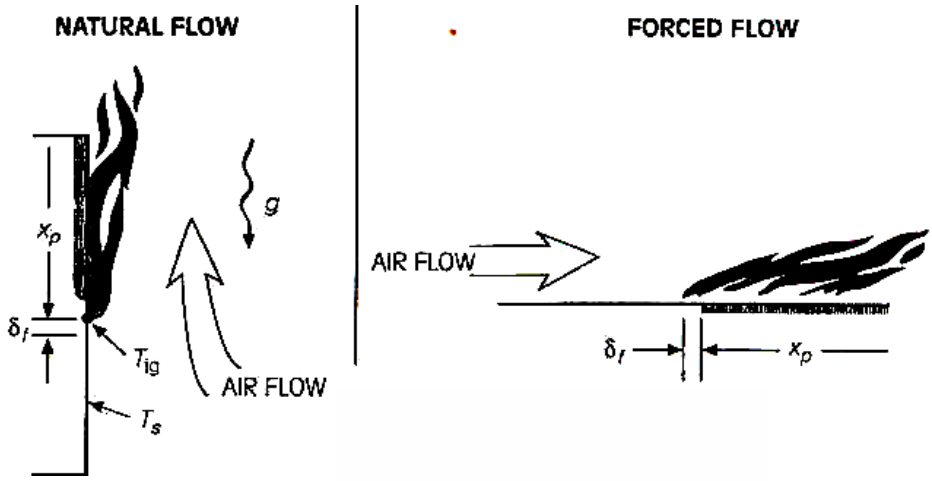

Figure 1 Opposed Flow Flame Spread – Reproduced from Quintiere (1998)

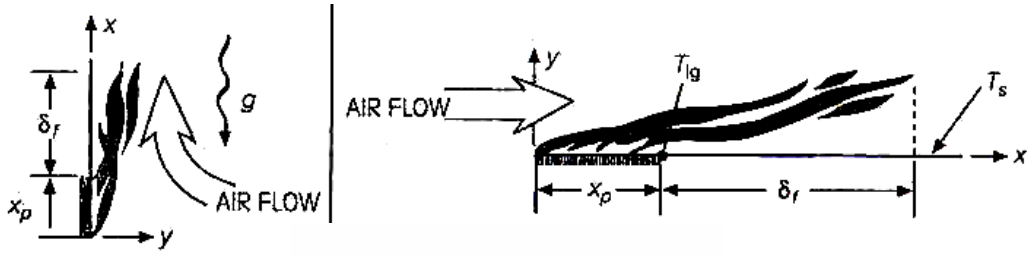

Figure 2 Wind-Aided Flame Spread – Reproduced from Quintiere (1998)

Wind-aided and opposed-flow flame spreads are the terms used to describe the permutations of fire spread that can occur. Wind-aided flame spread is in the direction of the air flow and also encompass the vertically-upward and ceiling flame spread. Even in still air vertically-upward and ceiling flame spread are referred to as wind-aided due to the buoyant flow of the fire itself. Permutations of opposed-flow flame spread include vertically-downward and lateral wall flame spread. In opposed-flow flame spread dependency is on the air flow and fuel surface as flame spread will only occur if the surface temperature is above the critical ignition value.

The process of flame spread, whether it is wind-aided or opposed flow, can be described in general terms. As depicted in Figure 1 and Figure 2 the flame spread velocity is defined as the rate of motion at position x_p. The x_p position represents the extent of the pyrolysis (vaporising) region. The pyrolysis region is driven by the

burning rate of the fire. The burning rate of the fire is in turn controlled by factors such as the temperature and composition of the material.

The pyrolysis process is caused by heat transfer from the advancing flame to the surface of the specimen. The pyrolysis process is a necessary step to sustain the flame spread process. The advancing face of the flame spread, which is the region denoted by δ_f, can be described as two different fronts: the flame in the gas phase, and the pyrolysis region in the condensed phase. The flame in the gas phase may easily be measured by an observer. The pyrolysis region in the condensed phase is more difficult to measure. The flame spread velocity is the rate of movement of the pyrolysis region in the condensed phase. The flame spread velocity is calculated using the theorems set out in Quintiere (1981).

3 The LIFT test apparatus and the Cone Calorimeter

Flame spread properties are commonly found using one of two testing methods and apparatus:

- The Lateral Ignition Flame Transport (LIFT) test or
- The Cone Calorimeter

The LIFT test is useful in determining ignition times as well as measuring opposed flow flame spread. The Cone Calorimeter is a test with multi-variable outputs.

3.1 Lateral Ignition Flame Transport (LIFT)

ASTM E 1321 – The test method for determining material ignition and flame spread properties.

ASTM E 1321 is also known as the lateral ignition flame transport (LIFT) test. The initial design for the LIFT test was created by Robertson (1969). The design evolved from work conducted by Robertson for the Intergovernmental Maritime Consultative Organisation (IMCO) in the 1970s. The LIFT test is used to determine the material properties relating to piloted ignition. The LIFT test consists of two aspects:

- Measuring the ignition; and
- Measuring the lateral fame spread.

The LIFT experiments provide a series of outputs:

- The minimum ignition surface flux, $\dot{q}''_{0,ig}$;
- The minimum ignition temperature, T_{ig};
- The minimum lateral spread flux, $\dot{q}''_{0,s}$;
- The minimum lateral spread temperature, $T_{s,min}$;
- The thermal inertia value, $k\rho c$; and
- The flame heating parameter, Φ

The LIFT test can also be used to predict the time to ignition, t_{ig}, and the velocity, V, of the lateral flame spread on a vertical surface subject to a specified external flux. This is discussed in section 5.1.

During experimental testing using the LIFT test the specimen is subject to the following constraints:

- The specimen is placed vertically; and
- A constant heat flux is applied.

The lateral flame spread on the vertical surface is recorded as a function of time.

The specimens are exposed to the heat from a vertical air-gas fuelled radiant-heat source inclined at 15° to the specimen (see Figure 3). The specimens are exposed to a graduated heat flux that is approximately 5kW/m² higher at the hot end than the minimum heat flux necessary for ignition. The specimens measure 155mm by 800mm. There is a piloted acetylene-air ignition source which forms part of this apparatus, this is used to ignite the air-gas fuelled radiant panel and also provide a means to ignite the specimens during flame spread tests.

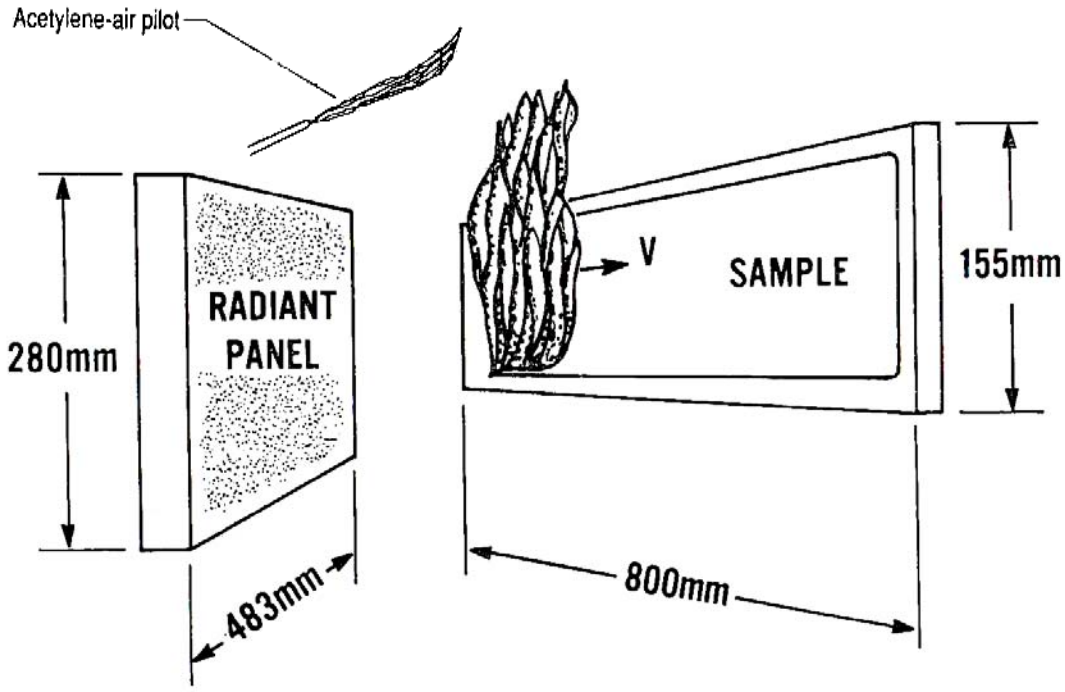

Figure 3 Schematic of the Apparatus during a LIFT test – Reproduced from Quintiere (1981)

As well as conducting flame spread tests, the LIFT test is capable of conducting ignition tests. For the ignition tests, a series of 155mm by 155mm specimens, are exposed to a nearly uniform heat flux. The irradiance over the range of 155mm is approximately uniform as illustrated in Figure 4. The results of the ignition tests allow for the time for ignition to be calculated as well as the critical minimum heat flux required for ignition. The ignition data is then used to derive preheat times, t^* needed for the flame spread tests, the preheat time, t^* represent the time that is required for the specimen to reach thermal equilibrium (steady state). The preheat time is a function of the critical heat flux required for ignition and is derived from the ignition correlations (*refer to section 5.2 for further details*).

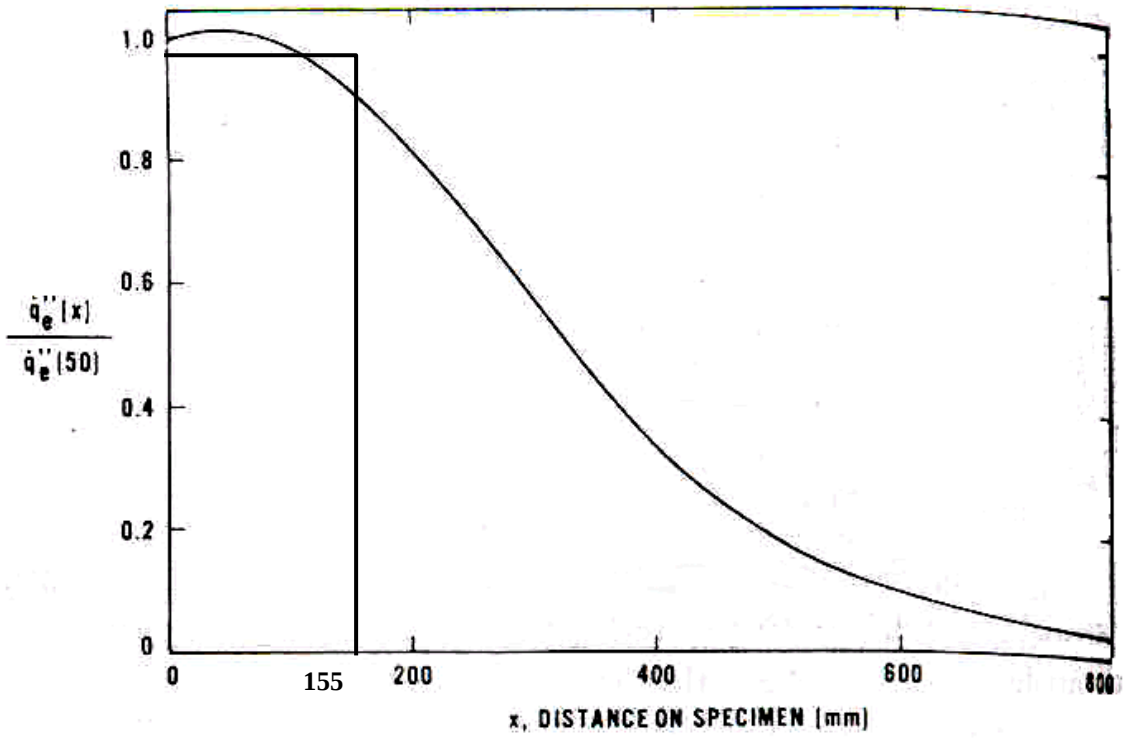

Figure 4 Normalised Heat Flux over Specimen – Reproduced from Quintiere (1981)

Prior to ignition in the flame spread tests, the specimens are preheated until thermal equilibrium is reached. Once the preheat time has been reached the pilot flame ignitor is placed so that the specimen can ignite. The pyrolysing flame front progressing along the horizontal length of the specimen can be recorded as a function of time.

The popularity of the LIFT is partly due to the availability of theory which is available to interpret the results, ASTM E 1321 – 97a. The data obtained by the LIFT

is increasingly being used in fire modelling. Jianmin (1990) has suggested that alternative approaches may be desirable because of the following difficulties:

- Actual measurements in the LIFT are often quite difficult because of flashing or jumping of the flame front. At times it is impossible because of the melting behaviour of the specimen in the vertically orientated position.
- The flame spread properties may be obtained by several different ways with no consistency.
- The relationship between full-scale and bench scale flame spread is tenuous because of the unpredictability of material behaviour in fires, such as due to shrinkage, connection behaviour, and behaviour between elements. At times only full scale testing will reveal the problems that bench scale tests hide.

3.2 Cone Calorimeter

The Cone Calorimeter was developed by researchers at the National Institute of Standards and Technology (NIST) formerly known as the National Bureau of Standards (NBS). The findings of the work have been reported by Babrauskas (1984). The Cone Calorimeter was first conceived and designed by Robertson at the NBS in the 1970s. The Cone Calorimeter test apparatus has since been developed and refined and is defined in a range of international standards such as ISO 5660 (1993) and national standards such as ASTM E 1354 – 02 and AS/NZS 3837 (1998).

The *ASTM E 1354 – 02* describes the standard test for heat and visible smoke release rate for materials and products using an oxygen consumption calorimeter. The standard provides a means for measuring the response of materials exposed to controlled levels of radiant heat with or without an external source of ignition.

In Figure 5 an example of how the Cone Calorimeter is housed is shown with its connections to the gas analysers. The exhaust hood sits directly above the cone, with probes position along the duct to allow gas samples to be taken to allow for calculation of heat release rates by use of oxygen calorimetry. Oxygen Calorimetry is based on the oxygen concentration and the flow rate in the exhaust stream and is based on approximately 13.1MJ of heat is released per 1kg of oxygen consumed. The

calculation of the heat release rate using oxygen calorimetry is described in detail in the paper by Janssens (1991). The sample sits upon a load cell which allows for the calculation of the mass loss rate. The effective heat of combustion is determined from an associated measurement of specimen mass loss rate; the smoke development is measured by obscuration of light in the exhaust stream. The cone heater is capable of producing radiant heat fluxes of 0 – 100 kW/m². The associated ignition source is by electric spark.

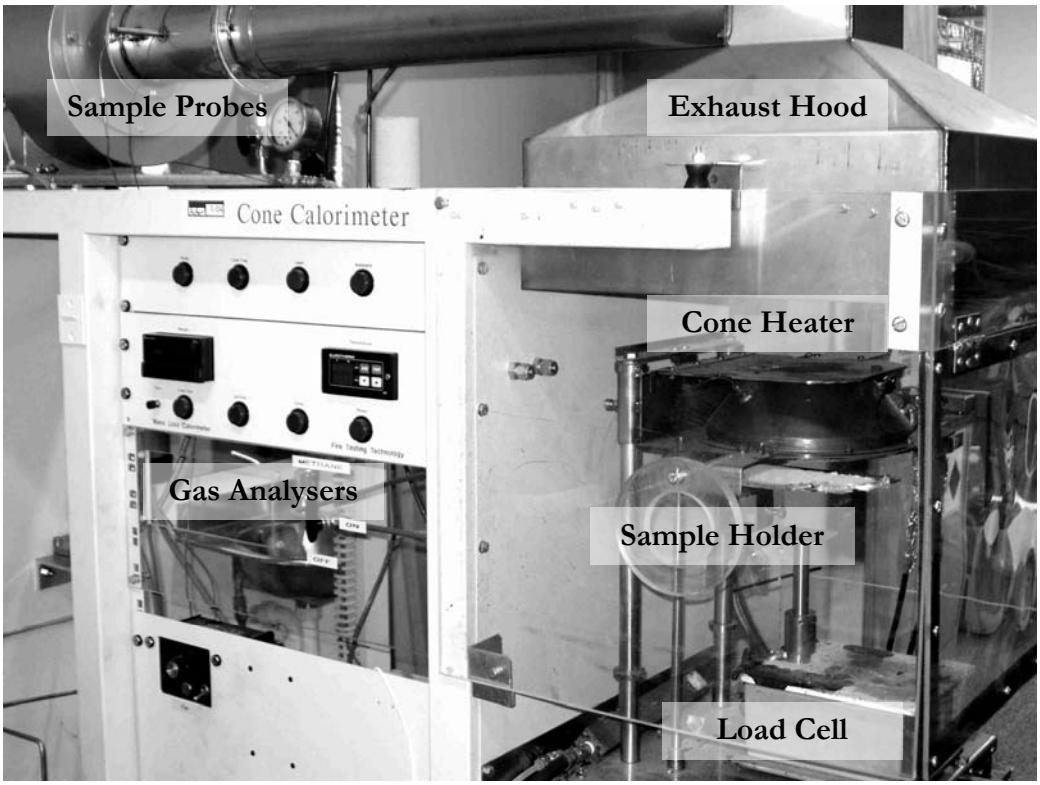

Figure 5 Exterior of the Cone Calorimeter

Figure 6 shows an example of the Cone Calorimeter setup in its conventional horizontal position; the pictures are of the same cone, shown at different perspectives. The right had side picture illustrate the tightly wound element forming the frustum. The spark ignitor is located 13mm away from the surface of the cone and is used in ignition tests. The heat shield can be seen in the open position, these are used in between tests to shield the irradiance from the cone while changing samples and protect the load cell from excessive exposure from the heat.

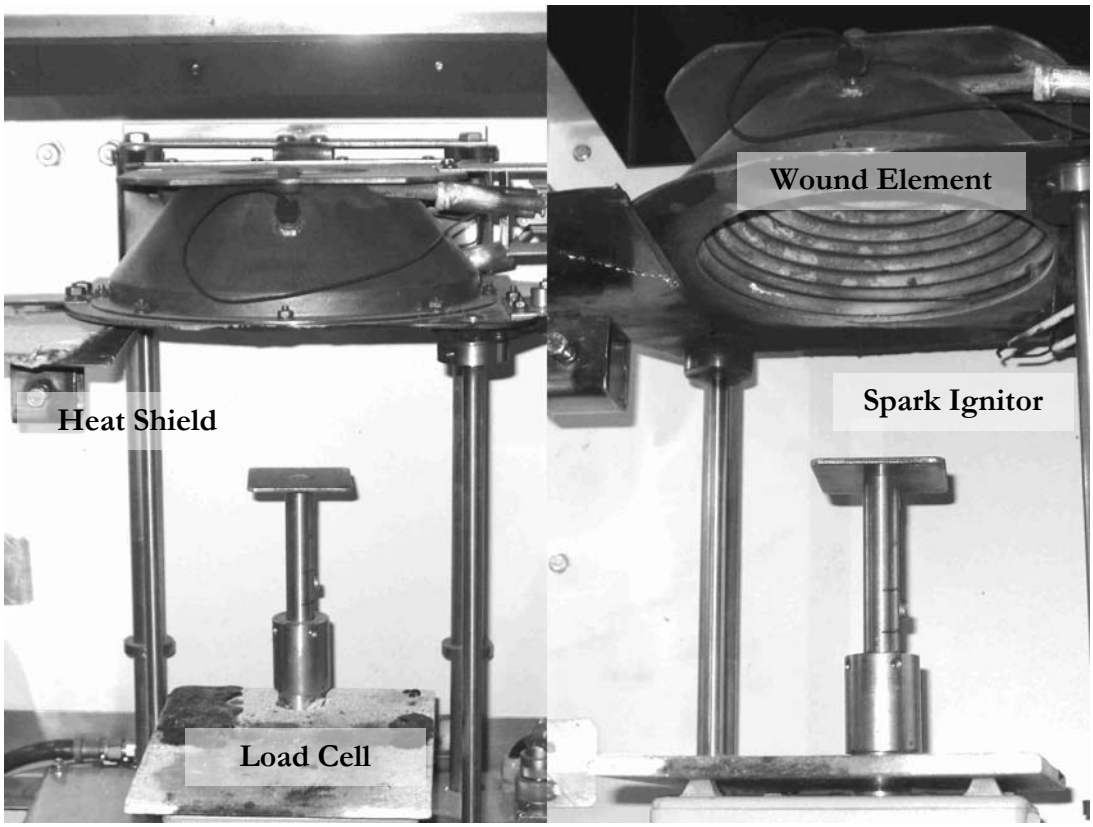

Figure 6 Cone Calorimeter - Split Perspectives

The Cone Calorimeter is used to obtain material properties in fire conditions by testing the behaviour of materials exposed to a controlled level of radiant heating. Parameters such as ignitability, the heat release rate, the mass loss rate, the heat of combustion, and the smoke release of materials can be determined from experiments undertaken in the Cone Calorimeter. The heating element within the cone is rated as 5000W at 240V, and consists of an element tightly wound into the shape of a truncated cone (frustum). The heating element is designed to deliver irradiances on the surface of the specimen of up to 100kW/m². Wilson et al (2002) conducted a series of experiments that showed that the heating element is capable of producing radiant heat fluxes with uniformity of ± 2% within a 50mm by 50mm area that is located 25mm directly below the frustum. The experiments were carried out in order to develop a model for the local configuration factor. The application of the Cone Calorimeter has proved to be very useful in fire applications because it is not a single variable test as many other fire tests are. As highlighted earlier, the versatile use of the Cone Calorimeter apparatus allows determining the ignitability, the heat release rates, the mass loss rate, the effective heat of combustion and the visible smoke

development. The Cone Calorimeter is broken down into finer details and are shown in Figure 7, Figure 8 and Figure 9.

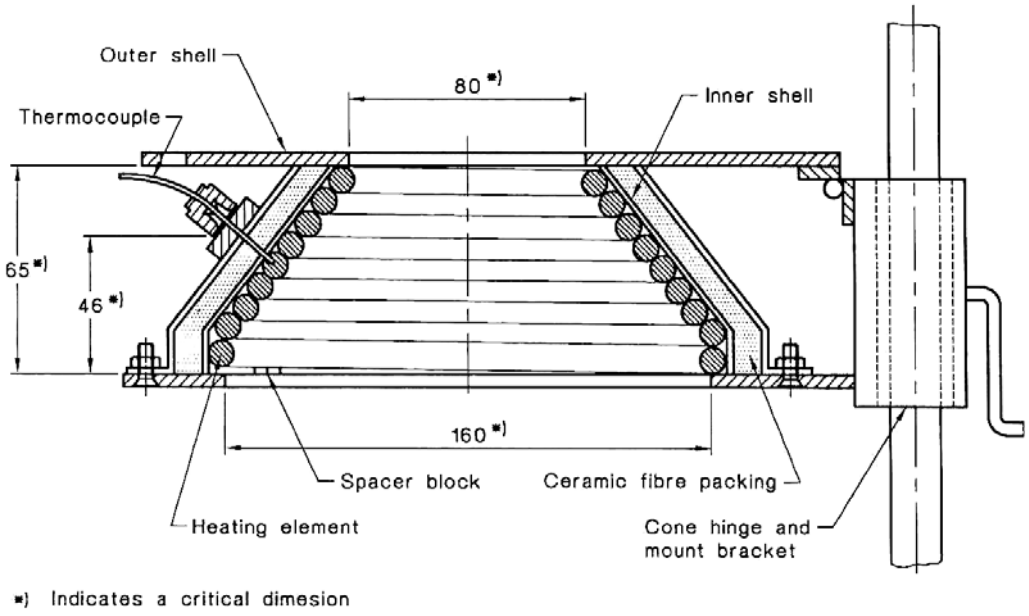

Figure 7 Cross-Sectional view Through the Heater – Reproduced from AS/NZS 3837:1998

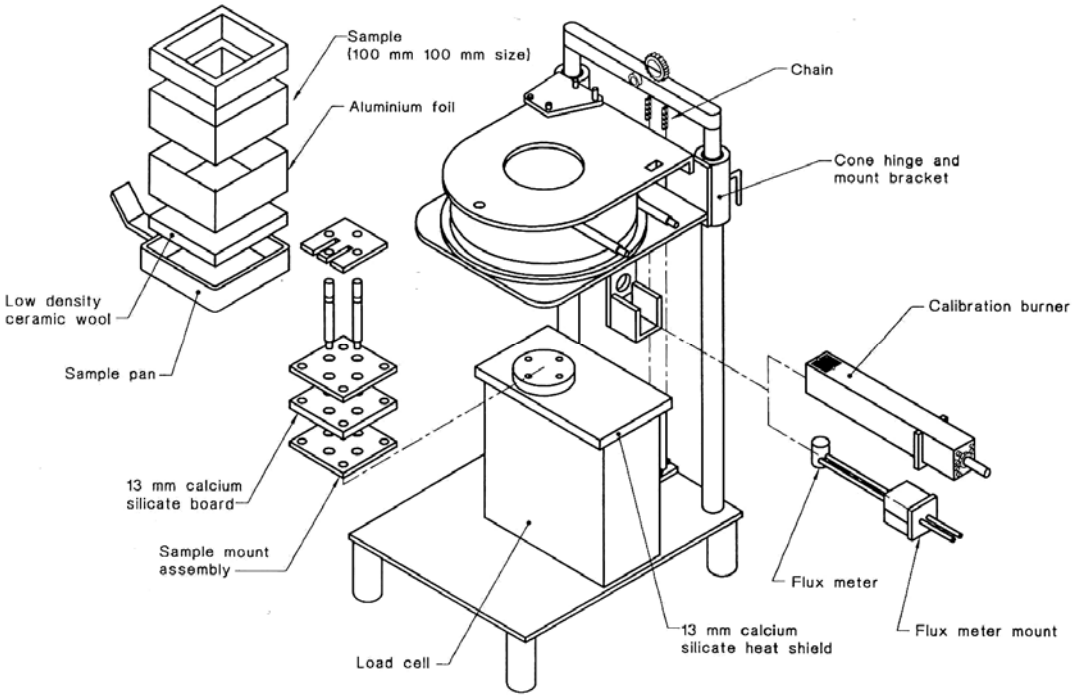

Figure 8 Exploded view, Horizontal Orientation – Reproduced from AS/NZS 3837:1998

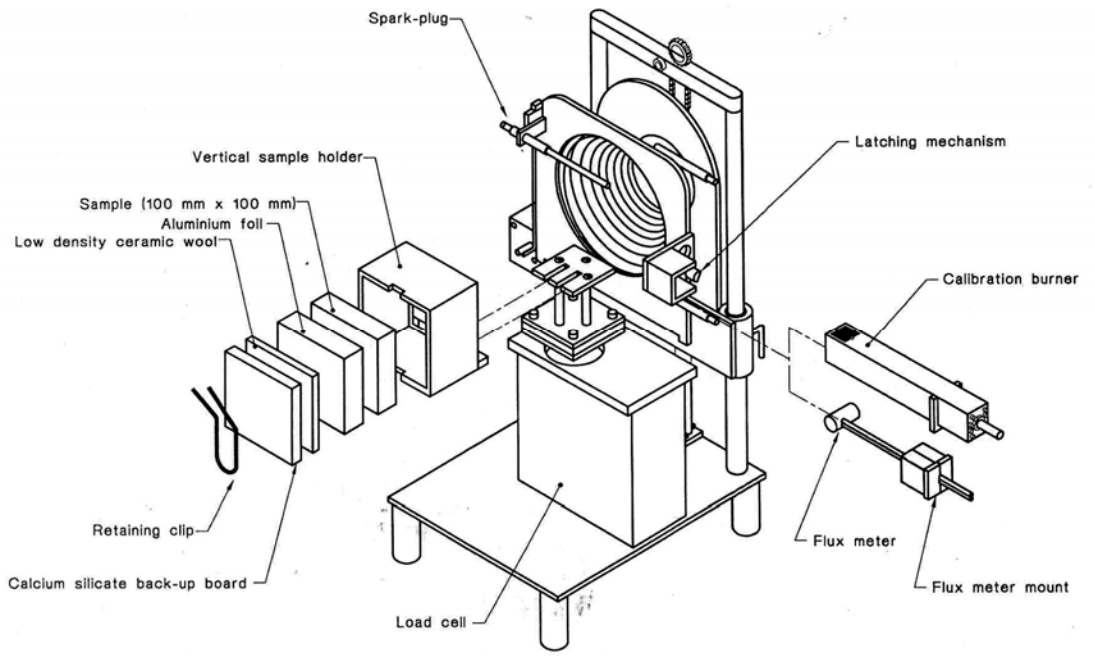

Figure 9 Exploded View, Vertical Orientation – Reproduced from AS/NZS 3837:1998

Figure 9 shows how the Cone Calorimeter can be used in the vertical orientation. Using the Cone Calorimeter in this vertical position a sample holder was developed to be able to hold the wood samples in a vertical position. A primary feature of the sample holder, is the flexibility of being able to set the holder at specified angles to the surface of the cone.

4 Literature Review

There have been many papers published which describe and assess the different experimental observations and theoretical models for calculating the flame spread process. The more notable ones include papers by: Fernandez-Pello and Hirano (1983); Williams (1985); Drysdale (1985); Wichman (1992); Babrauskas (1995) and Quintiere (2002). The papers highlight the lack of data on fire conditions and the failure to supply satisfactory information on the inputs for fire modelling.

4.1 Pioneering Work

4.1.1 De Ris (1969) - "Spread of Laminar Diffusion Flame"

The work undertaken by de Ris (1969), during the late 1960s reveals the original attempts to solve the problem of measuring flame spread both in the theoretical and experimental sense. In these times researchers did not have an existing base of knowledge to build research from but at the same time they also had the advantage of not being constrained by previous work.

The first studies of flame spread rose out of two different fields of study: (a) the defence field where the focus was on small scale flame spread over propellants; and (b) in the field of fire research where the focus was on large scale fire tests.

The work completed by de Ris has been instrumental in the development of flame spread models. De Ris developed a basic understanding of the flame propagation mechanism and achieved this by making physical assumptions based upon first principles. The problem is then able to be solved by deriving conservational equations and solved by using applied mathematics. De Ris describes the laminar diffusion flame spreading process as:

> "The hot flame heats the unburnt fuel bed which subsequently vaporises. The formulated model then treats the combustion as a diffusion flame for which the details of the reaction kinetics can be ignored by assuming infinite reaction rates."

In his work de Ris found that the flame spread mechanism was strongly influenced by:

(a) the adiabatic stoichiometric flame temperature; and

(b) the fuel bed thermal properties.

4.1.2 Williams (1976) – "Mechanism of Fire Spread"

William's article examines the mechanics of fire spread. The article describes the flame spread problem thoroughly by identifying the mechanisms involved. The mechanisms involved are simplified and sacrifices accuracy for the purpose of emphasising general aspects of heat transfer. Williams proposed an equation to represent the heat balance across the "surface of fire inception". The heat balance equation is a derivation of a universal flame spread equation which is given as: $q = \rho_s U_f \Delta h$ where q is the energy transferred across the separation line, S; ρ_s is the fuel density; and Δh is the thermal enthalpy difference between the fuel at ignition and ambient temperature. The heat balance equation is better represented when the gas-phase process dominates the flame spread, and not the solid phase process.

The article also examines flame spread over non-simple materials such as matchstick arrays and materials that drip or run during spread. Williams' work provides a framework for the field of flame spread which the various studies within flame spread can be grouped.

4.1.3 Fernandez-Pello (1977) – "A Theory of Laminar Flame Spread over Flat Surfaces of Solid Combustibles"

Fernandez-Pello introduced the use of finite rate chemistry into flame spread calculations. Fernandez-Pello proposed to establish a flame spread theory based on:

(a) a rigorous analysis of the gas phase equations, including equations for conservation of linear momentum;

(b) an analysis of the gas phase chemistry using high activation energy analysis.

Fernandez-Pello hypothesised that the bulk of the heat transfer ahead of the flame front occurred through the solid phase period. The observations made in this research proved this hypothesis to be correct, in that the solid phase does dominate the forward heat transfer particularly when the solid to gas ratio is small.

4.2 LIFT Related

4.2.1 Quintiere (1981) – "A Simplified Theory for Generalizing Results from a Radiant Panel Rate of Flame Spread Apparatus"

Quintiere (1981) sought to analyse the flame spread results from the test method as formulated by Robertson (1979) and generalise the results using a mathematical model. The model was developed for transient flame spread with external radiant heating and follows similar lines to Rockett's (1974) analysis of vertical downward spread. This work differs from that by de Ris (1969), and Fernandez-Pello and Williams (1977) as it is not completely based on fundamental properties but is also expressed in terms of fire parameters such as the flame's heat transfer rate and length.

Quintiere analysed experimental results on the rate of lateral flame spread and the time for piloted ignition under an externally imposed flux using a simple theoretical model. It was shown that the rate of flame spread, V_f can be correlated by:

$$V_f^{-1/2} = C(\dot{q}''_{0,ig} - \dot{q}''_e)$$

Where C is a material constant and $\dot{q}''_{0,ig}$ is the minimum heat flux required for piloted ignition.

4.2.2 Harkleroad/Quintiere/Walton 1983 - "Measurement of Material Flame Spread Properties"

The study undertaken by Harkleroad et al contained an analytical approach involving parameters and solutions arising from transient heat conditions in a semi infinite solid. The experimental data was generated using the apparatus that was design by Robertson (1979). These are the early tests carried out using the LIFT and hence subsequent work that has been carried out has been based on this early work. The flame spread rates and ignition events are measured against incident radiation and exposure time. As with a lot of flame spread experiments the outputs are intended to allow the prediction of downward or lateral flame spread on a vertical surface. The materials tested in this instance were selected to be representative of applications in aircraft (aircraft interior panelling, carpeting, seat cushion foam) and buildings (wood particle board, polymethymethacrylate (PMMA), and rigid low density foam). Although in this work a limited number of types of materials were tested, the application of the LIFT apparatus is not restricted to those mentioned. Any material that exhibits similar properties and under similar environmental conditions and orientation would be suitable to be tested.

4.2.3 Delichatsios (1999) – "New Interpretation of Data From LIFT (Lateral Ignition and Flame Transport) Apparatus and Modifications for Creeping Flame Spread"

Delichatsios attempted to reinterpret the measurements and results achieved by the LIFT apparatus. The findings of this study showed that one of the parameters deduced from the existing protocol was not a material property but in fact affected by the external heat flux applied at the front during the test. A new energy balance was proposed and used to determine the creeping flame spread. The resultant energy balance accounted for the dual effects of external heat flux on creeping flame spread, namely:

(a) the preheating of the solid ahead of the front; and
(b) the increasing the pyrolysis rate at the front.

It was observed that two creeping flame spread parameters are necessary to characterise the physics in 'normal' conditions. It was identified that the properties needed to predict creeping flame spread could not be obtained from a standard Cone Calorimeter apparatus. A test apparatus simpler than the LIFT was proposed by Delichatsios for obtaining the basic creeping flame spread properties. Instead of the one parameter, ϕ; two parameters are needed to characterise creeping flame spread, E the convective energy from the flame; and δ_f the gaseous thermal length.

4.3 Experimental Studies in the Field of Flame Spread

A number of experimental studies have been conducted into the effects of opposed flow flame spread. The majority of the studies undertaken have revolved around the use of the LIFT apparatus. The types of studies undertaken have varied. The earlier work by Quintiere and Harkleroad attempted to refine the LIFT experiments, later studies by Jianmin (1990) in Sweden and Nisted (1991) in Denmark were an attempt to predict flame spread results from standard Cone Calorimeter tests, Cleary (1992) and Janssens (1992, 1993) conducted tests to characterise flammability with the LIFT apparatus.

4.3.1 Quintiere/Harkleroad (1985) - "New Concepts for Measuring Flame Spread Properties"

In this paper Quintiere and Harkleroad discuss a method for deriving the parameters: $k\rho c$, referred to as the thermal inertia, ignition temperature and a flame spread factor suitable for use in mathematical models for piloted ignition and opposed flow flame spread. The method used for deriving the parameters are founded on existing flame spread theory.

It was identified within this study that the test methods did not yield results that were consistent with each other and did not reflect behaviour in actual fire tests. Although the results were not as consistent as hoped the results did compare relatively well with literature values for similar materials. The flame spread factor was defined as

representative of the available flame energy and applies solely to opposed-flow flame spread. The resulting findings from this work indicate that the parameters such as ignition temperature; thermal inertia; and the flame spread constant can be used in mathematical models to predict the performance of materials. The results found in this paper will be compared to the test results of the RIFT

4.3.2 Jianmin (1990) – "Prediction of Flame Spread Test Results From the Test Data of the Cone Calorimeter"

Jianmin (1990) presents a computational procedure to predict flame spread results by applying the LIFT method to data obtained from the Cone Calorimeter. The necessary input data for the model is the heat release rate at an irradiance level of 25kW/m² and a number of ignition times at various irradiance levels. These inputs were all obtained as outputs from the Cone Calorimeter tests.

The basic principles used in the model for prediction of the surface flame spread were as follows:

(a) In order for flame spread to occur the surface temperature is equal to the critical ignition temperature;
(b) Ignitability data is obtained from Cone Calorimeter tests, the thermal inertia properties, $k\rho c$ and critical ignitability temperature can be obtained from the results;
(c) The irradiance can be divided into two parts: external irradiance generated by radiation panel and irradiance generated by the flame from the sample; and
(d) The heat losses are accounted for due to lateral convection of air at ambient temperature.

4.3.3 Nisted, (1991), - "Flame Spread Experiments in Bench Scale, Project 5 of the EUREFIC Fire Research program"

Nisted's report represents a section of the work carried out by the Nordic research program "EUREFIC" European Reaction to Fire Classification. The aim of the project was to use and develop models to test flame spread over both thermally thick and thin materials. The report describes tests performed using the LIFT apparatus. The results obtained were then used in fire modelling. This report only details the analysis of the LIFT experiments and does not mention anything regarding what types of fire models the data was used for.

This work was part of the EUREFIC program and the other projects included:

1. Inter-laboratory calibration and repeatability of the Cone Calorimeter, ISO/DP 5660;
2. Inter-laboratory calibration and repeatability of the room/corner test NT Fire025, ISO/DP 9705;
3. Test in larger scale than NT Fire 025 and sensitivity analysis of the method;
4. Model for prediction of the fire growth in the room/corner test based on results from the Cone Calorimeter;
5. Models for flame spread and application of test data;
6. Correlation of test results with existing Nordic test methods;
7. Correlation of test results with other European test methods;
8. Preparation of a new classification system for surface products based on room/corner test and the Cone Calorimeter;
9. The effects of the new classification system on products and building costs; and
10. Coordination and information about Nordic research program.

Eleven materials were examined in the EUREFIC program. The results of the tests were calculated from the test data with a computer program provided by the National Institute for Standards and Technology (NIST). The results presented in the paper had been carried out as part of "Project 5 - Models for flame spread and application of

test data". This provides a good source of LIFT data in which results can be compared with.

4.3.4 Babrauskas/Wetterlund (1999) - "Comparative Data from LIFT and Cone Calorimeter Tests on 6 Products, Including Flame Flux Measurements"

This study by Babrauskas and Wetterlund (1999) was commissioned by the SP Swedish National Testing and Research Institute. This research examined how to predict opposed flow flame spread using Cone Calorimeter data. A lack of study in this area was highlighted in an earlier report by Babrauskas (1995), which comprised a literature survey to determine what was known about actual flame fluxes in the opposed flow flame spread geometry. The study revealed that very few studies could be found and none related to the LIFT geometry.

Babrauskas and Wetterlund discuss how the flame spread process is driven by the net heat flux to the specimen surface which included the flux from the flame itself. The flame flux is important as it is a major part of the driving force causing flame spread to occur. The literature review carried out by the authors showed that their existed very little studies where data on such flame fluxes could be obtained.

The work presented in this paper is summarised by the following:

(a) To provide set of detailed measurements of flame flux in the LIFT test
(b) Develops a small database of beach mark quality data for identical materials tested in the Cone Calorimeter and in the LIFT test; and
(c) Explores in detail the protocol of ASTM E 1321 – 90 and determines whether experiments can be performed in a controlled and routine manner.

4.3.5 Azhakesan (1998) – "Ignition and Opposed Flow Flame Spread Using a Reduced Scale Attachment to the Cone Calorimeter"

The work done by Azhakesan, Shields and Silcock (1998) at Fire SERT at the University of Ulster examines flame spread using a reduced scale ignition and flame spread technique (RIFT) incorporating the use of the Cone Calorimeter. Unlike some studies of experimental research that has been undertaken in the past, this work was carried out in an attempt to replicate LIFT experiments by using the Cone Calorimeter and applying the theory as detailed by Quintiere . It was found that the Cone Calorimeter allowed simultaneous measurements of ignition, flame propagation rate and mass loss rate. The data deduced from using the modified Cone Calorimeter and the parameters derived with reference to the existing theories of ignition and flame spread highlighted the correlational nature of the model. The results and analysis are presented in full in this paper by Azhakesan. The parameters derived using the RIFT compared favourably with those obtained using the standard LIFT apparatus.

It is from this experimental approach that this report and the experiments undertaken have been based upon.

4.4 Mathematical Fire Models

Many mathematical models have been studied in an attempt to model the opposed flow flame spread mechanisms. Such attempts have included numerical simulations which are characterised by trying to include as many features of the problem as possible. Numerical models are highly dependant on the input, therefore they tend to make these types of models very specialised, and Wichman (1992) has observed that "they make them good simulations but not good models". What that means is that numerical models simulate or mimic a particular scenario well however if a parameter or condition changes the numerical model can not adapt because it is too restrained. The other type of model is the simplified analytical models, which generally make poor simulations as they tend to generalise the problem. The analytical model accounts for the general parameters and conditions which means that it will not mimic

a specific scenario well because it is lacking the finer details however, any changes that may occur the model will be able to adapt and still provide an output.

Wichman (1992) has said that the development of a model is not necessarily to produce agreement with experiments or to simulate reality but rather to probe aspects of the problem by deriving formulas or improving theorems.

The following summaries are only but a couple of the models and types of work that have been undertaken in this field of study.

4.4.1 Ahmed Et Al (1994), "Calculating Flame Spread on Horizontal and Vertical Surfaces"

This paper examines a flame spread model which is an algorithm. It provides the capability to calculate a self consistent fire, based substantially on bench scale fire data. The model simulates object fire growth and burnout of a slab in a room. This algorithm produces an acceptable prediction of the spread of fire, smoke and toxic and non-toxic gases generation. The algorithm is based on data gathered from standard test apparatus, including the Cone Calorimeter and the LIFT.

An analytical tool such as this has the potential to reduce the number of full scale tests required and for providing the fire protection community with improved predictive capability for fire hazards, particularly evaluating new material in new environments.

4.4.2 Chen, Y et al (1998), - "A Prediction of Horizontal Flame Spread Using a Theoretical and Experimental Approach"

This paper discusses a new methodology that has been developed to obtain properties that characterise creeping flame spread. Creeping flame spread is another term used for opposed-flow flame spread as it is the aspect of flame spread that is against the air flow. Opposed-flow flame spread includes vertically downward, lateral and horizontal flame spread. Horizontal flame spread is faster than downward or lateral

flame spread because the fuel surface can receive significantly more radiation from its flame in horizontal position than in other orientations.

In this paper a general creeping flame spread relationship is discussed. Improvements to the relationship are accounted for by considering material thicknesses and allowing for varying external heat flux which includes the flame's irradiance.

The work presented by Chen et al is based on a new experimental methodology where some of the experimental uncertainties have been reduced. The experiment involves a constant speed horizontal flame spread (CSHFS) apparatus. Tests have shown that creeping flame spread properties are described by two parameters, the gaseous thermal convective length and the convective flame energy flux.

4.5 Literature Review Summary

The works briefly summarised above are only a fraction of the work that has been conducted in this field. The field of flame spread and ignitability encompasses such a wide range of factors that numerous studies have been undertaken. Others aspects of flame spread that have been studied includes:

- Charring over solids as studied by Atreya (1986) where the application of opposed flow flame spread was applied.
- Microgravity models as studied by Olsen (1987, 1991) at NASA where the conditions of negligible gravity were examined.
- Ignitability studies include those by Kanury (2002) which gives an overview of the criteria for ignition.
- The factors that contribute to ignition have been examined extensively and such studies include work by Atreya et al (1986) and Spearpoint et al (2000) who have looked at factors such as sample orientation and grain orientation at various heat flux levels.
- The irradiance studies that examine the configuration/view factors are catered for in books by Howell (1982), Siegel and Howell (1992) and Rohsenow, Hartnett and Choi (1998).

5 Theory Applied to LIFT Experiments

5.1 Flame Spread Theory

The opposed flow flame spread model was developed by Quintiere (1981) and is applied to derived material properties form the LIFT experiment. The subsequent work in this area has relied on the principle that the flame spread front exists at a position x_f, provided that the surface temperature, Ts arising from the imposed irradiance reaches the piloted ignition temperature, T_{ig}. Flame spread has been described by Drysdale (2000) as a continuous series of piloted ignitions occurring at the flame's leading edge. The model developed by Quintiere et al (1981, 1983, and 1985) is presented in Figure 10, the model takes into account the following considerations:

- One-dimensional unsteady state heat conduction occurs in the solid and is perpendicular to the surface;
- The position of the flame front is identified by x_f where the surface temperature has reached the ignition temperature, T_{ig};
- The external radiant heating flux, $\dot{q}_e^{"}$ depends on the position of the surface in relation to the radiant heat source and the time the surface reaches thermal equilibrium or ignition temperature and
- The heat transfer ahead of the pyrolysis front is considered to occur over a region, δ_f with a uniform heat flux of $\dot{q}_f^{"}$ which is independent of $\dot{q}_e^{"}$.

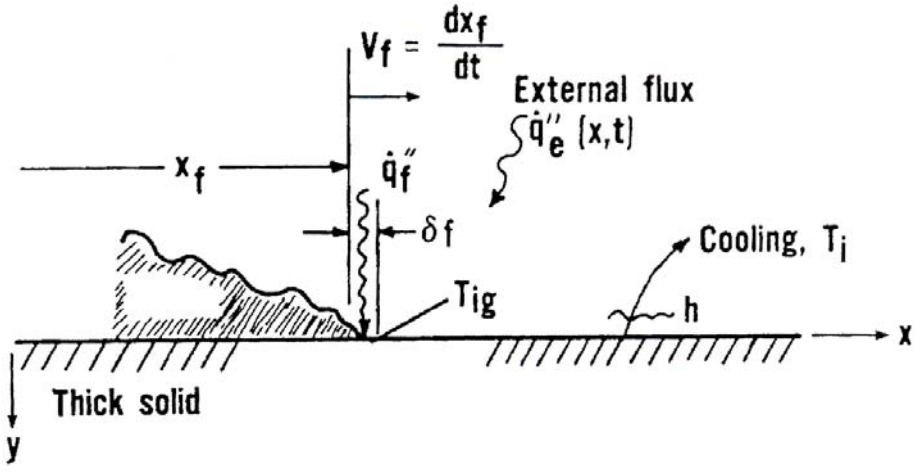

Figure 10 Components of Flame Spread Model – Reproduced from Quintiere (1981)

The flame heating distance, δ_f is assumed to be consistent with downward or lateral flame spread on a vertical wall. The model asserts that the flame front exists at $x = x_f$ provided the temperature of the surface has attained T_{ig}.

The rise in the surface temperature, ΔT to the ignition temperature must be equal to the flame heating. The rise in surface temperature is due to heating from the external source and can be expressed as:

$$T_{ig} - T_i = \Delta T_f + \Delta T_e \text{ at } x_f \quad \textbf{(1)}$$

The rise in temperature due to external radiant heating is given in the paper by Quintiere (1981) as:

$$\Delta T_e = T_s - T_i = \dot{q}_e''(x_f)[1 - \exp(at)\, erfc\sqrt{at}]/h \quad \textbf{(2)}$$

Equation 2 is for an infinitely thick solid, this is also known as a thermally thick solid. For thermally thick solids the heat loss is considered a linear approximation as detailed in Quintiere et al (1981, 1983, and 1985). In equation 2, h is a linearised convective heat transfer coefficient and $a = h^2 / k\rho c$. Equation 2 represents the time variation of the surface temperature while the temperature variation into the solid (y-direction) depends on time as well.

The theory described by Quintiere et al (1981, 1983, and 1985) goes on to explain that as the flame front approaches a region that has been heated by $\dot{q}_e''$, the surface temperature and its gradient in the solid will change with time. The flame then heats the region δ_f and it is assumed that the heating of the flame only affects the solid to a depth of $\Delta \approx \sqrt{\frac{kt}{\rho c}}$ and that the surface temperature, T_s is uniform over the depth Δ.

By applying an energy balance over the control volume, $\delta_f \times \Delta \times 1$,

where δf is the flame heating distance *(x-axis)*;

Δ is the depth of the solid *(y-axis)*; and

1 is to account for the unit width *(z-axis)*.

the flame front equation yields:

$$\rho c \Delta V_f (T_{ig} - T_s) \approx \dot{q}''_f \delta_f \tag{3}$$

Where V_f is the velocity relative to the control volume. This is also known as the flame spread velocity and is defined as:

$$V_f = \delta_f / \varepsilon = dx_f / dt \tag{4}$$

Where ε is the time for the flame to move a distance δ_f.

Equation 3 is a simplification of the process that is taking place in opposed flow flame spread, as heat losses have been ignored. The work by Quintiere et al (1981, 1983, and 1985) has revealed that serious errors can occur by ignoring these heat losses only when V_f is small. By substituting Δ and combining Equation 3 and Equation 4, this provides:

$$\Delta T_f = T_{ig} - T_s = \frac{\dot{q}''_f \sqrt{\delta_f} / \sqrt{k\rho c}}{\sqrt{V_f}} \tag{5}$$

Equation 5 is more consistent with solutions for surface flame spread as found in the early work by de Ris (1969). A more complete solution for flame spread velocity may be derived from Equations 1, 2 and 5 and is given by:

$$T_{if} - T_i = \left[\frac{\dot{q}''_f \sqrt{\delta_f}}{\sqrt{k\rho c}} \right] V_f^{-1/2} + \dot{q}''_e x_f [1 - \exp(at)\, erfc \sqrt{at}\,] / h \tag{6}$$

or

$$V_f^{-1/2} = C[h(T_{ig} - T_i) - \dot{q}''_e x_f F(t)] \tag{7}$$

Where $C = 1/\dot{q}''_f \sqrt{a\delta_f}$, is the flame heat transfer modulus and $F(t) = 1 - \exp(at)\, erfc \sqrt{at}$.

5.2 Ignition Theory

Similarly the theory behind ignition using the LIFT apparatus can be formulated along the same lines as the flame spread theory. An ignition relationship can be derived from Equation 2 by setting the surface temperature, T_s equal to the ignition temperature, T_{ig}. The results should be consistent with flame spread result as flame spread is considered a continuous series of piloted ignitions, Drysdale (2000). Accordingly the ignition temperature reached should be consistent with the flame spread correlation, regardless if it is derived from ignition tests or flame spread tests. It follows that from Equation 2 and Equation 7, ignition is governed by:

$$h(T_{ig} - T_i) - \dot{q}_e^{"} F(t) \qquad \textbf{(8)}$$

Since $F(t) \to 1 \; as \; t \to \infty$, the minimum radiative heat flux for piloted ignition is given as:

$$\dot{q}_{o,ig}^{"} = h(T_{ig} - T_i) \qquad \textbf{(9)}$$

The ignition temperature, T_{ig} can be found from a critical ignition irradiance at an arbitrarily defined heating time. Equation 9 can also be rewritten as a heat balance at the specimen's surface which defines $\dot{q}_{crit}^{"}$ as:

$$\dot{q}_{crit}^{"} = h_{ig}(T_{ig} - T_0) \qquad \textbf{(10)}$$

Azhakesan et al (1998) identified that the $\dot{q}_{crit}^{"}$ value was obtained from cone ignition data after a nominal exposure period of 20 minutes. The equation used to obtain the temperature rise from the initial surface temperature to the ignition temperature for a thermally thick solid subject to a constant irradiance with no heat losses from the surface is given by:

$$T_{if} - T_0 = 2\dot{q}_e^{"} \sqrt{t_{ig} / \pi k \rho c} \qquad \textbf{(11)}$$

Whereby:

$$\frac{1}{\sqrt{t_{ig}}} = m\dot{q}_e'' + const. \tag{12}$$

A plot of $1/\sqrt{t_{ig}}$ *versus* $\dot{q}_e''$ will yield an x-intercept of $\dot{q}_{crit}''$ which represents the heat flux corresponding to an infinite ignition time, t_{ig}. Following from the ignition correlation for flame spread, Equation 7 can be rewritten as:

$$V_f^{-1/2} = C[\dot{q}_{crit}'' - \dot{q}_e''(x) \cdot F(t)] \tag{13}$$

Where the ignition temperature, T_{ig} for a thermally thick solid at sustained ignition is given by:

$$T_{ig} = T_0 + \frac{\dot{q}_e''}{h_{ig}} F(t_{ig}) \tag{14}$$

The function $F(t_{ig})$ can be approximated by following the varying preheating times, up to a threshold equilibrium heating time, t^* at exposed irradiances. When $V_f \to \infty$ at sustained ignition, Equation 13 becomes:

$$\frac{\dot{q}_{crit}''}{\dot{q}_e''} = F(t_{ig}) = b\sqrt{t} \quad for \quad t \le t^* \tag{15}$$

$$\frac{\dot{q}_{crit}''}{\dot{q}_e''} = F(t_{ig}) = 1\sqrt{t} \quad for \quad t > t^* \tag{16}$$

where the slope $b = 2h_{ig} / \sqrt{\pi k \rho c}$, as derived by Quintiere et al (1983). The function $F(t_{ig})$ can be applied to flame spread data provided the surface temperature is less than T_{ig}. The ratio of $\dot{q}_{crit}'' / \dot{q}_e''$ can be viewed as the rate at which the surface temperature approaches its steady state value at the specified irradiance, Azhakesan et al (1998).

Thermally non-equilibrium flame spread conditions can be analysed with reference to Equation 13 and by plotting $\dot{q}_{crit}'' / \dot{q}_e''$ *versus* $\sqrt{t_{ig}}$ to obtain values for *b* and hence the values of *F(t)* from Equation 13.

Quintiere (1981) has also suggested the use of thermally thick flame spread correlations as proposed by de Ris (1969) as a frame-work for generalising Equation 13 to accommodate the variety of different materials examined.

By utilising Equations 10, 11, 13, 15 and de Ris's result, the flame spread velocity can be shown that:

$$V_f = 4\dot{q}_f^{1/2}\Delta / \pi k\rho c[1/(T_{ig} - T_s)]^2 \qquad \textbf{(17)}$$

or the equation can be rewritten as:

$$V_f = \frac{\phi}{k\rho c}\left[\frac{1}{\left(T_{ig} - T_s\right)^2}\right] \qquad \textbf{(18)}$$

Where $\phi = \frac{4}{\pi}\dot{q}_f^{"}\Delta = \frac{4}{\pi(Cb)^2}$

The parameter ϕ represents the composite influences of the environment, including the available flame energy, for opposed flow flame spread. By plotting the measured flame spread velocities, $V_f^{-1/2}(x)$ *versus* $\dot{q}_e^{"}(x)\cdot F(t)$, the slope C and the y-intercept $\dot{q}_{crit}^{"}$ can be determined. Using this approach an apparent thermal inertia, $k\rho c$ may be obtained from the slope since, $b = 2h_{ig}/\sqrt{\pi k\rho c}$, provided that h_{ig} is known. The linear slope crosses at $\dot{q}_{crit}^{"}/\dot{q}_e^{"} = 1$, the time needed for the surface of the material to reach thermally equilibrated conditions. The asymptote on the plot at large values of $V_f^{-1/2}(x)$ provides the lower irradiance bound for opposed flow flame spread, $\dot{q}_{0,s}^{"}$

The parameters that arise in the equations can be determined experimentally. The parameters have been identified as being dependent on the materials and on the conditions of flame spread. In opposed flow flame spread, the flow velocity induced by a developing fire should be relatively small and fairly constant, hence the parameters of C and h should not vary significantly. The parameter C depends on the opposed flow velocity and on the ambient oxygen concentration. Quintiere et al (1983) has shown that h is fairly constant under certain circumstances of natural convection.

5.3 The Schmidt-Boelter gauge

An objective of this work is to map the irradiance profile along the length of the sample. In this section a brief description of how the Schmidt – Boelter Gauge works is given, however for a thorough discussion and description of the gauge refer to the report published by Kidd and Nelson (1995). A number of testing facilities have presented work with respect to the calibration of high heat flux sensors. Papers that have been published include Murthy et al (1997) and Persson and Wetterlund (1997).

The Schmidt – Boelter gauge is one version of a proven heat flux measurement tool that uses the axial temperature gradient method. The gauge has been around since the 1950s and has gained wide acceptance because the transducer provides a high level, self generating output signal directly proportional to the heat flux incident at the surface. The general principle of operation of the gauge can be divided into two distinct categories: the thermal and thermoelectric functions. The thermal response of the gauge can be approximated by simple steady state equations. There are a number of different materials used in the construction of the gauge as shown in Figure 11. The transient temperature and heat conduction through the gauge can be more accurately characterised if finite element thermal analysis techniques are used. The thermoelectric characteristics define how the thermopile differential thermocouples measure the temperature difference between parallel planes. The analysis presented in the paper by Kidd and Nelson (1995) shows that the results are consistent with principles of thermoelectric thermometry as detailed in the ASTM "Manual on the Use of Thermocouples in Temperature Measurement".

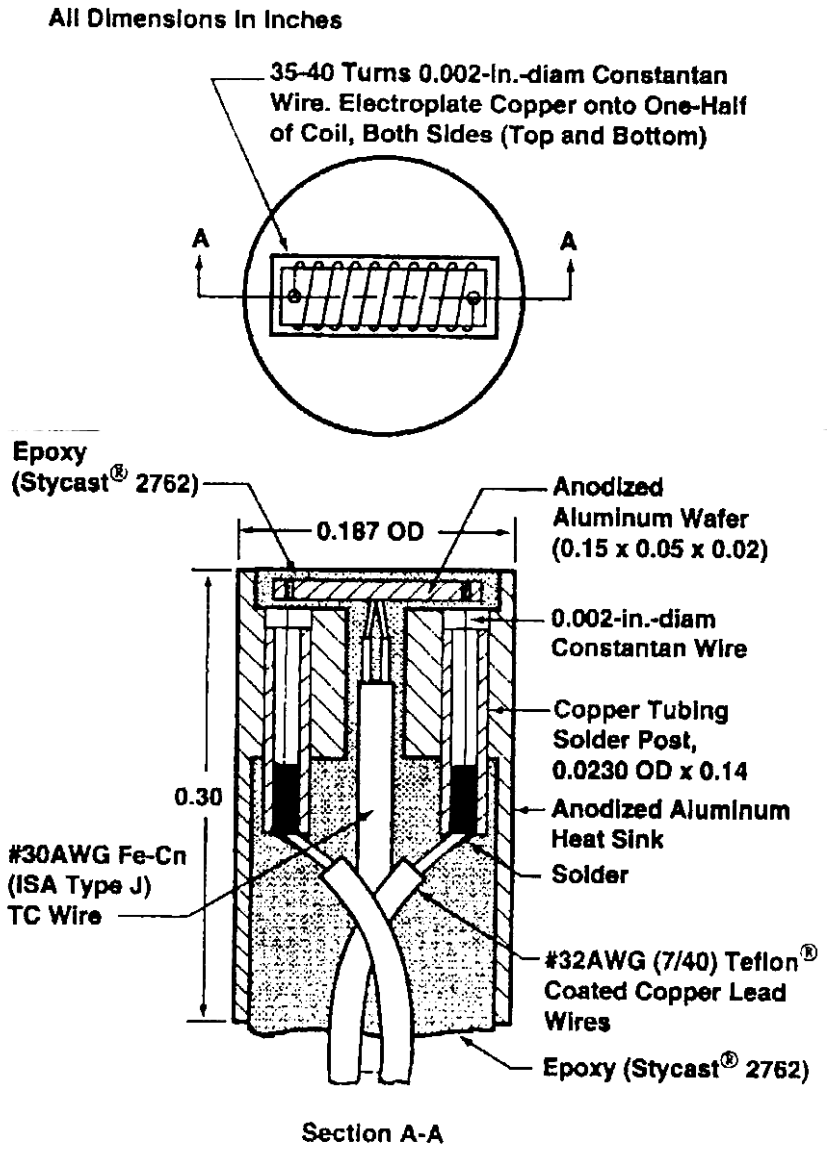

Figure 11 Cross-section of Heat Flux gauge – Reproduced from Kidd and Nelson, 1995

The radial temperature distribution of the Schmidt-Boelter gauge is shown in Figure 12. The family of curves as shown in the figure represents the temperature distribution between parallel plans at several axial locations. The sensitivity of the gauge is dependent on the epoxy thickness. The epoxy layer is found to be not very sensitive to small changes in thickness.

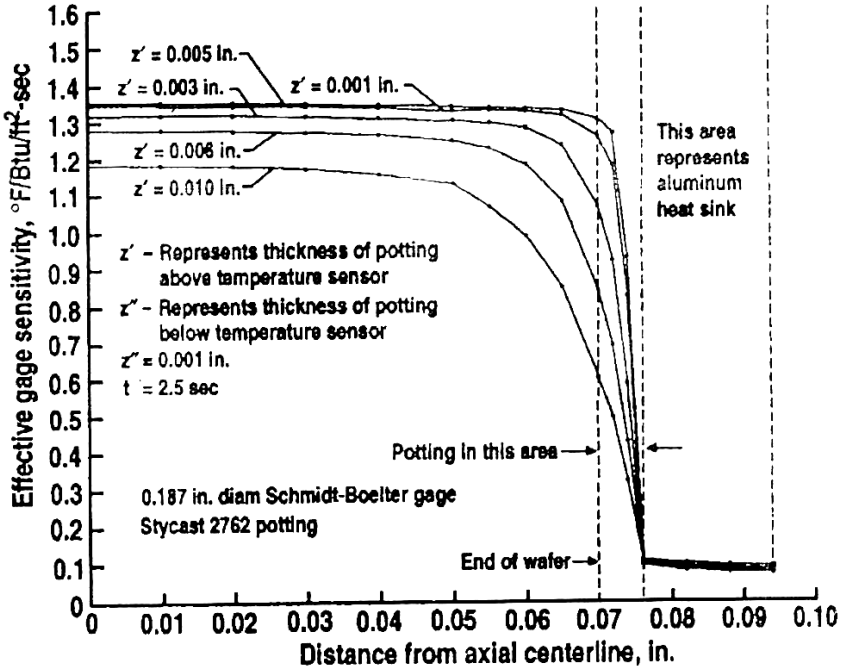

Figure 12 Thermal Analysis Range of the Heat Flux Gauge

Reproduced from Kidd and Nelson 1995

The time response of the Schmidt-Boelter gauge can be deduced from the same data set as the heat flux sensitivity analysis. The results of time response are illustrated in Figure 13. The curves show that in order to achieve a fast time response, the thickness of the protective layer over the temperature needs to be minimal.

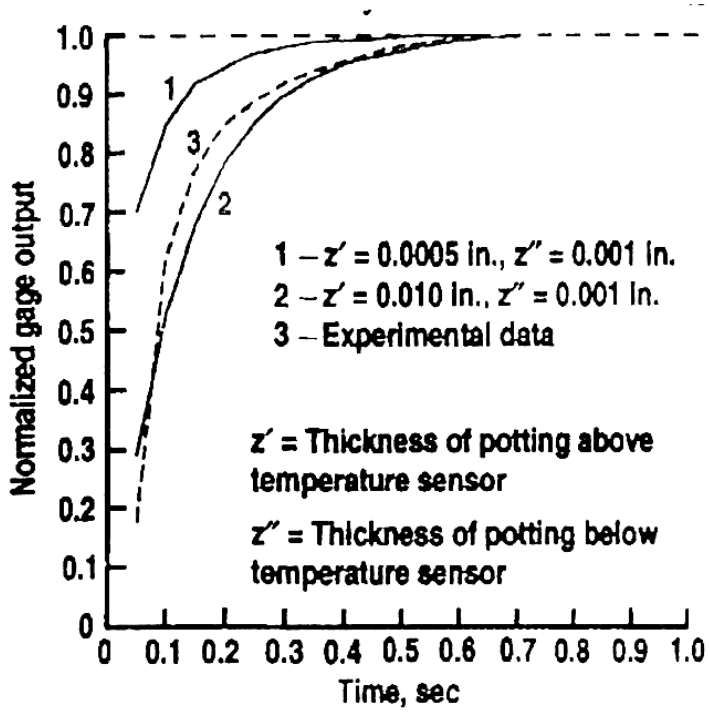

Figure 13 Time response of the Heat Flux Gauge – Reproduced from Kidd and Nelson, 1995

6 Experimental Design

This work is divided into two categories. Firstly the heat flux profile was examined by mapping the irradiance and applying view factors to estimate the irradiance profile along the length of the sample. The second category was the flame spread test themselves. Before flame spread tests can be conducted certain parameters are required which are obtained from ignition tests, these parameters were obtained from Ngu (2001). Where no data existed ignition tests were performed, in this instance namely for the particle board and the laminated veneer lumber.

6.1 Materials

The choice of wood type was based on previous work by Ngu (2001) at Canterbury University who looked at the various ignition correlations of New Zealand timbers. For cohesion between studies and the limited laboratory time available to conduct tests, the Ngu (2001) study was used in conjunction with this study of flame spread. Particle Board and LVL were not part of the Ngu study and therefore ignition experiments were conducted.

The flame spread tests were conducted on eight different wood types, these being:

- Radiata Pine;
- Rimu;
- Beech;
- Macrocarpa;
- Medium Density Fibre Board;
- Plywood;
- Particle Board; and
- Laminated Veneer Lumber.

6.2 Heat Flux Profile – Template

The irradiance exposure along the length of the sample was measured using a template. The template was constructed out of refractory brick and was cut to fit the specimen holder that was constructed as part of the reduced scale ignition and flame spread technique (RIFT). The nature of the refractory brick meant that a limited number of sampling holes could be drilled without the material breaking up. A configuration that would allow the greatest number of data points and utilised as much space as possible was chosen. The configuration used is shown in Figure 14. The numbering used to identify each sample hole is also illustrated in Figure 14, this numbering system is referred to throughout the experiments. The template was placed into the sample holder with sample holes 1 and 2 placed at the hot end, closest to the cone. Measurement of the heat flux involved holding the heat flux meter in each sampling point over a 30 second period where heat flux readings were recorded. The average heat flux value was then used for the remainder of this work.

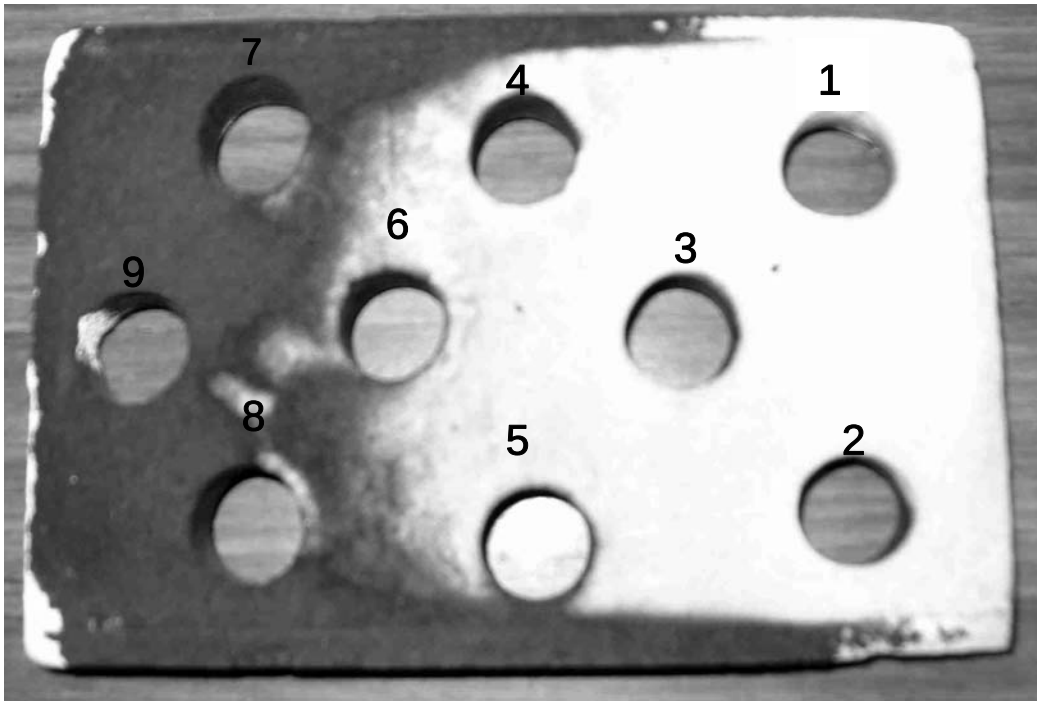

Figure 14 Template Used to Map Irradiance

6.3 Heat Flux Profile – Procedure

The Cone Calorimeter was heated to the required temperature. Once heated the Cone Calorimeter was allowed to stabilise for at least five minutes to ensure steady state was reached before experimental runs would begin. The guiding arm was then placed at the required angle and was fastened using a screw located in the guiding arm and a G-clamp. At the end of each run the angle was checked before the next test, to ensure the angle for each run was correct. The angles tested were 40°, 60° and 80°. The results of these tests were checked against the previous work of Pease (2001) and Perrin (2002) carried out at the University of Newcastle to ensure that continuity was maintained. The heat flux meter utilises an algorithm which automatically calculates the radiation over the end of the heat flux meter. The irradiance measurement is found by taking the difference in temperature of the water stream when it passes through the area exposed to the radiation source. The readings given by the computer software is the net radiation experienced at the surface of the template, which accounts for the radiative and convective components.

The heat flux settings were taken across a range which is considered "typical" in a house fire and therefore considered applicable in flame spread testing. The heat flux settings conducted were at 40kW/m², 50kW/m² and 60kW/m² at 25mm from the face of the cone. At these heat flux settings the surface of the cone were approximately 707°C, 770°C and 825°C respectively. The heat flux gauge was placed in the sampling holes and the readings were taken over 30 second intervals. This was repeated at each of the sampling points 1-9. The figure below illustrates how the heat flux meter was placed in the template in order to allow the irradiance to be measured.

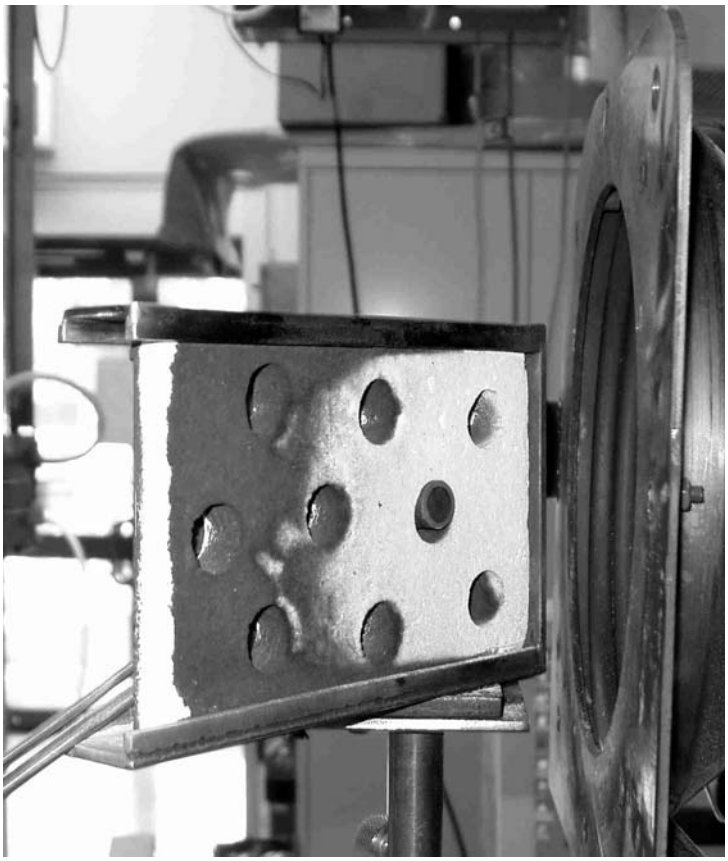

Figure 15 Heat Flux Measurements

6.3 Ignition Experiments

Ignition experiments were conducted using the Cone Calorimeter in the standard horizontal position. The experimental setup is as shown in Figure 16. The ignition samples were preconditioned as detailed in ISO 5660. The wood samples were placed in a controlled environment room of 23°C at 50% humidity. The samples tested were 100mm long by 100mm wide and 20mm thick. The pilot spark ignitor was located 13mm from the surface as defined by experimental protocol, ASTM E 1354. Each wood type was tested at four different heat fluxes and each test was repeated three times to check for repeatability. The irradiances tested were 20kW/m², 30kW/m², 35kW/m², and 40kW/m².

Figure 16 Experimental Setup of Ignition Tests

The test samples were subjected to a constant irradiance from the cone heater set to a fixed temperature. The testing of the sample was started when the cone had reached the desired temperature and had reached steady state. Firstly the irradiance at the surface, prior to adding the sample, was measured using a Schmitt-Boelter water cooled flux meter at 25mm from the surface of the cone heater. The time to piloted ignition was recorded from the time each sample was exposed, this was when the heat shield was removed, exposing the sample to the cone heater.

6.4 Flame Spread Experiments

The samples for the flame spread tests were held in a frame as depicted in Figure 17. The cone is in the vertical orientation and the sample's frame can be positioned at various angles. The wood samples were 250mm long, 90mm wide and about 20mm thick. The samples were backed by a non-combustible board, in this instance Calcium Silicate, $CaSiO_3$ was used. The board was approximately 10-12mm thick and slid in behind the sample. The purpose of the board is to satisfy the assumption of no heat loss through the specimen and in the process be said to be "thermally" thick

as prescribed in the standard. The design of the frame was such that the sample could be swivelled at various angles to the cone heater. A gas piloted flame ignitor was used. The flame was approximately 10mm long, and was located 5mm away from the sample face at the hot end of the sample. This differed from the ignitability test where a spark piloted lighter was used in the horizontal configuration. A schematic diagram illustrating the experimental apparatus is shown in Figure 18.

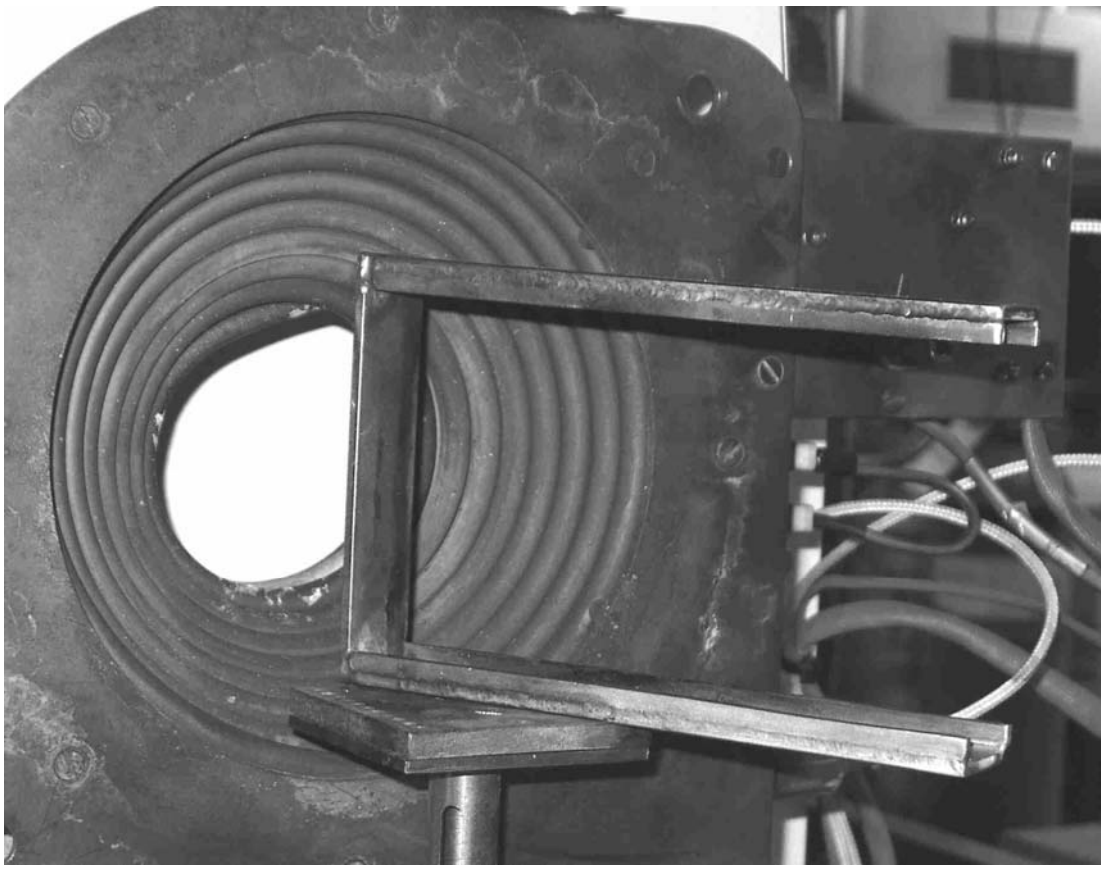

Figure 17 View of Sample Holder - Flame Spread Tests

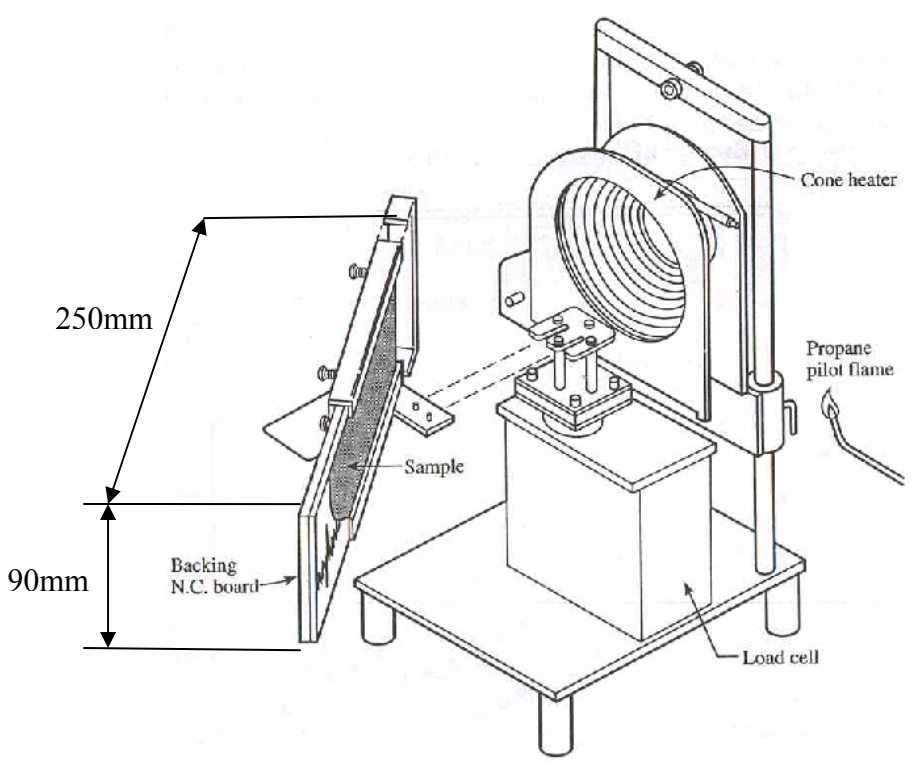

Figure 18 Reduced Scale Ignition and Flame Spread Attachment (RIFT)
Reproduced from Azhakesan et al (1998)

The irradiance gradient along the sample was determined using the template as shown in Figure 15. A video recording of the moving flame front position was taken in real time in order to derive the velocities. A picture of the experimental layout is shown in Figure 19. The position of the camera was perpendicular to the apparatus to give an unambiguous view of the flame front position. The location of the flame front was aided by lines drawn on the sample surface at 10mm intervals.

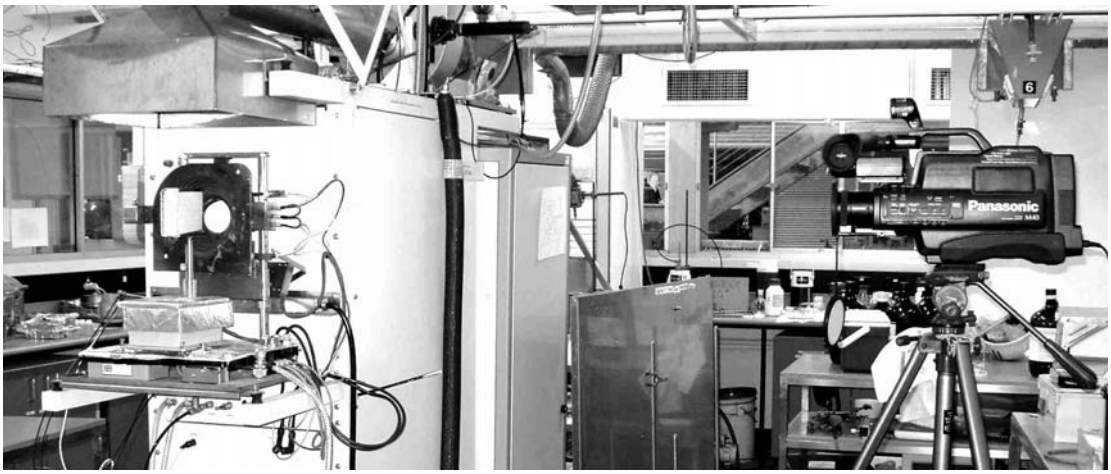

Figure 19 Experimental Setup - Flame Spread Tests

The specimen was allowed to preheat for the time t^* which is calculated from the ignition test data using Equation 15 and Equation 16. Once the specimen had reached the time, t^* a pilot flame was used to ignite the sample.

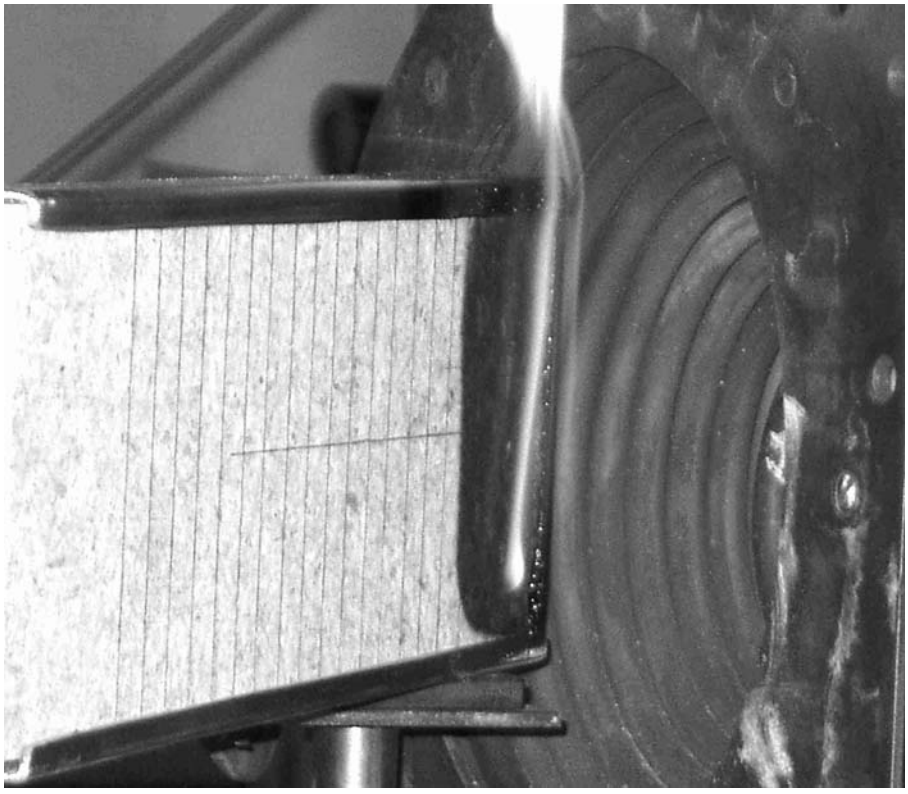

Figure 20 Close Up - Flame Spread Test

6.5 Flame Spread Data Analysis

As discussed earlier, flame spread can be categorised into two different classes; wind-aided flame spread and opposed flow flame spread. The conventional theory of wind aided flame spread requires only ignitability and heat release rate data which is readily available form the Cone Calorimeter. For opposed flow flame spread predictions, modellers have often used data from the LIFT test.

The LIFT apparatus can also be used to carry out radiant ignitability tests. The specimens used in these tests are 155mm long by 155mm wide. The resulting outputs are conceptually no different to the outputs from a Cone Calorimeter. However, in practise small variations will always be seen when different apparatus are used to measure any particular variable. In general it is considered that the Cone Calorimeter

and the LIFT ignition data are not much different for well behaved samples. The definition of well behaved samples are those that do not, buckle, greatly shrink, or show other problems while burning that might not perform similarly in the tests. These types of problems are more likely to be encountered for ignition tests, where for the LIFT testing the sample is in a vertical position compared with the Cone Calorimeter where the sample's orientation is horizontal.

The flame front velocity is calculated using the three point least squares fit to measure the flame front, where x is the position and *t* is the time.

$$V = \frac{\Sigma(tx) - \frac{\Sigma t \Sigma x}{3}}{\Sigma t^2 - \frac{(\Sigma t)^2}{3}} \qquad \textbf{(19)}$$

The surface flux configuration invariant, F(x) as defined in the ASTM 1321, is given by: $F(x) = \frac{\dot{q}_e^{"}(x)}{\dot{q}_e^{"}(crit)}$

Using this relationship the surface flux at a measured flame front position is given by:

$$\dot{q}_e^{"}(x) = F(x) \cdot \dot{q}_e^{"}(crit.) \qquad \textbf{(20)}$$

The flame spread data can then be shown as a plot of:

$$V^{-1/2} \ versus \ \dot{q}_e^{"}(x)F(t)$$

Where:

$$F(t) = \begin{cases} b\sqrt{t}, & t \le t^* \\ 1, & t \ge t^* \end{cases}$$

As a result from these plots the following outputs can be obtained:

- The minimum ignition surface flux, $q"_{0,ig}$
- The minimum ignition temperature, T_{ig}
- The minimum lateral spread flux, $q"_{0,s}$
- The minimum lateral spread temperature, $T_{s,min}$
- The thermal inertia value, $k\rho c$
- The flame spread parameter, C
- The flame heating parameter, Φ

7 Irradiance Mapping – Results and Discussion

The irradiance mapping was the first area of study, this examines the irradiance profile along the length of the sample. The irradiance was measured at the sampling location as detailed in section 6.3, and using this data the irradiance profile along the length of the sample can be examined and compared.

The irradiance profile was measured and compared with the typical irradiance profile of the LIFT apparatus. Comparisons were made at three different angles to determine which angle best matched the LIFT profile. The angles tested were 40°, 60° and 80°. The measurements were taken at three heat flux settings these were 40kW/m², 50kW/m² and 60kW/m². Plan views of the sample holder in relation to the face of the cone are illustrated in Figure 21, Figure 22 and Figure 23. These figures show that as the incident angle to the face of the cone increases the proportion of the sample directly exposed to the cone increases. In Figure 21 at 40° about 80mm of the sample is exposed to the cone, whereas in Figure 22 at 60° 120mm of the sample is exposed. Figure 23 shows that at 80° the sample is virtually vertical to the face of the cone and exposes the full length of the sample. However one would expect very little irradiance to the sample surface at 80° because at this angle the face of the sample is not directly exposed to the surface of the cone. The relative positions are marked on Figures 27, 28 and 29 where the dashed vertical line represent the proportion of the sample exposed to the radiant panel of the LIFT and the solid vertical line represents the proportion of the sample exposed to the cone heater of the RIFT. The measured data points were used as a comparison against an estimated irradiance profile, for the length of the sample, obtained from applying a view factor.

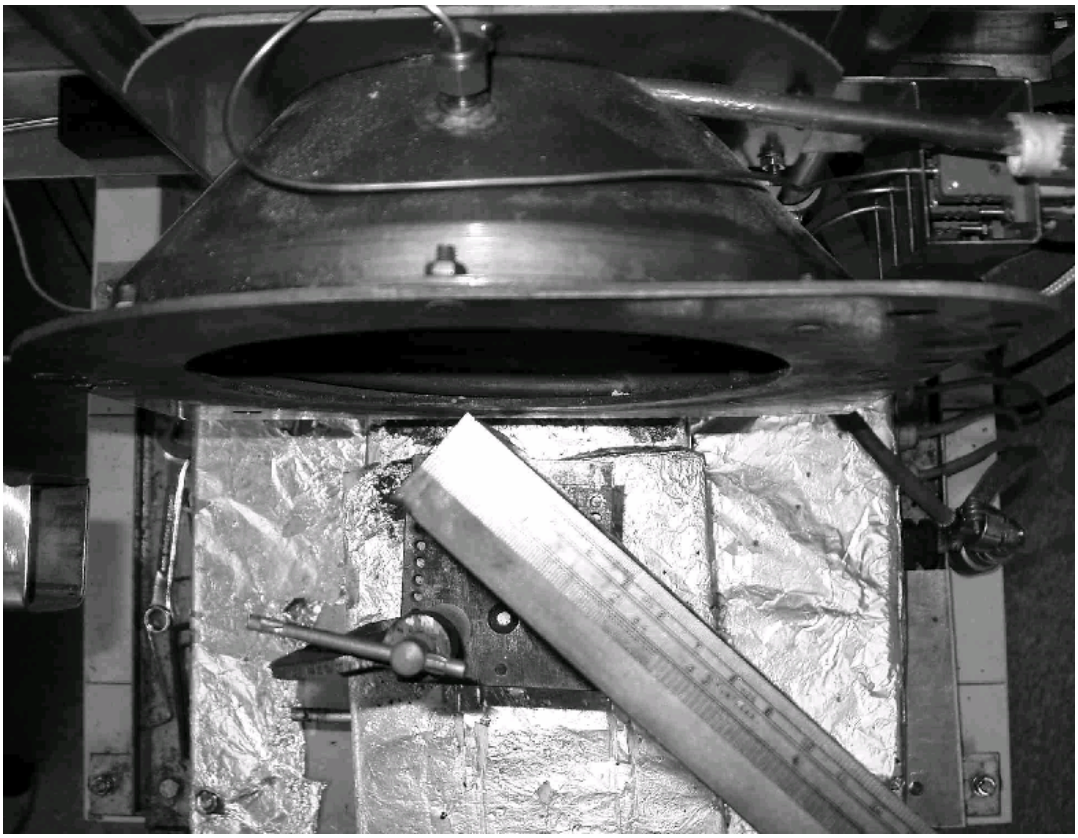

Figure 21 Sample holder at 40° to the face of the cone

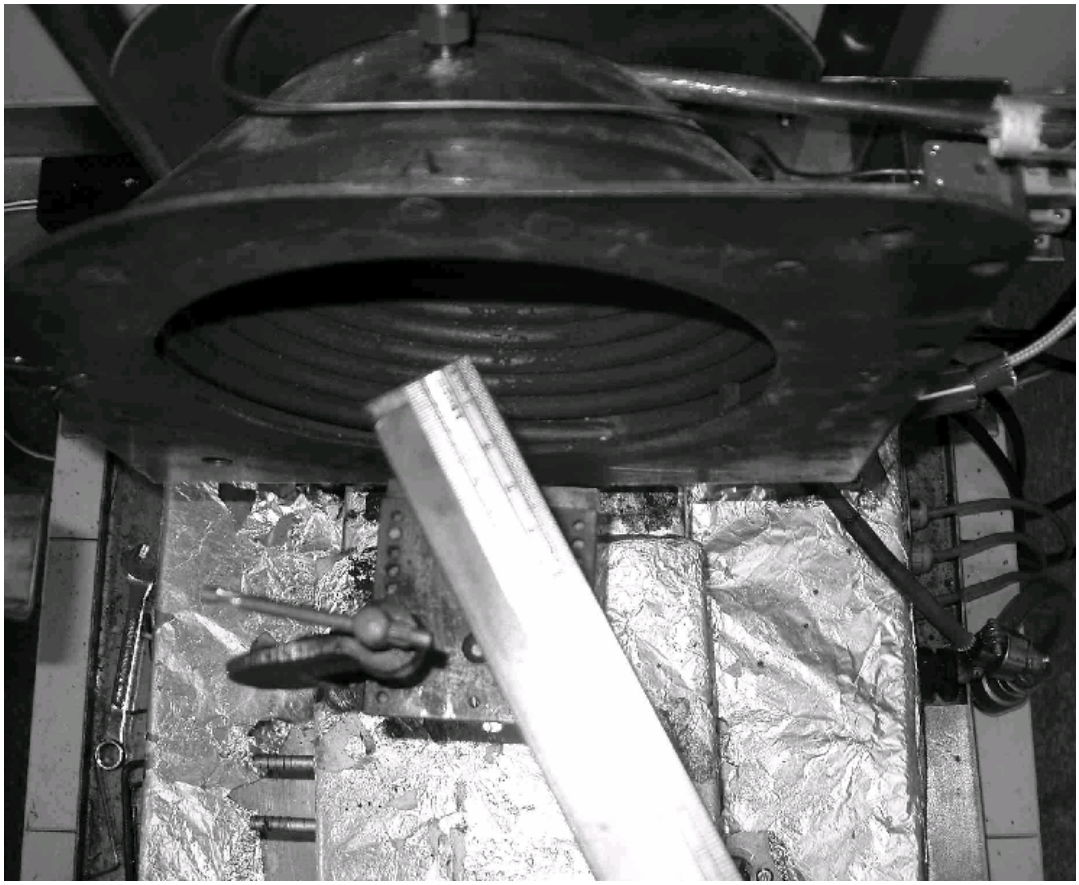

Figure 22 Sample holder at 60° to the face of the cone

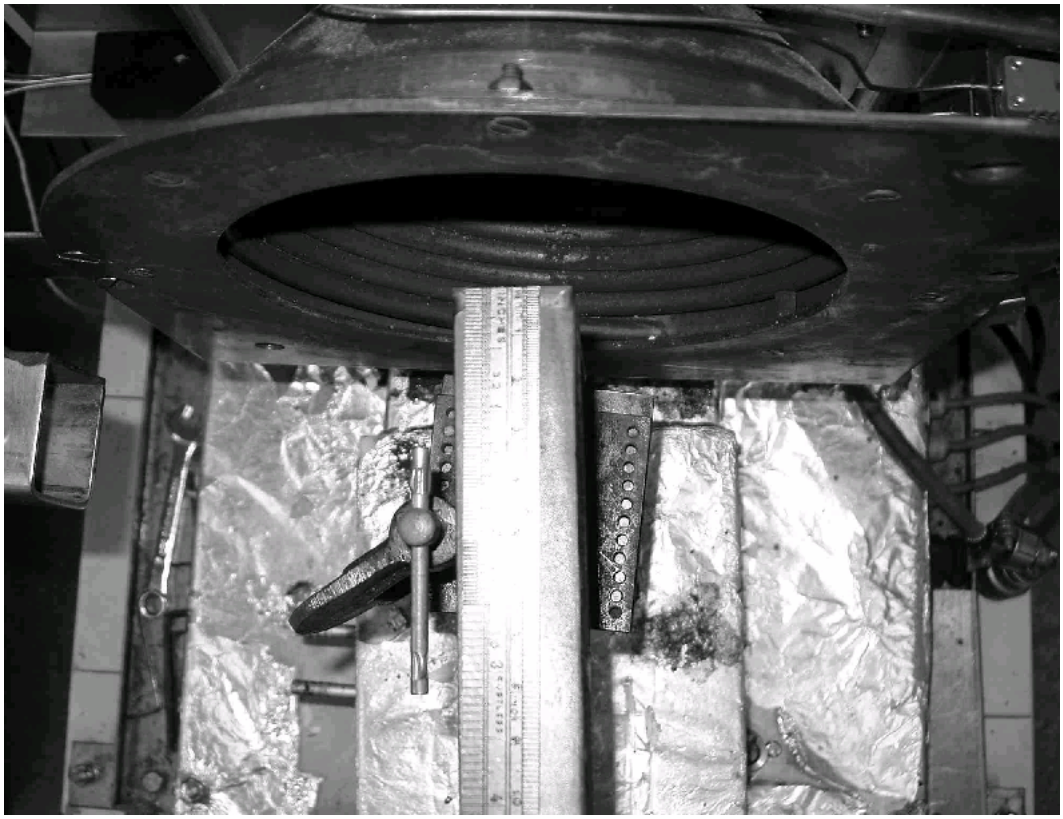

Figure 23 Sample holder at 80° to the face of the cone

7.1 Irradiance Profiles

Figure 24, Figure 25 and Figure 26 represent the irradiance profile along the length of the sample. Each plot represents a fixed irradiance, 40kW/m², 50kW/m² and 60kW/m², as measured by the heat flux gauge at 25mm from the cone surface and compared at three different angles. The graphs show that as the angle is increased the exposure of the irradiance on the sample decreases. At the lower angle (40°) the heat flux meter readings recorded the higher irradiances, as the angle was increased to 60° the irradiance values measured on the sample decreased by 37%. A further increase in the angle to 80° resulted in the irradiance readings decreasing by a further 32% of the value. The lowest measured heat flux was at sampling point 9, 120mm from the leading edge. At sampling point 9 the average irradiance measured was 3.5kW/m² within a range of 2.15kW/m² to 5.7kW/m². In all three profiles, a steeper gradient can be observed up to sampling position 5, 65mm, this observation was consistent for all tests independent of the angle or applied heat flux. After sampling position 5 the

gradients are much shallower. This pattern can easily be seen in Figure 27, Figure 28, and Figure 29.

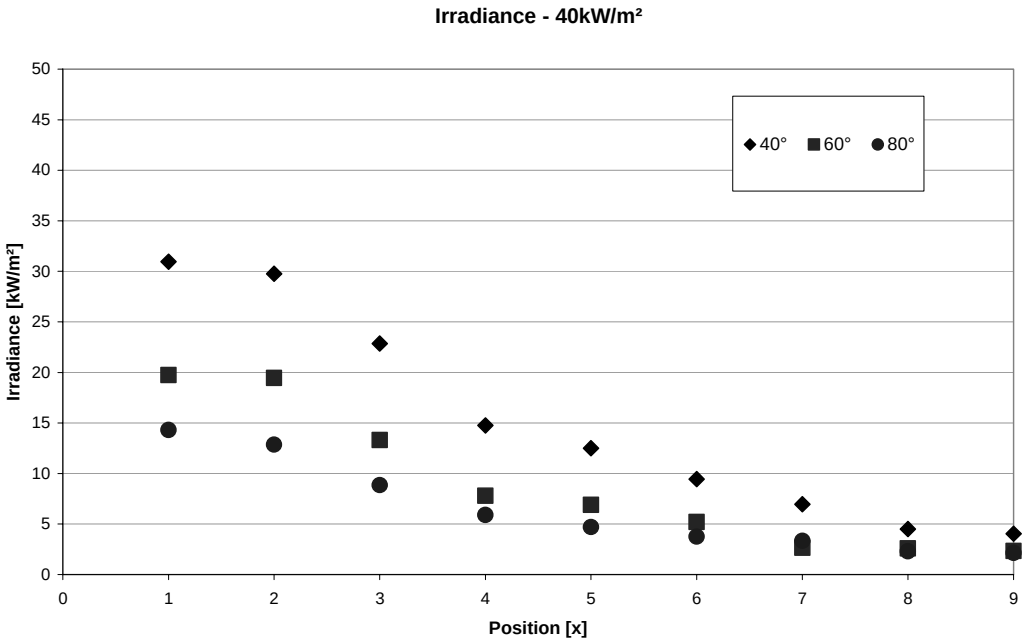

Figure 24 Irradiance Profile along Sample at Heat Flux of 40kW/m²

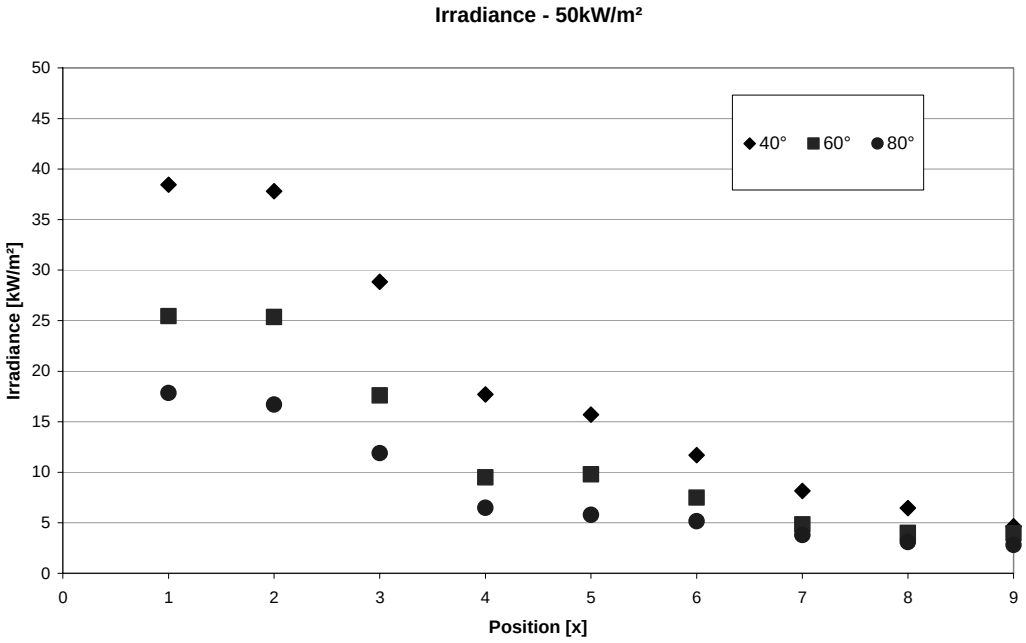

Figure 25 Irradiance Profile along Sample at Heat Flux of 50kW/m²

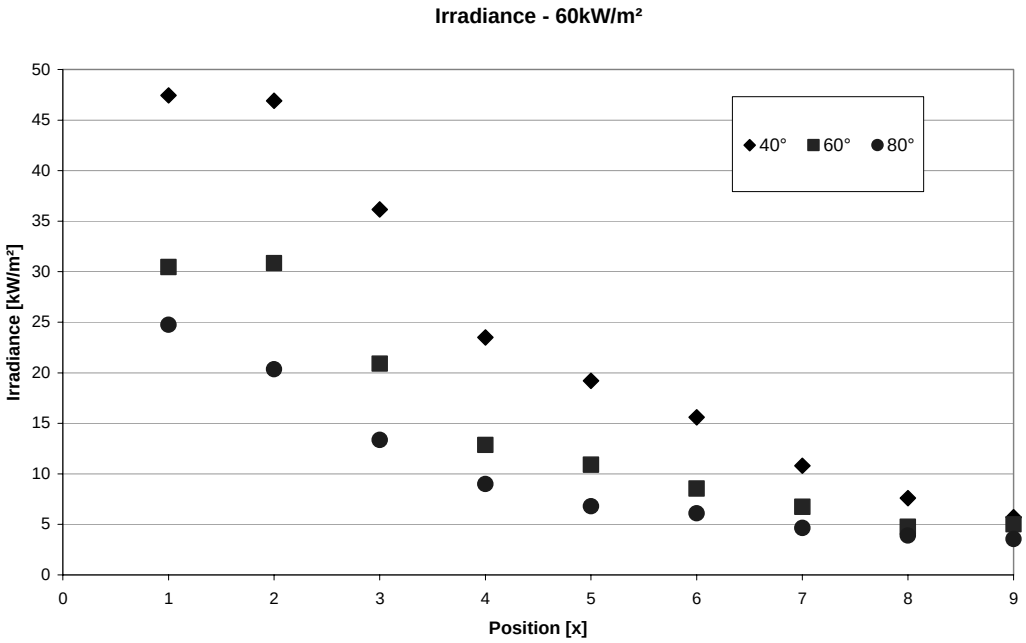

Figure 26 Irradiance Profile along Sample at Heat Flux of 60kW/m²

The above results were then normalised to compare the irradiance profile to that typical of the LIFT apparatus. These plots differ from the previous graphs as they directly compare the graduated heat flux along the length of the sample. The y-axis of each plot has been normalised to allow each graph to represent the irradiance profile and be compared with the LIFT profile at each angle.

In Figure 27, the sample holder is at 40°, the graph does not show a very good correlation to the LIFT profile. The values measured by the heat flux meter are higher relative to the same position of the LIFT. Figure 28 and Figure 29 show a much closer alignment with the LIFT until position 5, after this point the irradiance exposure is higher than the LIFT at the same relative position. What is meant by 'relative' is that the irradiance and the position along the sample is taken as a percentage. That is the graphs show that up to 50% along the sample the irradiance aligns quite well with the LIFT. As illustrated in the earlier plots of Figure 24, Figure 25, and Figure 26 the gradients taper off halfway along the sample. The LIFT profile shows that the irradiance exposure drops steadily until about three quarters along the length of the sample before it tapers off to 3% of the initial heat flux. In all three measured profiles, the irradiance tapers off to an average 14% of the initial heat flux, independent of the angle.

The percentage decrease in the irradiance measured is constant for each angle the experiments were conducted (40°, 60° or 80°) and were found to be independent of the applied irradiance whether it was 40kW/m², 50kW/m² or 60kW/m². A common characteristic shown is that as the sampling position moves further from the hot end of the sample, the difference gets smaller between the measured irradiance, regardless of angle. What is meant by 'hot end' is the end that is positioned at the center of the cone (frustum).

An aspect to note is the position of the sampling points as illustrated in Figure 14. There are three pairs of sampling points, these being; 1, 2; 4, 5; and 7, 8. The upper sampling points are; 1, 4 and 7. The upper sampling points consistently recorded higher irradiance values than their lower counterpart, even though each sampling pair was an equal distance from the "hot end". The difference in the values within each pair is small and the higher values were consistently measured at the upper sampling points. By observation the effect is smallest at the hot end, position 1 and 2, however as the sampling points move further from the hot end the effect increases gradually. Comparing the measurements, position 2 on average was 4% lower than its upper counterpart (position 1). Similarly position 5 on average was 15% lower than its upper counterpart (position 4), at the cool end position 8 on average was 23% lower than its upper counterpart (position 7).

In future studies this aspect should be examined more closely possibly introducing an additional parameter to account for the exhaust hood, or implement a method to minimise the effects.

The behaviour shown in Figure 24, Figure 25, and Figure 26 are indicative of what was found in the study by Perrin (2001) who carried out irradiance measurements at 10° increments. As the angle was increased the measured irradiance decreased with each movement away from the hot end. Similarly the percentage decrease, with the change in angle remained constant, indicating the applied irradiance is an independent factor.

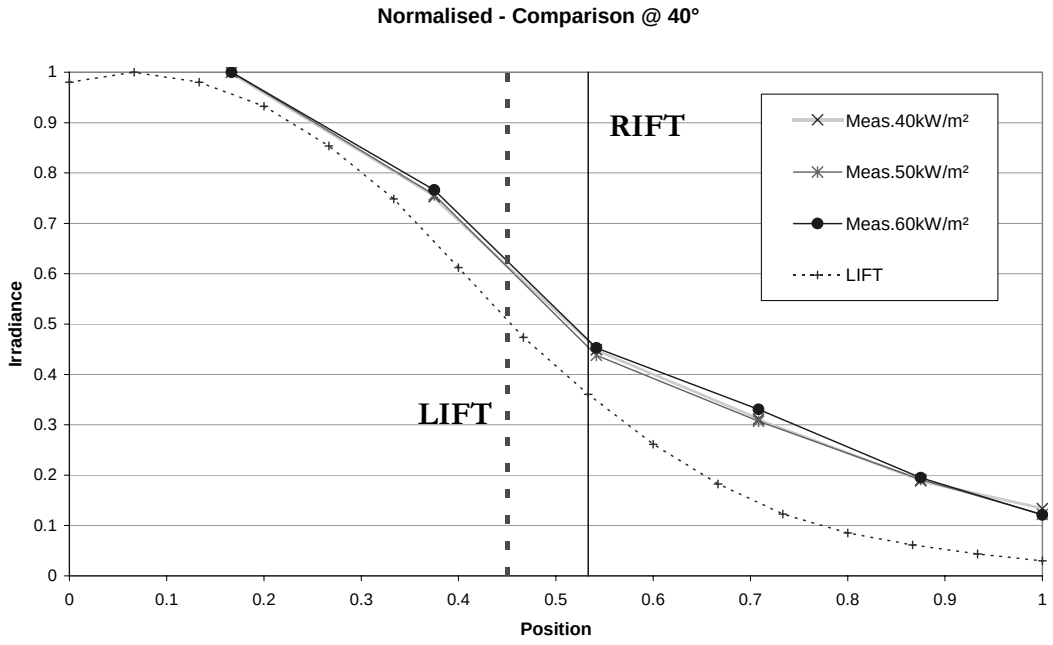

Figure 27 Normalised Irradiance profile along Length of Sample at 40°

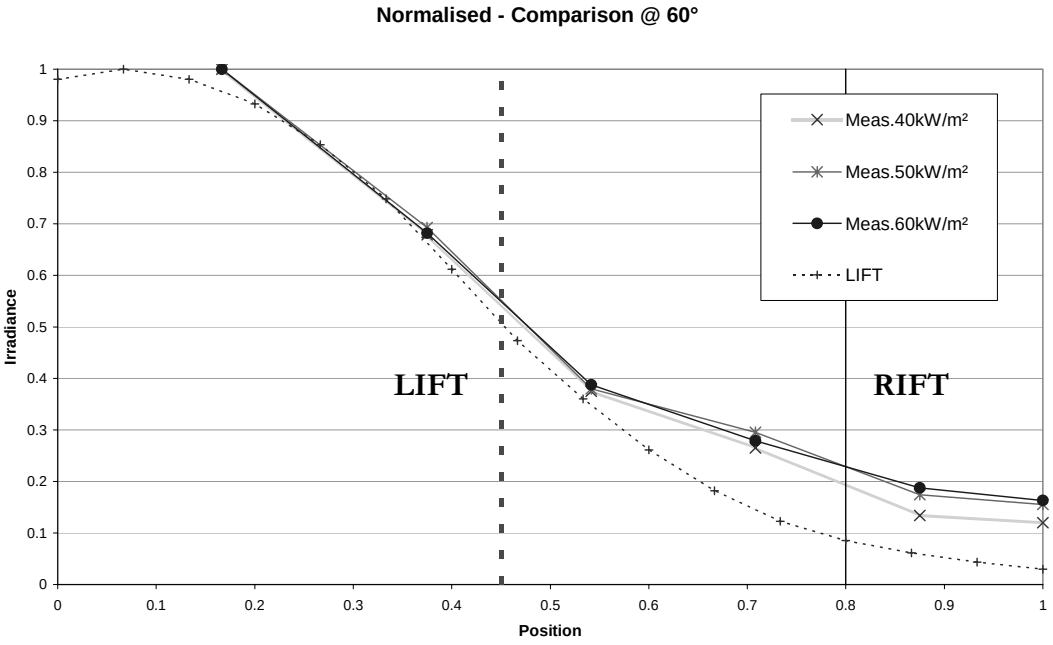

Figure 28 Normalised Irradiance profile along Length of Sample at 60°

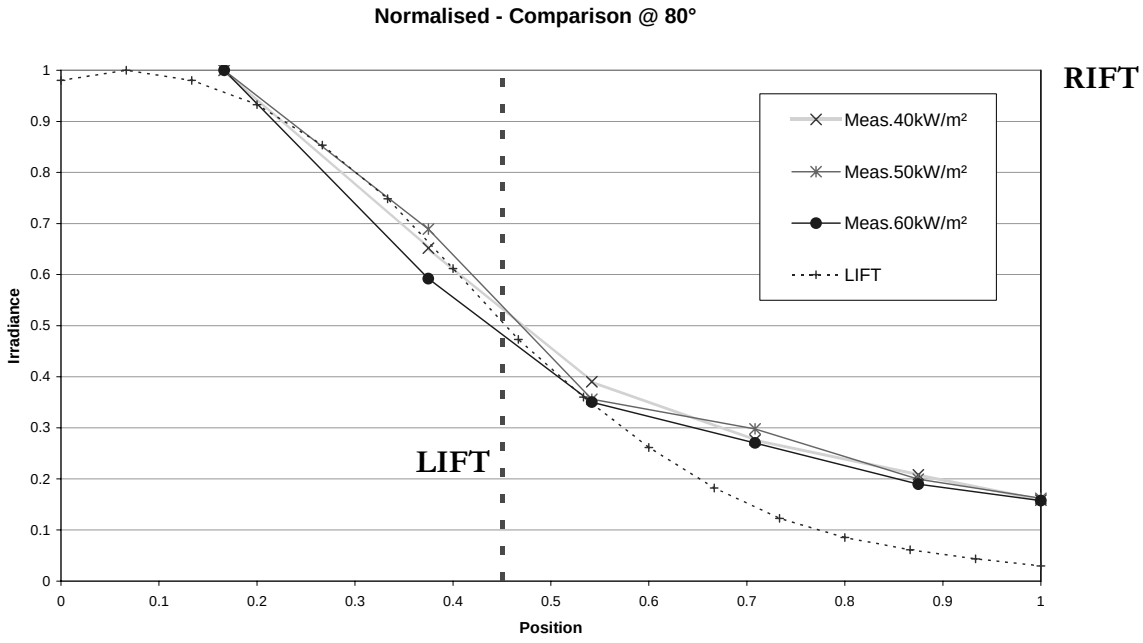

Figure 29 Normalised Irradiance profile along Length of Sample at 80°

A comparison of Figure 27, Figure 28 and Figure 29 reveal that the 60° angle is best suited to continue with the flame spread experiments. At 60° the measured irradiance shows a closer correlation with the irradiance profile shown from LIFT tests. In all the tests, the results showed that the irradiance exposed to the sample is much higher at the far end of the sample than that of the LIFT sample at an equivalent distance.

7.2 Irradiance Mapping

Radiative heat transfer is the process used to describe the exchange of energy between two surfaces. In general terms the radiative heat transfer can be expressed as:

$$\dot{q}''_{rad} = F_{1-2}\varepsilon\sigma T_s^4 \qquad \textbf{(21)}$$

Where: F_{1-2} is the configuration (view) factor

ε is the emissivity term;

σ is the Stefan-Boltzmann constant; and

T_s is the surface temperature.

The exchange of energy is dependent on the surface geometry and orientation, $F_{1\text{-}2}$; radiative properties, ε; and temperature, T_s.

Using the measured irradiance taken along the sample, a configuration factor was applied to estimate the irradiance exposed to the sample '*x*' distant away from the 'hot end'. A literature review could not find any view factor that exists that addresses the irradiance profile along the length of the LIFT specimen. Therefore an attempt to provide a method of estimating the irradiance profile was undertaken. Two methods were applied, firstly a simplified method where the irradiance emitted from the frustum was considered constant, this method was developed by Naraghi and Chung as detailed in Siegel and Howell (1992). The second method was an application of a modified configuration factor developed by Wilson et al (2002). The configuration factor by Wilson et al (2002) was a more accurate view factor as more parameters were calculated in relation to the position of the elemental point being considered.

7.2.1 Naraghi and Chung – Configuration Factor

The first approach in mapping the irradiance from the frustum to the sample's surface involved simplifying the parameters. The simplification was to assume a constant irradiance from the cone, ignoring completely the effect of the frustum's shape and radiative properties, ε. By assuming the frustum as a disk, A_2 and the sample surface as a rectangular surface, dA_1, at an angle to the cone, θ, the configuration factor of Naraghi and Chung could be applied. Figure 30 illustrates the assumed configuration.

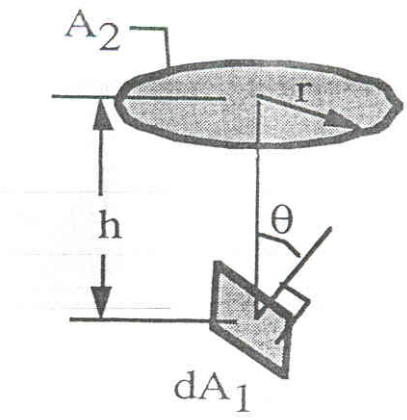

Figure 30 Configuration Factor for Tilted Planar Element to Disk
(Reproduced from Siegel and Howell, 1992)

This method assumes that 100% of the disk is over the point of consideration. It is recognised that this method will over predict the irradiance exposed to the surface of the sample. For the initial estimate of the irradiance it was important to apply a simple model with a known outcome to allow for initial comparisons between mathematical values against experimental results. This helps identify any mathematical shortfalls and highlights the key parameter required to refine the configuration factor later. Key parameters used in the configuration factor by Naraghi and Chung include accounting for the distance from the disk and the angle that the rectangular surface is to the disk. The governing equations to match Figure 30 are given as:

$$F_{d1-2} = \frac{1}{1+H^2}\cos\theta; \quad for \quad \theta \le \cot^{-1}\left(\frac{1}{H}\right) \tag{22}$$

$$F_{d1-2} = \frac{-HX\sin\theta}{\pi(1+H^2)} + \frac{1}{\pi}\tan^{-1}\left(\frac{X\sin\theta}{H}\right) + \frac{\cos\theta}{\pi(1+H^2)}\left[\pi - \cos\theta^{-1}(H\cot\theta)\right]; \quad for \quad \theta \ge \cot^{-1}\left(\frac{1}{H}\right) \tag{23}$$

Where: $H = h/r;$

$$X = \left(1 - H^2\cot^2\theta\right)^{1/2}$$

The measured irradiance and those calculated using the Naraghi and Chung configuration factor were normalised to allow a relative comparison to be made. Figure 31, Figure 32 and Figure 33 show the comparison between the measured

irradiance and that predicted at 40°, 60° and 80° respectively. The normalised results show that the predicted results over estimate the irradiance compared with the profile of the LIFT test along the length of the sample. The method of showing the results as in Figure 31, Figure 32, and Figure 33 highlight the differences in percentages.

Figure 31 shows the sample holder set at 40°, the estimated heat flux at the far (cool) end of the sample was 47% of the fixed heat flux at the end of the sample compared to 13% for measured and only 3% during LIFT tests.

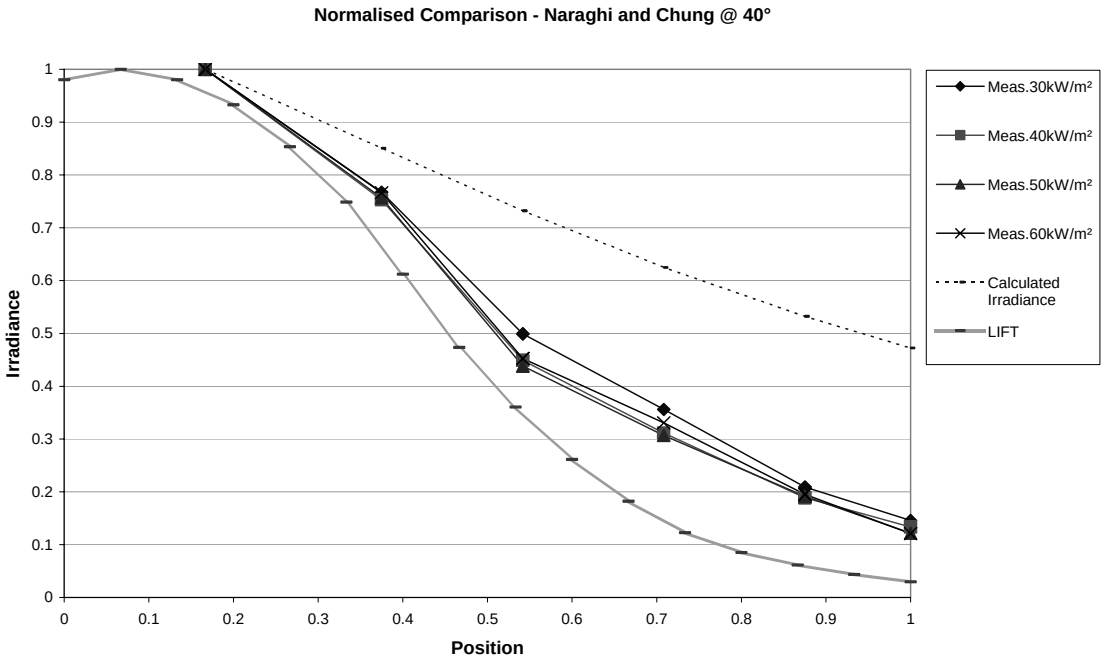

Figure 31 Normalised Comparison - Naraghi and Chung at 40°

Similarly in Figure 32 when the sample holder is at 60°, the irradiance estimated at the end of the sample is 36% of the fixed heat flux compared to the observed which is 15% of the fixed heat flux. Figure 33 illustrate the results when the sample holder is at 80°, the correlation improves marginally as the estimated irradiance falls to 31% of the fixed heat flux where as the measured stays around the 16% mark.

Figure 31, Figure 32 and Figure 33 clearly show how the Naraghi and Chung configuration factor over estimates the irradiance profile compared with the profile of the LIFT test along the length of the sample. As the incident angle increases the

correlation improves from 46% to 31%, whereby the measured results stay constant at around 15%.

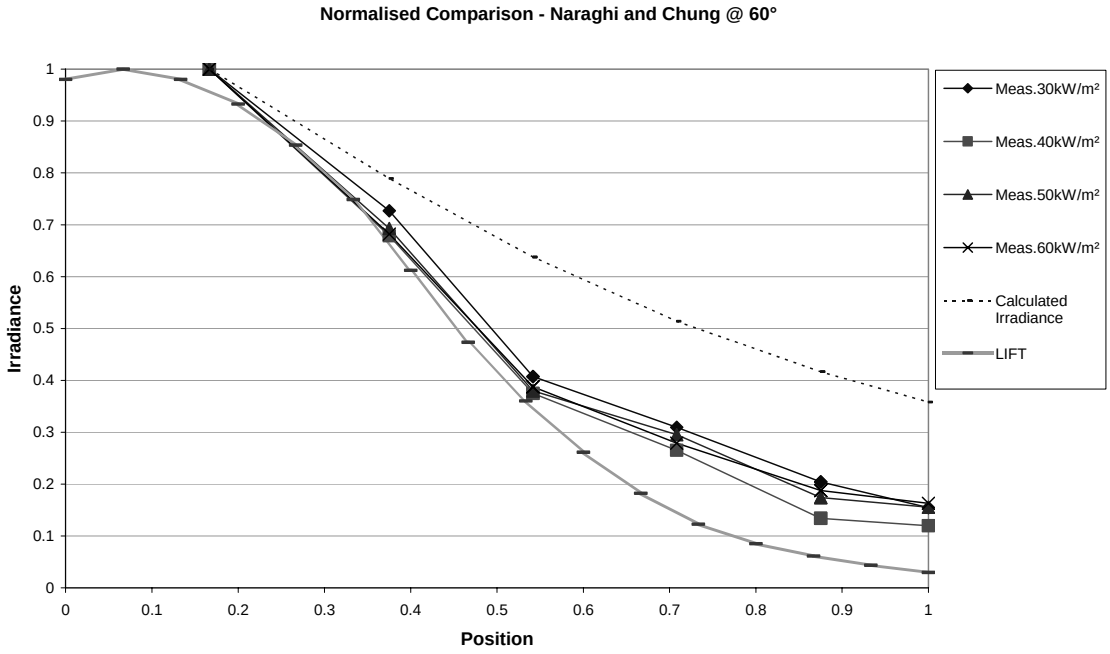

Figure 32 Normalised Comparison - Naraghi and Chung at 60°

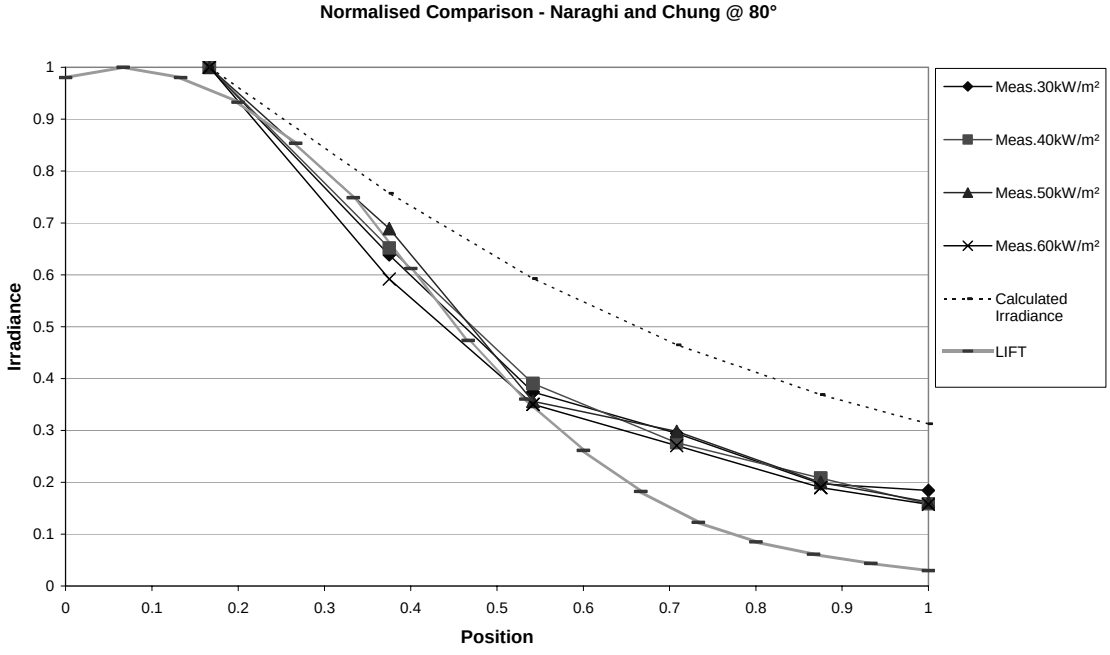

Figure 33 Normalised Comparison - Naraghi and Chung at 80°

The normalised results show the predicted results independent of the incident angle, this is due to the normalisation process, and as such do not show a true comparison.

As predicted earlier the method described by Naraghi and Chung would overestimate the irradiance measured at the sample's surface because the view factor assumes it is measuring an elemental point positioned in the middle of a radiant disk (Figure 30). In Figure 34 the expected behaviour is shown clearly in that the estimated irradiance along the length of the sample is much greater than those actually measured. The configuration factor assumes the elemental point is directly under the radiant disk resulting in an over estimation of the irradiance. At the 40° setting the percentage difference between them is quite interesting to note. The fixed heat flux setting is independent as the difference is accounted for in all the tests and therefore is not a contributing factor. Positions 1 and 2 show an average 11% variation where at position 3 the averaged variation is only 3%, because the view factor does not account for increasing distance the remaining sample points illustrate increasing variation. Positions 4-7 had an average 54% variation whereby the last 3 sample points had an average 174% variation.

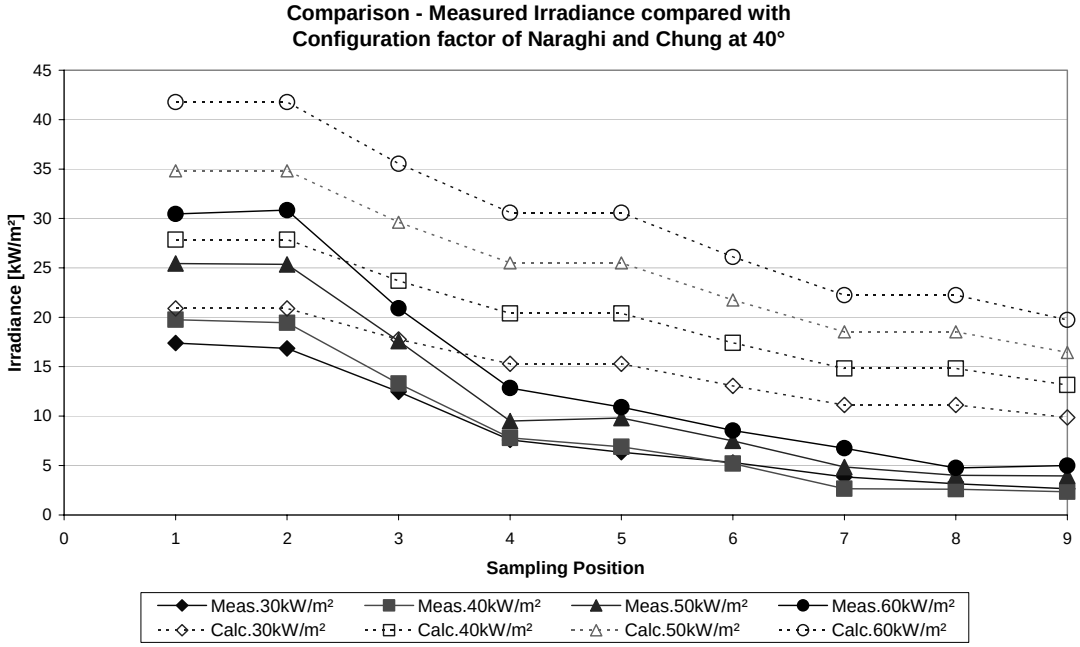

Figure 34 Comparison of Measured Irradiance with Naraghi and Chung at 40°

Figure 35 shows surprisingly comparative results between those measured and those estimated by the view factor. These results are more coincidental than actually meeting any criteria to simulate the results. The results are slightly better than at 40°, where the averaged variation across the length of the sample was 55%, which is lower than the averaged variation of 80% at 40°. As the normalised results show the irradiance profile resulting from the Naraghi and Chung view factor do not fall away the same way as the LIFT profile does having an overall effect of higher than expected irradiance levels.

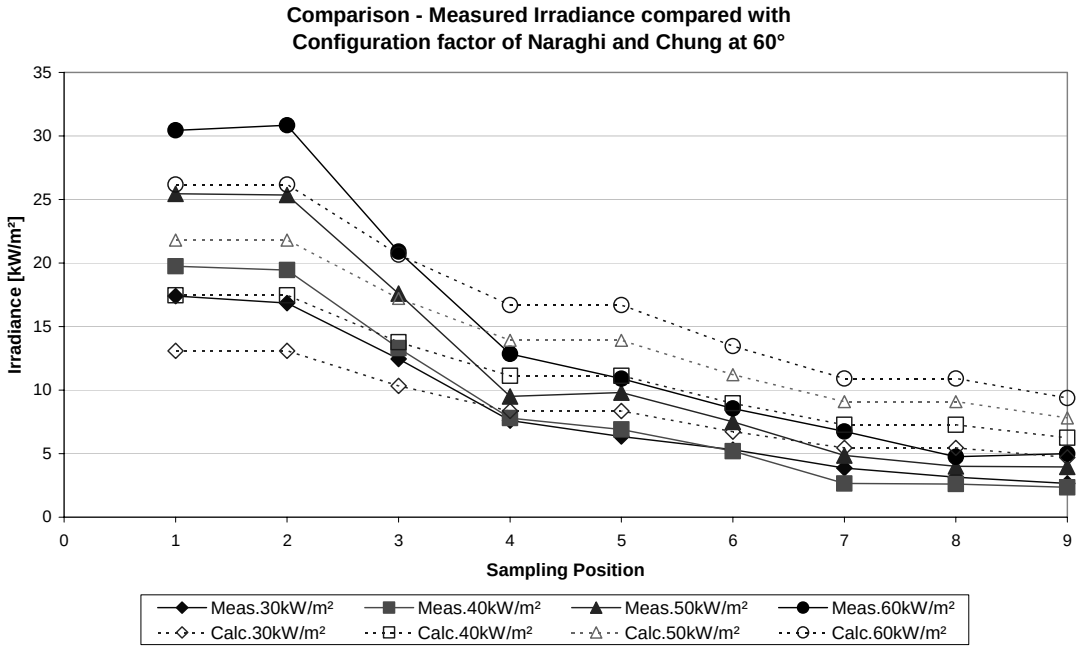

Figure 35 Comparison of Measured Irradiance with Naraghi and Chung at 60°

Figure 36 shows a contrasting effect in that the estimated results are below those measured. The angle which Figure 36 show, 80°, indicates that the sample's surface would experience very little of the irradiance emitted from the cone. Figure 23 show that the sample holder is almost vertical to that of the cone so it would be reasonable to assume that the level of irradiance emitted to the sample surface would be low. The results at 80° have the lowest percentage variation, 35%, this is mainly due to much lower irradiance levels therefore differences observed are smaller but are far from exhibiting any correlation.

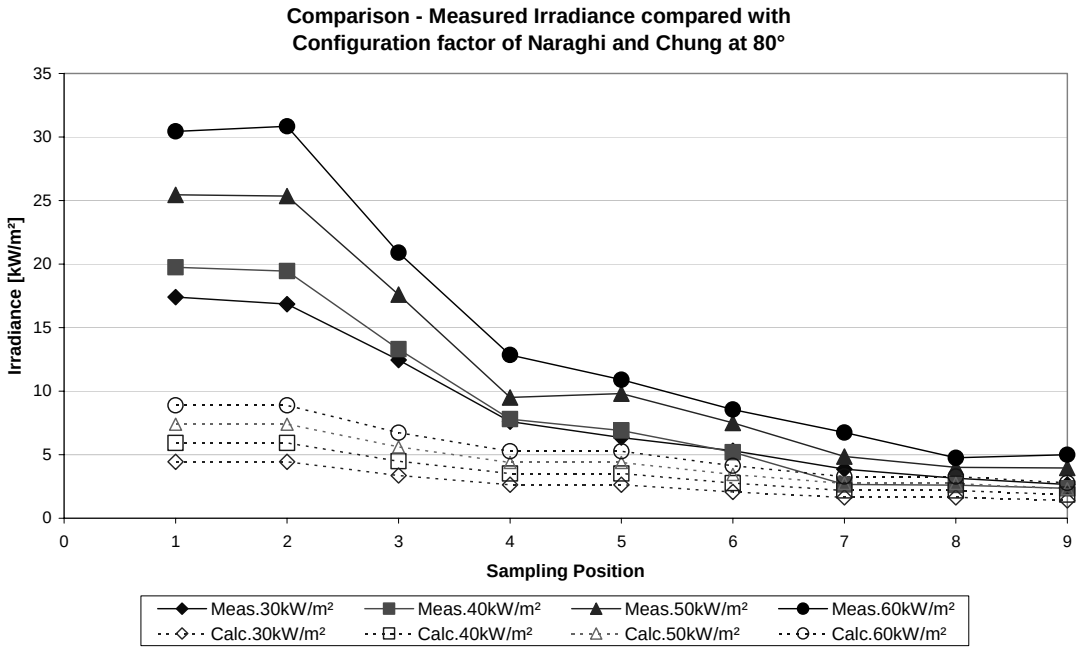

Figure 36 Comparison of Measured Irradiance with Naraghi and Chung at 80°

What the Naraghi and Chung view factor does is that it highlights the need for additional parameters to predict the irradiance along the length of the sample more accurately. Particularly to account for the sample's increasing distance from the cone in the *x* and *y* directions.

7.2.2 Wilson et al – Configuration Factor

The second approach in mapping the irradiance from the frustum to the sample's surface involved including as many parameters as practicable. Work undertaken by Wilson et al (2002) introduced a view factor that took into account the geometry interchange between the internal surface of the cone heater and an elemental area dA_1 located at the sample's surface. A slight modification was made to the view factor to accommodate for the fact the sample's surface, a rectangular surface, dA_1, is at an angle, θ, to the cone. This view factor assumes that the elemental area is exposed to 100% of the cone which is the same assumption made in the application of the view factor by Naraghi and Chung,. The assumption will mean an overestimation of the irradiance onto the surface of the sample, as in practise the sample is only exposed to half the cone's surface. The application of Wilson et al's view factor will indicate how well the estimated results compare to those measured. Figure 37 illustrates this

configuration which Wilson et al (2002) derived, showing the interchange between the frustum and the elemental area. The view factor can be described as:

$$F_{d1-3} = F_{d1-2} - F_{d1-4} \quad \textbf{(23)}$$

Where:

$F_{d1\text{-}2}$ configuration factor between elemental area dA_1 and surface 2

$F_{d1\text{-}3}$ configuration factor between elemental area dA_1 and surface 3

$F_{d1\text{-}4}$ configuration factor between elemental area dA_1 and surface 4

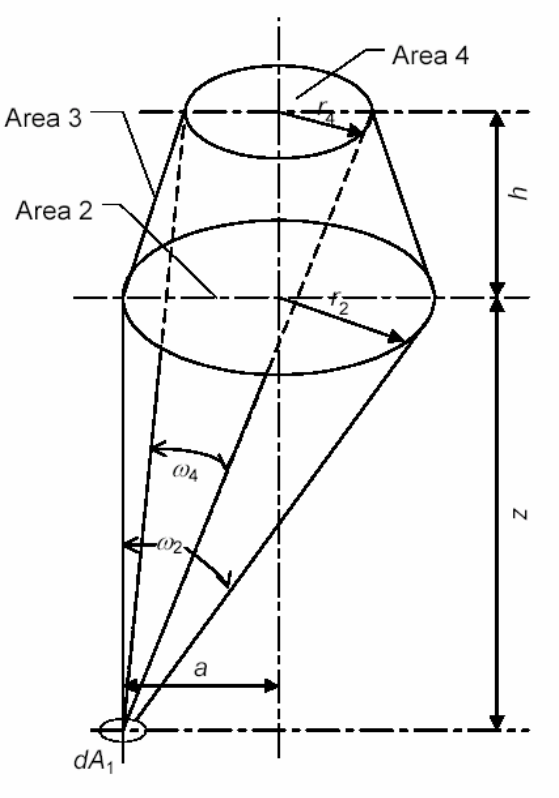

Figure 37 Schematic diagram of frustum radiating to an elemental surface dA_1
Reproduced from Wilson et al, 2002

$F_{d1\text{-}3}$ represents only a fraction of the radiative energy leaving area 3 and reaching the elemental surface dA_1. Furthermore the interchange within the frustum can be described by the following equation by Wilson et al (2002), further information regarding other geometries involving frusta is presented in Wang et al (1986) and Siegel and Howell (1992).

$$F_{d1-2} = \frac{1}{2}\left(1 - \frac{1 + H_2^2 - R_2^2}{\sqrt{Z_2^2 - 4R_2^2}}\right) \quad \textbf{(24)}$$

Where: $H_2 = z/a$;

$R_2 = r_2/a$; and

$Z_2 = 1 + H_2^2 + 4R_2^2$

Equation 24 can be simplified when the elemental area is at the centreline, the equation therefore when $a = 0$ becomes:

$$F_{d1-2} = \frac{r_2^2}{z^2 + r_2^2} \tag{25}$$

Similarly for $F_{d1\text{-}4}$ the following expressions are derived:

$$F_{d1-4} = \frac{1}{2}\left(1 - \frac{1 + H_4^2 - R_4^2}{\sqrt{Z_4^2 - 4R_4^2}}\right) \tag{26}$$

And at the centerline we get:

$$F_{d1-4} = \frac{r_4^2}{(z+h)^2 + r_4^2} \tag{27}$$

Where: $H_4 = (h+z)/a$;

$R_4 = r_4/a$; and

$Z_4 = 1 + H_4^2 + 4R_4^2$

By substituting the above equations into Equation 23 the interchange from the frustum to the elemental area can be expressed as:

$$F_{d1-3} = \frac{1}{2}\left[\left(1 - \frac{1 + H_2^2 - R_2^2}{\sqrt{Z_2^2 - 4R_2^2}}\right) - \left(1 - \frac{1 + H_4^2 - R_4^2}{\sqrt{Z_4^2 - 4R_4^2}}\right)\right] \tag{28}$$

Further, at the centreline the simplified expression is:

$$F_{d1-3} = \frac{r_2^2}{z^2 + r_2^2} - \frac{r_4^2}{(z+h)^2 + r_4^2} \tag{29}$$

The irradiance $\dot{q}''$ measured at the sample's surface can be expressed as:

$$\dot{q}^{"} = F_{d1-3}\varepsilon\sigma T^4 \quad \textbf{(30)}$$

This method provides a more accurate method in estimating the irradiance from the cone to the surface of the sample. The view factor, factors into the calculation the distance x and y away from the surface of the cone. The interchange within the frustum is accounted by calculating the effects of $F_{d1\text{-}2}$ and $F_{d1\text{-}4}$. A correcting factor, $\cos\theta$ is applied to the view factor in Equation 30 to account for the angle at which the sample is facing the surface of the frustum. Equation 30 is taken and is corrected by multiplying the view factor by cosine θ, this allows the following equation to be obtained:

$$\dot{q}^{"} = F_{d1-3}\cos\theta \cdot \varepsilon\sigma T^4 \quad \textbf{(31)}$$

As per the standard AS/NZS 3837 (1998), the cone was calibrated resulting in known heat flux readings at 25mm away from the surface of the cone. The first step to calculate the irradiance is to back calculate using Equation 31 to find the average surface temperature of the heating element relative to the heat flux calibration reading. The difference in the element temperature is shown in Table 1. The comparison is made between the measured results and those that resulted from the estimation. The angle proved to be independent when back calculating the element surface temperature. This is as expected as at the 25mm mark it is assumed the angle is zero and has no bearing on the irradiance reading. The temperature difference is a 10% rise compared to the measured results this equates to about a 60°C higher temperature value.

Heat Flux	30kW/m²	40kW/m²	50kW/m²	60kW/m²
Measured	640	707	770	825
Wilson et al	707	781	841	893
% Difference	10%	10%	9%	8%

Table 1 The average surface temperature of the heating element

The measured irradiance and those calculated using the Wilson et al configuration factor were compared. The first comparison was made by normalising the results and comparing the heat flux profiles observed and estimated to that of the LIFT test. Figure 38, Figure 39 and Figure 40 show the normalised results at 40°, 60° and 80°

respectively. The normalised results show that the predicted results over estimate the irradiance compared with the profile of the LIFT test along the length of the sample. Figure 38 shows the sample holder set at 40°, unlike that observed in the LIFT test the estimated heat flux is 23% of the fixed heat flux at the end of the sample compared to 13% for measured and a mere 3% observed during LIFT tests.

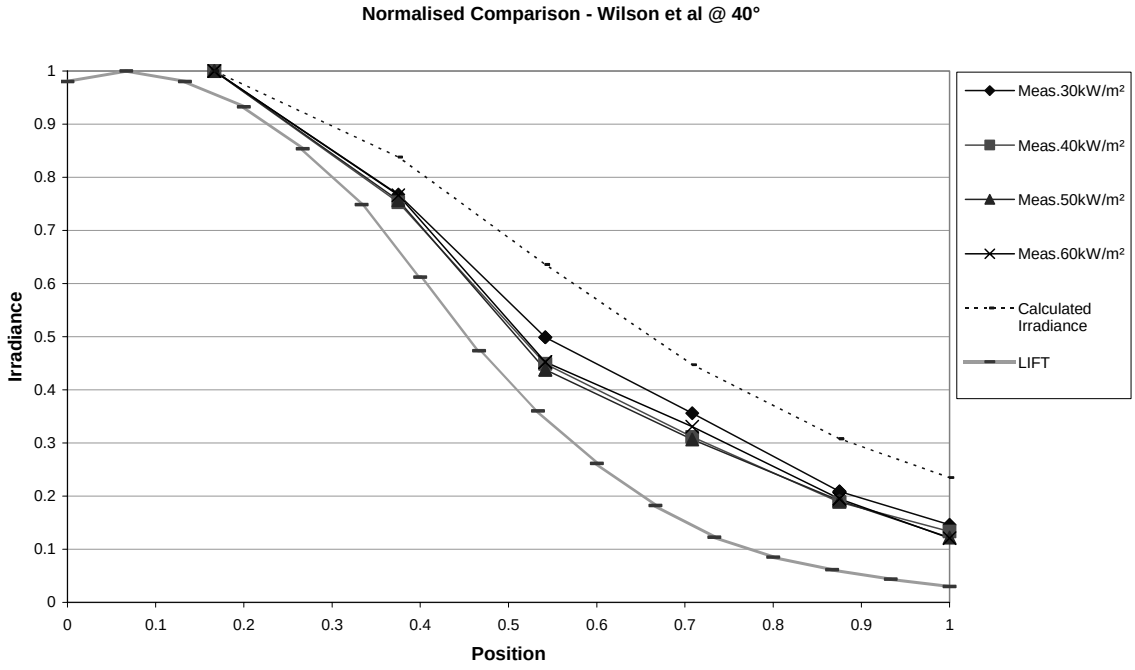

Figure 38 Normalised Comparison - Wilson et al at 40°

Figure 39 illustrates the results when the sample holder is at 60°. The results show less of a correlation. At the end of the sample, the estimated irradiance is only 29% of the fixed heat flux whereas measured are at 15%.

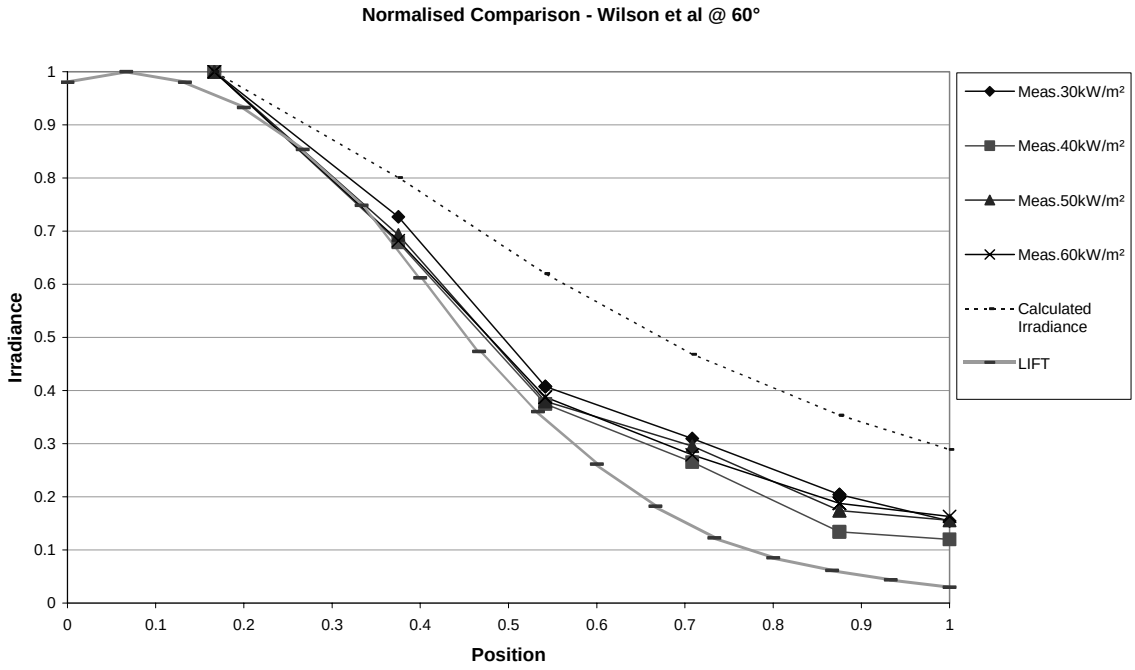

Figure 39 Normalised Comparison - Wilson et al at 60°

Figure 40 shows the results of the sample holder at 80°. The correlation for the estimated irradiance seems to worsen as the results at the end show that the estimated irradiance is 31% of the fixed irradiance compared to 16% for that measured.

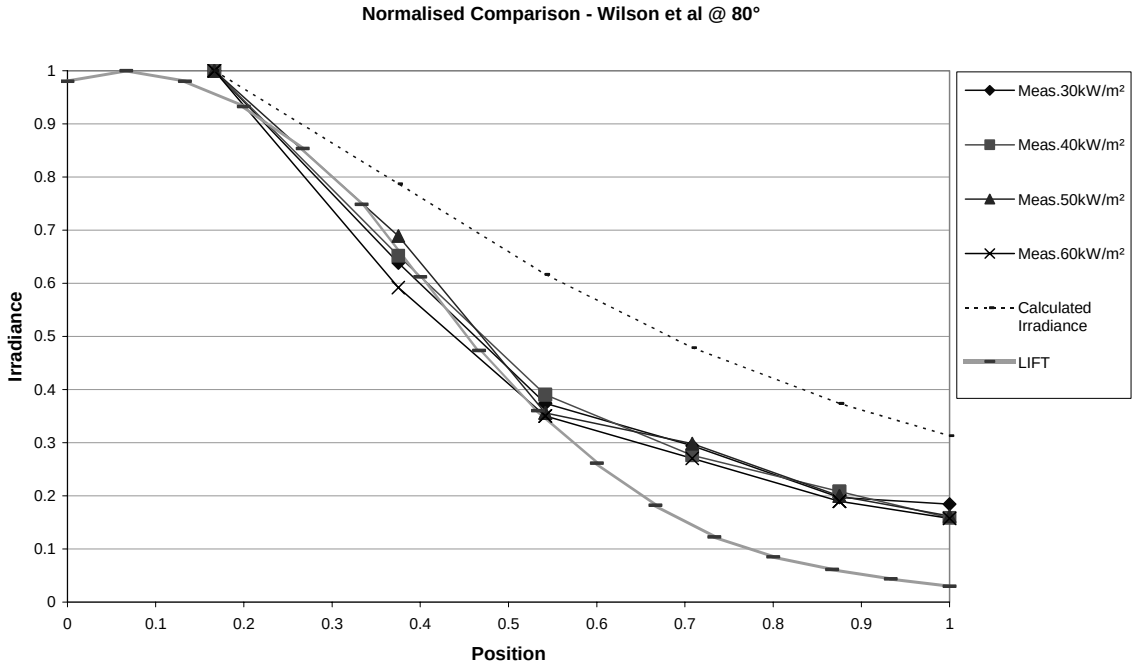

Figure 40 Normalised Comparison - Wilson et al at 80°

Figure 38, Figure 39 and Figure 40 are the result of applying the Wilson et al view factor. The graphs show that for all three angles tested they exhibit similar results to the Naraghi and Chung configuration factor that is the Wilson et al view factor overestimates the irradiance along the length of the sample. This was an expected observation as both view factors assumes that the elemental point is exposed to 100% of a radiant surface. The observations made applies to both view factors used. In Naraghi and Chung the correlation improved although small, the Wilson et al view factor got worse as the incident angle increased, a 23% variation at 40° increasing to a 31% variation at 80°.

A direct comparison of the estimated irradiance, using Wilson et al view factor, to those measured are shown in Figure 41, Figure 42 and Figure 43. These graphs show how well the actual numbers compare in terms of irradiance, kW/m² in relation to the sampling position.

Figure 41 illustrates the results when the sample holder is set at 40°. The comparison of irradiance values at the hot end of the sample shows a very close match. The first three sampling points demonstrates a close correlation with an average percentage difference of 5% between the measured values and those calculated using Wilson et al's view factor. The 5% difference at the hot end of the sample equates to a difference of about 2-3kW/m². However, as the remainder of Figure 41 illustrates the correlation gradually worsens as the view factor underestimates the heat loss along the length of the sample. At sampling points 4 to 6 the difference in the irradiance between that estimated and that measured had increased to an average value of 37%, which still equates to a difference of 2-3kW/m². At the tail end of the sample where irradiance values are expected to be around 3-6% of the fixed heat flux, we have values that are 23% and 13% for the estimated and measured respectively. The difference at the sampling point at the cool end of the sample between the estimated and measured is 66%. The actual irradiance difference is 3-4kW/m².

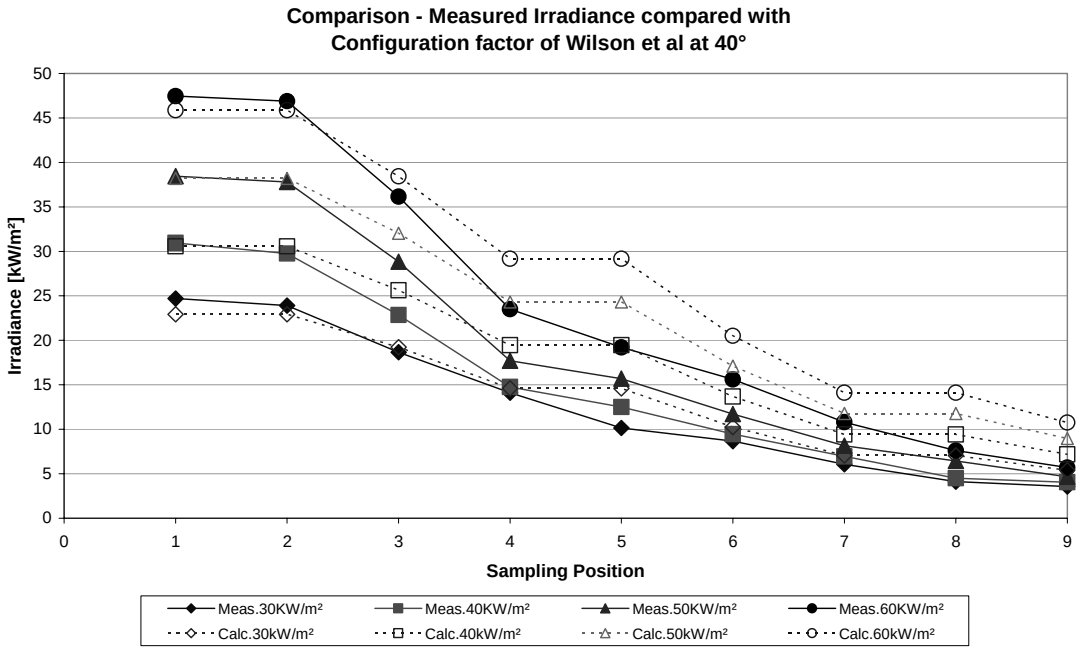

Figure 41 Comparison of Measured Irradiance with Wilson et al at 40°

The sample holder is set at 60° in Figure 42. The results similar to those shown in Figure 41 illustrate a close correlation at the hot end between the estimated irradiance and that measured. At the hot end of the sample, over sampling points 1-3, the average percentage difference was 6% equating to 2.5kW/m². At sampling points 4-6 the correlation worsens, with an average percentage difference of 52%, a 4.5kW/m² difference. By the cool end of the sample the correlation exhibits results similar to Naraghi and Chung's view factor with an average percentage difference of 94%, a difference of 4-5kW/m². The large percentage difference is a result of the view factor assuming that the elemental point is exposed to 100% of the radiant disk therefore the irradiance estimated is much higher than what is actually measured. The closeness of the results at the hot end is a result of the back calculation which is first required to find the temperature of the radiant surface.

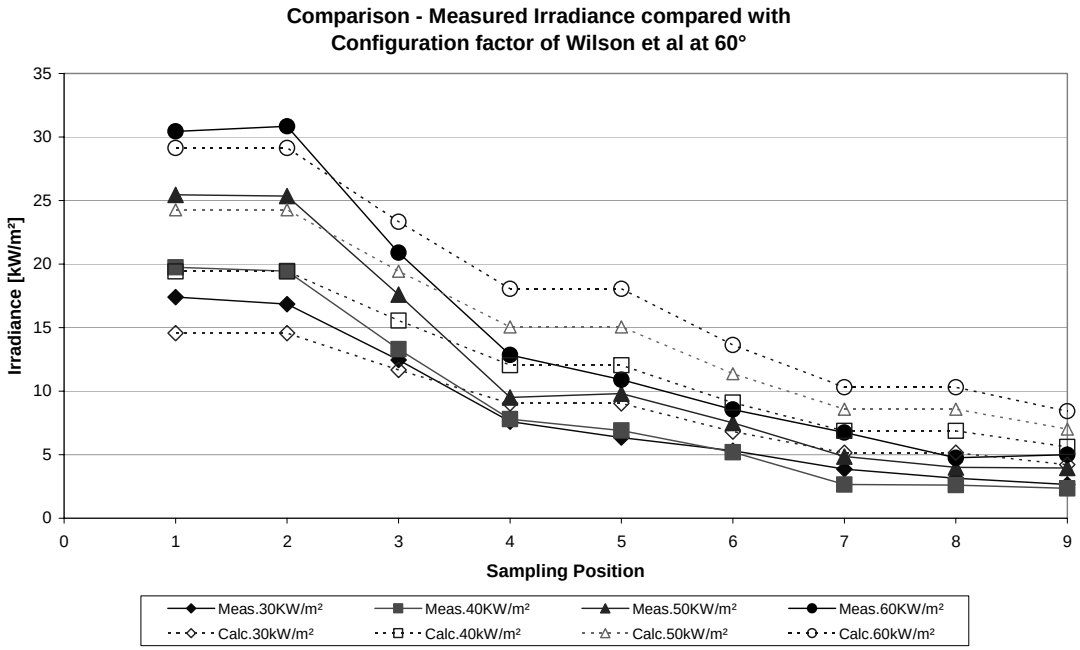

Figure 42 Comparison of Measured Irradiance with Wilson et al at 60°

Figure 43 illustrates the results of when the sample holder is at 80°. The prediction of the irradiance made using Wilson et al's view factor shows poor correlation at the hot end. This is the result of the view factor not properly accounting for the angle, resulting in the underestimation of the irradiance at sample points 1-3. The average percentage difference at the hot end is 48% a 6-7kW/m² difference. Unlike in the previous graphs of the sample holder at 40° and 60°, Figure 41 and Figure 42 respectively, the correlation between the measured and estimated seems to be very good. At sample points 4-6 the percentage difference is 19%, a 1kW/m² difference between the estimated and measured. Similarly at sampling points 7-9 the percentage difference improves further to a 11% difference, a 0.5kW/m² difference. This is a false indication of how well Wilson et al's view factor correlates with the measured results. The initial poor estimate, combining with the view factor overestimating the irradiance at the sample's surface means the results are more coincidental than anything else.

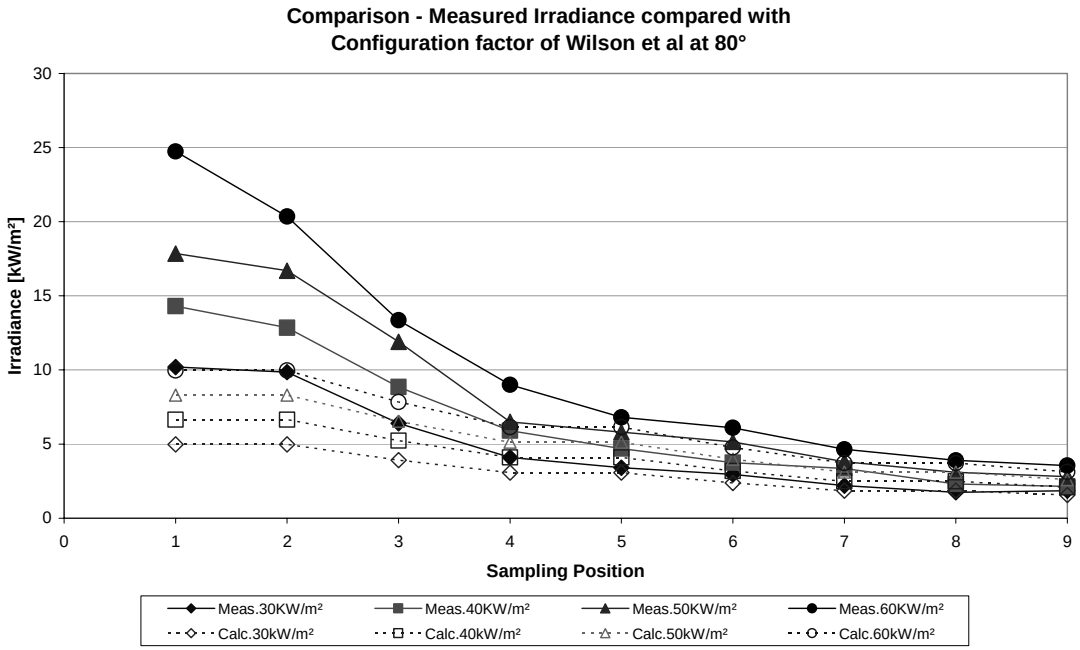

Figure 43 Comparison of Measured Irradiance with Wilson et al at 80°

Figure 41, Figure 42 and Figure 43 illustrate that Wilson et al's view factor is an improvement on the Naraghi and Chung's view factor in this application. This was expected because of the additional parameters that were taken into account by Wilson et al. The results shown are only an initial step and could form the foundations to derive a view factor more fitting of the configuration and interchange of the experimental setup.

7.2.3 Comparison of View factors

In Figure 44, the view factors calculated from the Naraghi and Chung and Wilson et al's model are compared. The results shown are for all scenario's, the heat flux applied is an independent factor in the calculation.

In the Naraghi and Chung model (solid lines), the angle the sample is placed in relation to the cone illustrates a strong influence. The value of the view factor clearly decreases as the angle increases. At 60° the value of the view factor decreases by 35% of the 40° value, at 80° the view factor decreases a further 65%. Expectantly the profile of the view factor is consistent and is shown to be independent of the angle.

The Wilson et al view factor is lower than the values obtained from Naraghi and Chung, these values show consistent behaviour based on the application of each model. That is in the model by Wilson et al there are more parameters taken into account for the view factor calculation, such as distance away from the centreline, distance from the cone surface and also angle of the sample's surface therefore affecting the final view factor, whereas the Naraghi and Chung model accounts for only angle and distance from the cone's surface. At 60° the value of the view factor decreases by 35% of the 40° value, at 80° the view factor decreases a further 65%. These values show the same decrease as shown by the Naraghi and Chung model. This steady decrease demonstrate that by modifying Wilson et al's model by multiplying Cosine of the angle, θ the result is consistent with a model that incorporates this angle factor in the derivation.

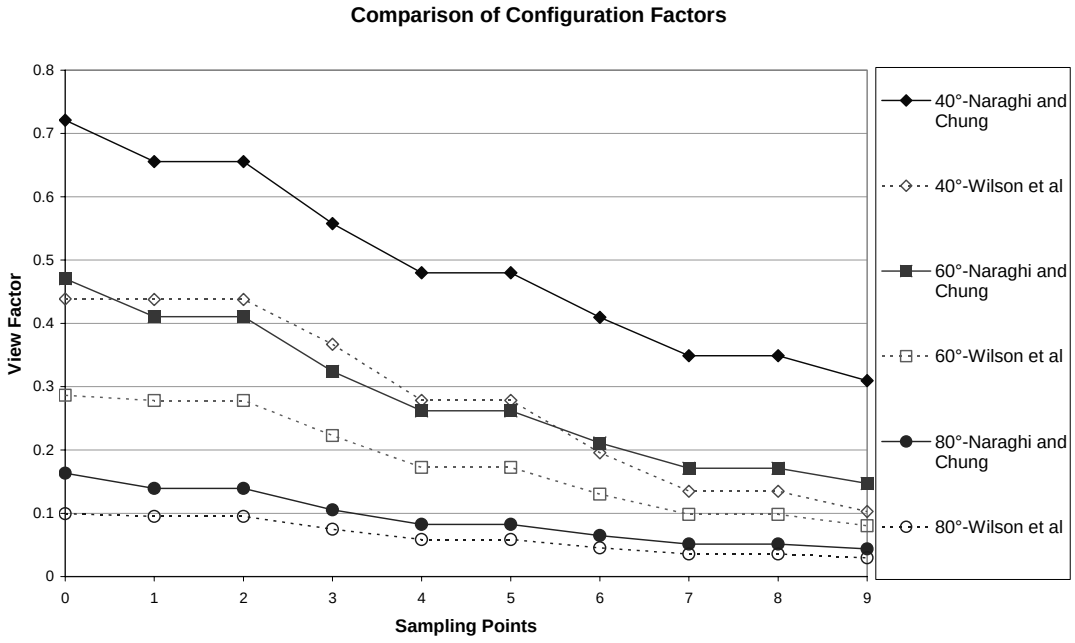

Figure 44 Comparison of Configuration factors

7.3 Summary of Irradiance Results and Recommendations

The comparison of the measured heat fluxes with the LIFT profile highlights the suitability of the sample holder at 60°. In testing at various angles it was observed that in all cases the heat flux across the length of the sample was greater than the

LIFT at the same proportional distance, but at the 60°, it showed the most promising results.

The application of view factors to estimate the irradiance along the length of the sample was carried out in twofold, firstly using a simplified approach by applying a view factor described by Naraghi and Chung. The second was to improve the estimations by including more parameter applicable to the interchange between the objects in this instance namely the cone heater and the angled specimen. It is acknowledged that these methods would over estimate the results which Figure 31, Figure 32 and Figure 33 (Naraghi and Chung) and Figure 38, Figure 39 and Figure 40 (Wilson et al) clearly shows. In terms of the irradiance level, the average percentage difference at 40° was 80%, whereas at 60° the average percentage difference is 55% and at 80° the averaged percentage difference is 35%. The application of a modified Wilson et al's configuration factor resulted in better results being observed although in many instances the estimate was still greater than those measured. At 40° the modified Wilson et al's view factor had an average percentage difference of 35%, at 60° the average percentage difference was 51% and at 80° the average percentage difference was 26%.

Highlighted in Figures 31 – 33 and Figures 38 – 40, are the overestimation of the irradiance at the sample's surface compared with that measured at the equivalent distance. As mentioned previously, the assumption used by Naraghi and Chung and Wilson et al is that the elemental point is exposed to 100% of the radiant surface. In the experiments, as shown by photos of the setup (Figures 21 – 23), the sample in practise is only exposed to half the face of the cone. Changes in the experimental methodology could improve the correlation shown by Wilson et al's view factor. If the experiments were conducted using the full face of the cone, the application of Wilson et al's view factor would be more appropriate. The results to date indicate a better correlation would be gauged between the measured and that estimated as the overestimation as shown in these results would be eliminated. The other parameters used in the view factor of Wilson et al have addressed the other conditions of the experiment, namely the distance away from the cone (*z*, y-*axis*), the distance away from the centreline (*a*, *x-axis)*, the effects of the frustum, and also then include the

effects of the elemental point being at an angle to the cone, θ. It is hypothesised that Wilson et al's view factor would show a very close fitting correlation.

The actual length of the sample for the RIFT test (250mm) is much smaller than the sample used in LIFT test (800mm). The effect of using a smaller specimen means the amount of possible data points is reduced accordingly. To illustrate the difference in the sample length comparative plots were drawn to illustrate the allowable range in which to conduct the measurements. Figure 46 and Figure 47 illustrates the irradiance measurements of the sample at an angle of 60° and clearly show the limited data range in comparison to the LIFT.

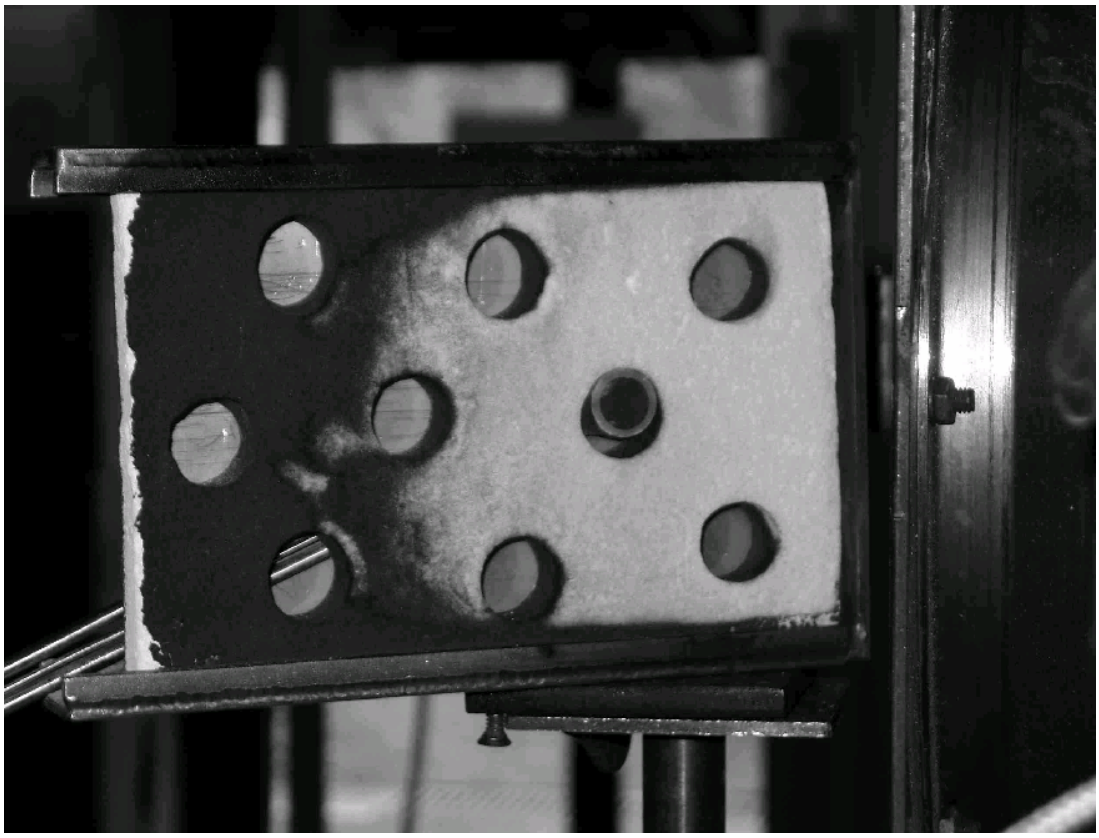

Figure 45 Positioning of heat flux meter in the sample template

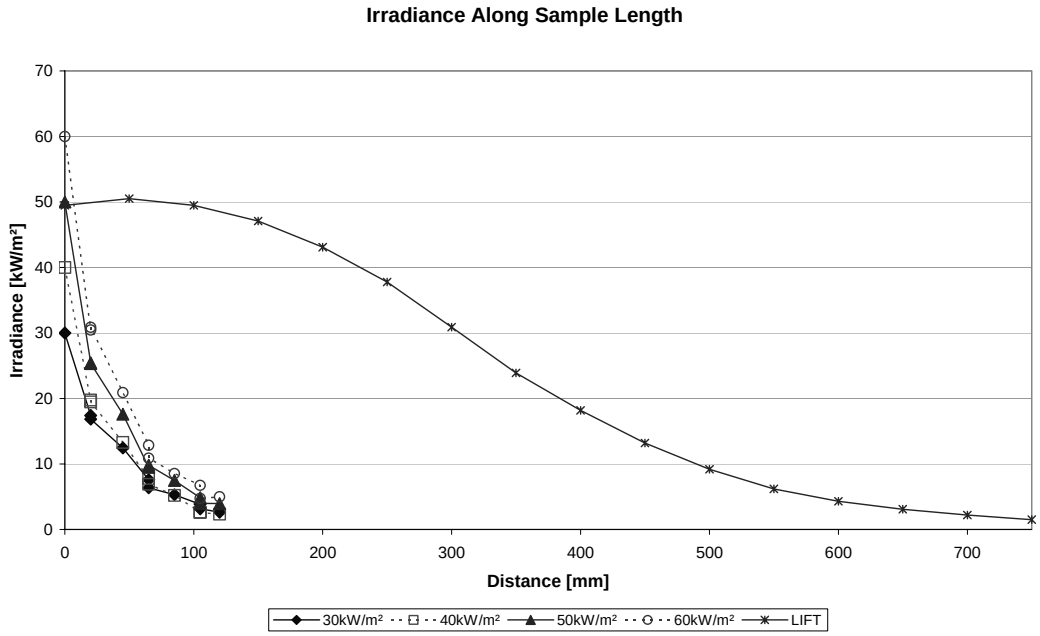

Figure 46Comparison of irradiance along sample lengths - 60°

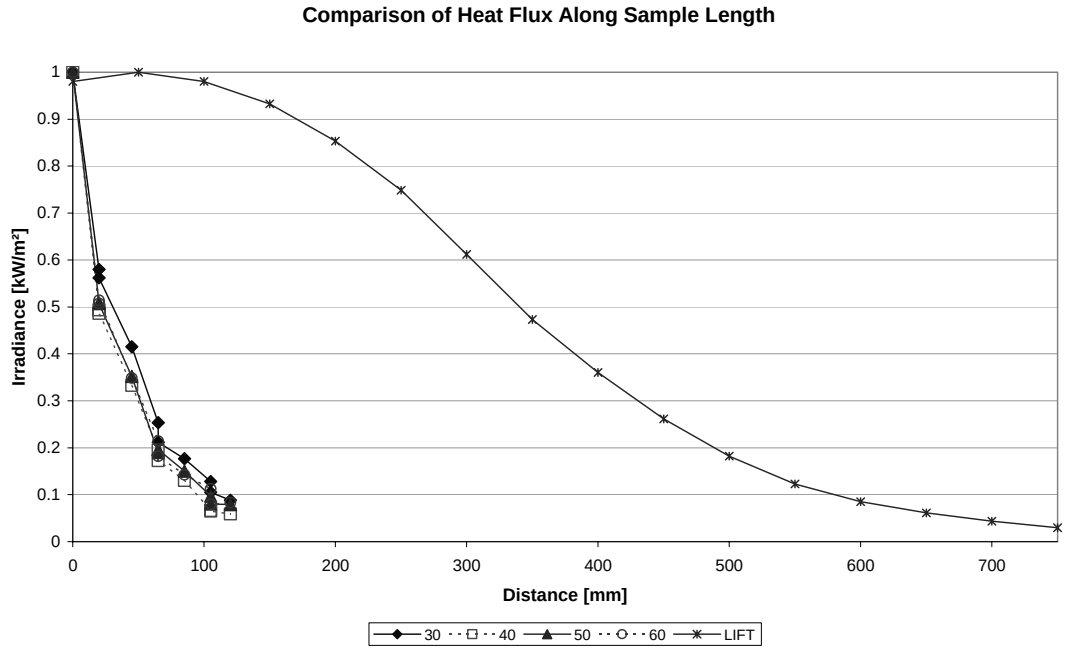

Figure 47 Comparison of Normalised Irradiance along length of sample

Given the limitation of the data range it is suggested that a modification to the way the experiments are conducted be made to allow a wider spread and increase the availability of data points. At present the samples are placed in the middle of the cone as shown in Figures 20 – 23. It is suggested that the sample be placed to the far left of the cone allowing the full face of the cone to radiate onto the sample face.

By using the full face of the cone, it is expected that the sample size could be increased allowing more data points to be collected, up to 250mm. Although sample sizes in this study were cut to 250mm in the flame spread tests it can be seen in Figure 92 that results at most were at 120mm. By having available a wider sampling area to collect data it is envisaged that their will be a larger number of results which will allow a clearer picture of the irradiance profile to be shown. This in turn will allow refinement of the configuration factor in mapping the irradiance. At present the results are too clustered to give a clear picture of what is required. The clustered results also mean that any errors will be proportionally larger, when standardised against the LIFT. The LIFT specimen is five and a half times the size of the RIFT samples therefore theoretically any errors will be magnified proportionally when the results are normalised for comparison.

Data collection is an area that will need to be addressed. The limited sampling points meant that a comparison of the estimated irradiances to those measured were only a best fit attempt. By using a sample template similar to that used in testing by Wilson et al (2002) as shown in Figure 48, a much larger number of sampling points could be used. The use of a metallic material such as that shown would not have a significant effect on measured irradiance, and therefore could prove to be satisfactory.

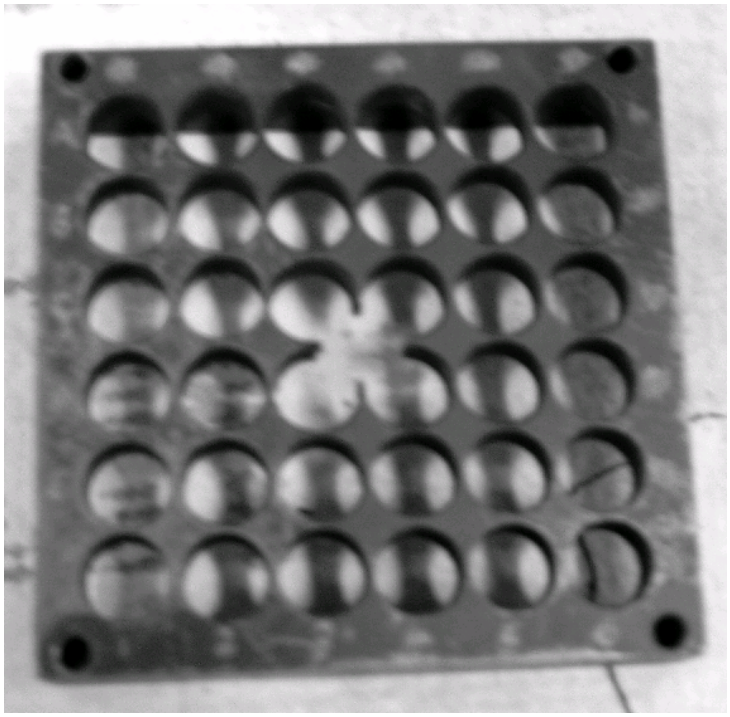

Figure 48 Template used by Wilson et al (2002)

Figure 49 show how the template used by Wilson et al (2002) could be used in a vertical orientation. The template could easily be made longer and a sample holder adapted to hold the template. The nature of this design would allow the heat flux meter to easily slide into the sampling position. A result of having higher number of sampling points is that a clearer picture of the irradiance across the sample could be found.

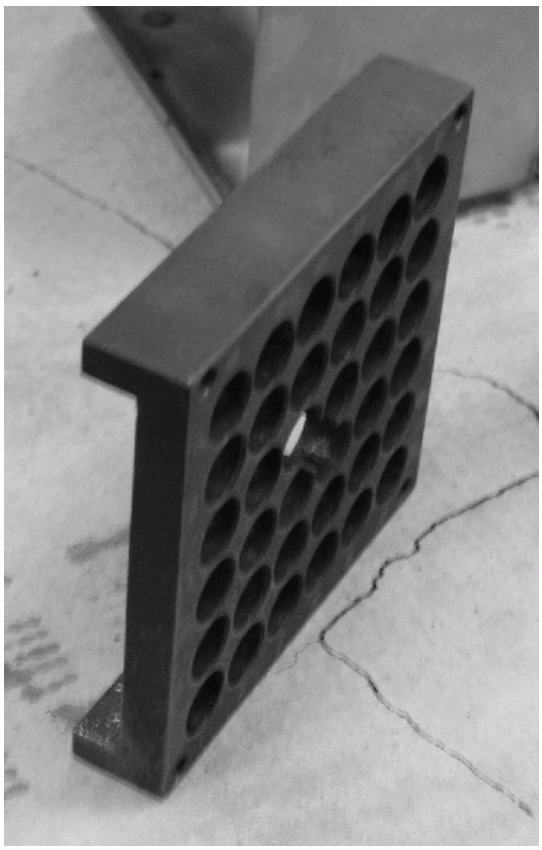

Figure 49 Vertical orientation of template used by Wilson et al (2002)

8 Ignition Tests – Results and Discussion

The ignition tests were conducted using the cone calorimeter in the horizontal orientation. The positioning of the sample is shown in Figure 16. The raw results for the particle board and laminated veneer lumber (LVL) obtained from these test can be found in Appendix D. For test results of the other wood species refer to the appendix of study undertaken by Ngu (2001). The data obtained from the results of Ngu (2001) were used for the majority of the wood species, to utilise available time and resources. More wood species were examined here than in the Ngu study, therefore further ignition tests were required, namely for the particle board and LVL.

The Quintiere and Harkleroad ignition model was applied to these test results where the gathered data was then tabulated and graphs plotted to obtain and show the material properties under ignition conditions. From the model the critical heat flux could be extrapolated and the thermal properties could then be estimated. According to the LIFT theory the ignition data are plotted as $\dot{q}''_{o,ig} / \dot{q}''_e$ *versus* $\sqrt{t}$. Once the points are plotted a straight line to fit the data is made as specified in ASTM E 1321. The fit to data is subjective as no specific guidance is given, and the points which were considered extreme were excluded. This process is dependent on the judgement of the individual and results can vary accordingly. The lack of protocol has been noted by Babrauskas (1999).

8.1 ASTM E 1321- Ignition Plots

Figure 52 illustrates the legend used in the ignition plots by Ngu (2001). The ignitability plots, graphed according to the ASTM standard E 1321 are given in Figures 50 – 58.

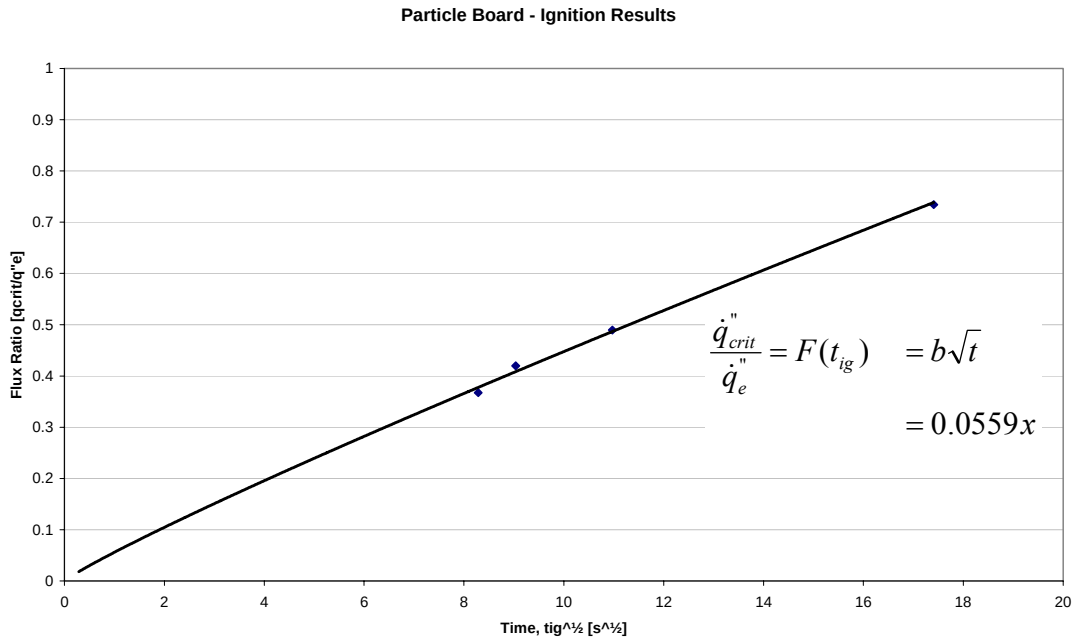

Figure 50 Ignition Plot - ASTM E 1321, Particle Board

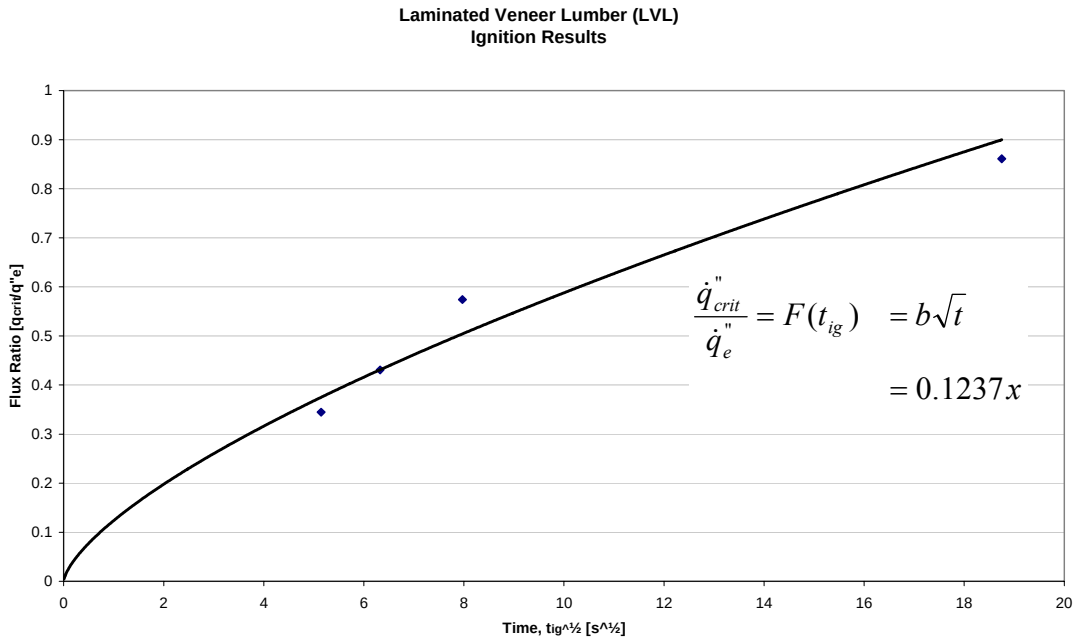

Figure 51 Ignition Plot - ASTM E 1321, LVL

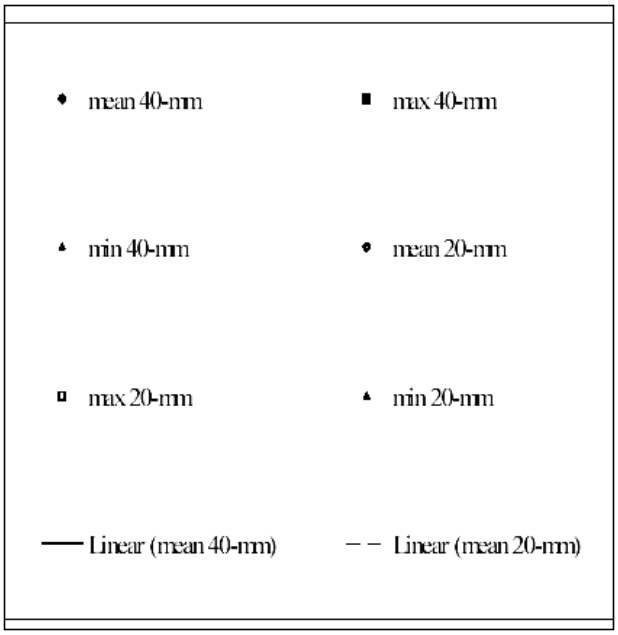

Figure 52 Legend used in the plots by Ngu (2001) - Reproduced from Ngu (2001)

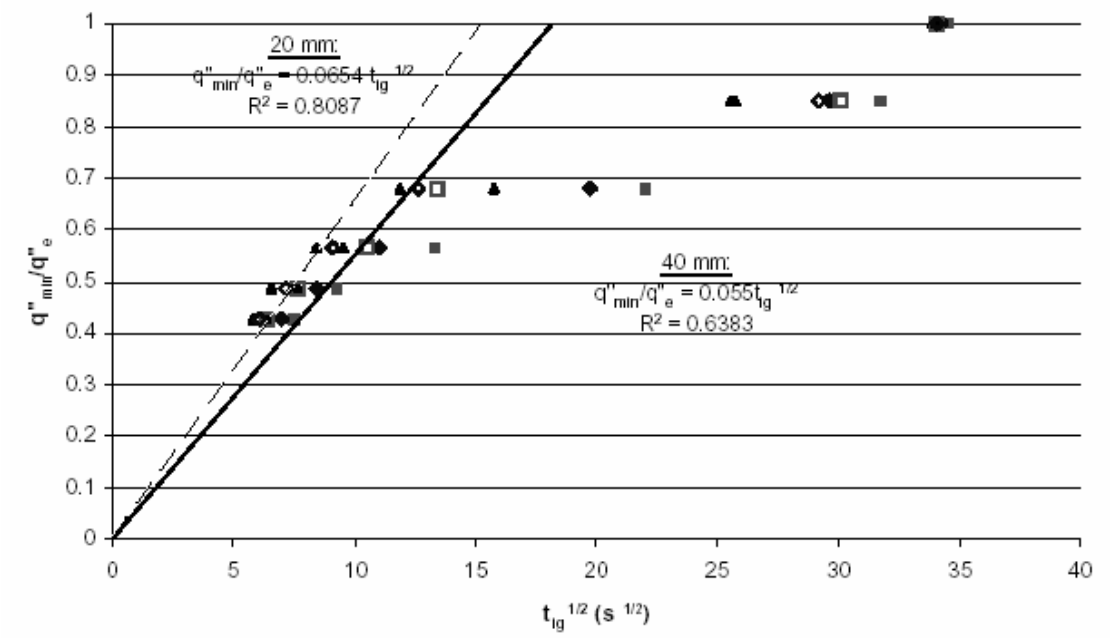

Figure 53 Ignition Plot - ASTM E 1321, Macrocarpa, Reproduced from Ngu (2001)

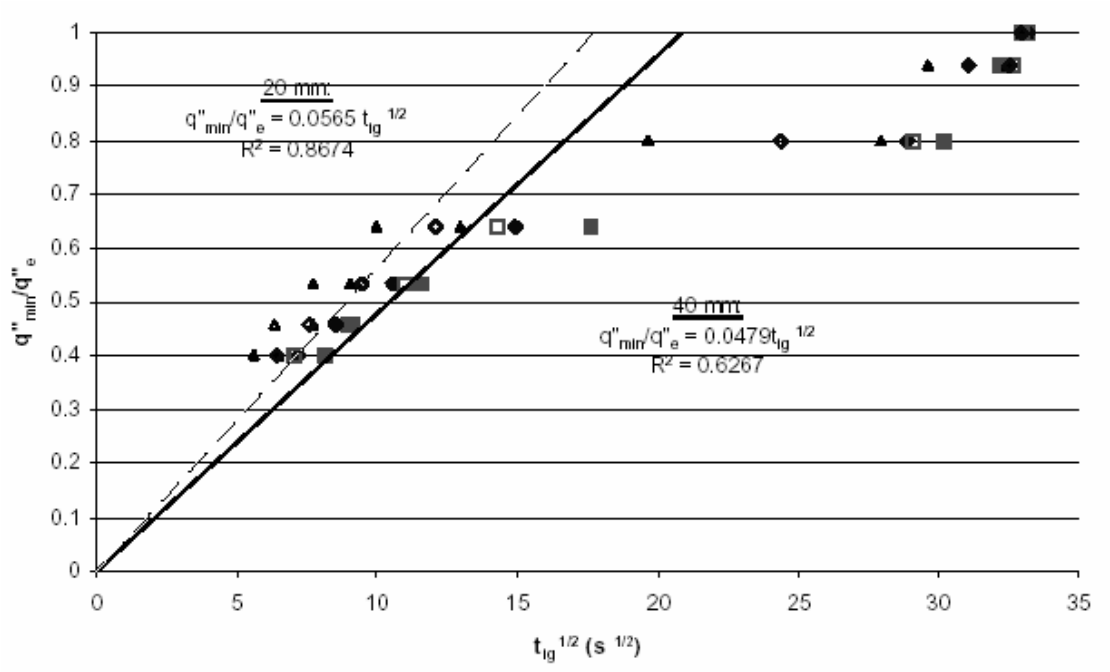

Figure 54 Ignition Plot - ASTM E 1321, Beech, Reproduced from Ngu (2001)

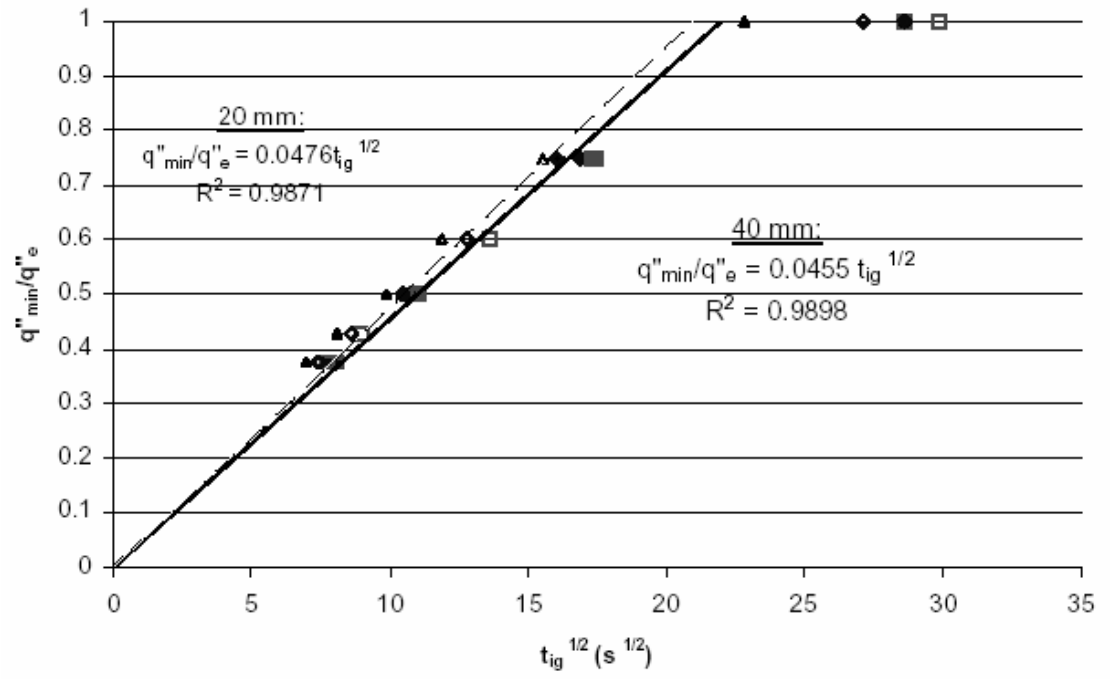

Figure 55 Ignition Plot - ASTM E 1321, Medium Density Fibre Board (MDF), Reproduced from Ngu (2001)

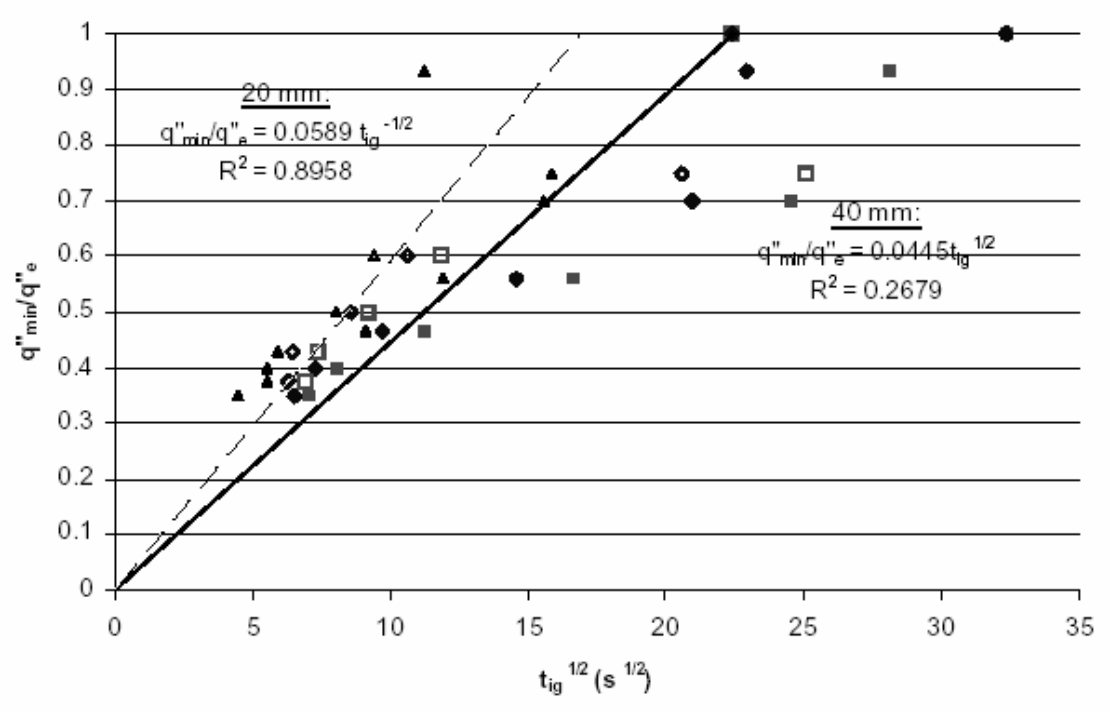

Figure 56 Ignition Plot - ASTM E 1321, Radiata Pine, Reproduced from Ngu (2001)

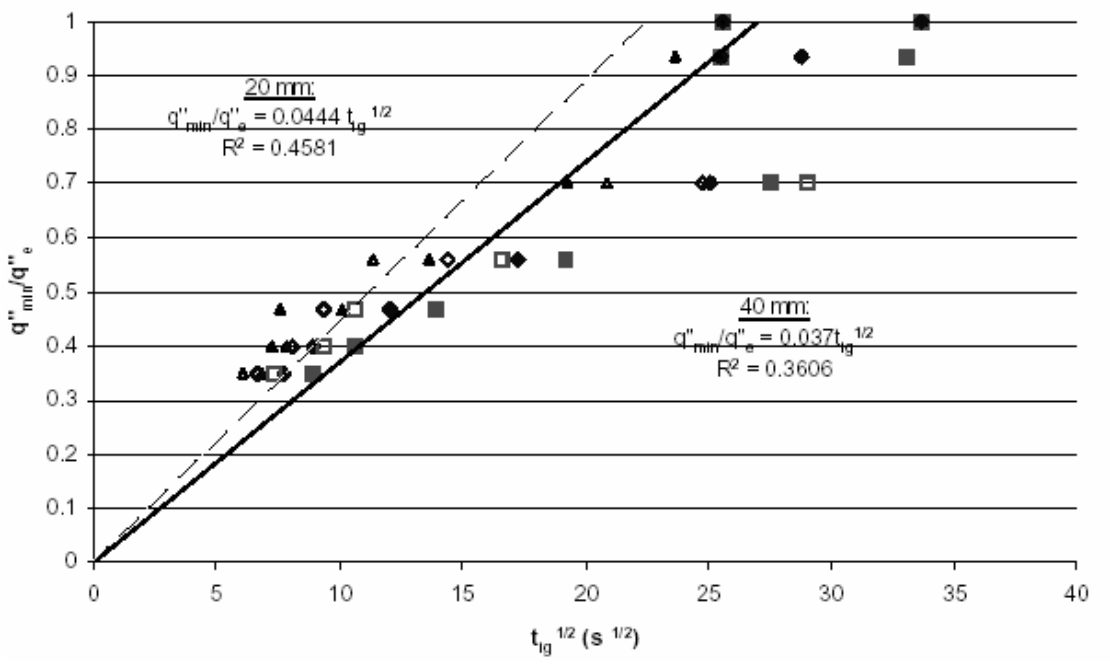

Figure 57 Ignition Plot - ASTM E 1321, Rimu, Reproduced from Ngu (2001)

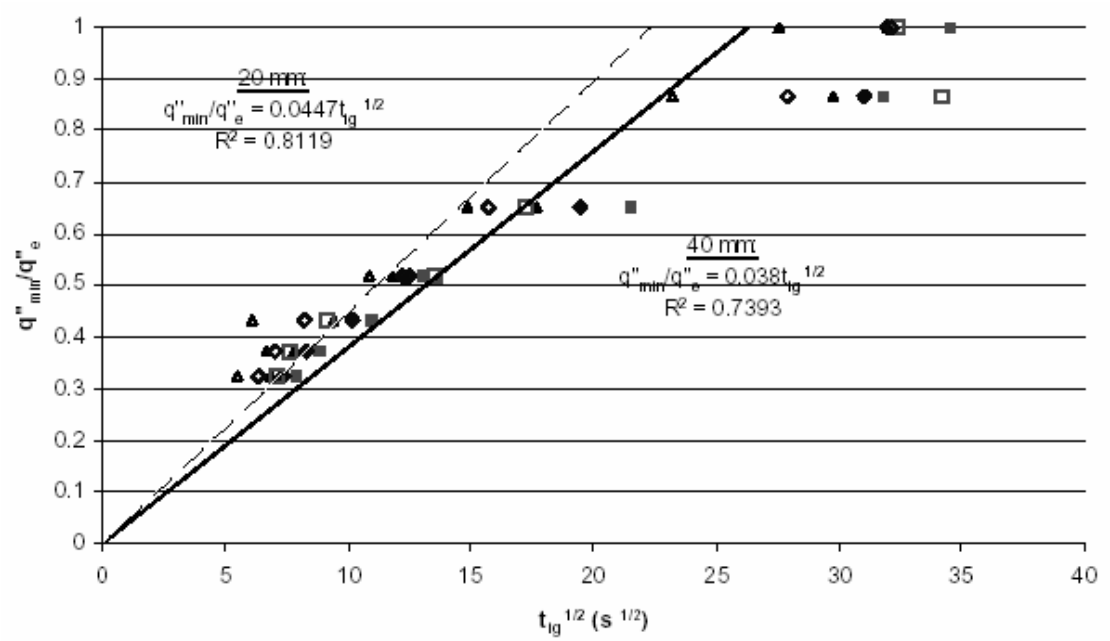

Figure 58 Ignition Plot - ASTM E 1321, Plywood, Reproduced from Ngu (2001)

The graphs shown in Figures 50 – 58 are the averaged results of the experimental tests. There were three ignition tests conducted at each heat flux setting for the particle board and the LVL specimens. The particle board samples were tested at 40kW/m²; 35kW/m², 30kW/m² and 20kW/m² whereas the LVL samples were tested at heat flux settings of 50kW/m², 40kW/m²; 30kW/m² and 20kW/m². In Ngu's study there were five repetitions at each heat flux of 40kW/m²; 35kW/m², 30kW/m², 25kW/m²; 20kW/m², 17kW/m², 16kW/m² and 15kW/m². The repeatability of the results were mixed for all wood species, this is shown in Table 2. As expected as the heat flux was decreased the variation in ignition time increased

Timber Type	Radiata Pine	Rimu	Beech	Macrocarpa	MDF	Plywood	Particle Board	LVL
Incident Flux	Δt_{ig} [s]	Δt_{ig} [s]	Δt_{ig} [s]	Δt_{ig} [s]	Δt_{ig} [s]	Δt_{ig} [s]	Δt_{ig} [s]	Δt_{ig} [s]
40kW/m²	17	17	19	7	11	20	8	8
30kW/m²	20	56	33	12	24	20	13	16
20kW/m²	201	407	120	345	58	62	120	23

Table 2 Variation in ignition times

At the high heat flux of 40kW/m² the time to ignition varied from 7 seconds (Macrocarpa) to 20 seconds (Plywood) (see Table 2). The lower the applied heat flux, the larger in the variation in ignition times. At 20kW/m², the ignition time variation was as large as 407 seconds (Rimu) compared with only a 23 second variation for the

LVL wood species. The time variation between wood types is interesting to note, for natural woods such as Radiata Pine, Rimu, Beech, and Macrocarpa the ignition times had at least a two minute difference, whereas for the wood composites the ignition times varied up to two minutes. It is observed that as the critical ignition heat flux draws nearer the time variation to ignition increases. At the lower applied heat flux, the effect of smouldering was more evident, the effect of smouldering has varying effects on the wood's chemistry. The chemistry in natural wood is complex therefore at the lower heat fluxes the ignition times are widely varied because of the complexity of many different reactions that can take place, Dietenberger (1994) and Kanury (2002). Comparing this to the wood composites which contain adhesive resins to keep the wood together, the resin's chemistry is less complex in comparison so time variation are not as great as shown by the deviation of the results of the repeatability tests in Table 2.

The theory of Quintiere and Harkleroad (1985) uses a thermal conduction model to analyse the results of the ignition from the LIFT tests. The application of the theory relies on the sample being thermally thick. In reports by Fernandez-Pello and Hirano (1983) and Quintiere (2002), solids with thicknesses, $\delta > 1$mm can be regarded as thermally thick. Thicknesses of 10 to 20mm also depend on the substrate material adjacent to the solid. Another condition is that the ignition time of the wood sample has to be less than the thermal equilibrium time, t*. In all instances this has been the case as shown in Table 3. No tests were conducted at the 30kW/m² irradiance levels.

		Macrocarpa				Beech				Rimu				Radiata Pine			
q_{crit}''	[kW/m²]	17	17	17	17	16	16	16	16	14	14	14	14	15	15	15	15
b		0.065	0.065	0.065	0.065	0.057	0.057	0.057	0.057	0.044	0.044	0.044	0.044	0.059	0.059	0.059	0.059
q_e''	[kW/m²]	30	40	50	60	30	40	50	60	30	40	50	60	30	40	50	60
q_{crit}'' / q_e''		0.567	0.425	0.340	0.283	0.533	0.400	0.320	0.267	0.467	0.350	0.280	0.233	0.500	0.375	0.300	0.250
time to Ignition [s]		-	6	3	2	-	4	2	2	-	5	3	4	-	7	4	3
t*	[s]	75	42	27	19	89	50	32	22	110	62	40	28	72	41	26	18
		Plywood				**MDF**				**Particle Board**				**LVL**			
q_{crit}''	[kW/m²]	13	13	13	13	15	15	15	15	14.7	14.7	14.7	14.7	17.2	17.2	17.2	17.2
b		0.047	0.047	0.047	0.047	0.048	0.048	0.048	0.048	0.056	0.056	0.056	0.056	0.121	0.121	0.121	0.121
q_e''	[kW/m²]	30	40	50	60	30	40	50	60	30	40	50	60	30	40	50	60
q_{crit}'' / q_e''		0.433	0.325	0.260	0.217	0.500	0.375	0.300	0.250	0.490	0.368	0.294	0.245	0.573	0.430	0.344	0.287
time to Ignition [s]		-	6	4	3	-	10	7	5	-	15	10	8	-	1	1	1
t*	[s]	83	47	30	21	110	62	40	28	77	43	28	19	22	13	8	6

Table 3 Thermal Equilibrium Times for Applied Heat Fluxes

The results from the ignition test data have been tabulated and are presented in Table 4.

Ignition Data	Wood Species		Macrocarpa	Beech Wood	Rimu	Radiata Pine	Plywood	Medium Density Fibre Board (MDF)	Particle Board	Laminated Veneer lumber
	q_{ig}''	[kW/m²]	17	16	14	15	13	15	14.7	17.2
	T_{ig}	[°C]	508	494	464	480	447	480	464	508
	b	$s^{-1/2}$	0.065	0.057	0.044	0.059	0.047	0.048	0.056	0.121
	h	[kW/m²·K]	0.0348	0.0338	0.0315	0.0326	0.0304	0.0326	0.0331	0.0352
	kρc	$[kW/m^2 \cdot K]^2 \cdot s$	0.3657	0.4465	0.6539	0.3889	0.5343	0.5876	0.4450	0.1080

Table 4 Parameters derived from the ignitability tests

As the table suggests the critical ignition heat flux varies between wood species and does not show any preference between wood types. The lowest critical ignition heat flux was that of the plywood sample at 13kW/m². The highest critical heat flux was that of the Macrocarpa and the LVL sample at 17kW/m².

As detailed in the ignition theory section, the function $F(t_{ig})$ can be approximated by Equation 15. In Figures 51 – 58 the slope is equal to $b = 2h_{ig} / \sqrt{\pi k \rho c}$, as derived by Quintiere et al (1983). The function $F(t_{ig})$ can be then be applied to the flame spread data analysis provided the surface temperature is less than T_{ig}. Using Equation 15 the time to thermal equilibrium, t^* can be calculated at each heat flux for each wood type. The time to thermal equilibrium decreases as the applied heat flux increases. A common trend was observed between the thermal equilibrium times and applied heat flux. At the 20kW/m² irradiance the thermal equilibrium times were highest, at 30kW/m² the thermal equilibrium times decreased to 44% of the previous time. Similarly at 40kW/m² the thermal equilibrium time decreased a further 36% and at the 60kW/m² irradiance the thermal equilibrium time decreased a further 30%.

The heat transfer coefficient, h changes very little between wood species. The heat transfer coefficient is dependant on:

$$h = \frac{\dot{q}_{ig}''}{T_{ig} - T_{\infty}} \tag{32}$$

where T_∞ is the ambient temperature. The effective thermal property is given as:

$$k\rho c = \frac{4}{\pi}\left(\frac{h}{b}\right)^2 \qquad \textbf{(33)}$$

The product of the thermal conductivity, k, density, ρ and specific heat, C is also known as the thermal inertia. The time to ignition of material depends on the thermal inertia of the material itself, Buchanan (2001). It is expected that those materials with low thermal inertia will heat more rapidly than materials with higher thermal inertia which would lead to much more rapid ignition. Timber's thermal property range from 108$W^2 \cdot s/m^4 \cdot K^2$ (LVL) to 654$W^2 \cdot s/m^4 \cdot K^2$ (Rimu), these values are low in comparison to other materials such as 1.6×10^9 $W^2 \cdot s/m^4 \cdot K^2$ (Steel) and $2\times10^6 W^2 \cdot s/m^4 \cdot K^2$ (Concrete), Buchanan (2001). The calculated thermal property of the wood suggests that these materials ignite more readily than others. Contrasting this theory is the ignition results which show the Rimu (14kW/m²) igniting at a lower heat flux than the LVL (17kW/m²) samples.

9 Flame Spread Tests – Results and Discussions

The flame spread tests were conducted using the cone calorimeter in the vertical orientation. The positioning of the sample is shown in Figure 59 and Figure 60. The raw results obtained from the video analyse are presented in Appendix A. The flame spread results as calculated from the video analysis are shown in Figure 61, Figure 62 and Figure 63. As with the ignition analysis the flame spread analysis was carried out in accordance with ASTM E 1321.

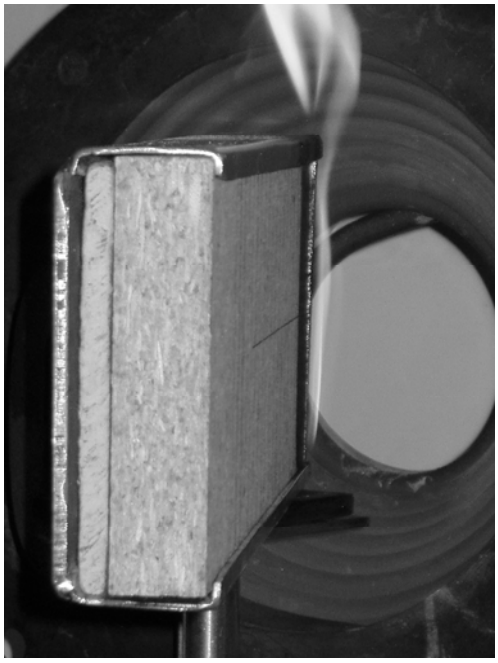

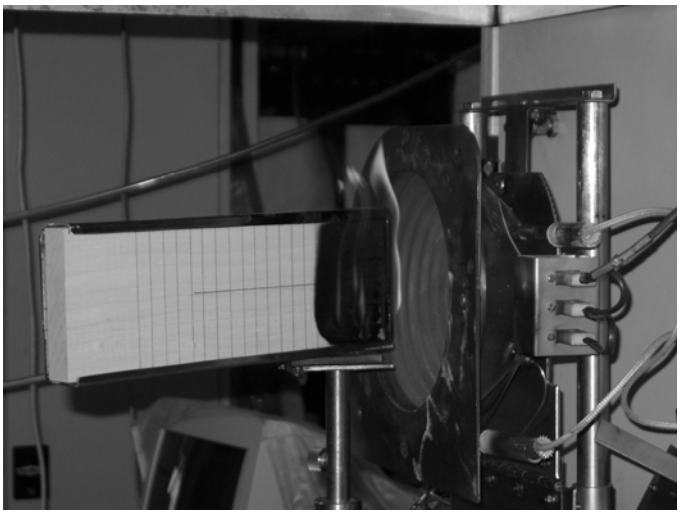

Figure 59 (Left) Flame spread experiment for Particle board specimen

Figure 60 (Above) Flame spread experiment for Macrocarpa specimen

The Quintiere et al flame spread model was applied to these test results. The data gathered was then tabulated and graphs were plotted to obtain the necessary outputs and parameters. The following theory is a excerpt out of section 6.5. The flame front velocity is calculated using the three point least squares fit to measure the flame front, where x is the position and *t* is the time.

$$V = \frac{\Sigma(tx) - \frac{\Sigma t \Sigma x}{3}}{\Sigma t^2 - \frac{(\Sigma t)^2}{3}} \qquad \textbf{(19)}$$

The surface flux configuration invariant, F(x) as defined in the ASTM 1321, is given by: $F(x) = \frac{\dot{q}_e''(x)}{\dot{q}_e''(crit.)}$

Using this relationship the surface flux at a measured flame front position is given by:

$$\dot{q}_e''(x) = F(x) * \dot{q}_e''(crit.) \quad \textbf{(20)}$$

The flame spread data can then be shown as a plot of:

$$V^{-1/2} \ versus \ \dot{q}_e''(x)F(t)$$

Where:

$$F(t) = \begin{cases} b\sqrt{t}, & t \le t^* \\ 1, & t \ge t^* \end{cases}$$

This method of calculating the flame front velocity is used in the ASTM E1321 standard and to maintain consistency was applied to results. Difficulties arose in interpreting the results as it was felt the standard was unclear in the calculation of the flame front velocity. For instance taking the equation for V as written in the standard:

$V = \frac{\Sigma tx - \frac{\Sigma t \Sigma x}{3}}{\Sigma t^2 - \frac{(\Sigma t)^2}{3}}$, the term Σtx can be interpreted in three ways, these are:

$\Sigma t \cdot x$ **or** $\Sigma t \cdot \Sigma x$ **or** $\Sigma(t \cdot x)$

By recalculating previous data from a LIFT research, Nisted (1991) the latter proved to be the correct method. It was assumed that the method used by Nisted (1991) was correct as the data was calculated using computer software from NIST.

Once the flame front velocity is found, the critical ignition heat flux can then be extrapolated and the various thermal properties can also be calculated. As mentioned in section 6.4 the fit of the data is subjective as no specific guidance is given in the standard to want warrants a straight line fit. This part of the analysis is dependent on

the judgment of the individual therefore the results can vary accordingly. The lack of protocol within the standard has been noted by Babrauskas (1999).

9.1 Flame Front Velocities

The flame fronts positions are shown against time in Figure 61 (40kW/m²), Figure 62 (50kW/m²) and Figure 63 (60kW/m²). Each plot shown is an average of three repeatability tests carried out at each heat flux for each wood species. In all graphs the results are plotted against the same scaled *x* and *y* axis to make obvious the effect of increasing the applied heat flux. The behaviour of each wood species shows that wood type to be independent of the applied heat flux. The effect of the higher heat flux is that the flame front velocity is quicker. This is shown by the shallower gradients of each wood species as the applied heat flux is increased. As expected, the higher heat flux the flame front can be seen to travel further along the wood sample as expected, and in doing so the flame front travels for a longer period of time.

The behaviour shown by the wood species is consistent for each heat flux setting. The MDF has the slowest flame front velocity, whereas the LVL sample consistently has the fastest flame front velocity. No correlation is evident from these results to show whether or not natural wood has a slower flame front velocity than wood composites or vice versa. Table 5, sets out the densities and moisture content of the wood species. No pattern emerged with each wood species behaving independent of any factor. The figures, however do show that the flame front velocity seems to be consistent through wood type. Ranked from slowest flame front velocity to fastest is: MDF; Pine; Plywood; Rimu; Particle Board; Beech; Macrocarpa and LVL. This order is repeated each time for each different applied heat flux test.

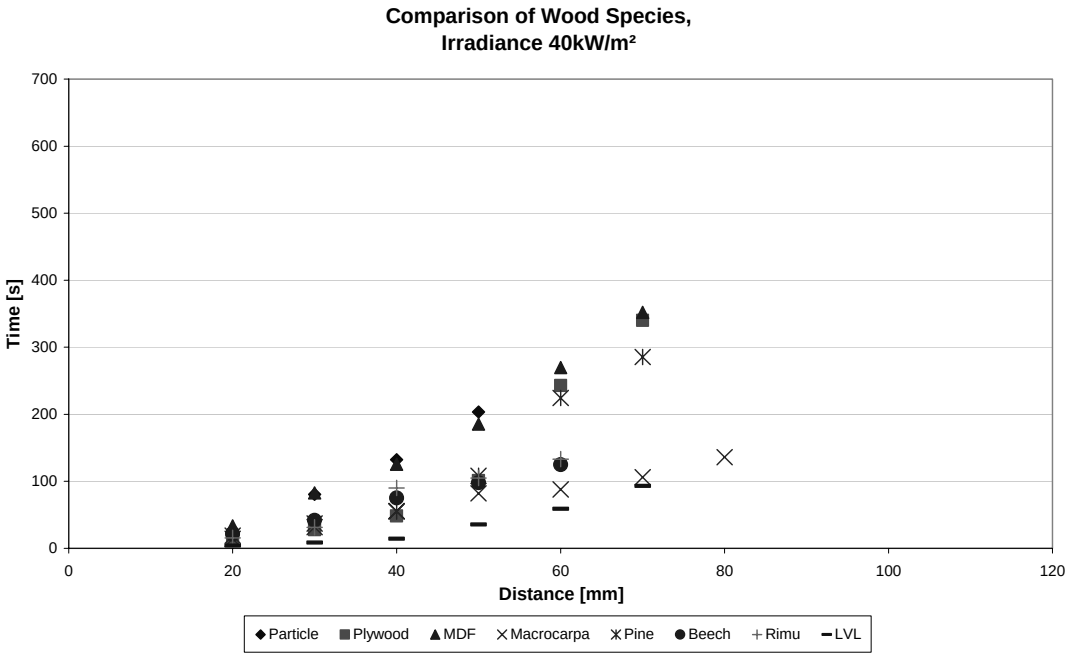

Figure 61 Comparison of surface flame spread 40kW/m² - 707°C

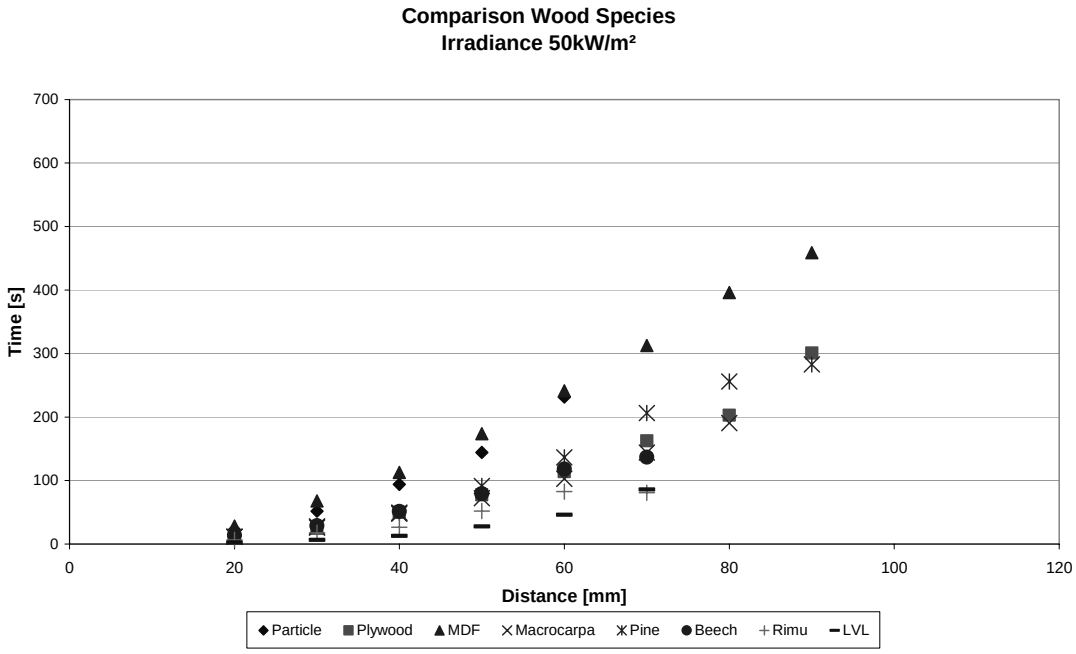

Figure 62 Comparison of surface flame spread 50kW/m² - 770°C

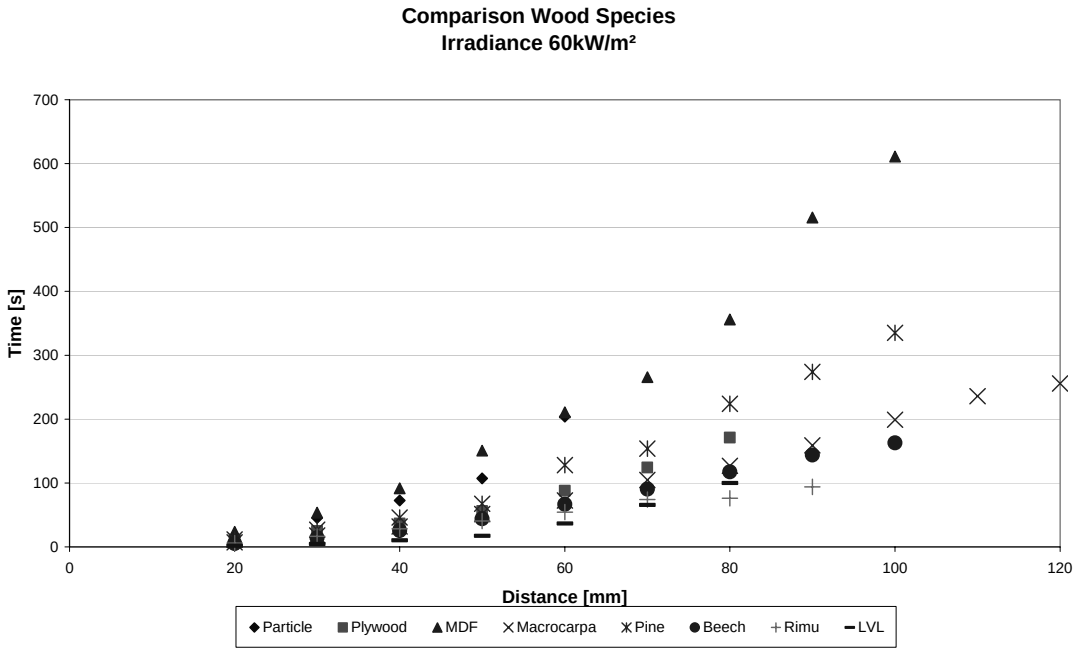

Figure 63 Comparison of surface flame spread 60kW/m² - 825°C

	density	$X_{initial}$ (%)	X_{final} (%)
mdf	727	8.4	8.5
Beech	586	13.5	12.6
Rimu	568	14.8	13.4
Macrocarpa	517	13.5	11.6
Plywood	507	10.6	10.5
Radiata Pine	454	11.9	11.4

Table 5 Density and Moisture content of 20mm samples – Reproduced from Ngu (2001)

9.2 Flame Spread Correlation – Velocity Plots

The theory by Quintiere suggests that flame spread time, t_s be the same as or less than the thermal equilibrium time, t*. In the model by Quintiere the preheating times before the flame front was inadequate to achieve thermal equilibrium at the exposed surface. The thermal response function, F(t), is introduced to correct the failure to meet thermal equilibrium in the preheating time. The thermal response function is multiplied by $\dot{q}_e^{"}(x)$ which is the measured incident flux at position x along the sample. In Figures 64 – 87 the result of plotting the function $\dot{q}_e^{"}(x) \cdot F(t) \, versus \, \sqrt{V}$ is shown. The graphs are grouped by wood type showing the results for each wood species at each applied heat flux. The general order of the graphs are 40kW/m², 50kW/m² and 60kW/m².

9.2.1 Flame velocity Plots for Particle Board

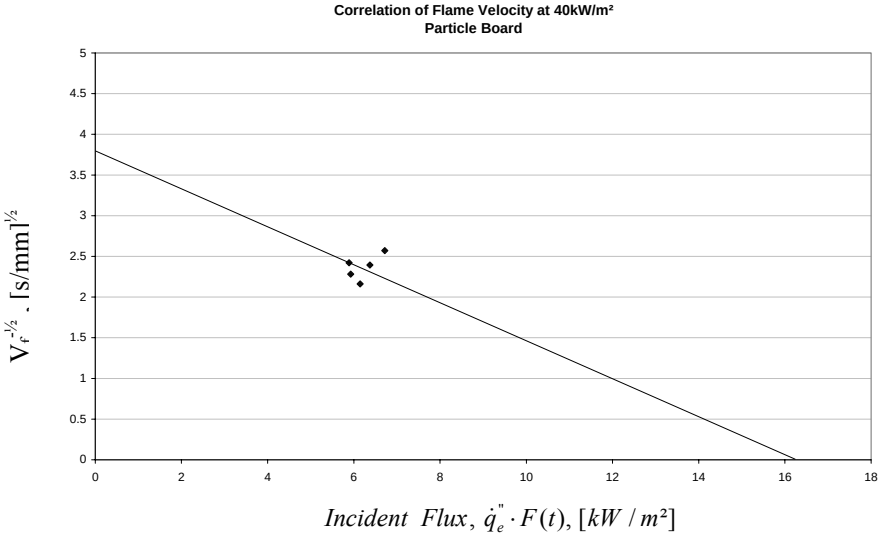

Figure 64 Flame velocity plot for Particle Board, 40kW/m²

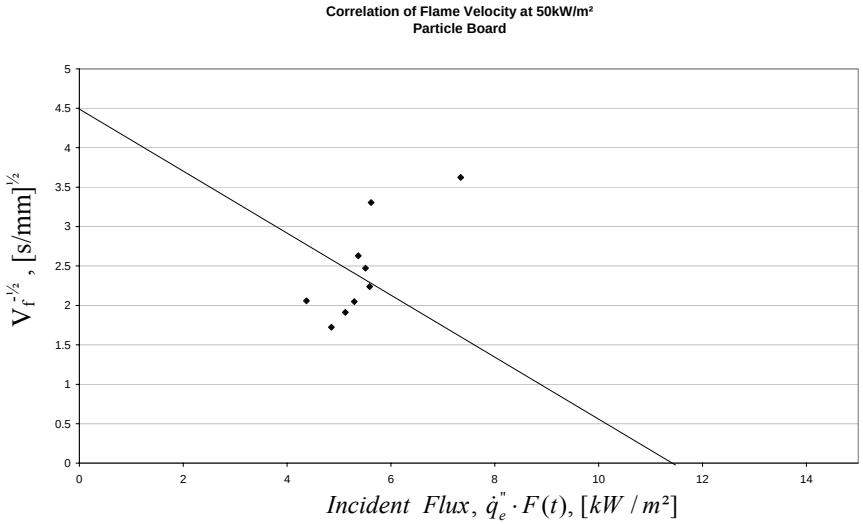

Figure 65 Flame velocity plot for Particle Board, 50kW/m²

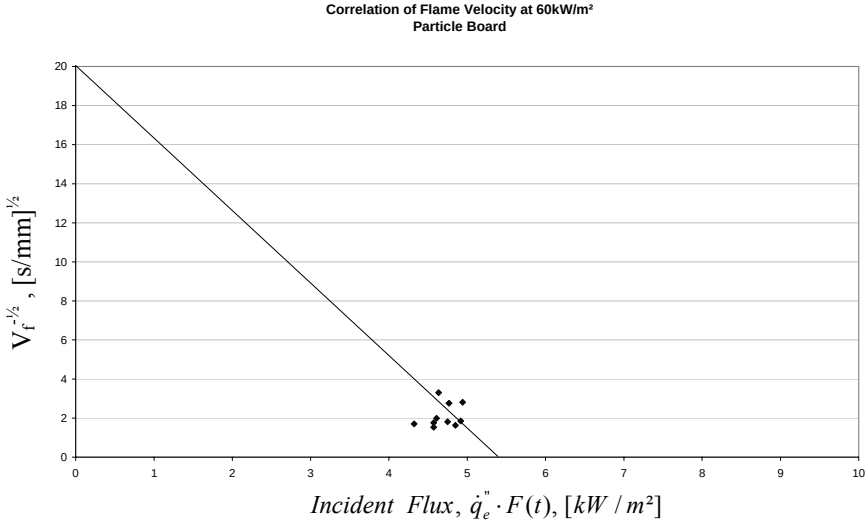

Figure 66 Flame velocity plot for Particle Board, 60kW/m²

9.2.2 Flame velocity Plots for Plywood

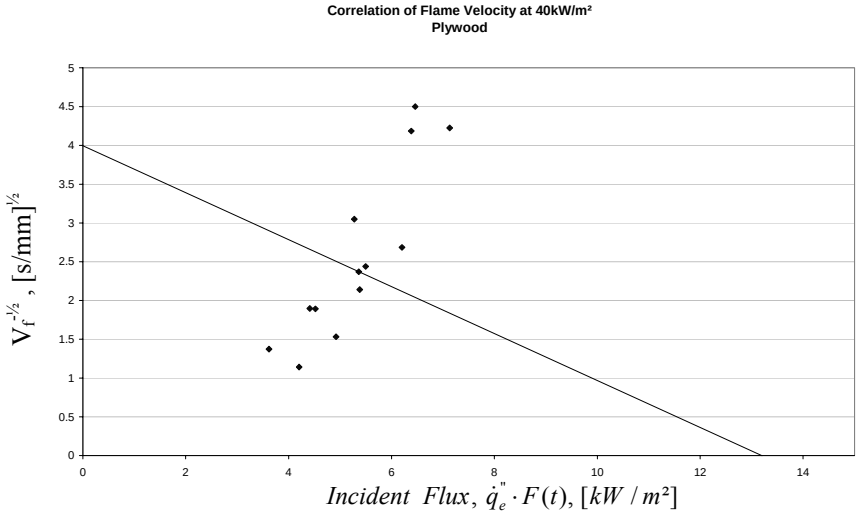

Figure 67 Flame velocity plot for Plywood, 40kW/m²

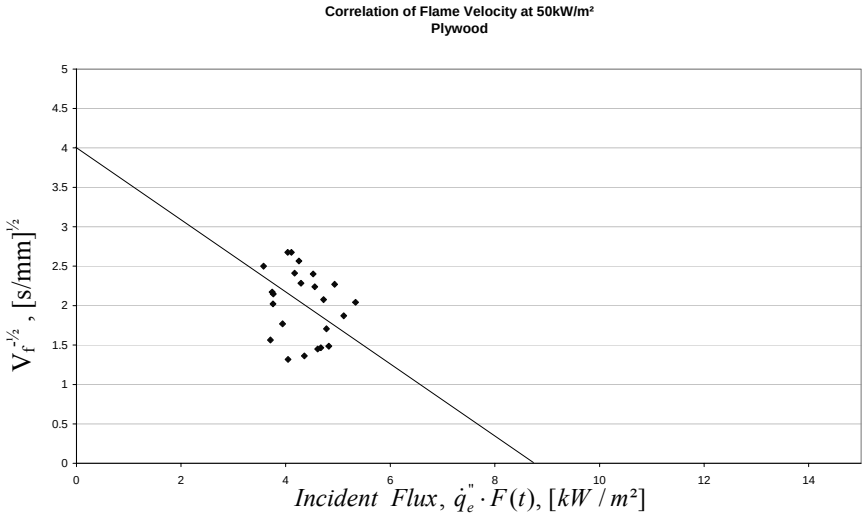

Figure 68 Flame velocity plot for Plywood, 50kW/m²

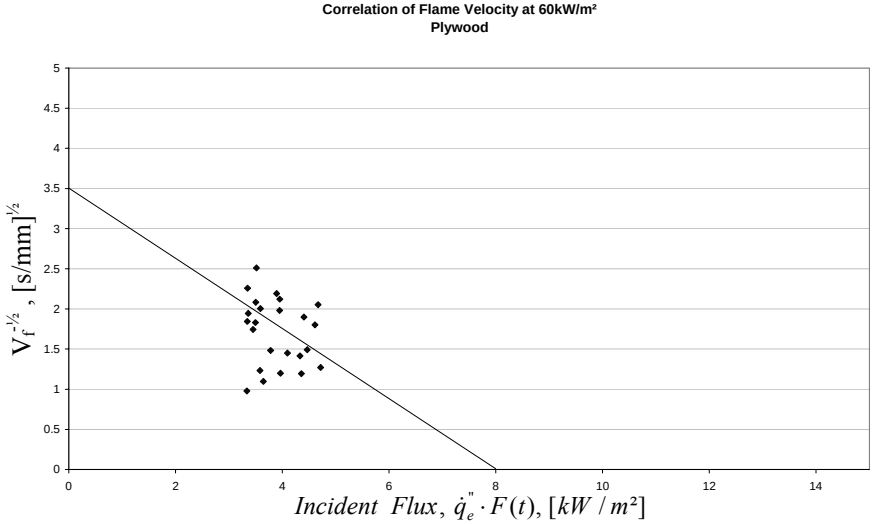

Figure 69 Flame velocity plot for Plywood, 60kW/m²

9.2.3 Flame velocity Plots for Medium Density Fibre Board (MDF)

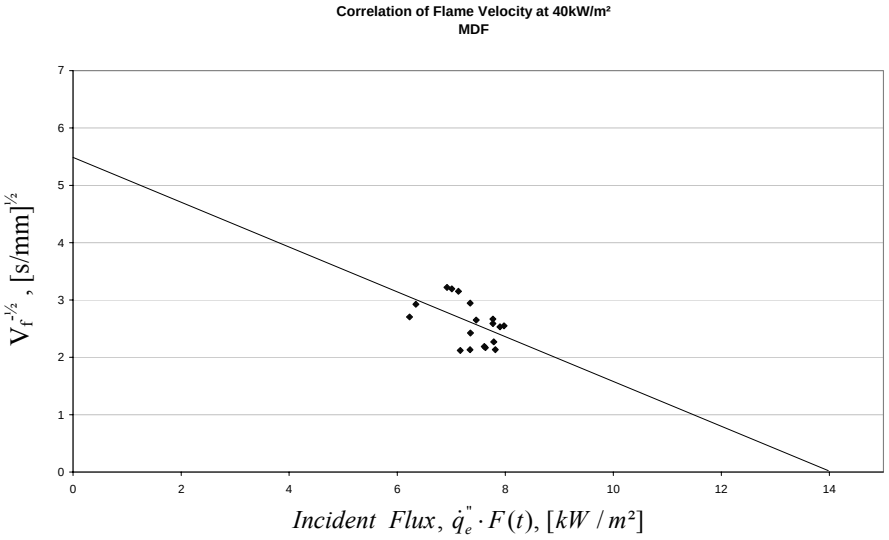

Figure 70 Flame velocity plot for MDF, 40kW/m²

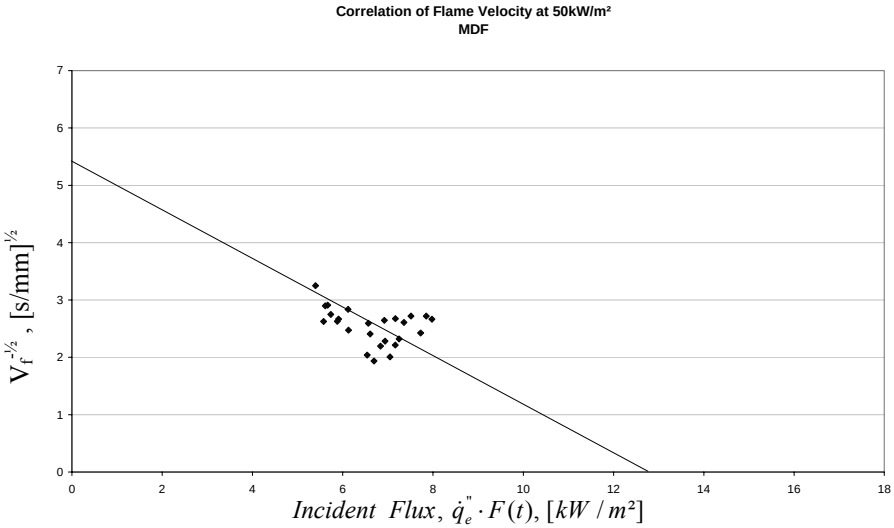

Figure 71 Flame velocity plot for MDF, 50kW/m²

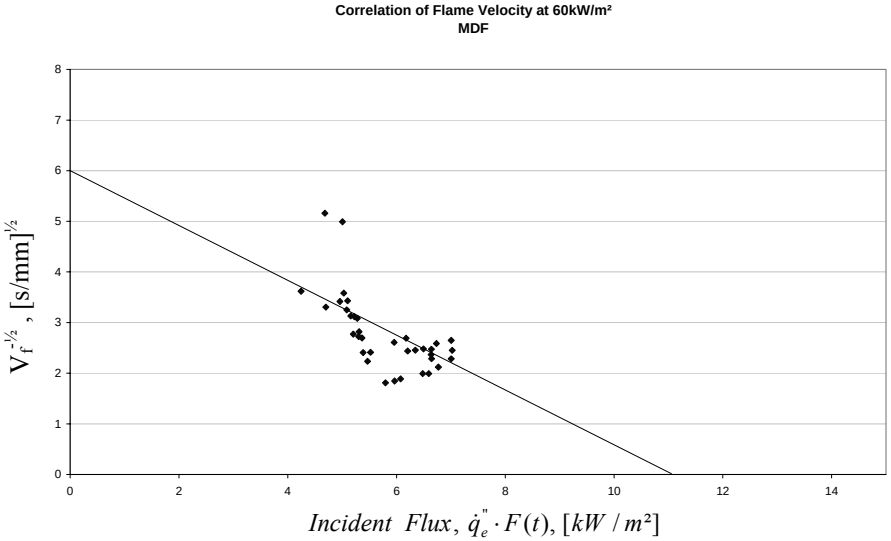

Figure 72 Flame velocity plot for MDF, 60kW/m²

9.2.4 Flame velocity Plots for Macrocarpa

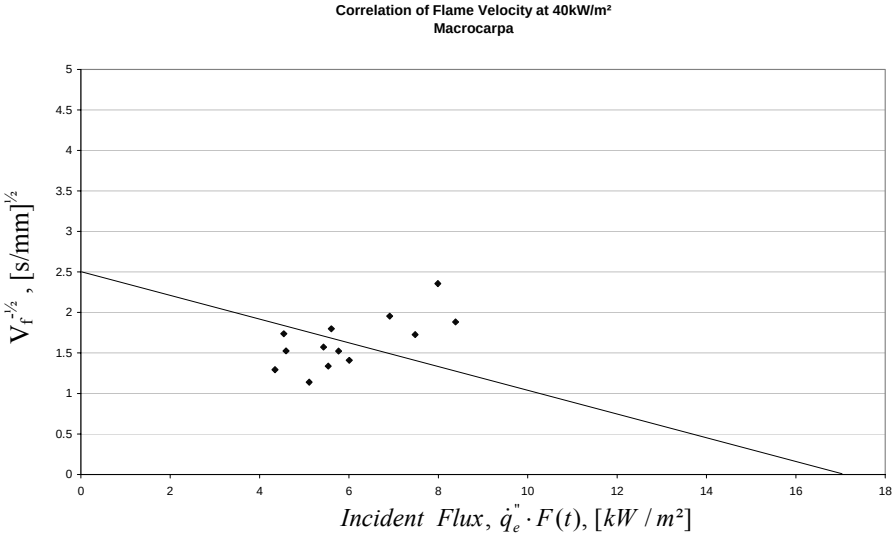

Figure 73 Flame velocity plot for Macrocarpa, 40kW/m²

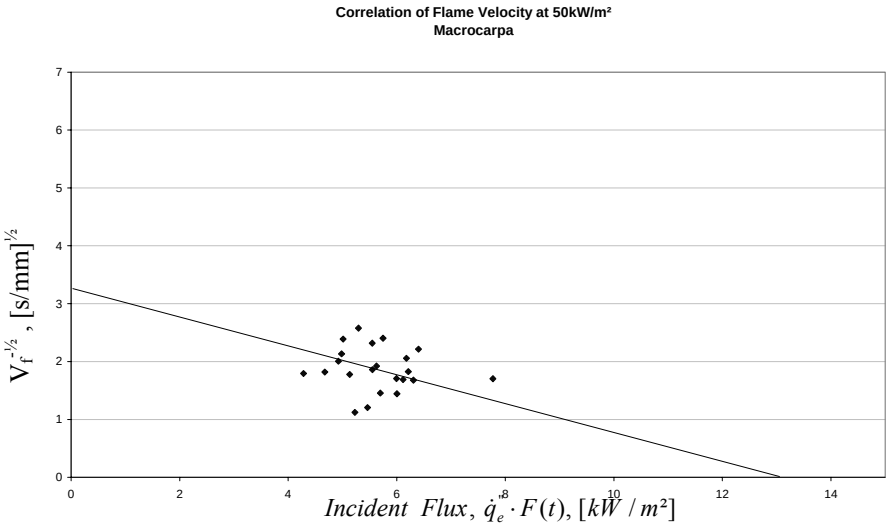

Figure 74 Flame velocity plot for Macrocarpa, 50kW/m²

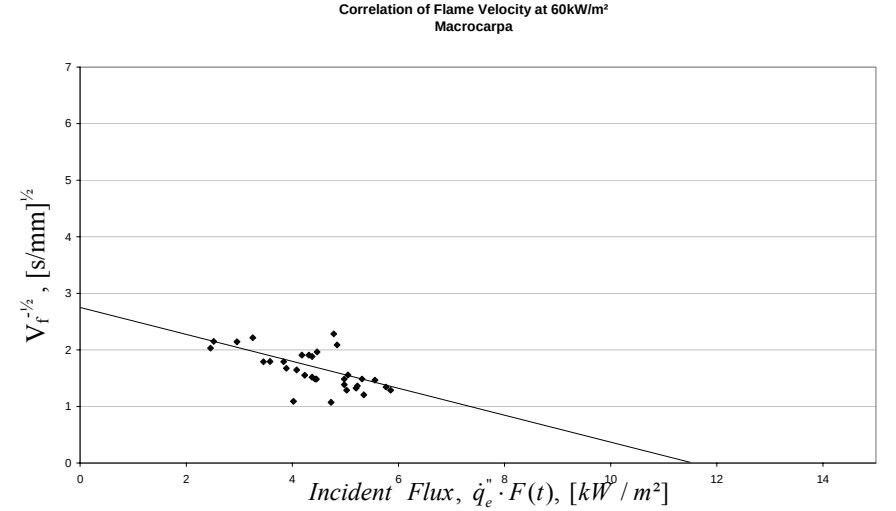

Figure 75 Flame velocity plot for Macrocarpa, 60kW/m²

9.2.5 Flame velocity Plots for Radiata Pine

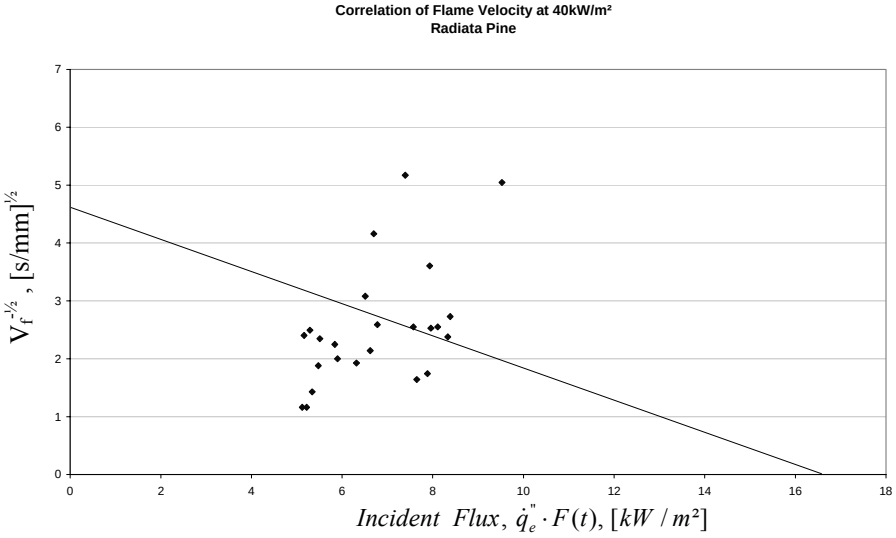

Figure 76 Flame velocity plot for Radiata Pine, 40kW/m²

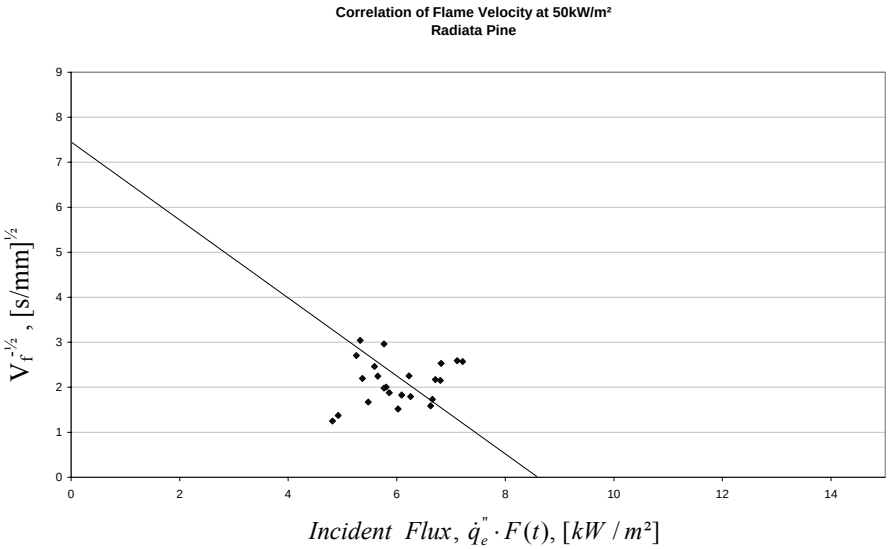

Figure 77 Flame velocity plot for Radiata Pine, 50kW/m²

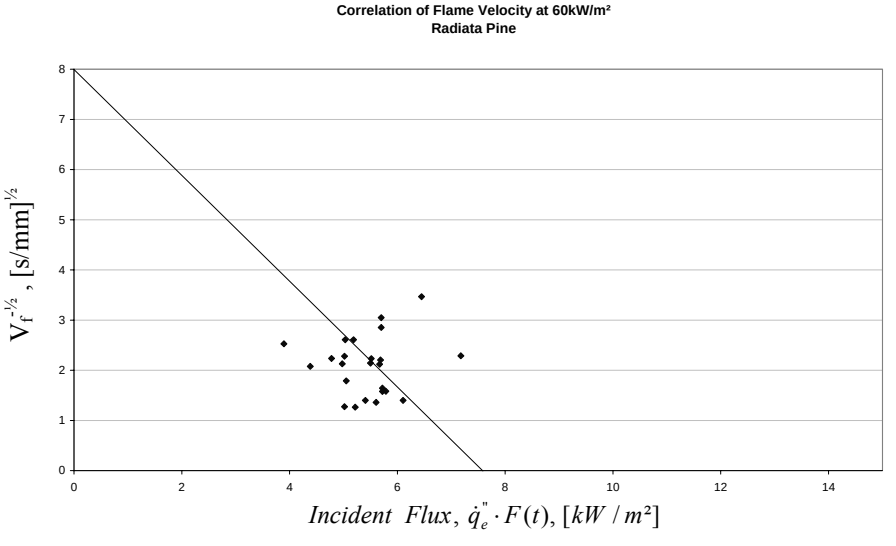

Figure 78 Flame velocity plot for Radiata Pine, 60kW/m²

9.2.6 Flame velocity Plots for Beech

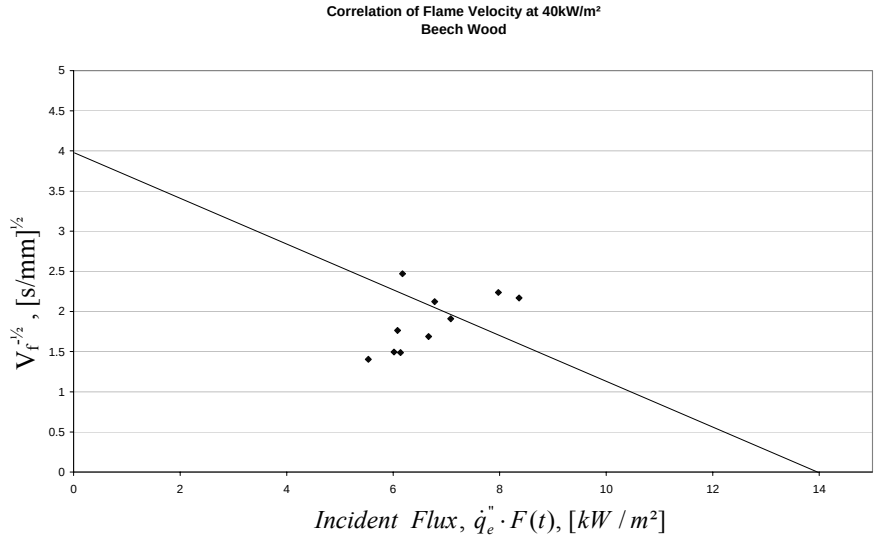

Figure 79 Flame velocity plot for Beech, 40kW/m²

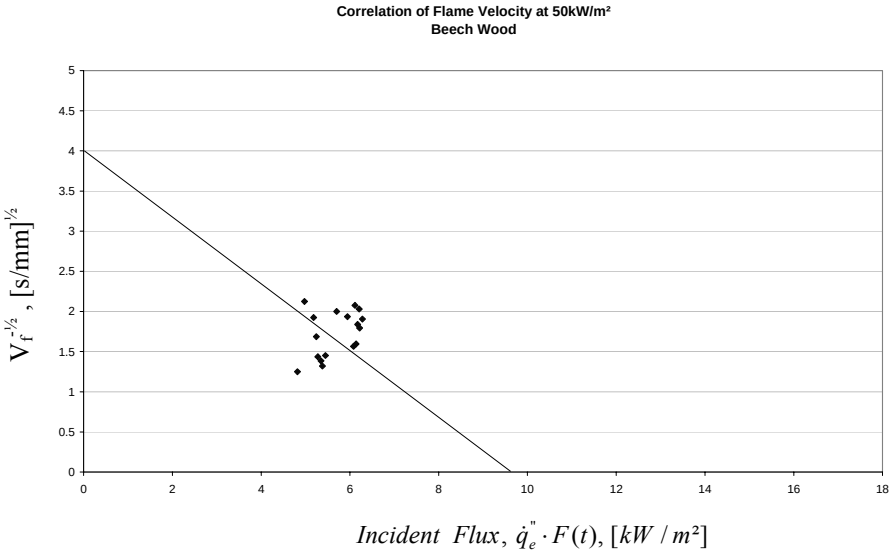

Figure 80 Flame velocity plot for Beech, 50kW/m²

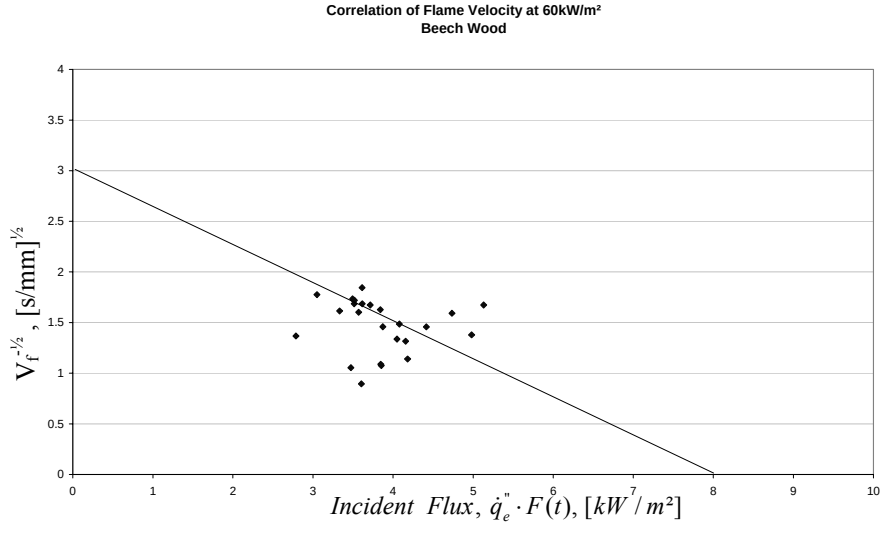

Figure 81 Flame velocity plot for Beech, 60kW/m²

9.2.7 Flame velocity Plots for Rimu

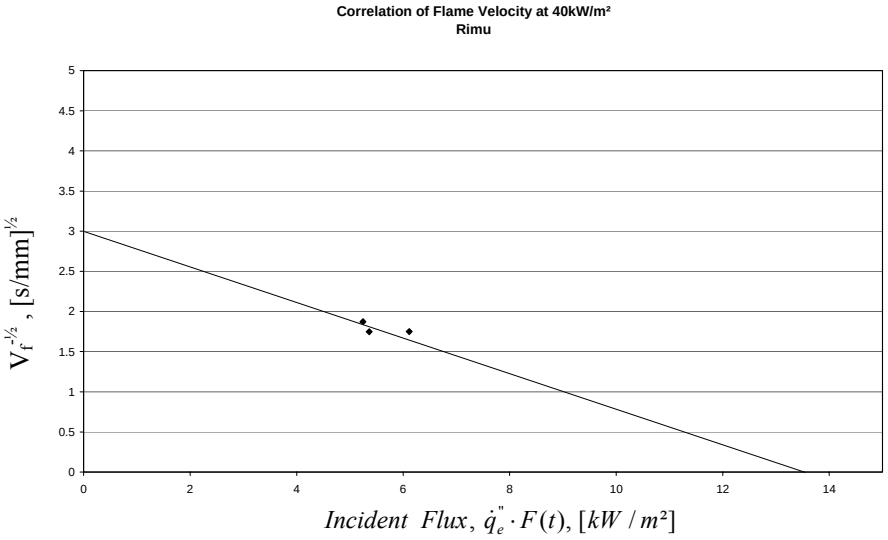

Figure 82 Flame velocity plot for Rimu, 40kW/m²

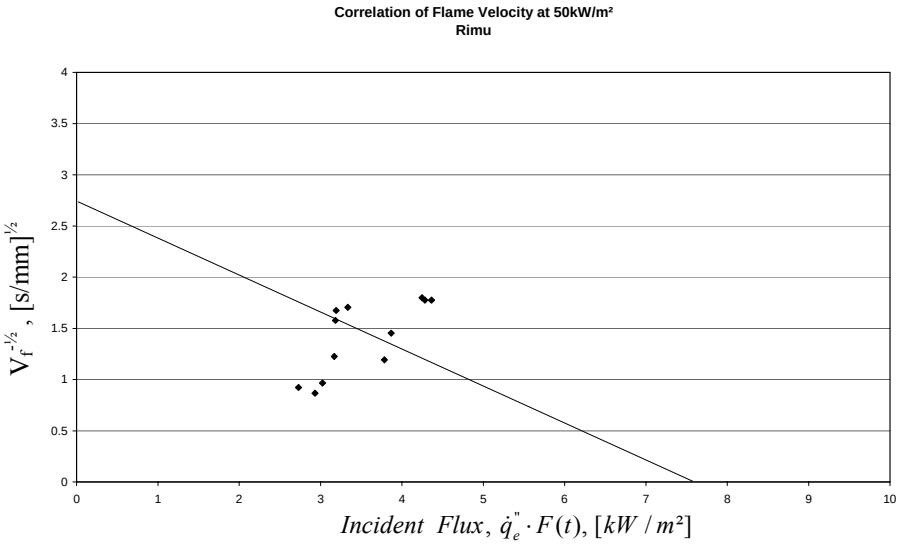

Figure 83 Flame velocity plot for Rimu, 50kW/m²

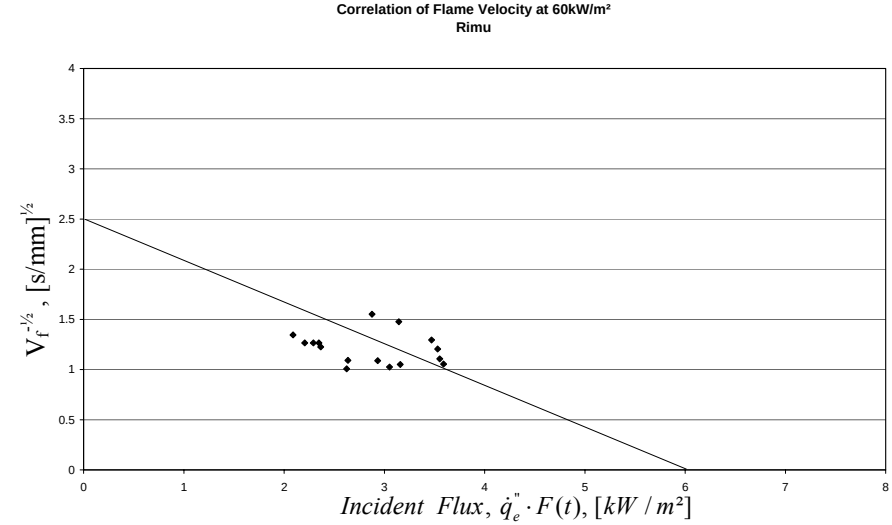

Figure 84 Flame velocity plot for Rimu, 60kW/m²

9.2.8 Flame velocity Plots for Laminated Veneer Lumber

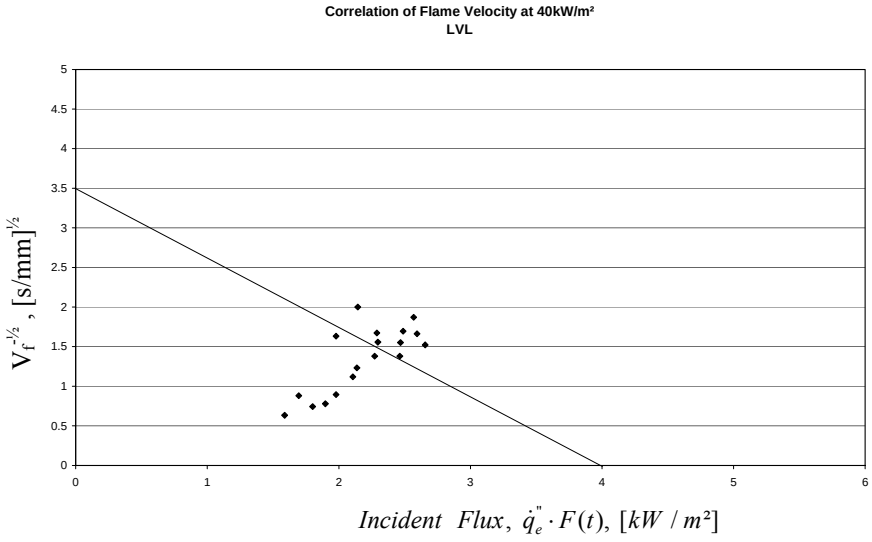

Figure 85 Flame velocity plot for LVL, 40kW/m²

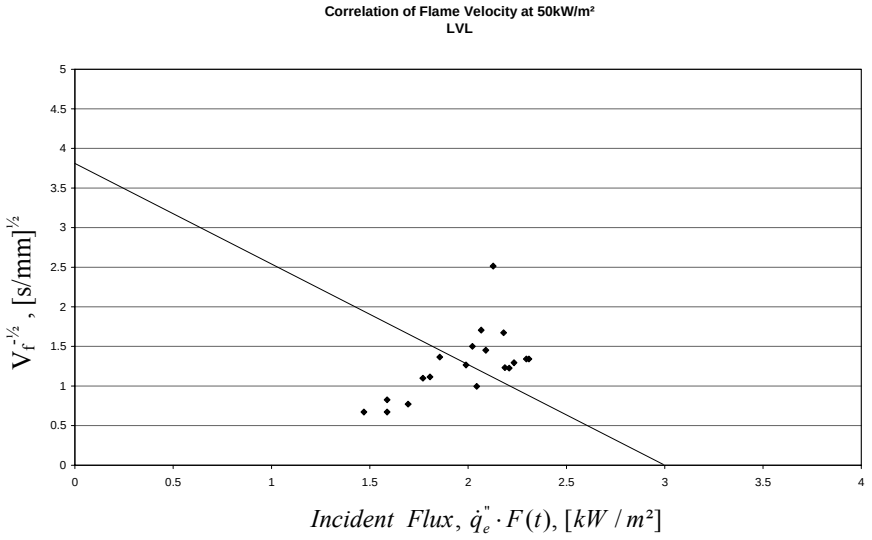

Figure 86 Flame velocity plot for LVL, 50kW/m²

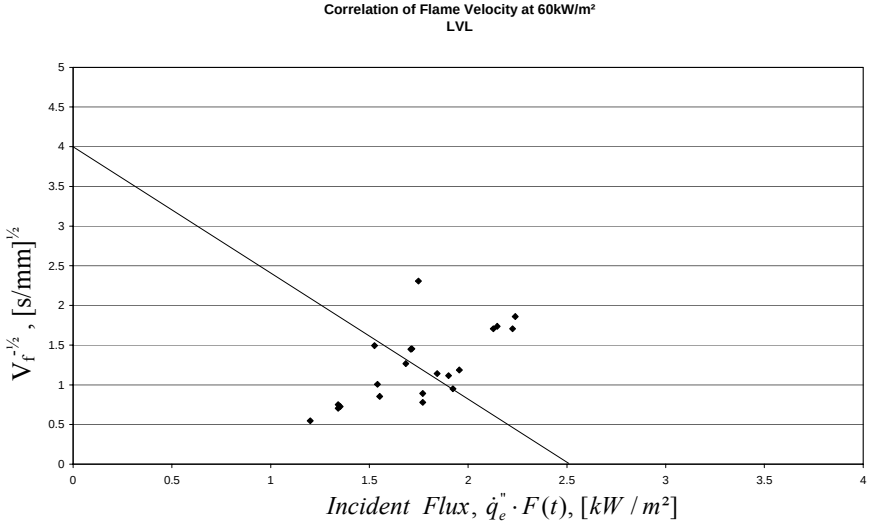

Figure 87 Flame velocity plot for LVL, 60kW/m²

The velocity data contained in Figures 64 – 87 is plotted according to ASTM E 1321. In all cases the data points show very poor linear relationship. The variation shown by the scatter in the data points indicate that very little confidence can be expressed in these results. In LIFT results by Quintiere et al (1985), Nisted (1991) and Babrauskas (1999), it has been observed that the data points illustrate quite a good correlation to a straight line fit. In comparison, RIFT tests have shown to vary widely. The results of this study show that for some wood species that is MDF and Macrocarpa a reasonable straight line correlation exists, whereas for the others, the straight line has been drawn more for completeness. Other experiments using the RIFT have shown widely varying results, Azhakesan (1998) produced reasonable data and had a good correlation with Quintiere's theory. The results by Pease (2001) had a similar outcome to those obtained in this study with wide variation in data points. The poor correlation can be attributed to the function *F(t)* as this function is to account for varying preheating times. Quintiere et al (1983, 1985) found that flame spread correlation departs from a linear relationship at low preheating times. The result shown in Figures 64 – 87 highlights these observations particularly those with short preheat time such as LVL and radiata pine. A comparison of the studies is shown by the reproduced results for plywood in Figure 88 and Figure 89 for Azhakesan et al and Pease respectively.

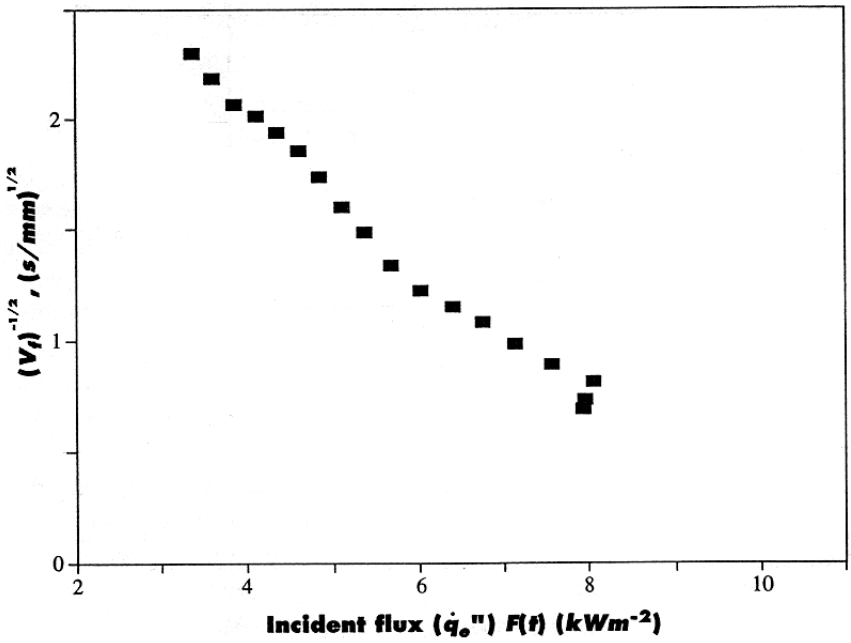

Figure 88 Correlation of Spread velocity, Plywood - Reproduced from Azhakesan et al (1998)

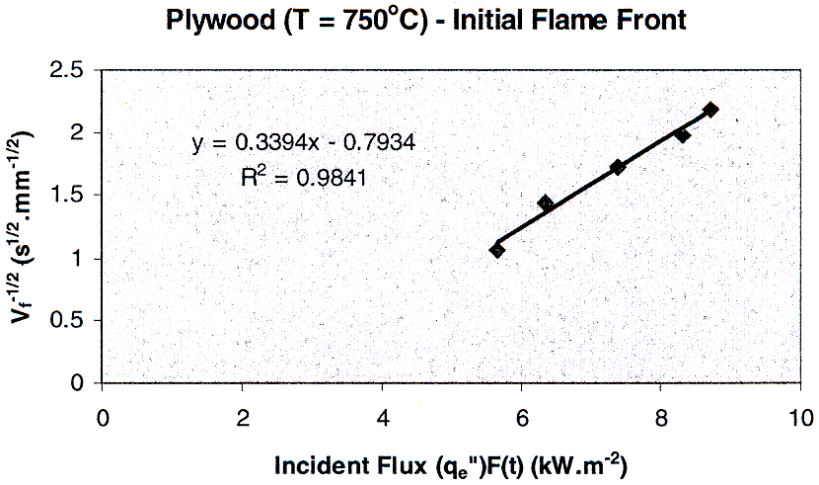

Figure 89 Flame Spread Correlation, Plywood - Reproduced from Pease (2001)

There is a significant difference between studies in the range of data obtained. Figure 90 illustrates the results for plywood from Azhakesan et al (1998), it can be seen the flame spreads up to 200mm of the sample's surface whereas in Pease (2001) shown in Figure 91 the flame spread is only 90mm of the sample's surface. The results shown by Pease (2001) are indicative of the results obtained in this study. The results of Pease and of this study do not produce the same consistency as shown by Azhakesan. As suggested in section 7.3, by modifying the apparatus so that the sample is exposed to the full face of the cone, quite possibly a wider range of data could be obtained, this could provide analytical advantages. The results would effectively double and enable further data points to be plotted. Photos of test specimens are shown in Figure 93

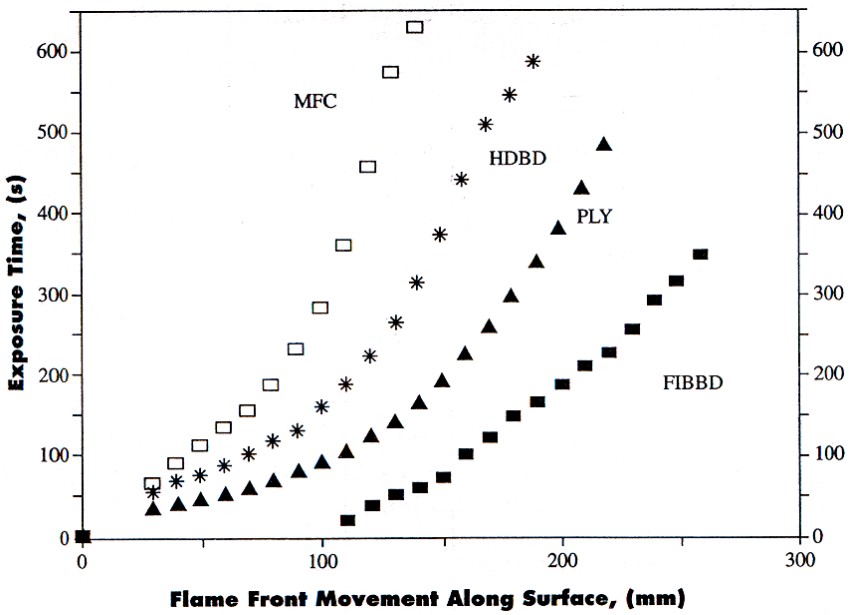

Figure 90 Surface Flame Spread Rate - Reproduced from Azhakesan et al (1998)

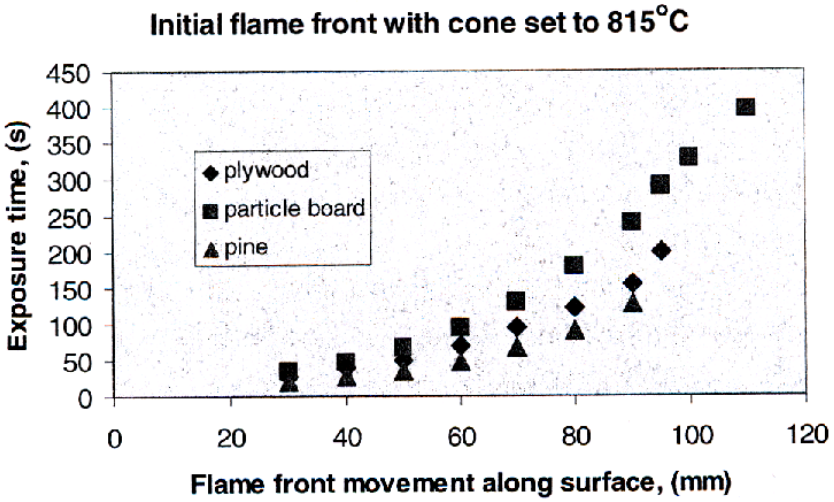

Figure 91 Surface Flame Spread Rate - Reproduced from Pease (2001)

A common test specimen between the RIFT studies is plywood. At the University of Ulster the plywood was tested at 755°C, the equivalent tests conducted by Pease at the University of Newcastle and from this study are at 50kW/m², with temperature readings of the cone element of 750°C and 770°C respectively. By isolating the plywood results and making a direct comparison of the flame spread rate it can be shown that Azhakesan had considerably more flame spread along the sample compared to the Australasian studies. At 50kW/m², we achieved flame spread of only 90mm along the sample and in Pease's study he was observed to attain 100mm whereas Azhakesan obtained results double the Australasian studies with flame spread of up to 220mm along the length of the sample. It is unsure, as to why a difference exists as the repeatability tests in the Australasian studies produced consistent results and did not extend further than 100mm even at a higher applied heat flux of 60kW/m², a cone temperature of 825°C.

The comparison shown in Figure 92 confirms the observations made from Figure 46 and Figure 47, which is the results in the Australasian studies are too clustered to allow any correlations to be drawn. The correlation flame velocity plots of Figures 67 – 87 are of all test results, if only averaged data points were shown as by Azhakesan (Figure 90) there would be too few points on the graph to be meaningful. This reinforces the fact that to overcome this "clustered" problem a means of testing is required to be achieve the lengths necessary to be able to analyse the results more meaningfully.

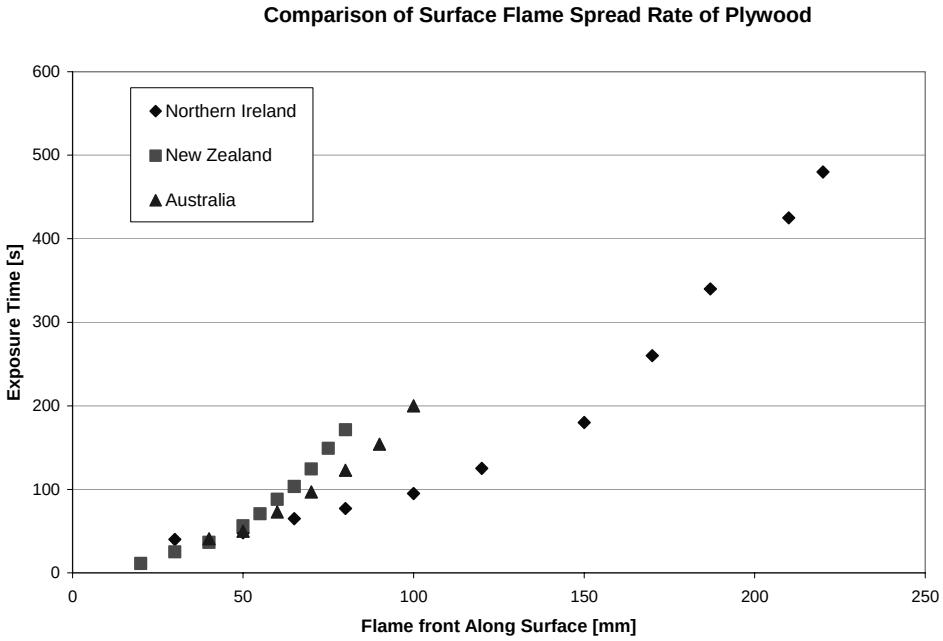

Figure 92 Comparison of surface flame spread rate of plywood

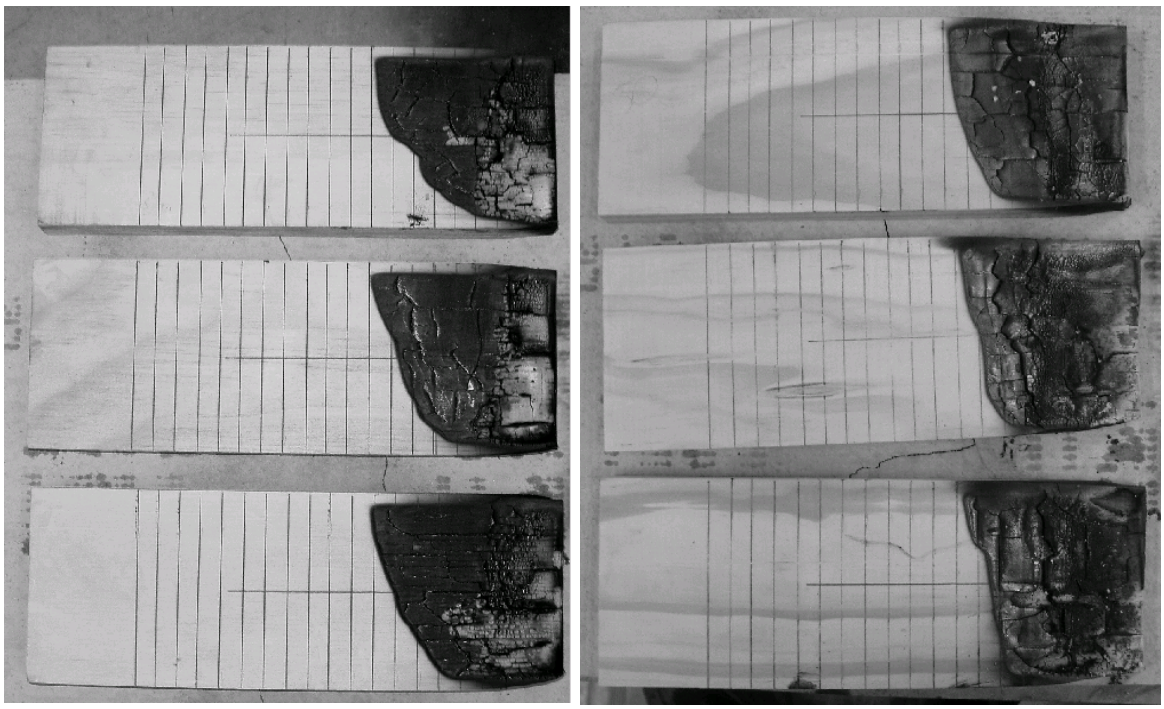

Figure 93 Tests results Plywood (Left), [Top 40kW/m², Middle 50kW/m² and Bottom 60kW/m²]
Test Radiata Pine (Right), [Top 40kW/m², Middle 50kW/m² and Bottom 60kW/m²]

As shown by Figure 93 the flame front along each sample is not uniform. The flame front profile in these samples is consistent and is independent of the applied heat flux. The profile confirms the higher heat flux measurements at the top of the specimens with flame front further than at the bottom of the sample. The density of the wood was thought to play a significant role in the final position of the flame front but the results as illustrated in Figures 61-63, show no such correlation. The higher density woods are thought to limit how far the flame front travels because of higher thermal inertial properties. The denser woods in theory require longer times to reach thermal equilibrium and therefore the time to reach the ignition and flame spread temperatures are larger. The results are inconclusive as when the data is applied to Quintiere's model the results deviate from linearity and do not produce confident conclusions. The reason for the deviation from linearity is because of the effects of the low preheating times, the results are consistent to previous work by Azhakesan et al (1998) and Pease (2001).

The material properties for the wood species can be obtained from flame spread correlation plots (Figures 64 – 87). Specifically the following three variables can be obtained directly from these plots:

C flame spread, heat transfer factor, $m^{s/2}/kW \cdot s^{½}$;

$\dot{q}''_{0,ig}$ critical flux for ignition, kW/m^2; and

$\dot{q}''_{0,s}$ critical flux for spread, kW/m^2

The value of C is the slope of the graphs. In the theory C is defined as $C = -slope$. Calculating the correct value of C is difficult as the units in the standard ASTM E 1321 are inconsistent. This has been identified by Babrauskas (1999) and also in an inter-laboratory study by ASTM, Fowell (1993), who identified that the several calculations had errors. The misinterpretation by participating laboratories included calculations errors, wrong units, and omitted data points. To make the C value consistent they converted it from mm/s to m/s by multiplying $\sqrt{1000}$ to the slope, C. The obtain the C value the following equation was applied: $C = -\sqrt{1000} \cdot slope$.

The second parameter $\dot{q}''_{0,ig}$ can be obtained from the x-axis intercept. This parameter is also referred to as the minimum ignition flux. A similar parameter is also derived from ignition correlations, however, it has been identified by Babrauskas (1999) as being physically different. The difference lies in the experimental procedure, the minimum ignition flux as calculated from ignition tests is the experimentally determined flux for ignition, whereas the minimum ignition flux from flame spread correlations is by extrapolation. A further discussion of the differences between the parameters is discussed by Janssen in the context of ignitability, Babrauskas (1999). The differences observed between the parameters in this instance are not clear as the results are not consistent and do not provide conclusive results.

The third parameter $\dot{q}''_{0,s}$ is obtained from the flame spread plot. The value is obtained by directly examining the minimum value in the flame velocity plots. Once the final position of the flame front is known, from the heat flux profile the corresponding heat flux can be found.

Other parameters that are derived are the corresponding temperature values for the flux variables, namely:

T_{ig} ignition temperature, °C

$T_{s,\,min}$ minimum temperature for spread, °C

These values are derived from extrapolating the flux – temperature profile at each corresponding flux.

The flame spread parameter, ϕ can be obtained from the following expression:

$$\phi = \frac{4/\pi}{(Cb)^2}$$

A summary of the material properties obtained from the flame spread correlation are tabulated in Table 6. The top row contains the results of the natural woods, the second column contains the results of the wood composites.

	Wood Species		Macrocarpa			Beech Wood			Rimu			Radiata Pine		
	Angle	[°]		60			60			60			60	
	Flux	[kW/m²]	40	50	60	40	50	60	40	50	60	40	50	60
	Temp	[°C]	707	770	825	707	770	825	707	770	825	707	770	825
Flame Spread	q_{ig}"	[kW/m²]	17	13.2	11.5	14	9.8	8	13.5	7.7	6	16.6	8.6	7.7
	T_{ig}	[°C]	508	447	409	464	363	336	447	305	270	494	336	305
	Max Distance [mm]		80	80	120	60	70	100	60	70	90	70	90	100
	q_s"	[kW/m²]	6	8	5	9	9	6	9	9	8	7	7	6
	Ts	[°C]	229	305	229	336	363	270	336	363	305	270	270	270
	C[1]	$m^{3/2}/kW \cdot s^{1/2}$	-4.65	-7.67	-7.70	-9.03	-12.91	-11.86	-7.03	-11.29	-13.18	-8.76	-27.21	-32.86
	ϕ	kW^2/m^3	13.93	5.13	5.08	4.80	2.35	2.79	13.32	5.16	3.79	4.76	0.49	0.34

	Wood Species		Plywood			Medium Density Fibre Board (MDF)			Particle Board			Laminated Veneer lumber		
	Angle	[°]		60			60			60			60	
	Flux	[kW/m²]	40	50	60	40	50	60	40	50	60	40	50	60
	Temp	[°C]	707	770	825	707	770	825	707	770	825	707	770	825
Flame Spread	q_{ig}"	[kW/m²]	13.2	8.8	8	14	12.8	11	16.2	11.5	5.4	4	3	2.5
	T_{ig}	[°C]	447	336	336	464	429	409	494	409	229	178	100	70
	Max Distance [mm]		70	90	80	70	90	100	50	60	60	70	70	80
	q_s"	[kW/m²]	7	7	9	7	7	6	12	12	14	7	9	9
	Ts	[°C]	270	270	363	270	270	270	409	409	464	270	100	70
	C[1]	$m^{3/2}/kW \cdot s^{1/2}$	-9.58	-14.37	-13.82	-12.42	-13.09	-17.25	-7.42	-12.37	-117.00	-27.67	-40.06	-50.60
	ϕ	kW^2/m^3	6.28	2.79	3.02	3.58	3.22	1.86	7.38	2.65	0.03	0.11	0.05	0.03

Note 1: The Flame Spread Parameter has been multiplied by sqrt(1000) to convert velocites from mm/s to m/s

Table 6 Material Properties derived from Flame Spread Correlation

9.3 Comparisons of Material Properties

A comparison of the values obtained in this study and those found in literature are presented in Table 7 and Table 8. It is important to note that the comparisons made are arbitrary as materials compared against were not co-ordinated with the other research projects. The results obtained from the RIFT are compared with those from LIFT tests. The top three rows are RIFT results, the remainder are results obtained from LIFT tests. The top row is from this work, followed by the Australian and Northern Ireland results by Pease (2001) and Azhakesan (1998) respectively.

Ignition Correlation

Minimum flux required for Ignition $\dot{q}''_{0,ig}$

	Testing Location	Particle Board	Plywood	Radiata Pine
RIFT	NZ	14.7	13	15
	Aust	5.2	10.7	9.4
	NI	17	11	
	NIST (1985)	17	14	
LIFT	NIST (1994)		14.7	
	UL (1994)		17.5	
	Safety Eng. Lab.		17	
	FRS (Canada)		14	
	SP	10		

Table 7 Comparison of Minimum Ignition Flux, Ignition Correlation

Flame Spread Correlation

Minimum flux required for Ignition $\dot{q}''_{0,ig}$

	Testing Location	Particle Board	Plywood	Radiata Pine
RIFT	NZ	11	10	17
	Aust	16	16	17
	NI	14	10	
	NIST (1985)	18	16	
LIFT	NIST (1994)		17.3	
	UL (1994)		22	
	Safety Eng. Lab.		18.7	
	FRS (Canada)		19.8	
	SP	15		

Table 8 Comparison of Minimum Ignition Flux, Flame Spread Correlation

The results are within a span of 2:1, for the minimum ignition heat flux. Generally speaking the results of the RIFT are on the lower end of the range of results obtained. However, in most instances the values are plausible when compared to the data of the LIFT. The exception is the 5.2kW/m² recorded by the particleboard. This heat flux is at the low end of what would be expected as a minimum ignition flux. The results for the minimum flame spread flux had a span of 3:1 in most instances. The RIFT results in this instance tended to be on the high end of the range of results.

	Minimum flux required for flame spread, $\dot{q}''_{0,s}$		
	Testing Location	Plywood	Particle Board
RIFT	NZ	7	12
	Aust	24	17
	NI	4	12
	NIST (1985)	4	6
	NIST (1994)	3	
LIFT	UL (1994)	2.8	
	Safety Eng. Lab.	2.9	
	FRS (Canada)	2.7	
	SP		4

Table 9 Comparison of Minimum Flame Spread Flux

	Flame Spread Parameter, ϕ			
	Testing Location	Particle Board	Plywood	Pine
RIFT	NZ	2.65	2.79	0.49
	Aust	3.46	10.27	2.86
	NI	1.43	7.8	
	NIST (1985)	6	12.9	
	NIST (1994)		32.3	
LIFT	UL (1994)		22.5	
	Safety Eng. Lab.		43.1	
	FRS (Canada)		47.6	
	SP	16.7		

Table 10 Comparison of Flame Spread Parameter

The results show quite wide variances between research studies. The results between the RIFT and LIFT tests are mixed, and therefore observations between the experiments are inconclusive. The comparison is limited to those that had tested similar wood species. The limitation of test materials to compare makes stating conclusive remarks difficult. Previous research using the LIFT test has shown that the reproducibility of inter-laboratory results does exist and this statistical finding has been highlighted in the report by Fowell (1993). The findings revealed that values such as the thermal inertia and flame spread parameter had a span of 2:1 for well behaved specimens and where difficulties were experienced in the experiments and/or calculations the span was as great as 10:1.

The ignition correlation and the flame spread correlation are compared to see if one particular method consistently showed higher results. In Figure 94, the results show that the flame spread correlation produced higher results than the ignition correlation.

A comparison of the ignition correlation and the flame spread correlation by laboratory is shown in Figure 95. The ignition correlation results produced by the RIFT tests were generally higher. These conclusions are preliminary due to the limitation of specimens to compare. The flame spread correlations is shown to calculate higher minimum ignition flux than the ignition correlation and these results are independent of the wood type. Further tests are required using the RIFT on other materials to draw further conclusions regarding the effect of the apparatus type.

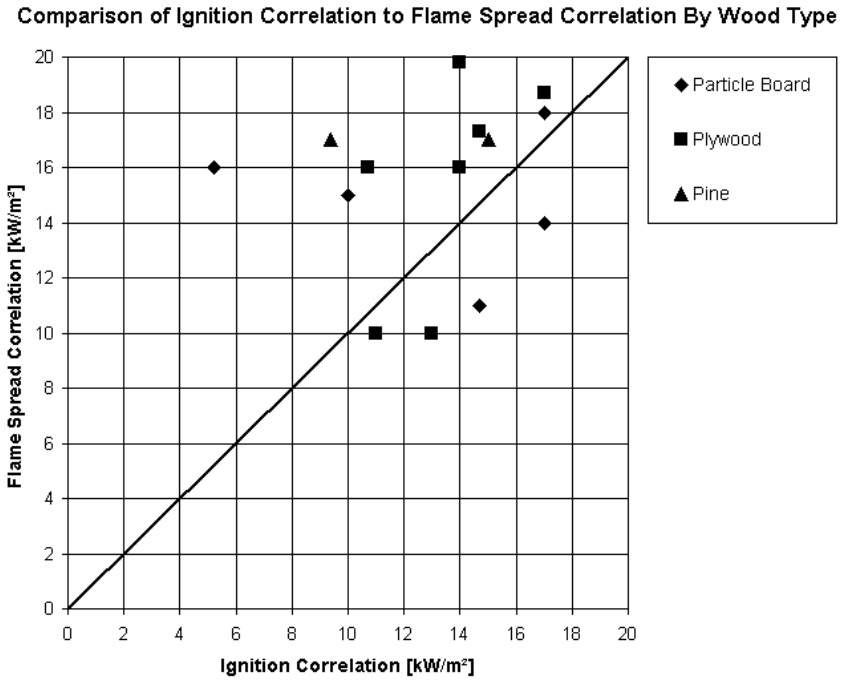

Figure 94 Comparison of Correlations, By Wood type

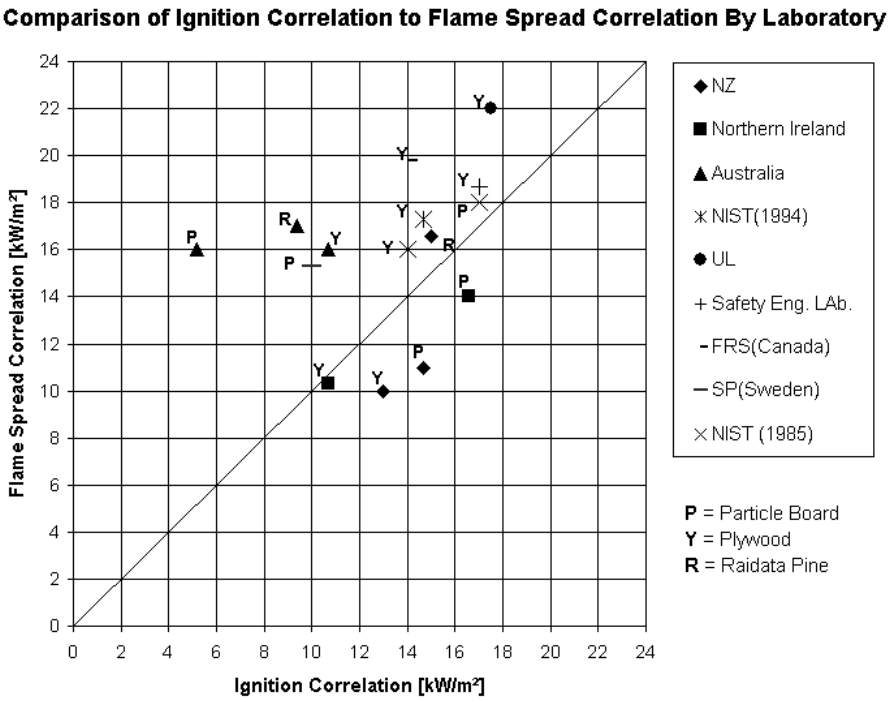

Figure 95 Comparison of Correlations, By Laboratory

The plots of the flame spread parameter and minimum flame spread flux are shown in Figure 96 and Figure 97 respectively. The graphs do not exhibit any correlation with testing locations. In Figure 97 the minimum flame spread flux is shown to be greater with respect to results from the LIFT tests when compared with those obtained from RIFT experiments.

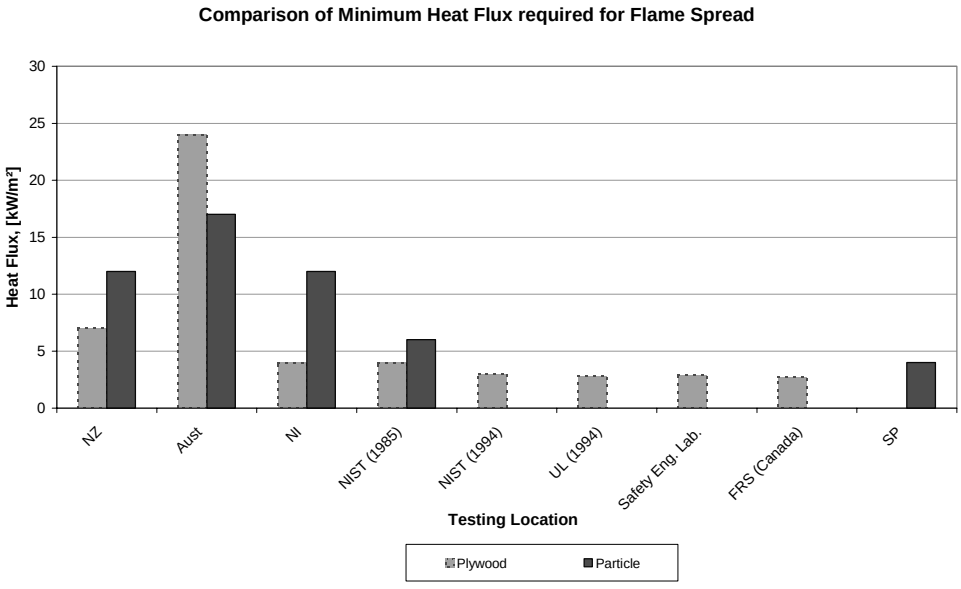

Figure 96 Comparison of the Flame Spread Parameter

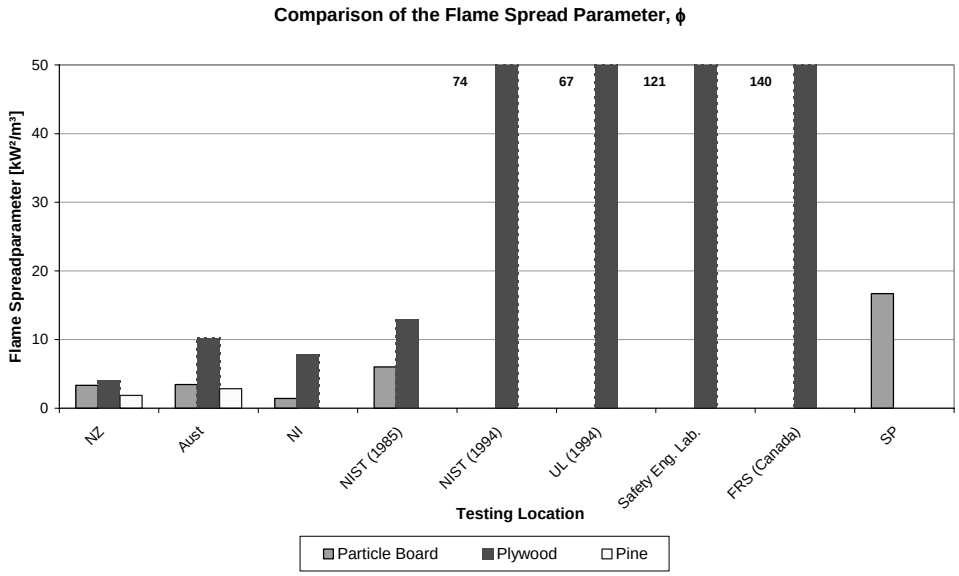

Figure 97 Comparison of the Minimum Flame Spread Flux

9.4 Summary of Flame Spread Results

The results of this study show that some wood species such as MDF and Macrocarpa exhibits a correlation with Quintiere's model. Other work with the RIFT have shown also shown widely varying results, Azhakesan (1998) produced reasonable data and had a good correlation with Quintiere's theory, whereas the results by Pease (2001) had a similar outcome to this work with wide variation in data points. The poor correlation can be attributed to the function *F(t)* as this function is to account for varying preheating times. Quintiere et al (1983, 1985) found that flame spread correlation departs from a linear relationship at low preheating times. A recommendation for the future would be to conduct the required ignition tests in the same instance that the flame spread tests are to be done. An advantage of this would be for consistency with material preparation and testing methodology/observations coming from the same operator, as in this instance previous ignition results are relied upon.

An inter-laboratory study was conducted in 1993 by the ASTM Institute for Standards Research. The project's objective was to provide precise and accurate data. What was found was that the results had a large scatter. On examination calculation errors, wrong units and omitted data points were found. The problems experienced by the

laboratories highlighted the fact that the ASTM E 1321 standard that has been in existence since the early 1980s still has its shortcomings. The results shown by the RIFT are only preliminary and limited to timber products. Further tests would be required to provide material properties to enable comparison of a wider range of materials, such as Gypsum Board; Polyurethane foam; and Polymethymethacrylate, PMMA. The results shown to date indicate that the RIFT does have possibilities and with fine tuning, such as using the full face of the cone and testing wider range of data, conclusive findings could be gauged.

Despite the substantial progress made in understanding and measuring creeping flame spread, inconsistencies still exists between bench scale fire tests and their suitability to derive thermophysical properties of test samples, Dietenberger (1995). As already identified flame spread can be an integral feature of a fire growth model, and flame spread properties are derived from tests such as the LIFT and RIFT. The preheating often causes surface properties to change significantly (such as charring). Further the results in a lateral surface temperature profile are not anticipated by models, therefore causing variation between similar wood species.

The parameters obtained, however, have shown a correlational nature with Quintiere's model in obtaining material properties as shown in this work as well as other such as Azhakesan (1998), Babrauskas (1999) and Fowell (1993).

10 Conclusions

This report investigated the use of an adaptation of the Cone Calorimeter to measure opposed flow flame spread. The Cone Calorimeter is typically used in a horizontal orientation for ignition testing. This report looked at using the Cone Calorimeter in a vertical orientation to test flame spread and compared the results to those from LIFT experiments. This modification was successfully carried out at The University of Newcastle and enabled the measurement of lateral surface flame spread on a vertical orientated sample.

An application of a view factor developed from horizontal Cone Calorimeter tests, Wilson et al (2002) was modified and applied to the vertical orientation of the Cone Calorimeter. The use of the view factor was to estimate the profile of the heat flux along the length of the sample. The results calculated compared well with the measured results and indicated a correlational nature however experimental modifications are required to enable confirmation of findings.

The comparison of the measured heat fluxes with the LIFT profile highlights the suitability of the sample holder being used at 60°. In testing at various angles it was observed that in all cases the heat flux across the length of the sample was greater than the LIFT at the same proportional distance. The application of view factors to estimate the irradiance along the length of the sample was carried out in twofold, firstly using a simplified approach by applying a view factor described by Naraghi and Chung. The second was to improve the estimations by including more parameter applicable to the interchange between the objects in this instance namely the cone heater and the angled specimen. The application of a modified Wilson et al's configuration factor resulted in better results being observed although in many instances the estimate was still greater than those measured.

The assumption used by Naraghi and Chung and Wilson et al is that the elemental point is exposed to 100% of the radiant surface. In the experiments, as shown by the photos of the setup (Figures 21 – 23), the sample is only exposed to half the face of the cone. If the experiments were conducted using the full face of the cone, the

application of Wilson et al's view factor would be more appropriate. The parameters used in the view factor of Wilson et al have addressed the other conditions of the experiment, namely the distance away from the cone (*z, y-axis*), the distance away from the centreline (*a*, *x-axis)*, the effects of the frustum, and by adding the Cosine θ to account for the elemental point being at an angle to the cone, θ.

The flame spread velocities as plotted from the results of the video analysis shows that the wood species is consistent throughout each heat flux setting. The MDF show that it has the slowest flame front velocity, whereas the LVL sample consistently has the fastest flame front velocity

The results of the flame spread study show that some wood species such as MDF and Macrocarpa exhibits a correlation with Quintiere's model. Other work with the RIFT have shown also shown widely varying results, Azhakesan (1998) produced reasonable data and had a good correlation with Quintiere's theory, whereas the results by Pease (2001) had a similar outcome to this work with wide variation in data points. The poor correlation can be attributed to the function *F(t)* as this function is to account for varying preheating times. Quintiere et al (1983, 1985) found that flame spread correlation departs from a linear relationship at low preheating times.

The limitation of flame travel as illustrated in Figures 46, 47 and 92 highlight that the results currently produced are too clustered and because of the this, the range of data to analyse is too small to give meaningful results.

The flame spread properties obtained by the RIFT are only preliminary and further tests would be required to provide material properties to enable comparison of wider range of materials, such as Gypsum Board; Polyurethane foam; Polymethymethacrylate, PMMA. The application of Quintiere's model on opposed flow flame spread used in LIFT tests were applied to the RIFT test to obtain material properties. The results from the RIFT analysis have shown that the flame spread variables are comparable with those obtained from LIFT tests.

10.1 Recommendations

Given the limitation of the data range it is suggested that a modification to the way the experiments are conducted be made to allow a wider range and increase the availability of data points. At present the samples are placed in the middle of the cone as shown in Figures 20 – 23. It is suggested that the sample be placed to the far left of the cone allowing the full face of the cone to radiate onto the sample face.

The limitation of flame travel as highlighted in Figures 46, 47 and 92 highlight that results currently produced are too clustered and that the analysis from these produce very little confidence. By using the full face of the cone, it is expected that the sample size could be increased allowing more data points to be collected, up to 250mm. Although sample sizes in this study were cut to 250mm in the flame spread tests it can be seen in Figure 92 that results at most were at 90mm. By having available a wider sampling area to collect data it is envisaged that their will be a larger number of results which will allow a clearer picture of the irradiance profile to be shown. This in turn will allow refinement of the configuration factor in mapping the irradiance.

For further tests, it is recommended that the same operator conduct the required ignition tests in the same instance that the flame spread tests are to be done. An advantage of this would be for consistency with material preparation and testing methodology/observations coming from the same operator. The flame spread correlations are dependent on ignition results therefore by having a consistent operator, results can be assured. In this instance the results do not show that there is any real gains to be made as specimens where ignition and flame spread tests were conducted by the same operator results were similar to the others.

A higher number of ignition tests is recommended, it was found that the range of heat fluxes conducted to be inadequate. Further test in the lower range by the ignition heat flux would provide more accurate results. This value is critical in terms of flame spread correlation as it provides the preheating time for the flame spread so an accurate result would assure flame spread tests are off on the right path.

The heat flux measurements were conducted using the template depicted in Figure 14. By using a template similar to one used by Wilson et al (Figure 37) would provide more sampling points and enable an accurate profile of the length of the sample be gauged.

For further flame spread tests it is recommended to test a wider range of materials. Materials that have been tested by the LIFT include Gypsum Board; Polyurethane foam; and Polymethymethacrylate, PMMA. By comparing against a wider range of materials other than timber products, a comprehensive comparison between the LIFT and RIFT can be conducted and be able to provide conclusive observations.

References

Ahmed GN; Dietenberger MA; Jones WW; "Calculating Flame Spread on Horizontal and Vertical Surfaces", NISTIR report 5392, Building and Fire Research Laboratory, NIST, 1994.

Anon., "Method of test for heat and smoke release rates for materials and products using an oxygen consumption calorimeter", AS/NZS 3837, 1998

Anon., "Reaction to Fire Tests – Spread of Flames – Part 1: Guidance on Flame Spread, BS ISO TR 5658-1:1997

Anon., "Reaction to Fire Tests – Spread of Flames – Part 2: Lateral Spread on Building Products in Vertical Configuration, BS ISO TR 5658-2:1996

Anon., "Reaction to Fire Tests – Spread of Flames – Part 4: Intermediate-Scale test of Vertical Spread of Flame with Vertically Orientated Specimen, BS ISO TR 5658-4:2001

Anon., "Standard Test Method for Determining Material Ignition and Flame Spread Properties", ASTM E 1321 – 97a

Anon., "Standard Test Method for Heat Release Rates for Materials and Products using an Oxygen Consumption Calorimeter", ASTM E 1354 – 02

Atreya A; Carpentier C; and Harkleroad M; "Effect of Sample Orientation on Piloted Ignition and Flame Spread", Fire Safety Science, Proceeding of the 1st International Symposium, pp 91-109, 1986.

Azhakesan MA; Shields TJ; Silcock GWH; "Ignition and Opposed Flow Flame Spread Using a Reduced Scale Attachment to the Cone Calorimeter", Ulster University., Northern Ireland, Fire Technology, Vol. 34, No. 2, pp 99 - 115, 1998.

Babrauskas V, "Flame Fluxes in Opposed-Flow Flame Spread: A Review of the Literature", Swedish National Testing Institute, Boras, Sweden, SP Report, 1995

Babrauskas V, Development of the Cone Calorimeter – A Bench Scale Heat Release Rate Apparatus Based on Oxygen Consumption, Fire and Materials, Wiley Heyden Ltd, Vol 8, No. 2 1984

Babrauskas V and Wetterlund I, "Comparative Data from LIFT and Cone Calorimeter Tests on 6 Products, Including Flame Flux Measurements", Swedish National Testing and Research Institute, Boras, Sweden, SP Report, 1999

Babrauskas V and Wetterlund I, "Role of Flame Flux in Opposed-Flow Flame Spread", Fire Science and Technology, Inc., Fire and Materials, Vol. 16, No. 6, pp 275 - 281, 1995,

Chen Y; Motevalli V; Delichatsios MA and Tatem P, "A Prediction of Horizontal Flame Spread Using a Theoretical and Experimental Approach", Combustion Institute, Twenty Seventh Symposium (International) on Combustion, Combustion Institute, Pittsburgh, PA, pp 2797-2805, 1998.

Cleary TG, "Flammability Characterization with the LIFT Apparatus and the Cone Calorimeter", Fire Retardant Chemicals Association, March 29-April 1, Orlando, FL, Technomic Publishing Co., Lancaster, PA, pp 99 - 115, 1992.

De Ris JN, "Spread of Laminar Diffusion Flame", Twelfth Symposium (International) on Combustion, The Combustion Institute, Pittsburgh, Pennsylvania, Pp 241 – 252, 1968

Delichatsios MA, "New Interpretation of Data from LIFT (Lateral Ignition and Flame Transport) Apparatus and Modifications for Creeping Flame Spread", Interflam '99**,** International Interflam Conference, 8th Proceedings. Volume 1, Interscience Communications Ltd., London, England, pp 591 - 603, 1999.

Dietenberger MA, "Protocol for ignitability, Lateral Flame Spread and Heat release rte Using the LIFT Apparatus", Fire and Polymers II, American Chemical Society, pp 435-449, 1995

Drysdale D, "Introduction to Fire Dynamics", John Wiley and Sons, New York, USA, 2000.

Fernandez-Pello AC and Hirano T., "Controlling Mechanisms of Flame Spread", Combustion Science and Technology, Vol 32, pp 1 - 31, Gordon and Breach Science Publishers Inc, 1983.

Fernandez-Pello AC and Williams FA, "A Theory of laminar Flame Spread Over Flat Services of Solid Combustibles", Combustion Flame, Vol 28, pp 251 - 277, 1977

Fowell A, "Inter-laboratory Test Program on ASTM E1321, Standard Test Method for Determining Material Ignition and Flame Spread Properties", National Institute of Standards and Technology, Building and Fire Research Laboratory, 1993

Harkleroad M; Quintiere JG and Walton W, "Radiative Ignition and Opposed Flow Flame Spread Measurements on Materials" Report No. DOT/FAA/CT-83/28, National bureau of Standards, Washington, 1983

Howell JR; "A Catalogue of radiation Configuration Factors", McGraw-Hill Book Co., New York, 1982.

Janssens ML, "Measuring rate of heat Release by Oxygen Consumption", Fire Technology, pp 234 – 249, August, 1991

Janssens ML, "Improved Method of Analysis for the LIFT Apparatus. Part 1. Ignition", American Forest and Paper Assoc., Washington, Interscience Communications Limited, Fire and Materials International Conference, 2nd. September 23-24, 1993, Arlington, VA, pp 37-46, 1993.

Janssens ML; "Determining Flame Spread Properties from Cone Calorimeter Measurements. Part A. General Concepts, Chapter 9, "Heat Release in Fires", Elsevier Applied Science, NY, Babrauskas, V.; Grayson, S. J., Editors, pp 265 – 281, 1992.

Jianmin Q, "Determining Flame Spread Properties from Cone Calorimeter Measurements. Part C. Prediction of LIFT Data from Cone Calorimeter Measurements", Sichuan Fire Research Inst., China, Chapter 9, "Heat Release in

Fires", Elsevier Applied Science, NY, Babrauskas, V.; Grayson, S. J., Editors, pp 293 - 306, 1992.

Jianmin Q, "Prediction of Flame Spread Test Results From the Test Data of the Cone Calorimeter", Swedish National Testing and Research Institute, Boras, Sweden, SP REPORT 1990:38, 1990.

Kanury AM, "Flaming Ignition of Solid Fuels", Section 2/Chapter 11, The SFPE Handbook of Fire Protection Engineering, 3rd Ed, National Fire Protection Association, Quincy, MA, 2002.

Karlsson B and Quintiere JG, "Enclosure Fire Dynamics", CRC Press LLC, Florida, USA, 2000.

Kidd CT and Nelson CG, "How the Schmidt-Boelter Really works", 41st International Instrumentations Symposium, Denver, 1995

Lukus C, "Communication: Measurement of Heat Flux in the Cone Calorimeter", Fire and Materials, Vol 19, pp 97-98, 1995

Mikkola E and Wichman IS, "On the Thermal Ignition of Combustion Materials", Fire and Material, Vol 14, John Wiley and Sons Ltd, 1989, pp 87 – 96

Murthy AV; Tsai BK and Sauders RD, "Aperture Proximity Effects in High Heat Flux Sensors Calibration", J. Res. Natl. Inst. Stand. Technol. 103, 621, 1998

Murthy AV; Tsai BK and Sauders RD, "Radiative Calibration of High Heat Flux sensors at NIST: Facilities and Techniques", J. Res Natl Inst. Stand. Technol, Vol 105, No 2, pp 293 – 305, 2000

Murthy AV; Tsai BK; Gibson CE, "Calibration of High Heat Flux sensors at NIST", J. Res Natl Inst. Stand. Technol, Vol 102, No 4, pp 479 – 488, 1997

Naraghi MHN and Chung BTF, "Radiation Configuration Factors Between Disks and a Class of Axisymmetric Bodies" Journal of Heat Transfer, Vol 104, Aug. 1982, pp 426-431, 1982.

Ngu CK, "Ignition Properties of New Zealand timbers", Master Fire Engineering Project, Department of Civil Engineering, University of Canterbury, Christchurch, NZ, 2001

Nisted T, "Flame Spread Experiments in Bench Scale, Project 5 of the EURIC Fire Research program", Dantest, Fire Technology, 1991

Olson S, "Mechanism of microgravity flame spread over a thin solid fuel: Oxygen and Opposed Flow Effects, Combustion Science and technology, Vol 76, pp 233-249, 1991

Olson S, "The effect of microgravity on flame spread over a thin fuel", NASA TM-100 195, 1987

Pease T, "A Study of Surface Flame Spread Using a Modified Cone Calorimeter", Undergraduate final year project, Department of Chemical Engineering, University of Newcastle, Australia, 2001

Perrin M, "A comparison between Cone Calorimeter and Lift Flame Spread Data", Undergraduate final year project, Department of Chemical Engineering, University of Newcastle, Australia, 2002

Persson B and Wetterlund I, "Tentative Guidelines for Calibration and Use of Heat Flux Meter", Swedish National Testing and Research Institute, Boras, Sweden, SP REPORT 1997:33; 1997.

Quintiere JG, "A Simplified Theory for Generalizing Results from a Radiant Panel Rate of Flame Spread Apparatus" Fire and Materials, Vol 5, No 2, Heyden and Son Ltd, 1981

Quintiere JG, "Principles of Fire Behaviour", Albany, N.Y, Delmar Publishers, c1998.

Quintiere JG, "Some Aspects of Fire Growth", Gaithersburg, Md,. : National Institute of Standards and Technology, Building and Fire Research Laboratory, 2000.

Quintiere JG, "Surface Flame Spread", Section 2/Chapter 12, The SFPE Handbook of Fire Protection Engineering, 3rd Ed, National Fire Protection Association, Quincy, MA, 2002.

Quintiere JG; Harkleroad M and Walton, D, "Measurement of Material Flame Spread Properties" Combustion of Science and Technology , Vol 32, pp67 -89, 1983., Pp67 -89

Quintiere JG and Harkleroad M, "New Concepts for Measuring Flame Spread Properties" Fire Safety and Engineering , STM STP 882 TZ Harmathy Ed., American Society for Testing and Materials, Philadelphia, pp 239 –267, 1985,

Robertson AF, "A Flammability test Based on Proposed ISO Spread of Flame Test", Third Progress Report, Intergovernmental Maritime Consultative Organisation, IMCO FP/215, 1979

Rockett JA, "Mathematical Modelling of Radiant Panel test Methods", Fire Safety Research, National Bureau of Standards, NBS SP 411, Nov 1974.

Rohsenow WM; Hartnett, JP and Choi YI, "Handbook of Heat Transfer", 3rd Ed, McGraw-Hill, New York, 1998

Shields TJ; Silcock GW and Murray JJ; "The effects of Geometry and Ignition Mode on Ignition Times Obtained Using a Cone Calorimeter and ISO Ignitability Apparatus", Fire and Materials 17, pp 25-35, 1993

Siegel R and Howell JR; "Thermal Radiation Heat Transfer", 3rd Edition, Hemisphere Pub. Corp, Washington D.C, 1992.

Spearpoint MJ and Quintiere JG, "Predicting The Piloted Ignition of Wood in the Cone Calorimeter using an Integral Model, effect of Species, Grain Orientation and Heat Flux", Fire Safety Journal, Vol 36, pp391-415, 2001.

Wang JCY; Lin S; Lee PM; Dai WL and Lou YS, "Radiant Interchange Configuration Factors Inside Segments of Frustum Enclosures of Right Circular Cones", Int. Comm. Heat Mass Transfer, Vol 13, pp 423-432, 1986

Wetterlund I, "Improving Heat Flux Meter Calibration for Fire Testing Laboratories (HFCAL), HFCAL Swedish National Testing and Research Institute, Boras, Sweden, 2002

Wichman IS, "Theory of Opposed Flow Flame Spread" Progress in Energy and Combustion Science, Vol 18, pp 553 – 592, Pergamon Press Ltd, 1992

Williams FA, "Combustion Theory", The Benjamin/Cummings, Co Inc, Menlo Park, CA, 1985

Williams FA, "Mechanism of Fire Spread", Sixteenth Symposium (International) on Combustion, The Combustion Institute, Pittsburgh, Pennsylvania, Pp 1281 – 1294, 1976

Williamson RB, "Fire Growth and Testing", Report No UCB FRG 78-2, Fire Research Group, University of California, Berkeley, 1978.

Wilson MT; Dlugogorski BZ and Kennedy EM, "Uniformity of Radiant Heat Fluxes in Cone Calorimeter", Process Safety and Environmental Protection Group, The University of Newcastle, Callaghan, Australia, 7th Symposium in Fires Science in Worcester, USA, 2002.

Appendix

Appendix A – Raw Data
- Irradiance: 40°; 60°; 80°
- Flame Spread
    - Particle Board
    - Plywood
    - MDF
    - Macrocarpa
    - Radiata Pine
    - Beech
    - Rimu
    - LVL

Appendix B – Irradiance Profile

Appendix C – Irradiance Mapping
- Naraghi and Chung
- Wilson et al

Appendix D – Ignition Calculations
- Particle Board
- LVL

Appendix E – Flame Spread Calculations
- Radiata Pine
- Macrocarpa
- Beech
- Rimu
- MDF
- Plywood
- Particle Board
- LVL

Appendix A – Raw Data

Irradiance measurements at 40°

Angle [°]	40
Flux [kW/m²]	30
Temp [°C]	640

Heat Flux Position												Max	Min	Average	Std Dev	Range
1	24.6	24.3	24.4	24.6	25.1	24.9	25	24.5	24.4	24.6	25	25.10	24.30	24.67	0.28	0.80
2	23.4	23.8	23.2	24.6	23.2	23.7	23.2					24.60	23.20	23.59	0.51	1.40
3	18.7	18.9	18.5	18.4	18.9	18.8	18.7	18.6	18.8	18.6		18.90	18.40	18.63	0.17	0.50
4	13.7	13.8	13.5	14	14.7	14.2	14.3	13.8	14.1	13.7	14	14.70	13.50	13.98	0.34	1.20
5	9.9	10	10.4	9.9	9.8	9.8	10	9.9				10.40	9.80	9.96	0.19	0.60
6	8.4	8.8	9	8.9	8.5	8.3	8.7	8.4	8.5	8.8	8.4	9.00	8.30	8.61	0.24	0.70
7	6.2	6.1	6.3	6	6.1	6.3	6.2	6.1	5.8	6	6.2	6.30	5.80	6.12	0.16	0.50
8	4.1	4.3	4.2	4.1	4	4.3	4.1	3.9	4.3	3.9	4.1	4.30	3.80	4.12	0.15	0.40
9	3.2	3.6	3.7	3.4	3.6	3.4	3.9	3.3	3.7	3.2		3.90	3.20	3.50	0.24	0.70

Angle [°]	40
Flux [kW/m²]	40
Temp [°C]	707

Heat Flux Position												Max	Min	Average	Std Dev	Range
1	30.2	30.9	31.1	30.2	30.5	30.6	31.5	31	31.7			31.70	30.20	30.86	0.53	1.50
2	23.4	23.6	23.8	23.7	23.9	30.1	23.9	23.8	23.7			30.10	23.40	23.77	0.20	0.70
3	22.8	22.7	22.5	22.6	22.5	22.7	22.8	22.9	23	23.2		23.20	22.50	22.77	0.22	0.70
4	14.4	14.5	14.3	14.3	14.6	15.1	14.6	14.5	14.9	15.2	15	15.20	14.30	14.67	0.32	0.90
5	12.1	12.6	12.5	12.7	12.9	12.3	12.9	12.4	12.2	12.7		12.90	12.10	12.53	0.28	0.80
6	9	9.3	10.3	9.6	9.7	9.1	8.9	8.7	8.9	8.7	8.6	10.30	8.60	9.16	0.52	1.70
7	7.7	6.8	7	6.6	6.5	6.7	6.6	6.5	6.3	7	6.9	7.70	6.50	6.91	0.36	1.20
8	4.7	4.8	4.7	4.6	4.8	4.3	5	4.3	4.6	4.7	4.8	5.00	4.30	4.72	0.18	0.70
9	4.3	4.5	4.3	4.1	4	3.9	3.9	4.1	3.8	3.7	3.8	4.50	3.60	4.00	0.27	0.90

Angle [°]	40
Flux [kW/m²]	50
Temp [°C]	770

Heat Flux Position												Max	Min	Average	Std Dev	Range
1	38.3	39	38.2	38.1	38.4	37.9	38.7	38.3	38.2	38.4	38.2	39.00	37.90	38.34	0.30	1.10
2	37.3	37.5	38	38.3	37.8	38.1	37.9	37.6	37.3	38	37.8	38.30	37.30	37.78	0.33	1.00
3	28.3	28.6	28.4	29.1	28.9	29.4	29.1	29	29.4	28.9		29.40	28.30	28.91	0.38	1.10
4	17.5	17.8	17.4	17.3	17.8	18.1	17.5	17.9	18.1	17.5		18.10	17.30	17.70	0.28	0.80
5	15.9	16	15.8	15.4	15.6	15.9	15.8	15.4	15.5	15.7		16.00	15.40	15.70	0.22	0.60
6	12.2	11.4	11.6	11.2	11.7	11.5	12	11.9	12			12.20	11.20	11.72	0.33	1.00
7	8	8.2	8.7	8.3	8.5	8.1	8	8.5	8.3	7.9	7.6	8.70	7.60	8.16	0.32	1.10
8	6.4	6.6	6.4	6.6	6.8	6.5	6.6	6.4	6.3	6.1	6.2	6.80	6.10	6.43	0.19	0.70
9	4.6	4.8	5	4.7	4.8	4.6	4.6	4.5	5	4.3	4.4	5.00	4.30	4.66	0.22	0.70

Angle [°]	40
Flux [kW/m²]	60
Temp [°C]	825

Heat Flux Position												Max	Min	Average	Std Dev	Range
1	47	47.4	47.3	47.4	47.8	47.4	47.8	47.3	47.1			47.90	47.00	47.46	0.32	0.90
2	46	46.6	46.1	47.1	46.2	46.6	46.9	47	47.8	47		47.80	46.00	46.73	0.55	1.80
3	35.8	35.3	35.7	36	35.8	36	35.6	36	37	36.1	36.5	37.00	35.30	35.98	0.46	1.70
4	23.7	23.3	23	23.4	23.9	23.6	23	23.9	24	23.3	23.1	24.00	23.00	23.47	0.37	1.00
5	19.4	19.1	19.5	19.4	19.3	19.1	19.3	19.1	19.4	19.2	18.9	19.50	18.90	19.23	0.17	0.60
6	15.8	15.9	15.3	15.8	15.7	15.9	15.7	16.2	15.8	15.6	15.5	16.20	15.30	15.75	0.23	0.30
7	10.2	10.6	10.7	11	10.8	11.1	11.4	11.1	10.8	11.3	10.8	11.40	10.20	10.91	0.33	1.20
8	7.5	7.7	7.6	7.5	7.6	7.4	7.3	7.7	7.4	7.6	7.3	7.30	7.30	7.56	0.16	0.60
9	5.7	6.2	5.5	5.6	5.4	6	5.6	5.3	5.2	5.3	5.7	6.20	5.20	5.58	0.30	1.00

Irradiance measurements at 60°

Angle [°]	60																		
Flux [kW/m²]	30																		
Temp [°C]	640															Max	Min	Average	Std Dev	Range
Heat Flux Position	1	17.3	17.6	16.3	17.6	17.2	17.3	17.6	17.7	17.3	17.6	17.3	17.8			17.30	16.30	17.48	0.23	1.00
	2	16.8	17	16.3	17.1	17	16.3	17	16.8	16.6	16.6					17.10	16.60	16.87	0.17	0.50
	3	12.3	12.5	12.6	12.7	12.5	12.4	12.2	12.3	12.5	12.3	12.6				12.70	12.20	12.45	0.16	0.50
	4	7.7	7.8	7.9	7.7	7.8	8	7.6	7.2	7.5	7.4					8.00	7.20	7.66	0.24	0.80
	5	6.3	6.2	6.3	6.6	6.1	6.2	6.3	6.2	6.1	6.3	6.3	6.2			6.60	6.10	6.26	0.13	0.50
	6	5.5	5	5.3	5.2	5.3	5.6	5.5	5.3	5.4						5.60	5.00	5.34	0.18	0.60
	7	4.2	3.6	3.7	4.1	4.1	3.3	3.8	3.5	3.6	3.9	3.6	3.9			4.20	3.50	3.83	0.23	0.70
	8	3	3.1	3.1	3.3	3.2	3	3.1	3.3	3.2						3.30	3.00	3.14	0.11	0.30
	9	2.6	2.7	2.9	2.6	2.4	2.6	2.5	2.7	2.6	2.4					2.30	2.40	2.60	0.15	0.50

Angle [°]	60																		
Flux [kW/m²]	40																		
Temp [°C]	707															Max	Min	Average	Std Dev	Range
Heat Flux Position	1	19.4	19.7	19.8	19.8	19.4	19.3	19.6	20.1	20.1						20.10	19.40	19.76	0.26	0.70
	2	19.2	19.4	19.3	19.6	19.5	19.4	19.7	19.2							19.70	19.20	19.41	0.18	0.50
	3	12.9	13.1	13.3	12.8	13.3	13.5	13.8	13.1	13.2	13.5					13.80	12.80	13.25	0.30	1.00
	4	7.9	8	7.7	7.5	7.9	8.1	7.9	8	8.1	7.8	8.1				8.10	7.50	7.91	0.19	0.60
	5	6.9	6.8	7	6.7	6.8	7	7.1	6.7	6.8	6.7	6.8	6.7	7.1	6.9	7.10	6.70	6.86	0.15	0.40
	6	4.9	5.1	5.2	5	5.2	5.5	5.2	5.3	4.9	5.3	5.1	4.9			5.50	4.90	5.13	0.19	0.60
	7	2.5	2.7	2.9	2.5	2.4	2.6	2.6	2.5	2.8						2.90	2.40	2.61	0.16	0.50
	8	2.5	2.6	2.7	2.8	2.4	2.7	2.4	2.5							2.80	2.40	2.58	0.15	0.40
	9	2.6	2.5	2.4	2.2	2.1	2.4	2.5	2.2	2.3	2.1					2.60	2.10	2.33	0.18	0.50

Angle [°]	60																		
Flux [kW/m²]	50																		
Temp [°C]	770															Max	Min	Average	Std Dev	Range
Heat Flux Position	1	25	24.9	25.1	25.3	24.9	25.3	25.1	26	25.7						26.00	24.30	25.26	0.37	1.10
	2	25.3	25.2	25.6	25.4	25.1	25.4	25.1	25.4							25.60	25.10	25.31	0.17	0.50
	3	17.8	17.5	17.6	17.9	17.2	18	17.6	17.9	17.6						18.00	17.20	17.68	0.25	0.80
	4	9.2	9.3	9.4	9.2	9.4	9.5	9.2	9.2	9.6	9.8					9.80	9.20	9.38	0.20	0.60
	5	9.6	9.8	9.9	9.6	9.9	10.1	9.8	9.7	9.6	9.5					10.10	9.50	9.75	0.18	0.60
	6	7.8	7.6	7.2	7.5	7	7	7	7.6	7.5	8					8.00	7.00	7.42	0.36	1.00
	7	4.8	5	4.9	5.2	4.7										5.20	4.70	4.92	0.13	0.50
	8	4	3.9	4	3.9	4.1	3.9	4.1								4.10	3.90	3.99	0.09	0.20
	9	4	3.9	3.8	3.8	3.7	4.1	3.9	4.2	4.1						4.20	3.70	3.94	0.17	0.50

Angle [°]	60																		
Flux [kW/m²]	60																		
Temp [°C]	825															Max	Min	Average	Std Dev	Range
Heat Flux Position	1	30.3	30	30.6	29.5	30.1	31.1	31.4	29.9							31.40	29.50	30.36	0.64	1.90
	2	30.3	31.4	30.9	31.2	30.6	30.7	31.2	30.8	30.5						31.40	30.30	30.84	0.36	1.10
	3	21.7	20.7	20.3	20.4	20.2	20.8	20.3	20.1	20.7						21.70	20.10	20.64	0.43	1.60
	4	12.7	12.3	13.3	13.4	13.1	12.5	13.2	13.2	13.4						13.40	12.30	13.01	0.41	1.10
	5	11	10.8	10.6	10.9	10.6	10.9	11	11.2							11.20	10.60	10.88	0.21	0.60
	6	8.8	8.1	8.9	8.6	9.3	8.8	8.1	8.5	9						9.30	8.10	8.68	0.40	1.20
	7	6.1	6.4	6.1	6.6	7.1	6.8	7.4	6.9	7.4	7					7.40	6.10	6.78	0.48	1.30
	8	4.7	4.6	4.8	4.5	4.7	4.8	4.7	5	4.5						5.00	4.50	4.70	0.16	0.50
	9	4.9	4.8	5.2	5.3	4.9	5.3	4.9	4.7	5.1						5.30	4.70	5.01	0.22	0.60

Irradiance measurements at 80°

Angle [°]	80
Flux [kW/m²]	30
Temp [°C]	640

Heat Flux Position											Max	Min	Average	Std Dev	Range
	1	10	10.2	10.1	10	10.2	10.4	10.4	10.3		10.40	10.00	10.20	0.16	0.40
	2	3.7	3.8	3.9	10	3.8	3.9	3.7	3.8		10.00	3.70	3.83	0.10	0.30
	3	6.5	6.4	6.5	6.6	6.2	6.6				6.60	6.20	6.47	0.15	0.40
	4	4.1	4.2	3.9	4.1	4.2	4.1	4.2	4.2	4.3	4.30	3.90	4.14	0.11	0.40
	5	3.6	3.4	3.4	3.2	3.4	3.4	3.3	3.4		3.60	3.20	3.39	0.11	0.40
	6	3.1	3	3	3.2	2.8	3.1	3	3.1		3.20	2.80	3.04	0.12	0.40
	7	2.4	2.2	2.3	2.4	2	2.1	2.3	2.1	2.4	2.40	2.00	2.24	0.15	0.40
	8	1.9	1.8	1.7	1.8	1.7	1.6				1.90	1.60	1.75	0.10	0.30
	9	1.8	2.1	1.7	2	1.7	1.8	1.9			2.10	1.70	1.86	0.15	0.40

Angle [°]	80
Flux [kW/m²]	40
Temp [°C]	707

Heat Flux Position											Max	Min	Average	Std Dev	Range
	1	14.4	14.3	14.1	14.4	14.1	14.4	14.5	14.5	14.2	14.4					14.50	14.10	14.33	0.15	0.40
	2	12.9	12.7	13.1	12.9	12.8	13	12.8	12.7	13	12.9					13.10	12.70	12.88	0.13	0.40
	3	8.8	8.7	8.9	8.7	8.6	8.7	8.6	8.1	8.6	8.3	3.1				9.10	8.60	8.79	0.13	0.50
	4	5.8	5.9	5.8	5.9	6										6.00	5.80	5.88	0.08	0.20
	5	4.3	4.4	4.6	4.5	4.3	5.1	4.6	4.9	4.8						5.10	4.30	4.61	0.28	0.80
	6	4	3.9	3.8	3.7	3.8	3.6	3.5	4	3.6	3.5					4.00	3.50	3.74	0.13	0.50
	7	3.5	3.3	3.2	3.4	3.5	3.6	3.5	3.6	3.1	3.6					3.60	3.10	3.43	0.18	0.50
	8	2.5	2.2	2.4	2.2	2.1	2.4	2.4								2.50	2.10	2.31	0.15	0.40
	9	2.2	2	2.1	2.2	2.4	2.1	1.9								2.40	1.90	2.13	0.16	0.50

Angle [°]	80
Flux [kW/m²]	50
Temp [°C]	770

Heat Flux Position											Max	Min	Average	Std Dev	Range
	1	17.9	18.2	17.8	17.9	18	18.1	17.9	18.2	17.8	17.9	17.5	17.8			18.20	17.50	17.92	0.13	0.70
	2	16.3	16.4	16.5	16.6	17	16.6	16.5	16.4							17.00	16.30	16.54	0.21	0.70
	3	11.7	11.9	11.8	11.7	11.8	11.7	12.2	11.6	11.7						12.20	11.60	11.79	0.18	0.60
	4	6.8	6.9	6.7	6.6	6.5	6.4	6.2	6.3	6.5	6.1					6.90	6.10	6.50	0.26	0.80
	5	5.6	5.3	5.5	5.8	5.9	6.1	6.3	5.8	9	5.4	5.5	5.9			9.00	5.30	6.01	0.33	3.70
	6	4.9	5	5.2	5.3	5.4	5.2	4.9	5.1	4.8	5.2	5				5.40	4.80	5.09	0.19	0.60
	7	3.7	3.9	3.8	4	4.1	3.8	3.9	3.5	3.7						4.10	3.50	3.82	0.18	0.60
	8	3.2	3	3.1	3.2	3.1	3.2	3.1	3.2	3.1						3.20	3.00	3.13	0.07	0.20
	9	2.9	2.5	2.6	2.7	2.8	2.9	3.1	2.9	2.7	2.6	2.7				3.10	2.50	2.76	0.17	0.60

Angle [°]	80
Flux [kW/m²]	60
Temp [°C]	825

Heat Flux Position											Max	Min	Average	Std Dev	Range
	1	23.8	24.2	24.4	25	24.4	25.7	24.4	24.6	23.9						25.70	23.80	24.43	0.58	1.90
	2	19.9	20.1	20.4	20.3	19.9	20	20.8	20.3	20.6	20.4	20.2				20.80	19.90	20.26	0.28	0.90
	3	13.4	13.2	13.4	13.9	13.4	12.8	13.5	13.1	13.8	13.6	13.4	13.5			13.90	12.80	13.42	0.29	1.10
	4	9.4	9.7	8.3	9	8.7	8.9	9	8.9	8.9	8.9	9.1				9.70	8.30	9.00	0.36	1.40
	5	7.1	6.6	6.5	6.8	6.9	6.5	7	6.8	7.5	6.8	7.1	6.9	7		7.50	6.50	6.88	0.27	1.00
	6	6	6.3	6.4	6.1	6	5.9	6.3	6.1	6	6	6.3	5.8			6.40	5.80	6.10	0.13	0.60
	7	5	5.4	4.8	5	4.8	4.7	4.8	4.2	4.6	5.1	5	4.3	4.6		5.40	4.20	4.79	0.33	1.20
	8	3.7	4.1	3.9	3.7	3.8	3.7	4	3.8	3.9						4.10	3.70	3.84	0.14	0.40
	9	3.5	3.6	3.3	3.4	3.6	3.7	3.8	3.5	3.6	3.4					3.80	3.30	3.54	0.15	0.50

Flame Spread Data

Laboratory	Newcastle University - Fire Lab
Date of Tests	7/02/03
Material	Particle Board
Specimen Dimension	250 * 90 * 20

Flame Front Position	Heat Flux	40					50						60						
	Specimen Number	1	2	3	Average		4	5	6	Average			7	8	9	Average			
	Time Ignition [s]	27	10.4	7			18	8	5				6	14	4				
	20		27	33	23	27.67		15	28	25	22.67			26	13	12	17.00		
	30		79	85	78	80.67		43	53	59	51.67			47	47	42	45.33		
	40		131	126	140	132.33		97	87	98	94.00			73	75	70	72.67		
	50			197	210	203.50		143	136	254	177.67			100	115	107	107.33		
	55									204	204.00			132	187	177	165.33		
	60							217	222	255	231.33			204					
	65																		
	70																		

Flame Spread Data

Laboratory Newcastle University - Fire Lab
Date of Tests 10/02/03
Material Plywood
Specimen Dimension 250 * 90 * 20

Flame Front Position

Heat Flux	40						50						60					
Specimen Number	1	2	3		Average		4	5	6		Average		7	8	9		Average	
Time Ignition [s]	7.5	4.5	5.4				4	3.7	2.8				5	1	4			
20		15	14	6	11.67		10	12	12	12	11.33		14	9	11	11	11.33	
30		27	37	20	28.00		21	25	29	29	25.00		24	17	34	34	25.00	
40		41	61	43	48.33		55	46	49	49	50.00		42	28	40	40	36.67	
50		92	123	89	101.33		91	68	73	73	77.33		68	41	60	60	56.33	
55		126	170	174	156.67				93	93	93.00		91	51	70	70	70.67	
60		151	288	290	243.00		138	88	116	116	114.00		110	73	81	81	88.00	
65			340		340.00		169	114	150	150	144.33		127	91	92	92	103.33	
70							187	135	166	166	162.67		149	107	117	117	124.33	
75								160	205	205	182.50		172	140	135	135	149.00	
80								175	231	231	203.00		197	170	147	147	171.33	
85								218	275	275	246.50							
90									301	301	301.00							
95																		
100																		

Flame Spread Data

Laboratory Newcastle University - Fire Lab
Date of Tests 10/02/03
Material Medium Density Fibre Board (MDF)
Specimen Dimension 250 * 90 * 20

Flame Front Position

Heat Flux	40					50					60				
Specimen Number	1	2	3		Average	4	5	6		Average	7	8	9		Average
Time Ignition [s]	6.8	11.8	10.1			3.4	6.4	9.7			5	4.8	5.8		
20		33	32	36	33.67	29	29	27		28.33	23	23	25		23.67
30		88	78	82	82.67	68	71	65		68.00	51	54	56		53.67
40		128	122	127	125.67	104	125	110		113.00	88	91	96		91.67
45		157		160	158.50	129	160			144.50	111	114	124		116.33
50		192	172	192	185.33	153	196	172		173.67	140	156	156		150.67
55		224	211	231	222.00	181	234	213		209.33	167	183	175		175.00
60		277	270	262	269.67	211	270	243		241.33	200	217	215		210.67
65		326	314		320.00	260	304	280		281.33	235	242	247		241.33
70		362	342		352.00	295	331	312		312.67	257	267	273		265.67
75						329	374	355		352.67	308	314	318		313.33
80								396		396.00	354	362	352		356.00
85								459		459.00	424	412	420		418.67
90											482	478	587		515.67
95											533	660			596.50
100											611				611.00
105															
110															

Flame Spread Data

Laboratory Newcastle University - Fire Lab
Date of Tests 11/02/03
Material Macroparpa
Specimen Dimension 250 * 90 * 20

Flame Front Position

Heat Flux	40					50					60				
Specimen Number	1	2	3	Average		4	5	6	Average		7	8	9	Average	
Time Ignition [s]	10.4	5.4	2.8			3.6	2.6	3.1			2.8	1.5	1.1		
20		14	8	21	14.33		11	12	11	11.33		7	9	5	7.00
30		29	21	45	31.67		22	32	24	26.00		18	23	13	18.00
35				66	66.00										
40		53	34	80	55.67		36	67	40	47.67		30	38	28	32.00
45		85			85.00										
50		108	56		82.00		63	89	65	72.33		52	56	46	51.33
55			69		69.00		79		90	84.50		62		56	59.00
60			88		88.00		92		114	103.00		74	74	70	72.67
65							113		132	122.50		84	85	98	89.00
70			106		106.00		122		166	144.00		96	96	122	104.67
75			123		123.00		150		189	169.50		107	119		113.00
80			136		136.00		179		202	190.50		120	134		127.00
85							194		249	221.50		134	155		144.50
90							212			212.00		148	170		159.00
95							226			226.00		166	187		176.50
100												196	202		199.00
105												210			210.00
110												236			236.00
115												256			256.00
120															

Flame Spread Data

Laboratory Newcastle University - Fire Lab
Date of Tests 11/02/03
Material Radiata Pine
Specimen Dimension 250 * 90 * 20

Heat Flux	40					50					60				
Specimen Number	1	2	3	Average		4	5	6	Average		7	8	9	Average	
Time Ignition [s]	9.3	7.6	3			6	3.6	2.9			3.1	1.8	3.5		
20		14	31	12	19.00		10	14	10	11.33		12	11	12	11.67
30		27	58	26	37.00		23	36	24	27.67		25	27	29	27.00
40		41	85	39	55.00		41	60	47	49.33		44	43	51	46.00
45			104	56	80.00			74	76	75.00			55		55.00
50		91	146	88	108.33		77	105	92	91.33		107	68	68	81.00
55		108	178	148	144.67		90	141	106	112.33		88	82	88	86.00
60		128	211	334	224.33		115	171	124	136.67		119	112	153	128.00
65		148	243	367	252.67		150	205	146	167.00		135	131	208	158.00
70		188	278	390	285.33		206	219	194	206.33		151	157		154.00
75		196		483	339.50		235			235.00			198		198.00
80		238			238.00		256			256.00			224		224.00
85							283			283.00			250		250.00
90													274		274.00
95													293		293.00
100													335		335.00

Flame Front Position

Flame Spread Data

Laboratory Newcastle University - Fire Lab
Date of Tests 11/02/03
Material Beech
Specimen Dimension 250 * 90 * 20

Flame Front Position

Heat Flux	40						50						60					
Specimen Number	1		2		3	Average	4		5		6	Average	7		8		9	Average
Time Ignition [s]	4.1		4.3		2.1		2.3		1.6		2.9		1.4		1.9		1.4	
20		22		25	17	21.33		12		13	16	13.67		4		6	6	5.33
30		39		54	33	42.00		25		32	30	29.00		13		16	14	14.33
35				80		80.00												
40		66		104	56	75.33		43		55	56	51.33		26		29	22	25.67
45		82		127	66	91.67		51		69	68	62.67				47		47.00
50		110			86	98.00		62		87	89	79.33		39		56	37	44.00
55					125	125.00		79		110	104	97.67				66	49	57.50
60								99		130	126	118.33		60		81	59	66.67
65								124		150		137.00		71			75	73.00
70														88			93	90.50
75														99			102	100.50
80														117			118	117.50
85																	132	132.00
90																	144	144.00
95																	163	163.00
100																		

Flame Spread Data

Laboratory Newcastle University - Fire Lab
Date of Tests 11/02/03
Material Rimu
Specimen Dimension 250 * 90 * 20

Flame Front Position

Heat Flux	40					50					60				
Specimen Number	1	2	3	Average		4	5	6	Average		7	8	9	Average	
Time Ignition [s]	4	5.6	6.3			1.8	4.2	3.2			4.4	3.2	3.2		
20	9	17	21	15.67		5	7	8	6.67		4	7	7	6.00	
30	15		48	31.50		13	15	25	17.67		12	22	15	16.33	
40			90	90.00		22	22	36	26.67		24	31	30	28.33	
45							29	55	42.00						
50			105	105.00			37	67	52.00		34	44	44	40.67	
55			133	133.00			53	86	69.50						
60							66	99	82.50		45	64		54.50	
65							81		81.00		52	77		64.50	
70											60	93		76.50	
75											68			68.00	
80											76			76.00	
85											84			84.00	
90											94			94.00	
95															
100															

Flame Spread Data

Laboratory: Newcastle University - Fire Lab
Date of Tests: 13/02/03
Material: Laminated Veneer Lumber (LVL)
Specimen Dimension: 250 * 90 * 20

Flame Front Position

Heat Flux	40					50					60				
Specimen Number	1	2	3		Average	4	5	6		Average	7	8	9		Average
Time Ignition [s]	1	1	1			1.5	1	1			0.5	0.6	0.9		
20		5	4	3	4.00		3	3	2	2.67		3		1	1.67
30		10	9	7	8.67		7	7	6	6.67		5		4	4.67
40		17	15	11	14.33		16	12	11	13.00		12		7	10.33
45		28	21	18	22.33		22		15	18.50		17			17.00
50		41	30	36	35.67		31	29	23	27.67		21		14	17.33
55		51	40	46	45.67		40	37	31	36.00		29		18	28.33
60		68	54	55	59.00		49	44	45	46.00		35		24	36.67
65		86	68		77.00		67	64	51	60.67		42		39	49.33
70			93		93.00		109		63	86.00		51			65.50
75												63			80.00
80												100			100.00
85															
90															

Appendix B – Irradiance Profiles

From ASTM 1321-97a

Distance	Normalised	Nominal Flux	Normalised
0	0	49.5	0.98
50	0.07	50.5	1.00
100	0.13	49.5	0.98
150	0.20	47.1	0.93
200	0.27	43.1	0.85
250	0.33	37.8	0.75
300	0.40	30.9	0.61
350	0.47	23.9	0.47
400	0.53	18.2	0.36
450	0.60	13.2	0.26
500	0.67	9.2	0.18
550	0.73	6.2	0.12
600	0.80	4.3	0.09
650	0.87	3.1	0.06
700	0.93	2.2	0.04
750	1.00	1.5	0.03

Interpolated

Distance along sample	Angle [°]	60			
	Flux [kW/m²]	30	40	50	60
	Temp [°C]	640	707	770	825
	0	31.5	42	53.5	63.5
	10	26.73	34.53	44.09	52.53
	15	21.95	27.06	34.69	41.57
	20	17.18	19.58	25.28	30.60
	25	16.23	18.32	23.76	28.61
	30	15.28	17.05	22.24	26.62
	35	14.34	15.78	20.72	24.63
	40	13.39	14.52	19.20	22.64
	45	12.45	13.25	17.68	20.64
	50	11.07	11.78	15.65	18.47
	55	9.70	10.32	13.62	16.29
	60	8.33	8.85	11.59	14.12
	65	6.96	7.38	9.57	11.94
	70	6.56	6.82	9.03	11.13
	75	6.15	6.26	8.49	10.31
	80	5.75	5.70	7.96	9.49
	85	5.34	5.13	7.42	8.68
	90	4.88	4.50	6.68	7.94
	95	4.41	3.86	5.94	7.21
	100	3.95	3.23	5.19	6.47
	105	3.48	2.59	4.45	5.74
	110	3.19	2.51	4.28	5.50
	115	2.89	2.42	4.11	5.25
	120	2.60	2.33	3.94	5.01

Appendix B – Irradiance Profiles

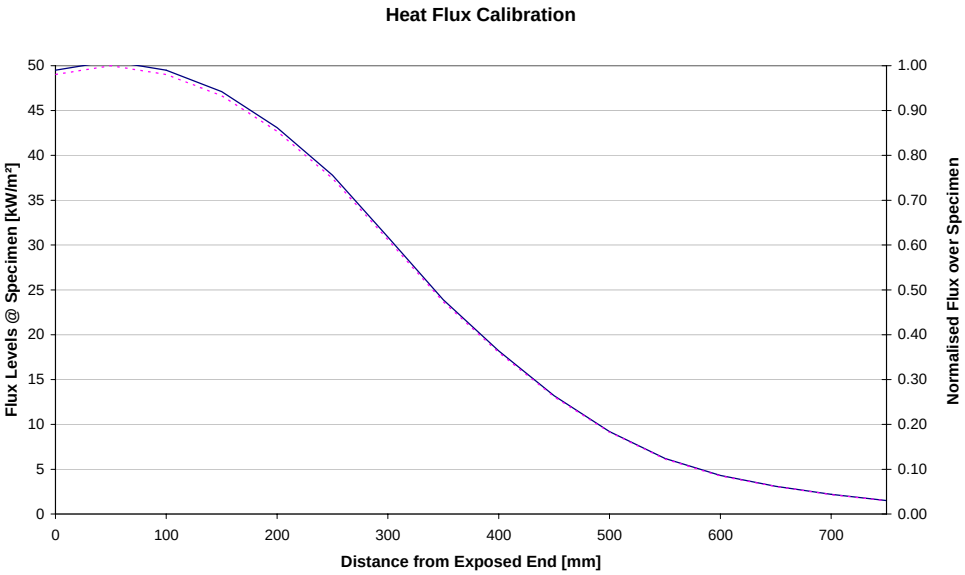

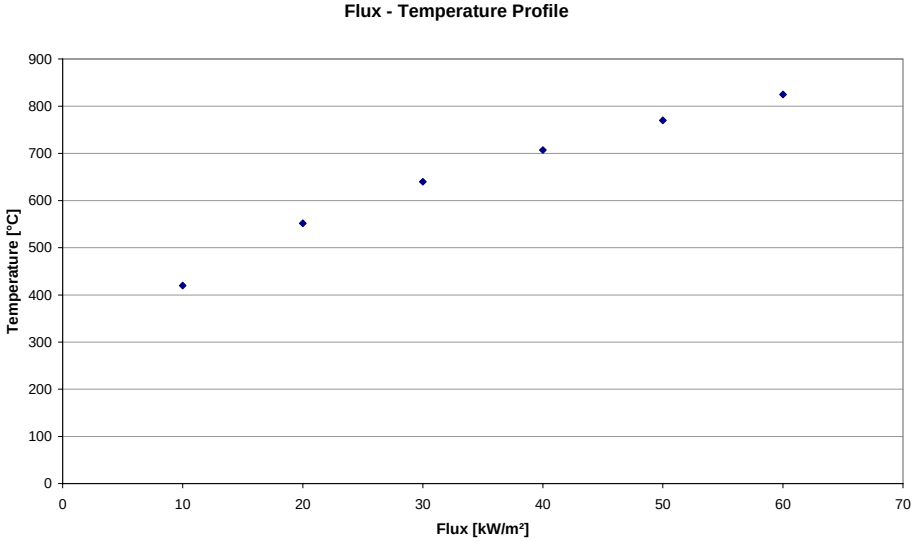

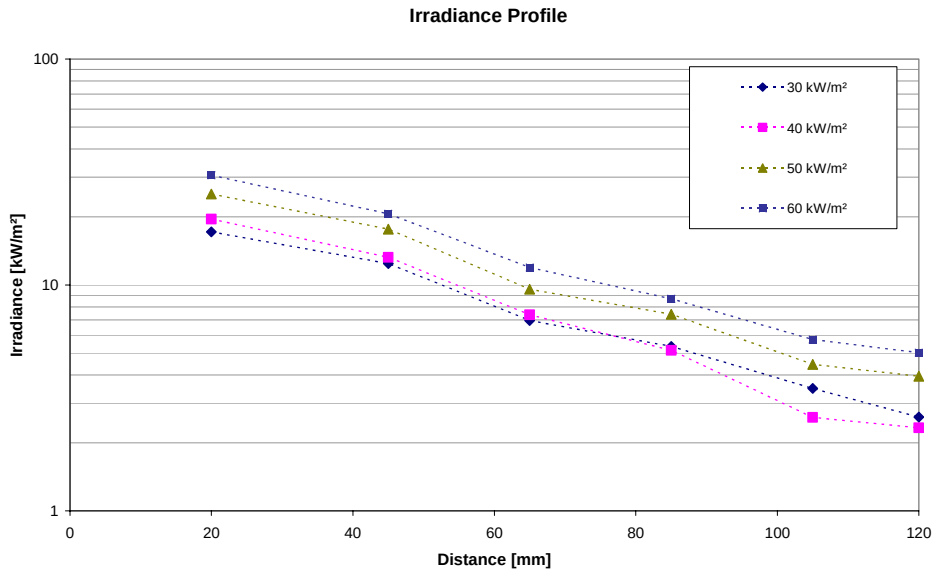

Appendix C – Irradiance Mapping

Measured

Distance	Heat Flux Position	Angle [] Temp [C]	40 640 Meas.30k w/m²	40 707 Meas.40k w/m²	40 770 Meas.50k w/m²	40 825 Meas.60k w/m²	60 640 Meas.30k w/m²	60 707 Meas.40k w/m²	60 770 Meas.50k w/m²	60 825 Meas.60k w/m²	80 640 Meas.30k w/m²	80 707 Meas.40k w/m²	80 770 Meas.50k w/m²	80 825 Meas.60k w/m²
20	1		24.70	30.95	38.45	47.45	17.40	19.75	25.45	30.45	10.20	14.30	17.85	24.75
20	2		23.90	29.75	37.80	46.90	16.85	19.45	25.35	30.85	9.85	12.85	16.70	20.35
45	3		18.65	22.85	28.85	36.15	12.45	13.30	17.60	20.90	6.40	8.85	11.90	13.35
65	4		14.10	14.75	17.70	23.50	7.60	7.80	9.50	12.85	4.10	5.90	6.50	9.00
65	5		10.15	12.50	15.70	19.20	6.35	6.90	9.80	10.90	3.40	4.70	5.80	6.80
85	6		8.65	9.45	11.70	15.60	5.30	5.20	7.50	8.55	2.95	3.75	5.15	6.10
105	7		6.05	6.95	8.15	10.80	3.85	2.65	4.85	6.75	2.20	3.35	3.80	4.65
105	8		4.10	4.50	6.45	7.60	3.15	2.60	4.00	4.75	1.75	2.30	3.10	3.90
120	9		3.55	4.05	4.65	5.70	2.65	2.35	3.95	5.00	1.85	2.15	2.80	3.55

Naraghi

Distance	Heat Flux Position	Angle [] Temp [C]	40 640 Calc.30k w/m²	40 707 Calc.40k w/m²	40 770 Calc.50k w/m²	40 825 Calc.60k w/m²	60 640 Calc.30k w/m²	60 707 Calc.40k w/m²	60 770 Calc.50k w/m²	60 825 Calc.60k w/m²	80 640 Calc.30k w/m²	80 707 Calc.40k w/m²	80 770 Calc.50k w/m²	80 825 Calc.60k w/m²
20	1		20.89	27.86	34.82	41.79	13.09	17.45	21.81	26.18	4.44	5.92	7.40	8.88
20	2		20.89	27.86	34.82	41.79	13.09	17.45	21.81	26.18	4.44	5.92	7.40	8.88
45	3		17.77	23.69	29.62	35.54	10.33	13.77	17.21	20.65	3.36	4.48	5.60	6.72
65	4		15.30	20.39	25.49	30.59	8.35	11.13	13.91	16.69	2.63	3.51	4.39	5.26
65	5		15.30	20.39	25.49	30.59	8.35	11.13	13.91	16.69	2.63	3.51	4.39	5.26
85	6		13.05	17.41	21.76	26.11	6.73	8.97	11.21	13.45	2.06	2.75	3.44	4.13
105	7		11.12	14.82	18.53	22.24	5.45	7.27	9.09	10.91	1.64	2.18	2.73	3.28
105	8		11.12	14.82	18.53	22.24	5.45	7.27	9.09	10.91	1.64	2.18	2.73	3.28
120	9		9.87	13.16	16.45	19.74	4.69	6.25	7.81	9.38	1.39	1.85	2.32	2.78

Wilson

Distance	Heat Flux Position	Angle [] Temp [C]	40 640 Calc.30k w/m²	40 707 Calc.40k w/m²	40 770 Calc.50k w/m²	40 825 Calc.60k w/m²	60 640 Calc.30k w/m²	60 707 Calc.40k w/m²	60 770 Calc.50k w/m²	60 825 Calc.60k w/m²	80 640 Calc.30k w/m²	80 707 Calc.40k w/m²	80 770 Calc.50k w/m²	80 825 Calc.60k w/m²
20	1		22.93	30.58	38.22	45.86	14.57	19.42	24.28	29.13	4.98	6.64	8.30	9.96
20	2		22.93	30.58	38.22	45.86	14.57	19.42	24.28	29.13	4.98	6.64	8.30	9.96
45	3		19.22	25.63	32.03	38.44	11.66	15.55	19.44	23.33	3.92	5.23	6.54	7.84
65	4		14.58	19.45	24.31	29.17	9.03	12.04	15.05	18.06	3.07	4.10	5.12	6.15
65	5		14.58	19.45	24.31	29.17	9.03	12.04	15.05	18.06	3.07	4.10	5.12	6.15
85	6		10.25	13.67	17.09	20.51	6.82	9.09	11.36	13.63	2.38	3.18	3.97	4.77
105	7		7.06	9.41	11.76	14.11	5.15	6.87	8.58	10.30	1.86	2.48	3.10	3.73
105	8		7.06	9.41	11.76	14.11	5.15	6.87	8.58	10.30	1.86	2.48	3.10	3.73
120	9		5.38	7.17	8.97	10.76	4.21	5.61	7.01	8.42	1.56	2.08	2.60	3.12

Normalised Results

Angle Temp Flux	[] [°C]	Measured 40				Naraghi 40				Wilson 40			
		640 Meas.30k.w/m²	707 Meas.40k.w/m²	770 Meas.50k.w/m²	825 Meas.60k.w/m²	640 Calc.30k.w/m²	707 Calc.40k.w/m²	770 Calc.50k.w/m²	825 Calc.60k.w/m²	640 Calc.30k.w/m²	707 Calc.40k.w/m²	770 Calc.50k.w/m²	825 Calc.60k.w/m²
0.167	1	1.000	1.000	1.000	1.000	1.000	1.000	1.000	1.000	1.000	1.000	1.000	1.000
0.167	2	0.968	0.961	0.983	0.988	1.000	1.000	1.000	1.000	1.000	1.000	1.000	1.000
0.375	3	0.755	0.738	0.750	0.762	0.851	0.851	0.851	0.851	0.838	0.838	0.838	0.838
0.542	4	0.571	0.477	0.460	0.495	0.732	0.732	0.732	0.732	0.636	0.636	0.636	0.636
0.542	5	0.411	0.404	0.408	0.405	0.732	0.732	0.732	0.732	0.636	0.636	0.636	0.636
0.708	6	0.350	0.305	0.304	0.329	0.625	0.625	0.625	0.625	0.447	0.447	0.447	0.447
0.875	7	0.245	0.225	0.212	0.228	0.532	0.532	0.532	0.532	0.308	0.308	0.308	0.308
0.875	8	0.166	0.145	0.168	0.160	0.532	0.532	0.532	0.532	0.308	0.308	0.308	0.308
1.000	9	0.144	0.131	0.121	0.120	0.472	0.472	0.472	0.472	0.235	0.235	0.235	0.235

Heat Flux Position / Distance

Angle Temp Flux	[] [°C]	Measured 60				Naraghi 60				Wilson 60			
		640 Meas.30k.w/m²	707 Meas.40k.w/m²	770 Meas.50k.w/m²	825 Meas.60k.w/m²	640 Calc.30k.w/m²	707 Calc.40k.w/m²	770 Calc.50k.w/m²	825 Calc.60k.w/m²	640 Calc.30k.w/m²	707 Calc.40k.w/m²	770 Calc.50k.w/m²	825 Calc.60k.w/m²
0.167	1	1.000	1.000	1.000	0.987	1.000	1.000	1.000	1.000	1.000	1.000	1.000	1.000
0.167	2	0.968	0.985	0.996	1.000	1.000	1.000	1.000	1.000	1.000	1.000	1.000	1.000
0.375	3	0.716	0.673	0.692	0.677	0.789	0.789	0.789	0.789	0.801	0.801	0.801	0.801
0.542	4	0.437	0.395	0.373	0.417	0.638	0.638	0.638	0.638	0.620	0.620	0.620	0.620
0.542	5	0.365	0.349	0.385	0.353	0.638	0.638	0.638	0.638	0.620	0.620	0.620	0.620
0.708	6	0.305	0.263	0.295	0.277	0.514	0.514	0.514	0.514	0.468	0.468	0.468	0.468
0.875	7	0.221	0.134	0.191	0.219	0.417	0.417	0.417	0.417	0.353	0.353	0.353	0.353
0.875	8	0.181	0.132	0.157	0.154	0.417	0.417	0.417	0.417	0.353	0.353	0.353	0.353
1.000	9	0.152	0.119	0.155	0.162	0.358	0.358	0.358	0.358	0.289	0.289	0.289	0.289

Heat Flux Position / Distance

Angle Temp Flux	[] [°C]	Measured 80				Naraghi 80				Wilson 80			
		640 Meas.30k.w/m²	707 Meas.40k.w/m²	770 Meas.50k.w/m²	825 Meas.60k.w/m²	640 Calc.30k.w/m²	707 Calc.40k.w/m²	770 Calc.50k.w/m²	825 Calc.60k.w/m²	640 Calc.30k.w/m²	707 Calc.40k.w/m²	770 Calc.50k.w/m²	825 Calc.60k.w/m²
0.167	1	1.000	1.000	1.000	1.000	1.000	1.000	1.000	1.000	1.000	1.000	1.000	1.000
0.167	2	0.966	0.899	0.936	0.822	1.000	1.000	1.000	1.000	1.000	1.000	1.000	1.000
0.375	3	0.627	0.619	0.667	0.539	0.757	0.757	0.757	0.757	0.787	0.787	0.787	0.787
0.542	4	0.402	0.413	0.364	0.364	0.593	0.593	0.593	0.593	0.617	0.617	0.617	0.617
0.542	5	0.333	0.329	0.325	0.275	0.593	0.593	0.593	0.593	0.617	0.617	0.617	0.617
0.708	6	0.289	0.262	0.289	0.246	0.465	0.465	0.465	0.465	0.479	0.479	0.479	0.479
0.875	7	0.216	0.234	0.213	0.188	0.369	0.369	0.369	0.369	0.374	0.374	0.374	0.374
0.875	8	0.172	0.161	0.174	0.158	0.369	0.369	0.369	0.369	0.374	0.374	0.374	0.374
1.000	9	0.181	0.150	0.157	0.143	0.313	0.313	0.313	0.313	0.313	0.313	0.313	0.313

Heat Flux Position / Distance

Naraghi and Chung Calculations @ 40°

General Data:

Gap	20	mm
L	56	mm
A_3	21111.5	mm'
r_2	80	mm
r_4	40	mm
h	65	mm
z	1	
σ	5.67E-08	W/m'K4

Flux 30 kW/m'

Temperature K °C

326 653

Angle 40 °

0.698132

cot (q) 1.191754

Incident Angle 50 °

0.872665

Condition										
cot (q) <= (1/H)	4.000	2.435	2.435	1.635	1.295	1.295	1.072	0.314	0.314	0.824
Position	0	1	2	3	4	5	6	7	8	9
Distance, x	0	20	20	45	65	65	85	105	105	120
Distance, y	0	70	20	45	70	20	45	70	20	45
a	0	15	15	34	50	50	65	80	80	92
z (h)	20	33	33	49	62	62	75	87	87	97
H	0.25	0.411	0.411	0.612	0.772	0.772	0.933	1.094	1.094	1.214
X	0.955	0.872	0.872	0.685	0.391	0.391	0.429	0.528	0.528	0.821
Fd1-2	0.721	0.655	0.655	0.558	0.480	0.480	0.410	0.349	0.349	0.310
q''	30000	20894	20894	17771	15296	15296	13055	11119	11119	9869
[kW/m']	30.00	20.89	20.89	17.77	15.30	15.30	13.05	11.12	11.12	9.87

Flux 40 kW/m'

Temperature K °C

395 722

Angle 40 °

0.6981

cot (q) 1.1918

Incident Angle 50 °

0.8727

Condition										
cot (q) <= (1/H)	4.000	2.435	2.435	1.635	1.295	1.295	1.072	0.314	0.314	0.824
Position	0	1	2	3	4	5	6	7	8	9
Distance, x	0	20	20	45	65	65	85	105	105	120
Distance, y	0	70	20	45	70	20	45	70	20	45
a	0	15	15	34	50	50	65	80	80	92
z (h)	20	33	33	49	62	62	75	87	87	97
H	0.25	0.411	0.411	0.612	0.772	0.772	0.933	1.094	1.094	1.214
X	0.955	0.872	0.872	0.685	0.391	0.391	0.429	0.528	0.528	0.821
Fd1-2	0.721	0.655	0.655	0.558	0.480	0.480	0.410	0.349	0.349	0.310
q''	40000	27858	27858	23695	20394	20394	17406	14825	14825	13158
[kW/m']	40.00	27.86	27.86	23.69	20.39	20.39	17.41	14.82	14.82	13.16

Flux 50 kW/m'

Temperature K °C

1051.636 778.6361

Angle 40 °

0.698132

cot (q) 1.191754

Incident Angle 50 °

0.872665

Condition										
cot (q) <= (1/H)	4.000	2.435	2.435	1.635	1.295	1.295	1.072	0.314	0.314	0.824
Position	0	1	2	3	4	5	6	7	8	9
Distance, x	0	20	20	45	65	65	85	105	105	120
Distance, y	0	70	20	45	70	20	45	70	20	45
a	0	15	15	34	50	50	65	80	80	92
z (h)	20	33	33	49	62	62	75	87	87	97
H	0.25	0.411	0.411	0.612	0.772	0.772	0.933	1.094	1.094	1.214
X	0.955	0.872	0.872	0.685	0.391	0.391	0.429	0.528	0.528	0.821
Fd1-2	0.721	0.655	0.655	0.558	0.480	0.480	0.410	0.349	0.349	0.310
q''	50000	34823	34823	29618	25493	25493	21758	18531	18531	16448
[kW/m']	50.00	34.82	34.82	29.62	25.49	25.49	21.76	18.53	18.53	16.45

Flux 60 kW/m'

Temperature K °C

1101 828

Angle 40 °

0.6981

cot (q) 1.1918

Incident Angle 50 °

0.8727

Condition										
cot (q) <= (1/H)	4.000	2.435	2.435	1.635	1.295	1.295	1.072	0.314	0.314	0.824
Position	0	1	2	3	4	5	6	7	8	9
Distance, x	0	20	20	45	65	65	85	105	105	120
Distance, y	0	70	20	45	70	20	45	70	20	45
a	0	15	15	34	50	50	65	80	80	92
z (h)	20	33	33	49	62	62	75	87	87	97
H	0.25	0.411	0.411	0.612	0.772	0.772	0.933	1.094	1.094	1.214
X	0.955	0.872	0.872	0.685	0.391	0.391	0.429	0.528	0.528	0.821
Fd1-2	0.721	0.655	0.655	0.558	0.480	0.480	0.410	0.349	0.349	0.310
q''	60000	41787	41787	35542	30591	30591	26109	22237	22237	19738
[kW/m']	60.00	41.79	41.79	35.54	30.59	30.59	26.11	22.24	22.24	19.74

Naraghi and Chung Calculations @ 60°

General Data:

Gap	20	mm
L	56	mm
A_s	21111.5	mm'
r_2	80	mm
r_4	40	mm
h	65	mm
ε	1	
σ	5.7E-08	W/m'K4

Flux	30	kW/m'	
Temperature	K	°C	
	1029.73	756.732	
Angle	60	°	
	1.047		
cot (q)	0.577		
Incident Angle	30	°	
	0.524		

Condition										
cot (q) <= (1/H)	4.000	2.144	2.144	1.357	1.049	1.049	0.855	0.721	0.721	0.646
Position	0	1	2	3	4	5	6	7	8	9
Distance, x	0	20	20	45	65	65	85	105	105	120
Distance, y	0	70	20	45	70	20	45	70	20	45
a	0	10	10	23	33	33	43	53	53	60
z (h)	20	37	37	59	76	76	94	111	111	124
H	0.250	0.467	0.467	0.737	0.954	0.954	1.170	1.387	1.387	1.549
X	0.930	0.963	0.963	0.905	0.835	0.835	0.737	0.599	0.599	0.447
Fd1-2	0.471	0.411	0.411	0.324	0.262	0.262	0.211	0.171	0.171	0.147
q"	30000	13089	13089	10326	8347	8347	6727	5453	5453	4688
[kW/m']	30.00	13.09	13.09	10.33	8.35	8.35	6.73	5.45	5.45	4.69

Flux	40	kW/m'	
Temperature	K	°C	
	1106.5	833.52	
Angle	60	°	
	1.047		
cot (q)	0.577		
Incident Angle	30	°	
	0.524		

Condition										
cot (q) <= (1/H)	4.000	2.144	2.144	1.357	1.049	1.049	0.855	0.721	0.721	0.646
Position	0	1	2	3	4	5	6	7	8	9
Distance, x	0	20	20	45	65	65	85	105	105	120
Distance, y	0	70	20	45	70	20	45	70	20	45
a	0	10	10	23	33	33	43	53	53	60
z (h)	20	37	37	59	76	76	94	111	111	124
H	0.250	0.467	0.467	0.737	0.954	0.954	1.170	1.387	1.387	1.549
X	0.930	0.963	0.963	0.905	0.835	0.835	0.737	0.599	0.599	0.447
Fd1-2	0.471	0.411	0.411	0.324	0.262	0.262	0.211	0.171	0.171	0.147
q"	40000	17452	17452	13769	11129	11129	8969	7270	7270	6251
[kW/m']	40.00	17.45	17.45	13.77	11.13	11.13	8.97	7.27	7.27	6.25

Flux	50	kW/m'	
Temperature	K	°C	
	1170	897.002	
Angle	60	°	
	1.047		
cot (q)	0.577		
Incident Angle	30	°	
	0.524		

Condition										
cot (q) <= (1/H)	4.000	2.144	2.144	1.357	1.049	1.049	0.855	0.721	0.721	0.646
Position	0	1	2	3	4	5	6	7	8	9
Distance, x	0	20	20	45	65	65	85	105	105	120
Distance, y	0	70	20	45	70	20	45	70	20	45
a	0	10	10	23	33	33	43	53	53	60
z (h)	20	37	37	59	76	76	94	111	111	124
H	0.250	0.467	0.467	0.737	0.954	0.954	1.170	1.387	1.387	1.549
X	0.930	0.963	0.963	0.905	0.835	0.835	0.737	0.599	0.599	0.447
Fd1-2	0.471	0.411	0.411	0.324	0.262	0.262	0.211	0.171	0.171	0.147
q"	50000	21815	21815	17211	13911	13911	11211	9088	9088	7814
[kW/m']	50.00	21.81	21.81	17.21	13.91	13.91	11.21	9.09	9.09	7.81

Flux	60	kW/m'	
Temperature	K	°C	
	1225	952	
Angle	60	°	
	1.047		
cot (q)	0.577		
Incident Angle	30	°	
	0.524		

Condition										
cot (q) <= (1/H)	4.000	2.144	2.144	1.357	1.049	1.049	0.855	0.721	0.721	0.646
Position	0	1	2	3	4	5	6	7	8	9
Distance, x	0	20	20	45	65	65	85	105	105	120
Distance, y	0	70	20	45	70	20	45	70	20	45
a	0	10	10	23	33	33	43	53	53	60
z (h)	20	37	37	59	76	76	94	111	111	124
H	0.250	0.467	0.467	0.737	0.954	0.954	1.170	1.387	1.387	1.549
X	0.930	0.963	0.963	0.905	0.835	0.835	0.737	0.599	0.599	0.447
Fd1-2	0.471	0.411	0.411	0.324	0.262	0.262	0.211	0.171	0.171	0.147
q"	60000	26178	26178	20653	16693	16693	13454	10906	10906	9376
[kW/m']	60.00	26.18	26.18	20.65	16.69	16.69	13.45	10.91	10.91	9.38

Naraghi and Chung Calculations @ 80°

General Data:

Gap	20	mm
L	56	mm
A_s	21112	mm'
r_2	80	mm
r_1	40	mm
h	65	mm
ε	1	
σ	6E-08	W/m'K4

Flux	30	kW/m'	
Temperature	K	°C	
	1341	1068	
Angle	80	°	
	1.396		
cot (q)	0.176		
Incident Angle	10	°	
	0.175		

Condition										
cot (q) <= (1/H)	4.000	2.015	2.015	1.244	0.352	0.352	0.771	0.648	0.648	0.579
Position	0	1	2	3	4	5	6	7	8	9
Distance, x	0	20	20	45	65	65	85	105	105	120
Distance, y	0	70	20	45	70	20	45	70	20	45
a	0	3	3	8	11	11	15	18	18	21
z (h)	20	40	40	64	84	84	104	123	123	138
H	0.250	0.496	0.496	0.804	1.050	1.050	1.296	1.543	1.543	1.727
X	0.999	0.996	0.996	0.990	0.983	0.983	0.974	0.962	0.962	0.952
Fd1-2	0.163	0.139	0.139	0.105	0.083	0.083	0.065	0.051	0.051	0.044
q''	30000	4441	4441	3362	2632	2632	2065	1638	1638	1390
[kW/m']	30.00	4.44	4.44	3.36	2.63	2.63	2.06	1.64	1.64	1.39

Flux	40	kW/m'	
Temperature	K	°C	
B	1441	1168	
Angle	80	°	
	1.396		
cot (q)	0.176		
Incident Angle	10	°	
	0.175		

Condition										
cot (q) <= (1/H)	4.000	2.015	2.015	1.244	0.352	0.352	0.771	0.648	0.648	0.579
Position	0	1	2	3	4	5	6	7	8	9
Distance, x	0	20	20	45	65	65	85	105	105	120
Distance, y	0	70	20	45	70	20	45	70	20	45
a	0	3	3	8	11	11	15	18	18	21
z (h)	20	40	40	64	84	84	104	123	123	138
H	0.250	0.496	0.496	0.804	1.050	1.050	1.296	1.543	1.543	1.727
X	0.999	0.996	0.996	0.990	0.983	0.983	0.974	0.962	0.962	0.952
Fd1-2	0.163	0.139	0.139	0.105	0.083	0.083	0.065	0.051	0.051	0.044
q''	40000	5922	5922	4483	3510	3510	2753	2184	2184	1853
[kW/m']	40.00	5.92	5.92	4.48	3.51	3.51	2.75	2.18	2.18	1.85

Flux	50	kW/m'	
Temperature	K	°C	
B	1524	1251	
Angle	80	°	
	1.396		
cot (q)	0.176		
Incident Angle	10	°	
	0.175		

Condition										
cot (q) <= (1/H)	4.000	2.015	2.015	1.244	0.352	0.352	0.771	0.648	0.648	0.579
Position	0	1	2	3	4	5	6	7	8	9
Distance, x	0	20	20	45	65	65	85	105	105	120
Distance, y	0	70	20	45	70	20	45	70	20	45
a	0	3	3	8	11	11	15	18	18	21
z (h)	20	40	40	64	84	84	104	123	123	138
H	0.250	0.496	0.496	0.804	1.050	1.050	1.296	1.543	1.543	1.727
X	0.999	0.996	0.996	0.990	0.983	0.983	0.974	0.962	0.962	0.952
Fd1-2	0.163	0.139	0.139	0.105	0.083	0.083	0.065	0.051	0.051	0.044
q''	50000	7402	7402	5603	4387	4387	3441	2730	2730	2316
[kW/m']	50.00	7.40	7.40	5.60	4.39	4.39	3.44	2.73	2.73	2.32

Flux	60	kW/m'	
Temperature	K	°C	
B	1595	1322	
Angle	80	°	
	1.396		
cot (q)	0.176		
Incident Angle	10	°	
	0.175		

Condition										
cot (q) <= (1/H)	4.000	2.015	2.015	1.244	0.352	0.352	0.771	0.648	0.648	0.579
Position	0	1	2	3	4	5	6	7	8	9
Distance, x	0	20	20	45	65	65	85	105	105	120
Distance, y	0	70	20	45	70	20	45	70	20	45
a	0	3	3	8	11	11	15	18	18	21
z (h)	20	40	40	64	84	84	104	123	123	138
H	0.250	0.496	0.496	0.804	1.050	1.050	1.296	1.543	1.543	1.727
X	0.999	0.996	0.996	0.990	0.983	0.983	0.974	0.962	0.962	0.952
Fd1-2	0.163	0.139	0.139	0.105	0.083	0.083	0.065	0.051	0.051	0.044
q''	60000	8883	8883	6724	5264	5264	4130	3276	3276	2779
[kW/m']	60.00	8.88	8.88	6.72	5.26	5.26	4.13	3.28	3.28	2.78

Wilson et al Calculations @ 40°

General Data:

Gap	20	mm
L	56	mm
A_g	21112	mm²
r_2	80	mm
r_1	40	mm
h	65	mm
z	1	
σ	5.67E-08	W/m²K⁴

Flux	30	kW/m²
Temperature	707	°C
	980	K
Angle	40	°
	0.698	
Incident Angl	50	°
	0.873	

Partition	0	1	2	3	4	5	6	7	8	9
Distance, x	0	20	20	45	65	65	85	105	105	120
Distance, y	0	70	20	45	70	20	45	70	20	45
a	0	15	15	34	50	50	65	80	80	92
z	20	33	33	49	62	62	75	87	87	97
H_2	N/A	2.14	2.14	1.42	1.24	1.24	1.15	1.09	1.09	1.06
H_4	N/A	6.39	6.39	3.30	2.55	2.55	2.14	1.90	1.90	1.76
R_2	N/A	5.22	5.22	2.32	1.61	1.61	1.23	0.99	0.99	0.87
R_4	N/A	2.61	2.61	1.16	0.80	0.80	0.61	0.50	0.50	0.44
Z_2	N/A	32.86	32.86	8.40	5.12	5.12	3.82	3.17	3.17	2.87
Z_4	N/A	48.61	48.61	13.27	8.13	8.13	5.98	4.84	4.84	4.30
$F_{2\text{-}2}$	0.671	0.848	0.848	0.669	0.505	0.505	0.363	0.258	0.258	0.203
$F_{4\text{-}4}$	0.099	0.276	0.276	0.190	0.142	0.142	0.107	0.083	0.083	0.069
$F_{4\text{-}3}$	0.573	0.571	0.571	0.479	0.363	0.363	0.255	0.176	0.176	0.134
q"	300000	22932	22932	19219	14584	14584	10253	7057	7057	5388
[kW/m²]	30.000	22.93	22.93	19.22	14.58	14.58	10.25	7.06	7.06	5.38

Flux	40	kW/m²
Temperature	781	°C
	1054	K
Angle	40	°
	0.698	
Incident Angl	50	°
	0.873	

Partition	0	1	2	3	4	5	6	7	8	9
Distance, x	0	20	20	45	65	65	85	105	105	120
Distance, y	0	70	20	45	70	20	45	70	20	45
a	0	15	15	34	50	50	65	80	80	92
z	20	33	33	49	62	62	75	87	87	97
H_2	N/A	2.14	2.14	1.42	1.24	1.24	1.15	1.09	1.09	1.06
H_4	N/A	6.39	6.39	3.30	2.55	2.55	2.14	1.90	1.90	1.76
R_2	N/A	5.22	5.22	2.32	1.61	1.61	1.23	0.99	0.99	0.87
R_4	N/A	2.61	2.61	1.16	0.80	0.80	0.61	0.50	0.50	0.44
Z_2	N/A	32.86	32.86	8.40	5.12	5.12	3.82	3.17	3.17	2.87
Z_4	N/A	48.61	48.61	13.27	8.13	8.13	5.98	4.84	4.84	4.30
$F_{2\text{-}2}$	0.671	0.848	0.848	0.669	0.505	0.505	0.363	0.258	0.258	0.203
$F_{4\text{-}4}$	0.099	0.276	0.276	0.190	0.142	0.142	0.107	0.083	0.083	0.069
$F_{4\text{-}3}$	0.573	0.571	0.571	0.479	0.363	0.363	0.255	0.176	0.176	0.134
q"	400000	30576	30576	25625	19446	19446	13671	9409	9409	7173
[kW/m²]	40.000	30.58	30.58	25.63	19.45	19.45	13.67	9.41	9.41	7.17

Flux	50	kW/m²
Temperature	841	°C
	1114	K
Angle	40	°
	0.698	
Incident Angl	50	°
	0.873	

Partition	0	1	2	3	4	5	6	7	8	9
Distance, x	0	20	20	45	65	65	85	105	105	120
Distance, y	0	70	20	45	70	20	45	70	20	45
a	0	15	15	34	50	50	65	80	80	92
z	20	33	33	49	62	62	75	87	87	97
H_2	N/A	2.14	2.14	1.42	1.24	1.24	1.15	1.09	1.09	1.06
H_4	N/A	6.39	6.39	3.30	2.55	2.55	2.14	1.90	1.90	1.76
R_2	N/A	5.22	5.22	2.32	1.61	1.61	1.23	0.99	0.99	0.87
R_4	N/A	2.61	2.61	1.16	0.80	0.80	0.61	0.50	0.50	0.44
Z_2	N/A	32.86	32.86	8.40	5.12	5.12	3.82	3.17	3.17	2.87
Z_4	N/A	48.61	48.61	13.27	8.13	8.13	5.98	4.84	4.84	4.30
$F_{2\text{-}2}$	0.671	0.848	0.848	0.669	0.505	0.505	0.363	0.258	0.258	0.203
$F_{4\text{-}4}$	0.099	0.276	0.276	0.190	0.142	0.142	0.107	0.083	0.083	0.069
$F_{4\text{-}3}$	0.573	0.571	0.571	0.479	0.363	0.363	0.255	0.176	0.176	0.134
q"	500001	38221	38221	32032	24307	24307	17089	11762	11762	8966
[kW/m²]	50.000	38.22	38.22	32.03	24.31	24.31	17.09	11.76	11.76	8.97

Flux	60	kW/m²
Temperature	893	°C
	1166	K
Angle	40	°
	0.698	
Incident Angl	50	°
	0.873	

Partition	0	1	2	3	4	5	6	7	8	9
Distance, x	0	20	20	45	65	65	85	105	105	120
Distance, y	0	70	20	45	70	20	45	70	20	45
a	0	15	15	34	50	50	65	80	80	92
z	20	33	33	49	62	62	75	87	87	97
H_2	N/A	2.14	2.14	1.42	1.24	1.24	1.15	1.09	1.09	1.06
H_4	N/A	6.39	6.39	3.30	2.55	2.55	2.14	1.90	1.90	1.76
R_2	N/A	5.22	5.22	2.32	1.61	1.61	1.23	0.99	0.99	0.87
R_4	N/A	2.61	2.61	1.16	0.80	0.80	0.61	0.50	0.50	0.44
Z_2	N/A	32.86	32.86	8.40	5.12	5.12	3.82	3.17	3.17	2.87
Z_4	N/A	48.61	48.61	13.27	8.13	8.13	5.98	4.84	4.84	4.30
$F_{2\text{-}2}$	0.671	0.848	0.848	0.669	0.505	0.505	0.363	0.258	0.258	0.203
$F_{4\text{-}4}$	0.099	0.276	0.276	0.190	0.142	0.142	0.107	0.083	0.083	0.069
$F_{4\text{-}3}$	0.573	0.571	0.571	0.479	0.363	0.363	0.255	0.176	0.176	0.134
q"	600000	45864	45864	38438	29168	29168	20506	14114	14114	10759
[kW/m²]	60.000	45.86	45.86	38.44	29.17	29.17	20.51	14.11	14.11	10.76

Wilson et al Calculations @ 80°

General Data:

Gap	20	mm
L	56	mm
A_1	21111.5	mm²
r_2	80	mm
r_4	40	mm
h	65	mm
z	1	
σ	5.7E-08	W/m²K4

Flux	30 kW/m²									
Temperature	707 °C									
	980 K									
Angle	80 °									
	1.396									
IncidentAngle	10 °									
	0.175									
Parition	0	1	2	3	4	5	6	7	8	9
Distance,x	0	20	20	45	65	65	85	105	105	120
Distance,y	0	70	20	45	70	20	45	70	20	45
a	0	3	3	∞	11	11	15	18	18	21
z	20	40	40	64	84	84	104	123	123	138
H_2	N/A	11.43	11.43	8.23	7.44	7.44	7.03	6.77	6.77	6.63
H_4	N/A	30.15	30.15	16.55	13.20	13.20	11.43	10.33	10.33	9.75
R_2	N/A	23.04	23.04	10.24	7.09	7.09	5.42	4.39	4.39	3.84
R_4	N/A	11.52	11.52	5.12	3.54	3.54	2.71	2.19	2.19	1.92
Z_2	N/A	662.26	662.26	173.56	106.64	106.64	79.75	66.06	66.06	59.71
Z_4	N/A	1042.44	1042.44	301.07	187.85	187.85	138.99	112.59	112.59	99.76
F_{41-2}	0.671	0.802	0.802	0.605	0.471	0.471	0.367	0.290	0.290	0.245
F_{41-4}	0.099	0.254	0.254	0.174	0.133	0.133	0.105	0.085	0.085	0.073
F_{41-3}	0.573	0.548	0.548	0.431	0.338	0.338	0.262	0.205	0.205	0.172
q^*	29947	4973	4973	3915	3067	3067	2381	1860	1860	1558
[kW/m²]	29.95	4.97	4.97	3.91	3.07	3.07	2.38	1.86	1.86	1.56

Flux	40 kW/m²									
Temperature	781 °C									
	1054 K									
Angle	80 °									
	1.396									
IncidentAngle	10 °									
	0.175									
Parition	0	1	2	3	4	5	6	7	8	9
Distance,x	0	20	20	45	65	65	85	105	105	120
Distance,y	0	70	20	45	70	20	45	70	20	45
a	0	3	3	∞	11	11	15	18	18	21
z	20	40	40	64	84	84	104	123	123	138
H_2	N/A	11.43	11.43	8.23	7.44	7.44	7.03	6.77	6.77	6.63
H_4	N/A	30.15	30.15	16.55	13.20	13.20	11.43	10.33	10.33	9.75
R_2	N/A	23.04	23.04	10.24	7.09	7.09	5.42	4.39	4.39	3.84
R_4	N/A	11.52	11.52	5.12	3.54	3.54	2.71	2.19	2.19	1.92
Z_2	N/A	662.26	662.26	173.56	106.64	106.64	79.75	66.06	66.06	59.71
Z_4	N/A	1042.44	1042.44	301.07	187.85	187.85	138.99	112.59	112.59	99.76
F_{41-2}	0.671	0.802	0.802	0.605	0.471	0.471	0.367	0.290	0.290	0.245
F_{41-4}	0.099	0.254	0.254	0.174	0.133	0.133	0.105	0.085	0.085	0.073
F_{41-3}	0.573	0.548	0.548	0.431	0.338	0.338	0.262	0.205	0.205	0.172
q^*	40000	6643	6643	5229	4097	4097	3180	2484	2484	2081
[kW/m²]	40.00	6.64	6.64	5.23	4.10	4.10	3.18	2.48	2.48	2.08

Flux	50 kW/m²									
Temperature	841 °C									
	1114 K									
Angle	80 °									
	1.396									
IncidentAngle	10 °									
	0.175									
Parition	0	1	2	3	4	5	6	7	8	9
Distance,x	0	20	20	45	65	65	85	105	105	120
Distance,y	0	70	20	45	70	20	45	70	20	45
a	0	3	3	∞	11	11	15	18	18	21
z	20	40	40	64	84	84	104	123	123	138
H_2	N/A	11.43	11.43	8.23	7.44	7.44	7.03	6.77	6.77	6.63
H_4	N/A	30.15	30.15	16.55	13.20	13.20	11.43	10.33	10.33	9.75
R_2	N/A	23.04	23.04	10.24	7.09	7.09	5.42	4.39	4.39	3.84
R_4	N/A	11.52	11.52	5.12	3.54	3.54	2.71	2.19	2.19	1.92
Z_2	N/A	662.26	662.26	173.56	106.64	106.64	79.75	66.06	66.06	59.71
Z_4	N/A	1042.44	1042.44	301.07	187.85	187.85	138.99	112.59	112.59	99.76
F_{41-2}	0.671	0.802	0.802	0.605	0.471	0.471	0.367	0.290	0.290	0.245
F_{41-4}	0.099	0.254	0.254	0.174	0.133	0.133	0.105	0.085	0.085	0.073
F_{41-3}	0.573	0.548	0.548	0.431	0.338	0.338	0.262	0.205	0.205	0.172
q^*	50001	8303	8303	6536	5121	5121	3975	3105	3105	2601
[kW/m²]	50.00	8.30	8.30	6.54	5.12	5.12	3.97	3.10	3.10	2.60

Flux	60 kW/m²									
Temperature	893 °C									
	1166 K									
Angle	80 °									
	1.396									
IncidentAngle	10 °									
	0.175									
Parition	0	1	2	3	4	5	6	7	8	9
Distance,x	0	20	20	45	65	65	85	105	105	120
Distance,y	0	70	20	45	70	20	45	70	20	45
a	0	3	3	∞	11	11	15	18	18	21
z	20	40	40	64	84	84	104	123	123	138
H_2	N/A	11.43	11.43	8.23	7.44	7.44	7.03	6.77	6.77	6.63
H_4	N/A	30.15	30.15	16.55	13.20	13.20	11.43	10.33	10.33	9.75
R_2	N/A	23.04	23.04	10.24	7.09	7.09	5.42	4.39	4.39	3.84
R_4	N/A	11.52	11.52	5.12	3.54	3.54	2.71	2.19	2.19	1.92
Z_2	N/A	662.26	662.26	173.56	106.64	106.64	79.75	66.06	66.06	59.71
Z_4	N/A	1042.44	1042.44	301.07	187.85	187.85	138.99	112.59	112.59	99.76
F_{41-2}	0.671	0.802	0.802	0.605	0.471	0.471	0.367	0.290	0.290	0.245
F_{41-4}	0.099	0.254	0.254	0.174	0.133	0.133	0.105	0.085	0.085	0.073
F_{41-3}	0.573	0.548	0.548	0.431	0.338	0.338	0.262	0.205	0.205	0.172
q^*	60000	9964	9964	7843	6145	6145	4770	3726	3726	3121
[kW/m²]	60.00	9.96	9.96	7.84	6.15	6.15	4.77	3.73	3.73	3.12

Wilson et al Calculations @ 80°

General Data:

Gap	20	mm
L	56	mm
A_1	21111.5	mm²
r_2	80	mm
r_4	40	mm
h	65	mm
z	1	
σ	5.7E-08	W/m²K4

Flux	30 kW/m²								
Temperature	707 °C								
	980 K								
Angle	80 °								
	1.396								
IncidentAngl	10 °								
	0.175								
Paritian	0	1	2	3	4	5	6	7	8	9
Distance,x	0	20	20	45	65	65	85	105	105	120
Distance,y	0	70	20	45	70	20	45	70	20	45
a	0	3	3	∞	11	11	15	18	18	21
z	20	40	40	64	84	84	104	123	123	138
H_2	N/A	11.43	11.43	8.23	7.44	7.44	7.03	6.77	6.77	6.63
H_4	N/A	30.15	30.15	16.55	13.20	13.20	11.43	10.33	10.33	9.75
R_2	N/A	23.04	23.04	10.24	7.09	7.09	5.42	4.39	4.39	3.84
R_4	N/A	11.52	11.52	5.12	3.54	3.54	2.71	2.19	2.19	1.92
Z_2	N/A	662.26	662.26	173.56	106.64	106.64	79.75	66.06	66.06	59.71
Z_4	N/A	1042.44	1042.44	301.07	187.85	187.85	138.99	112.59	112.59	99.76
$F_{4:2}$	0.671	0.802	0.802	0.605	0.471	0.471	0.367	0.290	0.290	0.245
$F_{4:4}$	0.099	0.254	0.254	0.174	0.133	0.133	0.105	0.085	0.085	0.073
$F_{4:3}$	0.573	0.548	0.548	0.431	0.338	0.338	0.262	0.205	0.205	0.172
s^4	29947	4973	4973	3915	3067	3067	2381	1860	1860	1558
[kW/m²]	29.95	4.97	4.97	3.91	3.07	3.07	2.38	1.86	1.86	1.56

Flux	40 kW/m²								
Temperature	781 °C								
	1054 K								
Angle	80 °								
	1.396								
IncidentAngl	10 °								
	0.175								
Paritian	0	1	2	3	4	5	6	7	8	9
Distance,x	0	20	20	45	65	65	85	105	105	120
Distance,y	0	70	20	45	70	20	45	70	20	45
a	0	3	3	∞	11	11	15	18	18	21
z	20	40	40	64	84	84	104	123	123	138
H_2	N/A	11.43	11.43	8.23	7.44	7.44	7.03	6.77	6.77	6.63
H_4	N/A	30.15	30.15	16.55	13.20	13.20	11.43	10.33	10.33	9.75
R_2	N/A	23.04	23.04	10.24	7.09	7.09	5.42	4.39	4.39	3.84
R_4	N/A	11.52	11.52	5.12	3.54	3.54	2.71	2.19	2.19	1.92
Z_2	N/A	662.26	662.26	173.56	106.64	106.64	79.75	66.06	66.06	59.71
Z_4	N/A	1042.44	1042.44	301.07	187.85	187.85	138.99	112.59	112.59	99.76
$F_{4:2}$	0.671	0.802	0.802	0.605	0.471	0.471	0.367	0.290	0.290	0.245
$F_{4:4}$	0.099	0.254	0.254	0.174	0.133	0.133	0.105	0.085	0.085	0.073
$F_{4:3}$	0.573	0.548	0.548	0.431	0.338	0.338	0.262	0.205	0.205	0.172
s^4	40000	6643	6643	5229	4097	4097	3180	2484	2484	2081
[kW/m²]	40.00	6.64	6.64	5.23	4.10	4.10	3.18	2.48	2.48	2.08

Flux	50 kW/m²								
Temperature	841 °C								
	1114 K								
Angle	80 °								
	1.396								
IncidentAngl	10 °								
	0.175								
Paritian	0	1	2	3	4	5	6	7	8	9
Distance,x	0	20	20	45	65	65	85	105	105	120
Distance,y	0	70	20	45	70	20	45	70	20	45
a	0	3	3	∞	11	11	15	18	18	21
z	20	40	40	64	84	84	104	123	123	138
H_2	N/A	11.43	11.43	8.23	7.44	7.44	7.03	6.77	6.77	6.63
H_4	N/A	30.15	30.15	16.55	13.20	13.20	11.43	10.33	10.33	9.75
R_2	N/A	23.04	23.04	10.24	7.09	7.09	5.42	4.39	4.39	3.84
R_4	N/A	11.52	11.52	5.12	3.54	3.54	2.71	2.19	2.19	1.92
Z_2	N/A	662.26	662.26	173.56	106.64	106.64	79.75	66.06	66.06	59.71
Z_4	N/A	1042.44	1042.44	301.07	187.85	187.85	138.99	112.59	112.59	99.76
$F_{4:2}$	0.671	0.802	0.802	0.605	0.471	0.471	0.367	0.290	0.290	0.245
$F_{4:4}$	0.099	0.254	0.254	0.174	0.133	0.133	0.105	0.085	0.085	0.073
$F_{4:3}$	0.573	0.548	0.548	0.431	0.338	0.338	0.262	0.205	0.205	0.172
s^4	50001	8303	8303	6536	5121	5121	3975	3105	3105	2601
[kW/m²]	50.00	8.30	8.30	6.54	5.12	5.12	3.97	3.10	3.10	2.60

Flux	60 kW/m²								
Temperature	893 °C								
	1166 K								
Angle	80 °								
	1.396								
IncidentAngl	10 °								
	0.175								
Paritian	0	1	2	3	4	5	6	7	8	9
Distance,x	0	20	20	45	65	65	85	105	105	120
Distance,y	0	70	20	45	70	20	45	70	20	45
a	0	3	3	∞	11	11	15	18	18	21
z	20	40	40	64	84	84	104	123	123	138
H_2	N/A	11.43	11.43	8.23	7.44	7.44	7.03	6.77	6.77	6.63
H_4	N/A	30.15	30.15	16.55	13.20	13.20	11.43	10.33	10.33	9.75
R_2	N/A	23.04	23.04	10.24	7.09	7.09	5.42	4.39	4.39	3.84
R_4	N/A	11.52	11.52	5.12	3.54	3.54	2.71	2.19	2.19	1.92
Z_2	N/A	662.26	662.26	173.56	106.64	106.64	79.75	66.06	66.06	59.71
Z_4	N/A	1042.44	1042.44	301.07	187.85	187.85	138.99	112.59	112.59	99.76
$F_{4:2}$	0.671	0.802	0.802	0.605	0.471	0.471	0.367	0.290	0.290	0.245
$F_{4:4}$	0.099	0.254	0.254	0.174	0.133	0.133	0.105	0.085	0.085	0.073
$F_{4:3}$	0.573	0.548	0.548	0.431	0.338	0.338	0.262	0.205	0.205	0.172
s^4	60000	9964	9964	7843	6145	6145	4770	3726	3726	3121
[kW/m²]	60.00	9.96	9.96	7.84	6.15	6.15	4.77	3.73	3.73	3.12

Appendix D – Ignition Calculations

680 Research - Flame Spread
21 January 2003

Ignition Data

Particle Board
Raw Data

Heat Flux	Ignition time analysis			
[kW/m²]	t	t^{-1}	$t^{(-1/1.5)}$	$t^{-1/2}$
40	68	0.015	0.060	0.121
40	73	0.014	0.057	0.117
40	65	0.015	0.062	0.124
35	84	0.012	0.052	0.109
35	84	0.012	0.052	0.109
35	77	0.013	0.055	0.114
30	114	0.009	0.043	0.094
30	130	0.008	0.039	0.088
30	117	0.009	0.042	0.092
20	313	0.003	0.022	0.057
20	290	0.003	0.023	0.059
20	306	0.003	0.022	0.057

Average Reults

Heat Flux	Ignition time analysis					
[kW/m²]	t	t^{-1}	$t^{(-1/1.5)}$	$t^{-1/2}$	$t^{1/2}$	q_{crit} / q_e"
40	68.67	0.015	0.060	0.121	8.29	0.367
35	81.67	0.012	0.053	0.111	9.04	0.420
30	120.33	0.008	0.041	0.091	10.97	0.490
20	303.00	0.003	0.022	0.057	17.41	0.734
		Thin Soild [t^{-1}]	Inter. Soild [$t^{(-1/1.5)}$]	Thick Soild [$t^{-1/2}$]		

680 Research - Flame Spread
21 January 2003

Ignition Data

Laminated Veneer Lumber
Raw Data

Heat Flux	Ignition time analysis			
[kW/m²]	t	t^{-1}	$t^{(-1/1.5)}$	$t^{-1/2}$
50	29	0.034	0.106	0.186
50	24	0.042	0.120	0.204
50	26	0.038	0.114	0.196
40	36	0.028	0.092	0.167
40	44	0.023	0.080	0.151
40	41	0.024	0.084	0.156
30	70	0.014	0.059	0.120
30	57	0.018	0.068	0.132
30	63	0.016	0.063	0.126
20	291	0.003	0.023	0.059
20	412	0.002	0.018	0.049
20	312	0.003	0.022	0.057

Average Reults

Heat Flux	Ignition time analysis					
[kW/m²]	t	t^{-1}	$t^{(-1/1.5)}$	$t^{-1/2}$	$t^{1/2}$	q_{crit} / q_e"
50	26.33	0.038	0.113	0.195	5.13	0.344
40	40.33	0.025	0.085	0.157	6.35	0.431
30	63.33	0.016	0.063	0.126	7.96	0.574
20	338.33	0.003	0.021	0.054	18.39	0.861
		Thin Soild [t^{-1}]	Inter. Soild [$t^{(-1/1.5)}$]	Thick Soild [$t^{-1/2}$]		

Particle Board - Ignition Results

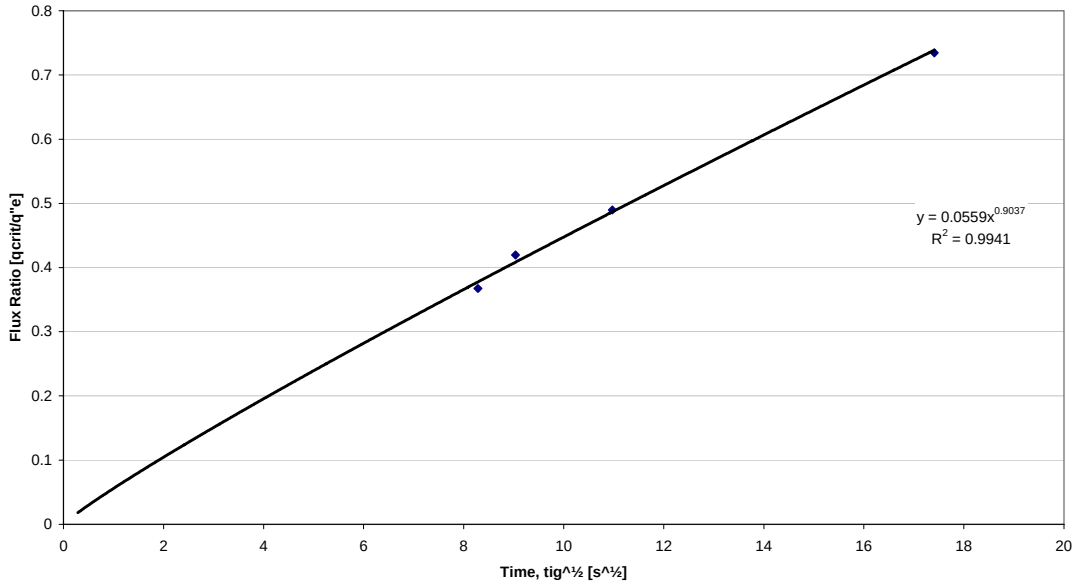

Laminated Veneer Lumber (LVL)
Ignition Results

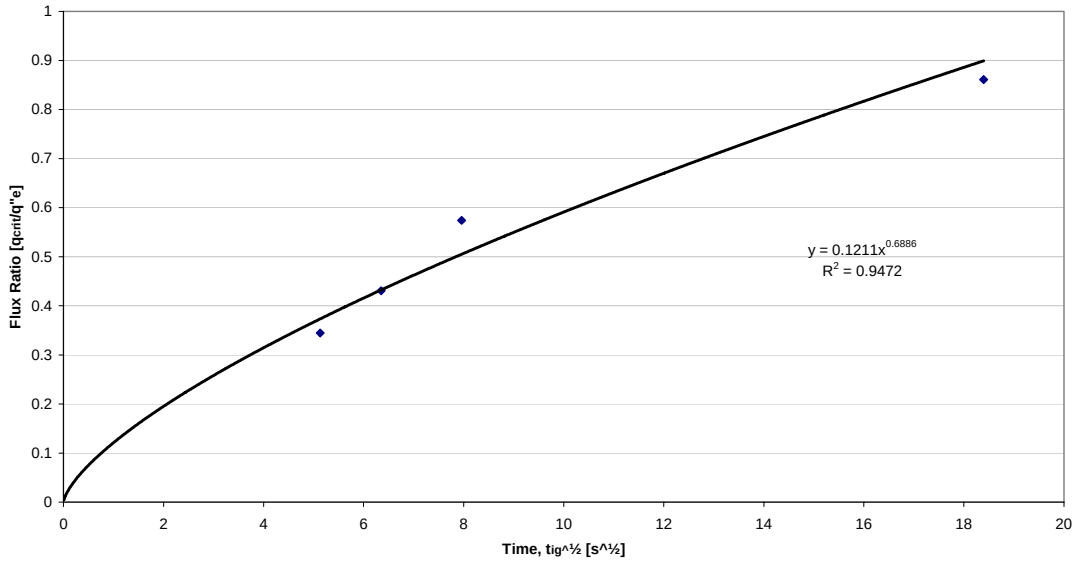

		Macrocarpa				Beech				Rimu				Radiata Pine			
q_{crit}"	[kW/m²]	17	17	17	17	16	16	16	16	14	14	14	14	15	15	15	15
b		0.065	0.065	0.065	0.065	0.057	0.057	0.057	0.057	0.044	0.044	0.044	0.044	0.059	0.059	0.059	0.059
q_e"	[kW/m²]	30	40	50	60	30	40	50	60	30	40	50	60	30	40	50	60
q_{crit}" / q_e"		0.567	0.425	0.340	0.283	0.533	0.400	0.320	0.267	0.467	0.350	0.280	0.233	0.500	0.375	0.300	0.250
t*	[s]	75	42	27	19	89	50	32	22	110	62	40	28	72	41	26	18

		Plywood				MDF				Particle Board				LVL			
q_{crit}"	[kW/m²]	13	13	13	13	15	15	15	15	14.7	14.7	14.7	14.7	17.2	17.2	17.2	17.2
b		0.047	0.047	0.047	0.047	0.048	0.048	0.048	0.048	0.056	0.056	0.056	0.056	0.121	0.121	0.121	0.121
q_e"	[kW/m²]	30	40	50	60	30	40	50	60	30	40	50	60	30	40	50	60
q_{crit}" / q_e"		0.433	0.325	0.260	0.217	0.500	0.375	0.300	0.250	0.490	0.368	0.294	0.245	0.573	0.430	0.344	0.287
t*	[s]	83	47	30	21	110	62	40	28	77	43	28	19	22	13	8	6

Appendix E – Flame Spread Calculations

Flame Spread Data

Laboratory	Newcastle University - Fire Lab
Date of Tests	7/02/03
Material	Particle Board
Specimen Dimension	250 * 90 * 20
b Value	0.0391

	Heat Flux	40									
	Flame Front Position	Σt	Σx	Σ(t²)	(Σt)²	Σ(t.x)	V	F(t)	Q	Q*F(t)	t/√V
Test 1	Ignition Time	27									
	20	27						0.203	19.58	3.98	
	30	79	237	90	24131	56169	8150	0.19	0.348	17.05	5.93	2.280
	40	131							0.448	14.52	6.50	
	50											
	55											
	60											
Test 2	Ignition Time	10.4									
	20	33							0.225	19.58	4.40	
	30	85	244	90	24190	59536	8250	0.21	0.360	17.05	6.15	2.161
	40	126	408	120	61910	166464	17440	0.17	0.439	14.52	6.37	2.395
	50	197							0.549	11.78	6.47	
	55											
	60											
Test 3	Ignition Time	7									
	20	23							0.188	19.58	3.67	
	30	78	241	90	26213	58081	8400	0.17	0.345	17.05	5.89	2.420
	40	140	428	120	63784	183184	18440	0.15	0.463	14.52	6.72	2.571
	50	210							0.567	11.78	6.68	
	55											
	60											

Laboratory	Newcastle University - Fire Lab
Date of Tests	7/02/03
Material	Particle Board
Specimen Dimension	250 * 90 * 20
b Value	0.0391

	Heat Flux	50										
	Flame Front Position		Σt	Σx	$\Sigma(t^2)$	$(\Sigma t)^2$	Σ(t.x)	V	F(t)	Q	Q*F(t)	1/√V
	Ignition Time	18										
Test 4	20	15							0.151	19.58	2.97	
	30	43	155	90	11483	24025	5470	0.24	0.256	17.05	4.37	2.058
	40	97	283	120	31707	80089	12320	0.20	0.385	14.52	5.59	2.238
	50	143	457	150	76947	208849	24050	0.16	0.468	11.78	5.51	2.472
	55											
	60	217							0.576	8.85	5.10	
	65											
	70											
	Ignition Time	8										
Test 5	20	28							0.207	19.58	4.05	
	30	53	168	90	11162	28224	5630	0.34	0.285	17.05	4.85	1.724
	40	87	276	120	28874	76176	11870	0.24	0.365	14.52	5.29	2.048
	50	136	445	150	75349	198025	23600	0.14	0.456	11.78	5.37	2.630
	55								0.000	10.32	0.00	
	60	222							0.583	8.85	5.16	
	65								0.000	7.38	0.00	
	70											
	Ignition Time	5										
Test 6	20	25							0.196	19.58	3.83	
	30	59	182	90	13710	33124	6190	0.27	0.300	17.05	5.12	1.912
	40	98	411	120	77601	168921	18390	0.09	0.387	14.52	5.62	3.305
	50	254	556	145	115736	309136	27840	0.08	0.623	11.78	7.34	3.623
	55	204	713	165	171157	508369	39220	0.00	0.558	10.32	5.76	
	60	255							0.624	8.85	5.53	
	65											
	70											

Laboratory	Newcastle University - Fire Lab
Date of Tests	7/02/03
Material	Particle Board
Specimen Dimension	250 * 90 * 20
b Value	0.0391

	Heat Flux	60										
	Flame Front Position		Σt	Σx	$\Sigma(t^2)$	$(\Sigma t)^2$	Σ(t.x)	V	F(t)	Q	Q*F(t)	1/√V
	Ignition Time	6										
Test 7	20	26							0.199	19.58	3.90	
	30	47	146	90	8214	21316	4850	0.42	0.268	17.05	4.57	1.536
	40	73	220	120	17538	48400	9330	0.38	0.334	14.52	4.85	1.628
	50	100	305	145	32753	93025	15180	0.25	0.391	11.78	4.61	1.995
	55	132	436	165	69040	190096	24500	0.09	0.449	10.32	4.63	3.303
	60	204							0.558	8.85	4.94	
	65											
	70											
	Ignition Time	14										
Test 8	20	13							0.141	19.58	2.76	
	30	47	135	90	8003	18225	4670	0.32	0.268	17.05	4.57	1.763
	40	75	237	120	21059	56169	10160	0.29	0.339	14.52	4.92	1.853
	50	115	377	145	53819	142129	19035	0.13	0.419	11.78	4.94	2.814
	55	187							0.535	10.32	5.52	
	60											
	65											
	70											
	Ignition Time	4										
Test 9	20	12							0.135	19.58	2.65	
	30	42	124	90	6808	15376	4300	0.34	0.253	17.05	4.32	1.703
	40	70	219	120	18113	47961	9410	0.31	0.327	14.52	4.75	1.809
	50	107	354	145	47678	125316	17885	0.13	0.404	11.78	4.77	2.761
	55	177							0.520	10.32	5.37	
	60											
	65											
	70											

Flame Spread Data

Laboratory	Newcastle University - Fire Lab
Date of Tests	10/02/03
Material	Plywood
Specimen Dimension	250 * 90 * 20
b Value	0.04747

	Heat Flux	40										
	Flame Front Position		Σt	Σx	$\Sigma(t^2)$	$(\Sigma t)^2$	Σ(t.x)	V	F(t)	Q	Q*F(t)	1/√V
	Time Ignition [s]	7.5										
Test 1	20	15							0.184	19.58	3.60	
	30	27	83	90	2635	6889	2750	0.77	0.247	17.05	4.21	1.141
	40	41	160	120	10874	25600	7050	0.28	0.304	14.52	4.41	1.898
	50	92	259	145	26021	67081	13170	0.18	0.455	11.78	5.37	2.370
	55	126	369	165	47141	136161	20590	0.17	0.533	10.32	5.50	2.438
	60	151							0.583	8.85	5.16	
	65											
	70											
	Time Ignition [s]	4.5										
Test 2	20	14							0.178	19.58	3.48	
	30	37	112	90	5286	12544	3830	0.43	0.289	17.05	4.92	1.533
	40	61	221	120	20219	48841	9700	0.22	0.371	14.52	5.38	2.140
	50	123	354	145	47750	125316	17940	0.14	0.526	11.78	6.20	2.684
	55	170	581	165	126973	337561	32780	0.06	0.619	10.32	6.39	4.185
	60	288	798	180	227444	636804	48730	0.06	0.806	8.85	7.13	4.225
	65	340							0.875	7.38	6.46	
	70											
	Time Ignition [s]	5.4										
Test 3	20	6							0.116	19.58	2.28	
	30	20	69	90	2285	4761	2440	0.53	0.212	17.05	3.62	1.373
	40	43	152	120	10170	23104	6770	0.28	0.311	14.52	4.52	1.892
	50	89	306	145	40046	93636	15740	0.11	0.448	11.78	5.28	3.049
	55	174	553	165	122297	305809	31420	0.05	0.626	10.32	6.46	4.501
	60	290							0.808	8.85	7.15	
	65											
	70											

Laboratory	Newcastle University - Fire Lab
Date of Tests	10/02/03
Material	Plywood
Specimen Dimension	250 * 90 * 20
b Value	0.04747

	Heat Flux	50										
	Flame Front Position		Σt	Σx	Σ(t²)	(Σt)²	Σ(t.x)	V	F(t)	Q	Q*F(t)	1/V
	Time Ignition [s]	4										
Test 4	20	10							0.150	19.58	2.94	
	30	21	86	90	3566	7396	3030	0.41	0.218	17.05	3.71	1.564
	40	55	167	120	11747	27889	7380	0.29	0.352	14.52	5.11	1.871
	50	91	284	150	30350	80656	15030	0.24	0.453	11.78	5.34	2.043
	55								0.000	10.32	0.00	
	60	138	398	175	55886	158404	23815	0.19	0.558	8.85	4.94	2.271
	65	169	494	195	82574	244036	32355	0.20	0.617	7.38	4.56	2.239
	70	187							0.649	6.82	4.43	
	75											
	80											
	Time Ignition [s]	3.7										
Test 5	20	12							0.164	19.58	3.22	
	30	25	83	90	2885	6889	2830	0.58	0.237	17.05	4.05	1.316
	40	46	139	120	7365	19321	5990	0.47	0.322	14.52	4.67	1.466
	50	68	202	150	14484	40804	10520	0.48	0.391	11.78	4.61	1.450
	55								0.000	10.32	0.00	
	60	88	270	175	25364	72900	16090	0.32	0.445	8.85	3.94	1.769
	65	114	337	195	38965	113569	22140	0.21	0.507	7.38	3.74	2.172
	70	135	409	210	56821	167281	28860	0.22	0.552	6.82	3.76	2.147
	75	160	470	225	74450	220900	35450	0.24	0.600	6.26	3.76	2.021
	80	175	553	240	103749	305809	44530	0.16	0.628	5.70	3.58	2.500
	85	218							0.701	5.13	3.60	
	90											
	Time Ignition [s]	2.8										
Test 6	20	12							0.164	19.58	3.22	
	30	29	90	90	3386	8100	3070	0.54	0.256	17.05	4.36	1.362
	40	49	151	120	8571	22801	6480	0.45	0.332	14.52	4.82	1.485
	50	73	215	145	16379	46225	10725	0.34	0.406	11.78	4.78	1.706
	55	93	282	165	27434	79524	15725	0.23	0.458	10.32	4.72	2.075
	60	116	359	180	44605	128881	21825	0.17	0.511	8.85	4.52	2.402
	65	150	432	195	63512	186624	28330	0.19	0.581	7.38	4.29	2.284
	70	166	521	210	92081	271441	36745	0.17	0.612	6.82	4.17	2.413
	75	205	602	225	122942	362404	45475	0.15	0.680	6.26	4.25	2.566
	80	231	711	240	171011	505521	57230	0.14	0.721	5.70	4.11	2.675
	85	275	807	255	219587	651249	68945	0.14	0.787	5.13	4.04	2.675
	90	301							0.824	4.50	3.70	

Laboratory: Newcastle University - Fire Lab
Date of Tests: 10/02/03
Material: Plywood
Specimen Dimension: 250 * 90 * 20
b Value: 0.04747

	Heat Flux	60										
	Flame Front Position		Σt	Σx	Σ(t²)	(Σt)²	Σ(t.x)	V	F(t)	Q	Q*F(t)	1/V
Test 7	Time Ignition [s]	5										
	20	14							0.178	19.58	3.48	
	30	24	80	90	2536	6400	2680	0.70	0.233	17.05	3.97	1.199
	40	42	134	120	6364	17956	5800	0.45	0.308	14.52	4.47	1.491
	50	68	201	145	14669	40401	10085	0.31	0.391	11.78	4.61	1.802
	55	91	269	165	25005	72361	15005	0.24	0.453	10.32	4.67	2.052
	60	110	328	180	36510	107584	19860	0.28	0.498	8.85	4.41	1.898
	65	127	386	195	50430	148996	25285	0.26	0.535	7.38	3.95	1.980
	70	149	448	210	67914	200704	31585	0.22	0.579	6.82	3.95	2.121
	75	172	518	225	90594	268324	39090	0.21	0.623	6.26	3.90	2.192
	80	197							0.666	5.70	3.79	
Test 8	Time Ignition [s]	1										
	20	9							0.142	19.58	2.79	
	30	17	54	90	1154	2916	1810	1.04	0.196	17.05	3.34	0.979
	40	28	86	120	2754	7396	3680	0.83	0.251	14.52	3.65	1.097
	50	41	120	145	5066	14400	5975	0.66	0.304	11.78	3.58	1.233
	55	51	165	165	9611	27225	9235	0.30	0.339	10.32	3.50	1.830
	60	73	215	180	16211	46225	13100	0.25	0.406	8.85	3.59	2.003
	65	91	271	195	25059	73441	17785	0.29	0.453	7.38	3.34	1.845
	70	107	338	210	39330	114244	23905	0.20	0.491	6.82	3.35	2.258
	75	140	417	225	59949	173889	31590	0.16	0.562	6.26	3.52	2.511
	80	170							0.619	5.70	3.53	
Test 9	Time Ignition [s]	4										
	20	11							0.157	19.58	3.08	
	30	34	85	90	2877	7225	2840	0.62	0.277	17.05	4.72	1.271
	40	40	134	120	6356	17956	5620	0.70	0.300	14.52	4.36	1.194
	50	60	170	145	10100	28900	8450	0.50	0.368	11.78	4.33	1.414
	55	70	211	165	15061	44521	11710	0.48	0.397	10.32	4.10	1.450
	60	81	243	180	19325	59049	14690	0.45	0.427	8.85	3.78	1.483
	65	92	290	195	28714	84100	19030	0.26	0.455	7.38	3.36	1.945
	70	117	344	210	40378	118336	24295	0.23	0.513	6.82	3.50	2.083
	75	135	399	225	53523	159201	30075	0.33	0.552	6.26	3.45	1.744
	80	147							0.576	5.70	3.28	

Flame Spread Data

Laboratory	Newcastle University - Fire Lab
Date of Tests	10/02/03
Material	Medium Density Fibre Board (MDF)
Specimen Dimension	250 * 90 * 20
b Value	0.0476

	Heat Flux	40										
	Flame Front Position		Σt	Σx	Σ(t²)	(Σt)²	Σ(t.x)	V	F(t)	Q	Q*F(t)	1/√V
	Time Ignition [s]	6.8										
Test 1	20	33							0.273	19.58	5.36	
	30	88	249.00	90	25217	62001	8420	0.21	0.447	17.05	7.61	2.188
	40	128	373.00	115	48777	139129	14825	0.22	0.539	14.52	7.82	2.135
	45	157	477.00	135	77897	227529	21785	0.16	0.596	13.25	7.90	2.534
	50	192	573.00	150	111689	328329	28985	0.15	0.660	11.78	7.77	2.589
	55	224	693.00	165	163769	480249	38540	0.12	0.712	10.32	7.35	2.945
	60	277	827.00	180	233181	683929	50130	0.10	0.792	8.85	7.01	3.195
	65	326	965.00	195	314049	931225	63150	0.12	0.859	7.38	6.35	2.927
	70	362							0.906	6.82	6.18	
	Time Ignition [s]	11.8										
Test 2	20	32							0.269	19.58	5.27	
	30	78	232.00	90	21992	53824	7860	0.22	0.420	17.05	7.17	2.121
	40	122	372.00	120	50552	138384	15820	0.21	0.526	14.52	7.63	2.169
	45								0.000	13.25	0.00	
	50	172	505.00	145	88989	255025	25085	0.17	0.624	11.78	7.36	2.425
	55	211	653.00	165	147005	426409	36405	0.10	0.691	10.32	7.13	3.152
	60	270	795.00	180	216017	632025	48215	0.10	0.782	8.85	6.92	3.221
	65	314	926.00	195	288460	857476	60550	0.14	0.843	7.38	6.23	2.705
	70	342							0.880	6.82	6.00	
	Time Ignition [s]	10.1										
Test 3	20	36							0.286	19.58	5.59	
	30	82	245.00	90	24149	60025	8260	0.22	0.431	17.05	7.35	2.133
	40	127	369.00	115	48453	136161	14740	0.19	0.536	14.52	7.79	2.270
	45	160	479.00	135	78593	229441	21880	0.15	0.602	13.25	7.98	2.550
	50	192	583.00	150	115825	339889	29505	0.14	0.660	11.78	7.77	2.669
	55	231	685.00	165	158869	469225	38025	0.14	0.723	10.32	7.46	2.652
	60	262							0.770	8.85	6.82	
	65											
	70											

Laboratory	Newcastle University - Fire Lab
Date of Tests	10/02/03
Material	Medium Density Fibre Board (MDF)
Specimen Dimension	250 * 90 * 20
b Value	0.0476

	Heat Flux	50										
	Flame Front Position		Σt	Σx	$\Sigma(t^2)$	$(\Sigma t)^2$	Σ(t.x)	V	F(t)	Q	Q*F(t)	1/V
	Time Ignition [s]	3.4										
Test 4	20	29							0.256	19.58	5.02	
	30	68	201.00	90	16281	40401	6780	0.27	0.393	17.05	6.69	1.937
	40	104	301.00	115	32081	90601	12005	0.25	0.485	14.52	7.05	2.007
	45	129	386.00	135	50866	148996	17615	0.20	0.541	13.25	7.16	2.214
	50	153	463.00	150	72811	214369	23410	0.19	0.589	11.78	6.94	2.283
	55	181	545.00	165	100691	297025	30265	0.17	0.640	10.32	6.61	2.409
	60	211	652.00	180	144882	425104	39515	0.12	0.691	8.85	6.12	2.838
	65	260	766.00	195	199146	586756	50210	0.12	0.768	7.38	5.67	2.912
	70	295	884.00	210	262866	781456	62225	0.14	0.818	6.82	5.58	2.627
	75	329							0.863	6.26	5.40	
	80											
	85											
	90											
	Time Ignition [s]	6.4										
Test 5	20	29							0.256	19.58	5.02	
	30	71	225.00	90	21507	50625	7710	0.21	0.401	17.05	6.84	2.197
	40	125	356.00	115	46266	126736	14330	0.17	0.532	14.52	7.73	2.426
	45	160	481.00	135	79641	231361	22000	0.14	0.602	13.25	7.98	2.665
	50	196	590.00	150	118772	348100	29870	0.14	0.666	11.78	7.85	2.721
	55	234	700.00	165	166072	490000	38870	0.14	0.728	10.32	7.51	2.721
	60	270	808.00	180	220072	652864	48830	0.14	0.782	8.85	6.92	2.646
	65	304	905.00	195	274877	819025	59130	0.16	0.830	7.38	6.13	2.475
	70	331	1009.00	210	341853	1018081	70980	0.14	0.866	6.82	5.91	2.669
	75	374							0.921	6.26	5.76	
	80											
	Time Ignition [s]	9.7										
Test 6	20	27							0.247	19.58	4.84	
	30	65	202.00	90	17054	40804	6890	0.24	0.384	17.05	6.54	2.040
	40	110	347.00	120	45909	120409	14950	0.19	0.499	14.52	7.25	2.323
	45								0.000	13.25	0.00	
	50	172	495.00	145	87053	245025	24715	0.15	0.624	11.78	7.36	2.609
	55	213	628.00	165	134002	394384	34895	0.14	0.695	10.32	7.17	2.675
	60	243	736.00	180	182818	541696	44495	0.15	0.742	8.85	6.57	2.593
	65	280	835.00	195	234793	697225	54620	0.14	0.797	7.38	5.88	2.629
	70	312	947.00	210	301769	896809	66665	0.13	0.841	6.82	5.73	2.748
	75	355	1063.00	225	380185	1129969	80145	0.12	0.897	6.26	5.61	2.899
	80	396	1210.00	240	493522	1464100	97320	0.09	0.947	5.70	5.40	3.249
	85	459							1.020	5.13	5.23	
	90											

Laboratory: Newcastle University - Fire Lab
Date of Tests: 10/02/03
Material: Medium Density Fibre Board (MDF)
Specimen Dimension: 250 * 90 * 20
b Value: 0.0476

Heat Flux: 60

	Flame Front Position	Σt	Σx	Σ(t²)	(Σt)²	I(t,x)	V	F(t)	Q	Q*F(t)	t/V
Test 7	Time Ignition [s]	5						0.228	19.58	4.47	
	20	23						0.228	19.58	4.47	
	30	51	162.00	30	10874	26244	5510	0.31	0.340	17.05	5.80	1.809
	40	88	250.00	115	22666	62500	10045	0.25	0.447	14.52	6.48	1.992
	45	111	333.00	135	39665	114321	15515	0.19	0.501	13.25	6.64	2.285
	50	140	418.00	150	53810	174724	21180	0.18	0.563	11.78	6.64	2.367
	55	167	501.00	165	87483	257043	28185	0.17	0.615	10.32	6.35	2.454
	60	200	602.00	180	123114	362404	36460	0.15	0.673	8.85	5.96	2.608
	65	235	632.00	195	161274	478864	45265	0.17	0.730	7.38	5.39	2.408
	70	257	800.00	210	216138	640000	56365	0.13	0.763	6.82	5.20	2.772
	75	308	919.00	225	286229	844561	63410	0.10	0.835	6.26	5.23	3.116
	80	354	1086.00	240	339356	1173336	87460	0.08	0.896	5.70	5.10	3.430
	85	424	1260.00	255	537416	1587600	107740	0.08	0.960	5.13	5.03	3.563
	90	482	1433.00	270	636183	2070721	130055	0.09	1.045	4.50	4.70	3.304
	95	533	1626.00	285	883734	######	155115	0.08	1.039	3.86	4.25	3.618
	100	611							1.177	3.23	3.80	
Test 8	Time Ignition [s]	4.8						0.228	19.58	4.47	
	20	23						0.228	19.58	4.47	
	30	54	168.00	30	11726	28224	5720	0.23	0.350	17.05	5.36	1.846
	40	91	253.00	115	24193	67081	10330	0.25	0.454	14.52	6.59	1.992
	45	114	361.00	135	45613	130321	16570	0.15	0.508	13.25	6.73	2.586
	50	156	453.00	150	70821	205209	22935	0.14	0.595	11.78	7.01	2.647
	55	183	556.00	165	104314	309136	30885	0.16	0.644	10.32	6.64	2.475
	60	217	642.00	180	133142	412164	38815	0.17	0.701	8.85	6.21	2.438
	65	242	726.00	195	176342	527076	47440	0.20	0.740	7.38	5.47	2.236
	70	267	823.00	210	228443	677329	57970	0.13	0.778	6.82	5.31	2.725
	75	314	943.00	225	300929	889249	71200	0.11	0.843	6.26	5.28	3.062
	80	362	1088.00	240	399384	1183744	87530	0.10	0.906	5.70	5.16	3.131
	85	412	1252.00	255	529272	1567504	107000	0.09	0.966	5.13	4.36	3.417
	90	478	1550.00	270	833828	######	140740	0.04	1.041	4.50	4.68	5.158
	95	660							1.223	3.86	4.72	
	100											
Test 9	Time Ignition [s]	5.8						0.238	19.58	4.66	
	20	25						0.238	19.58	4.66	
	30	56	177.00	30	12377	31329	6020	0.28	0.356	17.05	6.07	1.883
	40	96	276.00	115	27728	76176	11100	0.22	0.466	14.52	6.77	2.120
	45	124	376.00	135	48328	141376	17220	0.17	0.530	13.25	7.02	2.451
	50	156	455.00	150	70337	207025	23005	0.19	0.595	11.78	7.01	2.283
	55	175	546.00	165	101186	298116	30325	0.16	0.630	10.32	6.50	2.480
	60	215	637.00	180	137853	405769	38580	0.14	0.638	8.85	6.18	2.683
	65	247	735.00	195	181763	540225	48065	0.17	0.748	7.38	5.52	2.413
	70	273	838.00	210	236662	702244	53015	0.14	0.786	6.82	5.36	2.636
	75	318	943.00	225	293557	889249	71120	0.13	0.843	6.26	5.31	2.820
	80	352	1090.00	240	401428	1188100	87710	0.09	0.893	5.70	5.09	3.252
	85	420	1353.00	255	644873	1846881	116630	0.04	0.976	5.13	5.01	4.383
	90	587							1.153	4.50	5.19	
	95											
	100											

Laboratory	Newcastle University - Fire Lab
Date of Tests	11/02/03
Material	Macroparpa
Specimen Dimension	250 * 90 * 20
b Value	0.0654

	Heat Flux		40									
	Flame Front Position	t	Σt	Σx	$\Sigma(t^2)$	$(\Sigma t)^2$	Σ(t.x)	V	F(t)	Q	Q*F(t)	1/√V
	Time Ignition [s]	10.4										
Test 1	20	14							0.245	19.58	4.79	
	30	29	96	90	3846	9216	3270	0.50	0.352	17.05	6.00	1.409
	35								0.000	15.78	0.00	
	40	53	167	115	10875	27889	6815	0.26	0.476	14.52	6.91	1.954
	45	85	246	135	21698	60516	11345	0.18	0.603	13.25	7.99	2.356
	50	108							0.680	11.78	8.01	
	Time Ignition [s]	5.4										
Test 2	20	8							0.185	19.58	3.62	
	30	21	63	90	1661	3969	2150	0.77	0.300	17.05	5.11	1.140
	35								0.000	15.78	0.00	
	40	34	111	120	4733	12321	4790	0.56	0.381	14.52	5.54	1.337
	45								0.000	13.25	0.00	
	50	56	159	145	9053	25281	7955	0.43	0.489	11.78	5.77	1.523
	55	69	213	165	15641	45369	11875	0.31	0.543	10.32	5.60	1.799
	60	88	263	185	23741	69169	16495	0.40	0.614	8.85	5.43	1.573
	65								0.000	7.38	0.00	
	70	106	317	205	34109	100489	21925	0.43	0.673	6.82	4.59	1.525
	75	123	365	225	44861	133225	27525	0.33	0.725	6.26	4.54	1.737
	80	136	262	155	33633	68539	20105	0.61	0.763	5.70	4.34	1.280
	Time Ignition [s]	2.8										
Test 3	20	21							0.300	19.58	5.87	
	30	45	132	85	6822	17424	4080	0.34	0.439	17.05	7.48	1.727
	35	66	191	105	12781	36481	6860	0.28	0.531	15.78	8.39	1.883
	40	80							0.585	14.52	8.49	
	45											
	50											

Laboratory	Newcastle University - Fire Lab
Date of Tests	11/02/03
Material	Macroparpa
Specimen Dimension	250 * 90 * 20
b Value	0.0654

	Heat Flux	50										
	Flame Front Position	t	Σt	Σx	Σ(t²)	(Σt)²	Σ(t.x)	V	F(t)	Q	Q*F(t)	1/V
	Time Ignition [s]	3.6										
Test 4	20	11							0.217	19.58	4.25	
	30	22	69	90	1901	4761	2320	0.80	0.307	17.05	5.23	1.121
	35								0.000	15.78	0.00	
	40	36	121	120	5749	14641	5250	0.47	0.392	14.52	5.70	1.456
	45								0.000	13.25	0.00	
	50	63	178	145	11506	31684	8935	0.35	0.519	11.78	6.12	1.688
	55	79	234	165	18674	54756	13015	0.34	0.581	10.32	6.00	1.706
	60	92	284	180	27474	80656	17210	0.29	0.627	8.85	5.55	1.861
	65	113	327	195	36117	106929	21405	0.32	0.695	7.38	5.13	1.778
	70	122	385	210	50153	148225	27135	0.25	0.722	6.82	4.93	2.006
	75	150	451	225	69425	203401	34110	0.18	0.801	6.26	5.01	2.388
	80	179	523	240	92177	273529	42060	0.22	0.875	5.70	4.98	2.133
	85	194	585	255	114621	342225	49890	0.30	0.911	5.13	4.68	1.819
	90	212	632	270	133656	399424	57040	0.31	0.952	4.50	4.28	1.794
	95	226							0.983	3.86	3.80	
	100											
	Time Ignition [s]	2.6										
Test 5	20	12							0.227	19.58	4.44	
	30	32	111.00	90	5657	12321	3880	0.35	0.370	17.05	6.31	1.679
	35								0.000	15.78	0.00	
	40	67	188.00	120	13434	35344	8090	0.34	0.535	14.52	7.77	1.703
	45								0.000	13.25	0.00	
	50	89							0.617	11.78	7.27	
	55											
	60											
	Time Ignition [s]	3.1										
Test 6	20	11							0.217	19.58	4.25	
	30	24	75.00	90	2297	5625	2540	0.69	0.320	17.05	5.46	1.206
	35								0.000	15.78	0.00	
	40	40	129.00	120	6401	16641	5570	0.48	0.414	14.52	6.00	1.443
	45								0.000	13.25	0.00	
	50	65	195.00	145	13925	38025	9800	0.30	0.527	11.78	6.21	1.826
	55	90	269.00	165	25321	72361	15040	0.20	0.620	10.32	6.40	2.214
	60	114	336.00	180	38520	112896	20370	0.24	0.698	8.85	6.18	2.056
	65	132	412.00	195	57976	169744	27040	0.19	0.751	7.38	5.55	2.316
	70	166	487.00	210	80701	237169	34375	0.17	0.843	6.82	5.75	2.402
	75	189	557.00	225	104081	310249	41955	0.27	0.899	6.26	5.63	1.922
	80	202	640.00	240	138526	409600	51500	0.15	0.930	5.70	5.29	2.577
	85	249							1.032	5.13	5.30	
	90											

Laboratory	Newcastle University - Fire Lab
Date of Tests	11/02/03
Material	Macroparpa
Specimen Dimension	250 * 90 * 20
b Value	0.0654

	Heat Flux	60										
	Flame Front Position	t	Σt	Σx	$\Sigma(t^2)$	$(\Sigma t)^2$	Σ(t.x)	V	F(t)	Q	Q*F(t)	1/√V
	Time Ignition [z]	2.8										
Test 7	20	7							0.173	19.58	3.39	
	30	18	55	90	1273	3025	1880	0.87	0.277	17.05	4.73	1.073
	35								0.000	15.78	0.00	
	40	30	100	120	3928	10000	4340	0.57	0.358	14.52	5.20	1.323
	45								0.000	13.25	0.00	
	50	52	144	145	7448	20736	7210	0.47	0.472	11.78	5.56	1.464
	55	62	188	165	12024	35344	10450	0.45	0.515	10.32	5.31	1.485
	60	74	220	180	16376	48400	13310	0.45	0.563	8.85	4.98	1.485
	65	84	254	195	21748	64516	16620	0.45	0.599	7.38	4.43	1.485
	70	96	287	210	27721	82369	20205	0.43	0.641	6.82	4.37	1.517
	75	107	323	225	35065	104329	24345	0.42	0.677	6.26	4.23	1.551
	80	120	361	240	43805	130321	29015	0.37	0.716	5.70	4.08	1.644
	85	134	402	255	54260	161604	34310	0.36	0.757	5.13	3.89	1.673
	90	148	448	270	67416	200704	40480	0.31	0.796	4.50	3.58	1.794
	95	166	510	285	87876	260100	48690	0.20	0.843	3.86	3.26	2.214
	100	196	572	300	110072	327184	57420	0.22	0.916	3.23	2.96	2.143
	105	210	642	315	138212	412164	67610	0.24	0.948	2.59	2.46	2.030
	110	236	702	330	165332	492804	77450	0.22	1.005	2.51	2.52	2.151
	115	256							1.046	2.42	2.53	
	Time Ignition [z]	1.5							0.080			
Test 8	20	9							0.196	19.58	3.84	
	30	23	70	90	2054	4900	2390	0.69	0.314	17.05	5.35	1.204
	35								0.000	15.78	0.00	
	40	38	117	120	5109	13689	5010	0.60	0.403	14.52	5.85	1.286
	45								0.000	13.25	0.00	
	50	56	168	150	10056	28224	8760	0.56	0.489	11.78	5.77	1.342
	55								0.000	10.32	0.00	
	60	74	215	175	15837	46225	12765	0.52	0.563	8.85	4.98	1.385
	65	85	255	195	21917	65025	16685	0.45	0.603	7.38	4.45	1.483
	70	96	300	210	30602	90000	21170	0.28	0.641	6.82	4.37	1.882
	75	119	349	225	41333	121801	26365	0.26	0.713	6.26	4.46	1.964
	80	134	408	240	56142	166464	32820	0.28	0.757	5.70	4.31	1.906
	85	155	459	255	70881	210681	39195	0.28	0.814	5.13	4.18	1.906
	90	170	512	270	87894	262144	46240	0.31	0.853	4.50	3.84	1.790
	95	187	559	285	104673	312481	53265	0.31	0.894	3.86	3.45	1.790
	100	202							0.930	3.23	3.00	
	105											
	110											
	Time Ignition [z]	1.1										
Test 9	20	5							0.146	19.58	2.86	
	30	13	46	90	978	2116	1610	0.84	0.236	17.05	4.02	1.089
	35								0.000	15.78	0.00	
	40	28	87	120	3069	7569	3810	0.60	0.346	14.52	5.02	1.286
	45								0.000	13.25	0.00	
	50	46	130	145	6036	16900	6500	0.54	0.444	11.78	5.23	1.363
	55	56	172	165	10152	29584	9580	0.41	0.489	10.32	5.05	1.556
	60	70	224	180	17640	50176	13650	0.23	0.547	8.85	4.84	2.087
	65	98	290	195	29388	84100	19110	0.19	0.647	7.38	4.78	2.283
	70	122							0.722	6.82	4.93	

Laboratory	Newcastle University - Fire Lab
Date of Tests	11/02/03
Material	Radiata Pine
Specimen Dimension	250 * 90 * 20
b Value	0.0589

	Heat Flux	40										
	Flame Front Position	t	Σt	Σx	Σ(t²)	(Σt)²	Σ(t.x)	V	F(t)	Q	Q*F(t)	t^N/V
	Time Ignition [s]	9.3										
Test 1	20	14							0.220	19.58	4.32	
	30	27	82	90	2606	6724	2730	0.74	0.306	17.05	5.22	1.162
	40	41	159	120	10691	25281	7000	0.28	0.377	14.52	5.47	1.881
	45								0.000	13.25	0.00	
	50	91	240	145	21626	57600	12130	0.22	0.562	11.78	6.62	2.139
	55	108	327	165	36329	106929	18170	0.27	0.612	10.32	6.31	1.926
	60	128	384	180	49952	147456	23240	0.25	0.666	8.85	5.90	2.000
	65	148	464	195	73632	215296	30460	0.16	0.717	7.38	5.29	2.494
	70	188	532	210	95664	283024	37480	0.18	0.808	6.82	5.51	2.348
	75	196	622	225	130404	386884	46900	0.17	0.825	6.26	5.16	2.402
	80	238							0.909	5.70	5.18	
	Time Ignition [s]	7.6							0.162			
Test 2	20	31							0.328	19.58	6.42	
	30	58	174	90	11550	30276	5760	0.37	0.449	17.05	7.65	1.643
	40	85	247	115	21405	61009	9820	0.33	0.543	14.52	7.88	1.743
	45	104	335	135	39357	112225	15380	0.16	0.601	13.25	7.96	2.528
	50	146	428	150	63816	183184	21770	0.13	0.712	11.78	8.39	2.729
	55	178	535	165	97521	286225	29750	0.15	0.786	10.32	8.11	2.550
	60	211	632	180	135254	399424	38245	0.15	0.856	8.85	7.57	2.550
	65	243	732	195	180854	535824	47915	0.15	0.918	7.38	6.78	2.589
	70	278	921	210	296333	848241	65255	0.06	0.982	6.82	6.70	4.160
	75	400							1.178	6.26	7.37	
	80											
	Time Ignition [s]	3										
Test 3	20	12							0.204	19.58	4.00	
	30	26	77	90	2341	5929	2580	0.74	0.300	17.05	5.12	1.162
	40	39	121	115	5333	14641	4860	0.49	0.368	14.52	5.34	1.429
	45	56	183	135	12401	33489	8480	0.20	0.441	13.25	5.84	2.248
	50	88	292	150	32784	85264	15060	0.11	0.553	11.78	6.51	3.080
	55	148	570	165	141204	324900	32580	0.04	0.717	10.32	7.39	5.172
	60	334	849	180	268149	720801	52035	0.04	1.076	8.85	9.53	5.046
	65	367	1091	195	398345	1190281	71195	0.18	1.128	7.38	8.33	2.379
	70	390	1240	210	520078	1537600	87380	0.08	1.163	6.82	7.93	3.607
	75	483							1.294	6.26	8.10	

Laboratory	Newcastle University - Fire Lab
Date of Tests	11/02/03
Material	Radiata Pine
Specimen Dimension	250 * 90 * 20
b Value	0.0589

	Heat Flux	50										
	Flame Front Position	t	Σt	Σx	Σ(t²)	(Σt)²	Σ(t.x)	V	F(t)	Q	Q*F(t)	1/√V
	Time Ignition [s]	6										
Test 4	20	10							0.186	19.58	3.65	
	30	23	74	90	2310	5476	2530	0.64	0.282	17.05	4.82	1.250
	40	41	141	120	8139	19881	6180	0.36	0.377	14.52	5.47	1.673
	45								0.000	13.25	0.00	
	50	77	208	145	15710	43264	10440	0.30	0.517	11.78	6.09	1.826
	55	90	282	165	27254	79524	15700	0.25	0.559	10.32	5.76	1.981
	60	115	355	180	43825	126025	21600	0.17	0.632	8.85	5.59	2.461
	65	150	471	195	78161	221841	31070	0.11	0.721	7.38	5.33	3.043
	70	206	591	210	120161	349281	41795	0.11	0.845	6.82	5.77	2.964
	75	235	697	225	163197	485809	52525	0.20	0.903	6.26	5.65	2.246
	80	256	774	240	200850	599076	62160	0.21	0.942	5.70	5.37	2.197
	85	283							0.991	5.13	5.09	
	90											
	Time Ignition [s]	3.6										
Test 5	20	14							0.220	19.58	4.32	
	30	36	110	90	5092	12100	3760	0.43	0.353	17.05	6.03	1.517
	40	60	170	115	10372	28900	6810	0.40	0.456	14.52	6.62	1.587
	45	74	239	135	20101	57121	10980	0.21	0.507	13.25	6.71	2.171
	50	105	320	150	36382	102400	16335	0.15	0.604	11.78	7.11	2.591
	55	141	417	165	60147	173889	23265	0.15	0.699	10.32	7.22	2.573
	60	171	517	180	91147	267289	31340	0.16	0.770	8.85	6.82	2.531
	65	205	595	195	119227	354025	38915	0.20	0.843	7.38	6.23	2.253
	70	219							0.872	6.82	5.95	
	Time Ignition [s]	2.9										
Test 6	20	10							0.186	19.58	3.65	
	30	24	81	90	2885	6561	2800	0.53	0.289	17.05	4.92	1.373
	40	47	147	115	8561	21609	6020	0.28	0.404	14.52	5.86	1.878
	45	76	215	135	16449	46225	9900	0.22	0.513	13.25	6.80	2.151
	50	92	274	150	25476	75076	13850	0.33	0.565	11.78	6.66	1.733
	55	106	322	165	35076	103684	17870	0.31	0.606	10.32	6.26	1.794
	60	124	376	180	47928	141376	22760	0.25	0.656	8.85	5.80	2.003
	65	146	464	195	74328	215296	30510	0.14	0.712	7.38	5.25	2.706
	70	194							0.820	6.82	5.60	

Laboratory	Newcastle University - Fire Lab
Date of Tests	11/02/03
Material	Radiata Pine
Specimen Dimension	250 * 90 * 20
b Value	0.0589

	Heat Flux	60										
	Time Ignition [s]											
	Flame Front Position	t	Σt	Σx	Σ(t²)	(Σt)²	Σ(t.x)	V	F(t)	Q	Q*F(t)	1/√V
	Time Ignition [s]	3.1										
Test 7	20	12							0.204	19.58	4.00	
	30	25	81	90	2705	6561	2750	0.62	0.295	17.05	5.02	1.272
	40	44	176	120	14010	30976	7860	0.22	0.391	14.52	5.67	2.120
	45								0.000	13.25	0.00	
	50	107	239	145	21129	57121	11950	0.19	0.609	11.78	7.18	2.290
	55	88	314	165	33354	98596	17330	0.12	0.553	10.32	5.70	2.854
	60	119	342	180	40130	116964	20755	0.21	0.643	8.85	5.69	2.204
	65	135	405	195	55187	164025	26485	0.31	0.684	7.38	5.05	1.789
	70	151							0.724	6.82	4.94	
	Time Ignition [s]	1.8										
Test 8	20	11							0.195	19.58	3.83	
	30	27	81	90	2699	6561	2750	0.63	0.306	17.05	5.22	1.265
	40	43	125	115	5603	15625	5005	0.54	0.386	14.52	5.61	1.360
	45	55	166	135	9498	27556	7595	0.40	0.437	13.25	5.79	1.582
	50	68	205	150	14373	42025	10385	0.37	0.486	11.78	5.72	1.644
	55	82	262	165	23892	68644	14630	0.22	0.533	10.32	5.50	2.143
	60	112	325	180	36429	105625	19745	0.20	0.623	8.85	5.52	2.232
	65	131	400	195	54354	160000	26225	0.22	0.674	7.38	4.98	2.130
	70	157	486	210	81014	236196	34355	0.15	0.738	6.82	5.03	2.610
	75	198	579	225	114029	335241	43760	0.15	0.829	6.26	5.19	2.610
	80	224	672	240	151880	451584	54020	0.19	0.882	5.70	5.02	2.280
	85	250	748	255	187752	559504	63830	0.20	0.931	5.13	4.78	2.237
	90	274	817	270	223425	667489	73745	0.23	0.975	4.50	4.39	2.078
	95	293	902	285	273150	813604	85995	0.16	1.008	3.86	3.89	2.528
	100	335							1.078	3.23	3.48	
	Time Ignition [s]	3.5										
Test 9	20	12							0.204	19.58	4.00	
	30	29	92	90	3586	8464	3150	0.51	0.317	17.05	5.41	1.400
	40	51	148	120	8066	21904	6310	0.51	0.421	14.52	6.11	1.400
	45								0.000	13.25	0.00	
	50	68	207	145	14969	42849	10280	0.40	0.486	11.78	5.72	1.579
	55	88	309	165	35777	95481	17420	0.11	0.553	10.32	5.70	3.049
	60	153	449	180	74417	201601	27540	0.08	0.729	8.85	6.45	3.468
	65	208							0.849	7.38	6.27	

Laboratory	Newcastle University - Fire Lab
Date of Tests	11/02/03
Material	Beech
Specimen Dimension	250 * 90 * 20
b Value	0.0565

	Heat Flux	40										
	Flame Front Position	t	Σt	Σx	$\Sigma(t^2)$	$(\Sigma t)^2$	Σ(t.x)	V	F(t)	Q	Q*F(t)	1/√V
	Time Ignition [s]	4.1										
Test 1	20	22							0.265	19.58	5.19	
	30	39	127	90	6361	16129	4250	0.45	0.353	17.05	6.02	1.496
	35								0.000	15.78	0.00	
	40	66	187	115	12601	34969	7500	0.35	0.459	14.52	6.66	1.688
	45	82	258	135	23180	66564	11830	0.22	0.512	13.25	6.78	2.123
	50	110							0.593	11.78	6.98	
	55											
	60											
	Time Ignition [s]	4.3										
Test 2	20	25							0.283	19.58	5.53	
	30	54	159	85	9941	25281	4920	0.27	0.415	17.05	7.08	1.910
	35	80	238	105	20132	56644	8580	0.20	0.505	15.78	7.98	2.237
	40	104	311	120	33345	96721	12675	0.21	0.576	14.52	8.36	2.168
	45	127							0.637	13.25	8.44	
	50											
	55											
	60											
	Time Ignition [s]	2.1										
Test 3	20	17							0.233	19.58	4.56	
	30	33	106	90	4514	11236	3570	0.51	0.325	17.05	5.53	1.404
	35								0.000	15.78	0.00	
	40	56	155	115	8581	24025	6200	0.45	0.423	14.52	6.14	1.489
	45	66	208	135	14888	43264	9510	0.32	0.459	13.25	6.08	1.764
	50	86	277	150	27377	76729	14145	0.16	0.524	11.78	6.17	2.471
	55	125							0.632	10.32	6.52	
	60											

Laboratory	Newcastle University - Fire Lab
Date of Tests	11/02/03
Material	Beech
Specimen Dimension	250 * 90 * 20
b Value	0.0565

	Heat Flux	50										
	Flame Front Position	t	Σt	Σx	$\Sigma(t^2)$	$(\Sigma t)^2$	Σ(t.x)	V	F(t)	Q	Q*F(t)	1/√V
	Time Ignition [s]	2.3										
Test 4	20	12							0.196	19.58	3.83	
	30	25	80	90	2618	6400	2710	0.64	0.283	17.05	4.82	1.250
	35								0.000	15.78	0.00	
	40	43	119	115	5075	14161	4765	0.57	0.370	14.52	5.38	1.321
	45	51	156	135	8294	24336	7115	0.52	0.403	13.25	5.35	1.384
	50	62	192	150	12686	36864	9740	0.35	0.445	11.78	5.24	1.686
	55	79	240	165	19886	57600	13385	0.27	0.502	10.32	5.18	1.926
	60	99	302	180	31418	91204	18345	0.22	0.562	8.85	4.98	2.126
	65	124							0.629	7.38	4.65	
	70											
	Time Ignition [s]	1.6										
Test 5	20	13							0.204	19.58	3.99	
	30	32	100	90	4218	10000	3420	0.47	0.320	17.05	5.45	1.451
	35								0.000	15.78	0.00	
	40	55	156	115	8810	24336	6265	0.41	0.419	14.52	6.08	1.565
	45	69	211	135	15355	44521	9655	0.31	0.469	13.25	6.22	1.794
	50	87	266	150	24430	70756	13505	0.24	0.527	11.78	6.21	2.030
	55	110	327	165	36569	106929	18200	0.23	0.593	10.32	6.11	2.075
	60	130	390	180	51500	152100	23600	0.25	0.644	8.85	5.70	2.000
	65	150							0.692	7.38	5.11	
	70											
	Time Ignition [s]	2.9										
Test 6	20	16							0.226	19.58	4.43	
	30	30	102	90	4292	10404	3460	0.49	0.309	17.05	5.28	1.435
	35								0.000	15.78	0.00	
	40	56	154	115	8660	23716	6200	0.39	0.423	14.52	6.14	1.595
	45	68	213	135	15681	45369	9750	0.30	0.466	13.25	6.17	1.839
	50	89	261	150	23361	68121	13230	0.28	0.533	11.78	6.28	1.906
	55	104	319	165	34613	101761	17730	0.27	0.576	10.32	5.94	1.935
	60	126							0.634	8.85	5.61	
	65											

Laboratory	Newcastle University - Fire Lab
Date of Tests	11/02/03
Material	Beech
Specimen Dimension	250 * 90 * 20
b Value	0.0565

	Heat Flux	60										
	Flame Front Position	t	Σt	Σx	Σ(t²)	(Σt)²	Σ(t.x)	V	F(t)	Q	Q*F(t)	1/√V
	Time Ignition [s]	1.4										
Test 7	20	4							0.113	19.58	2.21	
	30	13	43	90	861	1849	1510	0.90	0.204	17.05	3.47	1.055
	35								0.000	15.78	0.00	
	40	26	78	120	2366	6084	3380	0.77	0.288	14.52	4.18	1.140
	45								0.000	13.25	0.00	
	50	39	125	150	5797	15625	6590	0.58	0.353	11.78	4.16	1.316
	55								0.000	10.32	0.00	
	60	60	170	175	10162	28900	10165	0.47	0.438	8.85	3.87	1.459
	65	71	219	195	16385	47961	14375	0.35	0.476	7.38	3.51	1.686
	70	88	258	210	22586	66564	18200	0.35	0.530	6.82	3.62	1.686
	75	99	304	225	31234	92416	22945	0.34	0.562	6.26	3.52	1.719
	80	117							0.611	5.70	3.48	
	85											
	90											
	Time Ignition [s]	1.9										
Test 8	20	6							0.138	19.58	2.71	
	30	16	51	90	1133	2601	1760	0.86	0.226	17.05	3.85	1.075
	35								0.000	15.78	0.00	
	40	29	92	115	3306	8464	3755	0.47	0.304	14.52	4.42	1.457
	45	47	132	135	6186	17424	6075	0.36	0.387	13.25	5.13	1.673
	50	56	169	150	9701	28561	8545	0.53	0.423	11.78	4.98	1.379
	55	66	203	165	14053	41209	11290	0.39	0.459	10.32	4.74	1.592
	60	81							0.509	8.85	4.50	
	65											
	70											
	Time Ignition [s]	1.4										
Test 9	20	6							0.138	19.58	2.71	
	30	14	42	90	716	1764	1420	1.25	0.211	17.05	3.60	0.894
	35								0.000	15.78	0.00	
	40	22	73	120	2049	5329	3150	0.84	0.265	14.52	3.85	1.089
	45								0.000	13.25	0.00	
	50	37	108	145	4254	11664	5425	0.56	0.344	11.78	4.05	1.336
	55	49	145	165	7251	21025	8085	0.45	0.396	10.32	4.08	1.485
	60	59	183	180	11507	33489	11110	0.38	0.434	8.85	3.84	1.627
	65	75	227	195	17755	51529	14925	0.29	0.489	7.38	3.61	1.845
	70	93	270	210	24678	72900	19035	0.36	0.545	6.82	3.72	1.673
	75	102	313	225	32977	97969	23600	0.39	0.571	6.26	3.57	1.602
	80	118	352	240	41752	123904	28310	0.33	0.614	5.70	3.50	1.733
	85	132	394	255	52084	155236	33620	0.38	0.649	5.13	3.33	1.614
	90	144	439	270	64729	192721	39665	0.32	0.678	4.50	3.05	1.776
	95	163	307	285	47305	94249	28445	-0.05	0.721	3.86	2.79	
	100											

Laboratory	Newcastle University - Fire Lab
Date of Tests	11/02/03
Material	Rimu
Specimen Dimension	250 * 90 * 20
b Value	0.0444

	Heat Flux	40										
	Flame Front Position	t	Σt	Σx	$\Sigma(t^2)$	$(\Sigma t)^2$	Σ(t.x)	V	F(t)	Q	Q*F(t)	1/√V
	Time Ignition [s]	4										
Test 1	20	9										
	30	15					**NO RESULT**					
	40											
	Time Ignition [s]	5.6										
Test 2	20	17										
	30						**NO RESULT**					
	40											
	Time Ignition [s]	6.3										
Test 3	20	21							0.203	19.58	3.98	
	30	48	159	90	10845	25281	5460	0.29	0.308	17.05	5.24	1.872
	40	90	243	120	21429	59049	10290	0.33	0.421	14.52	6.11	1.750
	45								0.000	13.25	0.00	
	50	105	328	145	36814	107584	16165	0.33	0.455	11.78	5.36	1.748
	55	133							0.512	10.32	5.28	

Laboratory	Newcastle University - Fire Lab
Date of Tests	11/02/03
Material	Rimu
Specimen Dimension	250 * 90 * 20
b Value	0.0444

	Heat Flux	50										
	Flame Front Position	t	Σt	Σx	$\Sigma(t^2)$	$(\Sigma t)^2$	Σ(t.x)	V	F(t)	Q	Q*F(t)	1/√V
	Time Ignition [s]	1.8										
Test 4	20	5							0.099	19.58	1.94	
	30	13	40	90	678	1600	1370	1.18	0.160	17.05	2.73	0.922
	40	22							0.208	14.52	3.02	
	Time Ignition [s]	4.2										
Test 5	20	7							0.117	19.58	2.30	
	30	15	44	90	758	1936	1470	1.33	0.172	17.05	2.93	0.867
	40	22	66	115	1550	4356	2635	1.07	0.208	14.52	3.02	0.966
	45	29	88	135	2694	7744	4035	0.67	0.239	13.25	3.17	1.226
	50	37	119	150	5019	14161	6070	0.40	0.270	11.78	3.18	1.578
	55	53	156	165	8534	24336	8725	0.34	0.323	10.32	3.33	1.706
	60	66	200	180	13726	40000	12140	0.36	0.361	8.85	3.19	1.675
	65	81							0.400	7.38	2.95	
	Time Ignition [s]	3.2										
Test 6	20	8							0.126	19.58	2.46	
	30	25	69	90	1985	4761	2350	0.70	0.222	17.05	3.79	1.192
	40	36	116	115	4946	13456	4665	0.47	0.266	14.52	3.87	1.453
	45	55	158	135	8810	24964	7265	0.32	0.329	13.25	4.36	1.776
	50	67	208	150	14910	43264	10555	0.32	0.363	11.78	4.28	1.776
	55	86	252	165	21686	63504	14020	0.31	0.412	10.32	4.25	1.799
	60	99							0.442	8.85	3.91	
	65											

Laboratory	Newcastle University - Fire Lab
Date of Tests	11/02/03
Material	Rimu
Specimen Dimension	250 * 90 * 20
b Value	0.0444

	Heat Flux	60										
	Flame Front Position	t	Σt	Σx	Σ(t²)	(Σt)²	Σ(t.x)	V	F(t)	Q	Q*F(t)	1/V
	Time Ignition [s]	4.4										
Test 7	20	4							0.089	19.58	1.74	
	30	12	40	90	736	1600	1400	0.99	0.154	17.05	2.62	1.007
	40	24	70	120	1876	4900	3020	0.91	0.218	14.52	3.16	1.050
	45								0.000	13.25	0.00	
	50	34	103	150	3757	10609	5360	0.95	0.259	11.78	3.05	1.025
	55								0.000	10.32	0.00	
	60	45	131	175	5885	17161	7780	0.84	0.298	8.85	2.64	1.091
	65	52	157	195	8329	24649	10280	0.67	0.320	7.38	2.36	1.226
	70	60	180	210	10928	32400	12680	0.63	0.344	6.82	2.35	1.265
	75	68	204	225	14000	41616	15380	0.63	0.366	6.26	2.29	1.265
	80	76	228	240	17456	51984	18320	0.63	0.387	5.70	2.20	1.265
	85	84	254	255	21668	64516	21680	0.55	0.407	5.13	2.09	1.344
	90	94							0.430	4.50	1.94	
	Time Ignition [s]	3.2										
Test 8	20	7							0.117	19.58	2.30	
	30	22	60	90	1494	3600	2040	0.82	0.208	17.05	3.55	1.107
	40	31	97	120	3381	9409	4100	0.90	0.247	14.52	3.59	1.055
	45								0.000	13.25	0.00	
	50	44	139	150	6993	19321	7280	0.60	0.295	11.78	3.47	1.294
	55								0.000	10.32	0.00	
	60	64	185	175	11961	34225	11045	0.46	0.355	8.85	3.14	1.477
	65	77	229	195	17769	52441	15005	0.42	0.390	7.38	2.88	1.551
	70	88							0.417	6.82	2.84	
	75											
	80											
	Time Ignition [s]	3.2										
Test 9	20	7							0.117	19.58	2.30	
	30	15	52	90	1174	2704	1790	0.84	0.172	17.05	2.93	1.089
	40	30	89	120	3061	7921	3850	0.69	0.243	14.52	3.53	1.204
	45								0.000	13.25	0.00	
	50	44							0.295	11.78	3.47	
	55											
	60											

Laboratory	Newcastle University - Fire Lab
Date of Tests	13/02/03
Material	Laminated Veneer Lumber (LVL)
Specimen Dimension	250 * 90 * 20
b Value	0.0352

	Heat Flux	40										
	Flame Front Position	t	Σt	Σx	Σ(t²)	(Σt)²	Σ(t.x)	V	F(t)	Q	Q*F(t)	1/√V
	Time Ignition [s]	1										
Test 1	20	5							0.079	19.58	1.54	
	30	10	32	90	414	1024	1080	1.65	0.111	17.05	1.90	0.778
	40	17	55	115	1173	3025	2240	0.80	0.145	14.52	2.11	1.118
	45	28	86	135	2754	7396	3990	0.42	0.186	13.25	2.47	1.551
	50	41	120	150	5066	14400	6115	0.43	0.225	11.78	2.66	1.521
	55	51	160	165	8906	25600	8935	0.36	0.251	10.32	2.59	1.661
	60	68	205	180	14621	42025	12475	0.29	0.290	8.85	2.57	1.871
	65	86							0.326	7.38	2.41	
	70											
	Time Ignition [s]	1										
Test 2	20	4							0.070	19.58	1.38	
	30	9	28	90	322	784	950	1.81	0.106	17.05	1.80	0.743
	40	15	45	115	747	2025	1815	1.25	0.136	14.52	1.98	0.894
	45	21	66	135	1566	4356	3045	0.66	0.161	13.25	2.14	1.233
	50	30	91	150	2941	8281	4645	0.53	0.193	11.78	2.27	1.379
	55	40	124	165	5416	15376	6940	0.41	0.223	10.32	2.30	1.556
	60	54	162	180	9140	26244	9860	0.36	0.259	8.85	2.29	1.673
	65	68	215	195	16189	46225	14170	0.25	0.290	7.38	2.14	2.001
	70	93							0.339	6.82	2.32	
	Time Ignition [s]	1										
Test 3	20	3							0.061	19.58	1.19	
	30	7	21	90	179	441	710	2.50	0.093	17.05	1.59	0.632
	40	11	36	115	494	1296	1460	1.29	0.117	14.52	1.69	0.880
	45	18	65	135	1741	4225	3050	0.38	0.149	13.25	1.98	1.631
	50	36	100	150	3736	10000	5140	0.35	0.211	11.78	2.49	1.696
	55	46	137	165	6437	18769	7630	0.53	0.239	10.32	2.46	1.379
	60	55							0.261	8.85	2.31	
	65											
	70											

Laboratory	Newcastle University - Fire Lab
Date of Tests	13/02/03
Material	Laminated Veneer Lumber (LVL)
Specimen Dimension	250 * 90 * 20
b Value	0.0352

	Heat Flux	50										
	Flame Front Position	t	Σt	Σx	Σ(t²)	(Σt)²	Σ(t.x)	V	F(t)	Q	Q*F(t)	t/V
	Time Ignition [s]	1.5										
Test 4	20	3							0.061	19.58	1.19	
	30	7	26	90	314	676	910	1.47	0.093	17.05	1.59	0.826
	40	16	45	115	789	2025	1840	1.01	0.141	14.52	2.04	0.996
	45	22	69	135	1701	4761	3180	0.66	0.165	13.25	2.19	1.233
	50	31	93	150	3045	8649	4740	0.56	0.196	11.78	2.31	1.342
	55	40	120	165	4962	14400	6690	0.56	0.223	10.32	2.30	1.342
	60	49	156	180	8490	24336	9495	0.36	0.246	8.85	2.18	1.673
	65	67	225	195	18771	50625	14925	0.16	0.288	7.38	2.13	2.514
	70	109							0.367	6.82	2.51	
	Time Ignition [s]	1										
Test 5	20	3							0.061	19.58	1.19	
	30	7	22	90	202	484	750	2.21	0.093	17.05	1.59	0.672
	40	12	48	120	1034	2304	2140	0.83	0.122	14.52	1.77	1.100
	45								0.000	13.25	0.00	
	50	29	78	145	2354	6084	3965	0.60	0.190	11.78	2.23	1.293
	55	37	110	165	4146	12100	6125	0.67	0.214	10.32	2.21	1.226
	60	44	145	180	7401	21025	8835	0.34	0.233	8.85	2.07	1.705
	65	64							0.282	7.38	2.08	
	70											
	Time Ignition [s]	1										
Test 6	20	2							0.050	19.58	0.97	
	30	6	19	90	161	361	660	2.21	0.086	17.05	1.47	0.672
	40	11	32	115	382	1024	1295	1.68	0.117	14.52	1.69	0.771
	45	15	49	135	875	2401	2265	0.80	0.136	13.25	1.81	1.116
	50	23	69	150	1715	4761	3530	0.63	0.169	11.78	1.99	1.265
	55	31	99	165	3515	9801	5555	0.44	0.196	10.32	2.02	1.502
	60	45	127	180	5587	16129	7720	0.47	0.236	8.85	2.09	1.451
	65	51	159	195	8595	25281	10425	0.54	0.251	7.38	1.86	1.366
	70	63							0.279	6.82	1.91	

Averaged Results - Surface Flame Spread

Heat Flux - 40kW/m²

Distance	Wood Species							
	Particle	Plywood	MDF	Macrocarpa	Pine	Beech	Rimu	LVL
20	27.67	11.67	33.67	14.33	19.00	21.33	15.67	4.00
30	80.67	28.00	82.67	31.67	37.00	42.00	31.50	8.67
40	132.33	48.33	125.67	55.67	55.00	75.33	90.00	14.33
50	203.50	101.33	185.33	82.00	108.33	98.00	105.00	35.67
60		243.00	269.67	88.00	224.33	125.00	133.00	59.00
70		340.00	352.00	106.00	285.33			93.00
80				136.00				

Heat Flux - 50kW/m²

Distance	Wood Species							
	Particle	Plywood	MDF	Macrocarpa	Pine	Beech	Rimu	LVL
20	22.67	11.33	28.33	11.33	11.33	13.67	6.67	2.67
30	51.67	25.00	68.00	26.00	27.67	29.00	17.67	6.67
40	94.00	50.00	113.00	47.67	49.33	51.33	26.67	13.00
50	144.33	77.33	173.67	72.33	91.33	79.33	52.00	27.67
60	231.33	114.00	241.33	103.00	136.67	118.33	82.50	46.00
70		162.67	312.67	144.00	206.33	137.00	81.00	86.00
80		203.00	396.00	190.50	256.00			
90		301.00	459.00		283.00			
100								

Heat Flux - 60kW/m²

Distance	Wood Species							
	Particle	Plywood	MDF	Macrocarpa	Pine	Beech	Rimu	LVL
20	17.00	11.33	23.67	7.00	11.67	5.33	6.00	1.67
30	45.33	25.00	53.67	18.00	27.00	14.33	16.33	4.67
40	72.67	36.67	91.67	32.00	46.00	25.67	28.33	10.33
50	107.33	56.33	150.67	51.33	67.67	44.00	40.67	17.33
60	204.00	88.00	210.67	72.67	128.00	66.67	54.50	36.67
70		124.33	265.67	104.67	154.00	90.50	74.00	65.50
80		171.33	356.00	127.00	224.00	117.50	76.00	100.00
90			515.67	159.00	274.00	144.00	94.00	
100			611.00	199.00	335.00	163.00		
110				236.00				
120				256.00				
130								

Laboratory	Newcastle University - Fire Lab
Date of Tests	13/02/03
Material	Laminated Veneer Lumber (LVL)
Specimen Dimension	250 * 90 * 20
b Value	0.0352

	Heat Flux	60										
	Flame Front Position	t	Σt	Σx	Σ(t²)	(Σt)²	Σ(t.x)	V	F(t)	Q	Q*F(t)	t/V
	Time Ignition [s]	0.6										
Test 7	20	3							0.061	19.58	1.19	
	30	5	20	90	178	400	690	2.01	0.079	17.05	1.34	0.704
	40	12	34	115	458	1156	1395	1.26	0.122	14.52	1.77	0.890
	45	17	50	135	874	2500	2295	1.11	0.145	13.25	1.92	0.951
	50	21	67	150	1571	4489	3410	0.80	0.161	11.78	1.90	1.116
	55	29	85	165	2507	7225	4745	0.71	0.190	10.32	1.96	1.187
	60	35	106	180	3830	11236	6425	0.77	0.208	8.85	1.84	1.141
	65	42	128	195	5590	16384	8400	0.62	0.228	7.38	1.68	1.268
	70	51	156	210	8334	24336	11025	0.47	0.251	6.82	1.71	1.454
	75	63	214	225	16570	45796	16295	0.19	0.279	6.26	1.75	2.308
	80	100							0.352	5.70	2.00	
	Time Ignition [s]	0.6										
Test 8	20	1							0.035	19.58	0.69	
	30	4	12	90	66	144	420	3.33	0.070	17.05	1.20	0.548
	40	7	25	120	261	625	1100	1.90	0.093	14.52	1.35	0.726
	45								0.000	13.25	0.00	
	50	14	39	145	569	1521	1970	1.37	0.132	11.78	1.55	0.854
	55	18	56	165	1096	3136	3130	0.99	0.149	10.32	1.54	1.007
	60	24	81	180	2421	6561	4965	0.45	0.172	8.85	1.53	1.493
	65	39							0.220	7.38	1.62	
	Time Ignition [s]	0.9										
Test 9	20	1							0.035	19.58	0.69	
	30	5	18	90	170	324	650	1.77	0.079	17.05	1.34	0.751
	40	12	34	120	458	1156	1480	1.65	0.122	14.52	1.77	0.778
	45								0.000	13.25	0.00	
	50	17	67	145	1877	4489	3420	0.48	0.145	11.78	1.71	1.448
	55	38	106	165	4334	11236	6000	0.29	0.217	10.32	2.24	1.861
	60	51	156	180	8534	24336	9505	0.34	0.251	8.85	2.22	1.706
	65	67	198	195	13490	39204	13015	0.34	0.288	7.38	2.13	1.706
	70	80	244	210	20298	59536	17230	0.33	0.315	6.82	2.15	1.737
	75	97							0.347	6.26	2.17	
	80											